UNIVERSITY OF NEWCASTLE UPON TYNE

Department of Civil Engineering

Movement of Solutes in Structured Soils During Intermittent Leaching: A Theoretical and Laboratory Study.

by
Mahmoud Al-Sibai

B. Sc. Civil Engineering (Al-Baath University, Syria)
M. Sc. Irrigation Engineering (University of Newcastle upon Tyne, UK)

A Thesis Submitted for the Degree of Doctor of Philosophy

September 1996

Abstract

Soil salinity is one of the major problems in arid and semi-arid zones, affecting up to 50% of arable land in Syria. Salt-affected soils are usually desalinized by leaching the excess salts out of the soil profile. Some studies have shown that applying the leaching water intermittently instead of continuously may result in more efficient leaching. This thesis aims to investigate, theoretically and experimentally, the benefits and limitations of intermittent leaching and to develop mathematical models able to simulate solute transport through structured soils under such conditions.

Laboratory leaching experiments were conducted on bi-continuum media, as an analogue of structured soils, created by packing porous aggregates (ceramic spheres or soil aggregates of uni- or multi- diameters) in glass columns. The columns were either leached continuously or intermittently and with different pore-water velocities. Intermittent leaching was undertaken either under saturated or drained conditions. Under "saturated conditions" the column remained saturated throughout the experiment, while under "drained conditions" the column was allowed to drain at the beginning of each rest period and remained like this until being saturated again for the next leaching period. The solute concentration in the leachate was monitored continuously (either using a flow-through conductivity cell, or by using ion-selective electrodes for K^+ and Br^-) to produce breakthrough curves. These curves were used to investigate solute transport through such media and validate the developed models.

The experiments showed that water savings of up to 22% under intermittent leaching from a soil aggregate column were possible under saturated conditions. Such saving increased with aggregate size, flow velocity and duration of rest period. Under drained conditions, for ceramic spheres, 12% more solute was leached with the same amount of water under intermittent leaching.

Two models were developed, the SIL (Saturated Intermittent Leaching) and the DIL (Drained Intermittent Leaching) models, for saturated and drained conditions respectively. The SIL model simulated solute transport in structured soils under intermittent leaching. The governing equations during displacement period were the mobile-immobile convection-dispersion equations. During the rest period the flow is stopped, and the solute transfers only by diffusion between immobile and mobile water regions. The DIL model simulated solute transport when the soil drained. Here, during the displacement period, the mobile water was drained. The model simulated this using the equations of the SIL model by assuming that air displaced the solution in a *piston*-type displacement. During the rest periods the solute diffuses within the aggregates establishing a more uniform concentration in the immobile water across the aggregate.

The models can be used with a wide range of column conditions and for both sorbed and non-sorbed solutes. Both models were verified against experimental results.

Acknowledgements

I would like to express my gratitude toward Dr. M.A. Adey and Dr. D.A. Rose for the invaluable guidance and supervision provided during this study, moreover for their readiness to listen and to advise on all matters.

Many thanks are due to the staff and colleagues of *salinity research group* for the valuable and lengthy discussion provided during the group meetings.

Thanks are due to Al-Baath University, Syria, for sponsoring my research study.

Thanks also to the staff of the Soil Physics & Soil Chemistry Laboratory, for their help and assistance.

I wish to thank my parents, brother and sisters for the inspiration, continuous concern and love they always gave.

Finally, I wish to thank my wife for her constant encouragement, support and her patience in enduring many inconveniences while I embarked on this study.

Table of contents

PART ONE

Solute transport through columns of ceramic spheres under saturated condition

PART TWO

Solute transport through columns of soil aggregates under saturated condition .

Appendices

List of main symbols

Symbol	Definition	Units
a	sphere radius	[L]
d	sphere or aggregate diameter	[L]
f	the fraction of adsorption sites that equilibrate with the mobile water phase	
k_f, k_b	the forward and backward rates of reactions	[T^{-1}]
q	water flux	[L^3 T^{-1}]
r^2	coefficient of determination (linear regresion)	
t	time	[T]
v	the average pore-water velocity	[L T^{-1}]
v_d	Darcy velocity ($v_d = \frac{q}{A}$)	[L T^{-1}]
v_m	average pore-water velocity in the mobile water region	[L T^{-1}]
x	distance	[L]
z	space co-ordinate (positive downwards)	[L]
A	cross-sectional area of the column	[L^2]
A_i	activity of the measured ions	[M L^{-3}]
C	solute concentration	[M L^{-3}]
C_e	concentration at equilibrium	[M L^{-3}]
$C_m(t)$	measured concentration of the external solution (for diffusion model)	[M L^{-3}]
$C_{im}(r,t)$	concentration of solute in the solution within the ceramic spheres (for diffusion model)	[M L^{-3}]

C_m	average solute concentration in the mobile water region	[M L^{-3}]
C_{im}	solute concentration in the immobile water region	[M L^{-3}]
C_{inp}	concentration of solute in the added water	[M L^{-3}]
C_0	initial concentration of solute in both the mobile and immobile solution	[M L^{-3}]
D_0	ionic diffusion coefficient in free water	[L^2 T^{-1}]
D_e	effective diffusion coefficient	[L^2 T^{-1}]
D_m	mechanical dispersion coefficient	[L^2 T^{-1}]
D_s	hydrodynamic dispersion coefficient	[L^2 T^{-1}]
F	mass fraction of type 1 "equilibrium" sites	
K	distribution coefficient	
L_r	length of the porous column	[L]
P	dimensionless variable (Table 6.2)	
R	total retardation factor	
R_m	retardation factors in the mobile water regions	
R_{im}	retardation factor in the immobile water region	
R^2	coefficient of determination (non-linear regresion)	
S	concentration of adsorbate, expressed as mass adsorbate per unit mass of dry soil	[M M^{-1}]
S_2	adsorption on type 2 "kinetic" sites	[M M^{-1}]
Sa	initial amount of potassium in the column including the adsorbed one	[M]
So	initial salt mass in the column	[M]
$Ss\ (t)$	salt mass in the column at time t	[M]
V	outflow volume	[L^3]
V_0	total volume of mobile and immobile water in the column	[L^3]
V_a	volume of added water needed to remove 90% of the initial salt load of the column	[L^3]

V_e	volume of external solution (for diffusion model)	[L^3]
V_{ws}	volume of solution inside the ceramic spheres	[L^3]
α	mass transfer rate coefficient between the mobile and immobile water regions	[T^{-1}]
α_k	first-order kinetic rate coefficient	[T^{-1}]
β	dimensionless variable (Table 6.2)	
θ_{sp}	sphere porosity	[L^3 L^{-3}]
θ	volumetric water content of the column	[L^3 L^{-3}]
θ_m	volume of mobile water as a proportion of total column volume	[L^3 L^{-3}]
θ_{im}	volume of immobile water as a proportion of total column volume	[L^3 L^{-3}]
λ	dispersivity	[L]
$\varphi(z,t)$	solute source or sink	[M L^{-3} T^{-1}]
ρ	soil bulk density	[M L^{-3}]
ρ_p	average particle density of the spheres	[M L^{-3}]
Φ	fraction of soil water that is mobile $(=\theta_m/\theta)$	
ω	dimensionless mass transfer coefficient.	

The above symbols represent the main variables and parameters, others will be defined through the text as necessary.

Chapter One

Introduction

The provision of adequate drainage and the accompanying problem of accumulation of salt in soil has plagued irrigated agriculture for centuries. Different factors can cause such salt accumulation. Saline irrigation water, low soil permeability, inadequate drainage conditions, low rainfall, and poor irrigation management, all contribute to the tendency of salt to accumulate in soils (*Yaron,* 1981). Excess salts in the soil solution influence the growth of plants by osmotic effects and toxicity of specific ions, and by changing the physical properties of the soils. Over time, salts may concentrate to such an extent that they hinder germination , seedling, vegetative growth, and the yield and quality of crops (*Tanji,* 1990), and ultimately render land sterile.

Historical records for the past 6000 years reveal that numerous societies based on irrigated agriculture failed due to salinity problems. One of the most highly publicised is that of ancient Mesopotamia, now Iraq. This once productive land appears to have suffered progressive salt damage from about 2400 BC to 1700 BC which contributed to decline of this civilisation (*Gelbured,* 1985; *Tanji,* 1990). Nowadays, salt-affected soils are to be found on all continents, covering about 10% of the total surface of dry land (*Szabolcs,* 1980), and about one-third of all irrigated land (*Yaron,* 1981).

The only way known to effectively remove excess salts from soil is by leaching (*Shalhevet,* 1973). Ponding water on the soil surface is the traditional method, but consumes large quantities of valuable water. During such leaching the water does not uniformly flow through the soil, but preferentially through macropores (*Tanji*, 1990; *Jury*, 1991). These tend to be inter-aggregate pores within a structured soil and such preferential flow results in a reduced effectiveness of leaching from *within* aggregates. More uniform leaching occurs if soil is leached in the unsaturated condition but this is slower and requires greater management control. In practice this requires a sprinkler irrigation system, which is unusual in arid and semi-arid environments.

Alternatively, if ponded leaching were intermittent, with a "rest period" during which the profile drained, solutes could diffuse to the exterior of the aggregates during the rest period even though macropore flow was not occurring. During the subsequent ponded-irrigation phase such solutes would quickly diffuse to the macropore region and be readily leached. Such a strategy should result in more efficient use of water for leaching purposes.

This study aims to optimise leaching using such intermittent ponded leaching of the soil profile.

Chapter Two

Literature review

This chapter consists of four main parts. The first will explain the idea of miscible displacement and will illustrate the different shapes of the resulting breakthrough curves. The second will consider the equation of solute transport through the soil and a general overview of the modelling approach of solute transport. The third part will introduce the idea of soil structure and the bi-continuum concept for modelling salt leaching from structured soils. The fourth part will summarise the comparative studies between continuous and intermittent leaching and will identify the most important factors affecting intermittent leaching.

2.1 Miscible displacement

2.1.1 Introduction

Miscible displacement (MD) is the process that occurs when one fluid mixes with and displaces another fluid (*Kirkham & Powers,* 1972). Leaching salts from a soil is an example of MD, because added water mixes with, and displaces, the solution in the soil. Another example of MD is the movement of water containing dissolved fertiliser or herbicides into and through the soil. One of the best known introductions of MD techniques to the field of soil science was made by *Nielsen & Biggar* in a series of papers in 1961 ,1962 and

1963. Since then MD techniques have gained widespread acceptance and use in the field of soil science .

Solutes in the displacing fluid are transferred through the soil by mass transport of the moving fluid and by diffusion (*Bear*, 1972; *Kirkham & Powers*, 1972; *Rose*, 1973). In a soil column this flow can be expected to be rather "*erratic*". It varies in magnitude and direction from point to point due to the complex pore geometry, and this erratic flow causes the solute to disperse between the displacing and the displaced fluid. The term "mechanical dispersion" is used to differentiate this spreading mechanism from that due to diffusion. This distinction is made because diffusion is caused by the random thermal motion of solute molecules, whereas dispersion is due to the erratic flow of the fluids through complex pore systems. *Mangold & Tsang* (1991) defined three processes occurring in the pore channels causing mechanical dispersion:

1) mixing within individual pore channels due to differences in velocity of the molecules between those in the middle of the channel and those subject to dragging forces along the pore walls,

2) mixing caused by differences in the sizes of the pore channels and hence velocities along the flow paths, and

3) differences caused by the branching of flow channel paths in the soil matrix.

The separation between mechanical and diffusion dispersion is, actually, rather artificial as they are inseparable. However, molecular diffusion depends on concentration differences (*Bear*, 1972), whereas mechanical dispersion depends only on velocity (*Wagenet*, 1983).

The coefficient of hydrodynamic dispersion (sometimes called effective diffusion coefficient (*Jury et al.*, 1981), or apparent diffusion coefficient

(*Biggar & Nielsen,* 1980; *Wagenet,* 1983), or simply the dispersion coefficient (*Nielsen et al.,* 1986)) is a term which is used to describe the spreading resulting from both mechanical dispersion and molecular diffusion (*Rose & Passioura,* 1971; *Passioura,* 1971; *Bear* ,1972; *Freeze & Cherry,* 1979).

2.1.2 Breakthrough curves

Because it is difficult to study the shape of the boundary between different fluids as they emerge from a pipe or soil column, it is common to monitor the concentration change of the displacing solute in the effluent. The manner in which the concentration changes can give some information about the porous medium and the physical behaviour of the fluid movement. Data are presented in a standard form called a breakthrough curve (BTC).

The BTC is a graph of concentration in the effluent relative to some standard concentration (usually the concentration of influent), plotted against the ratio of the volume of the collected effluent relative to the total pore volume in the column (*Krupp & Elrick,* 1968).

In the absence of dispersion (i.e., immiscible displacement), the BTC would take the form of the vertical line. This model, in which there is no dispersion, is called the *piston-flow* model of solute transport (Fig. 2.1), so named because the solute is displaced through the soil like a piston. Such displacement is seldom if ever encountered in practice (*Hillel,* 1980). What normally happens at the boundary (or the front between the two solutions) is a gradual mixing resulting from the hydrodynamic dispersion so that the boundary becomes increasingly diffuse about the mean position of the advancing front and the BTC will take a form of *S-shaped* curve (*Bear & Bachmat,* 1991; *Rose,* 1977). Shifting of the curve to the left indicates exclusion or "bypass" from a significant portion of the soil solution, while shifting to the right indicates adsorption or solute retention by soil. The symmetrical breakthrough curve which passes through the point of relative

concentration = 0.5 at pore volume =1 (showed by the dashed line in Fig. 2.1) called typical dispersion (or an ideal MD). Comprehensive discussions of the shapes of BTCs have been presented by *Nielsen & Biggar* (1962) and *Rose* (1977).

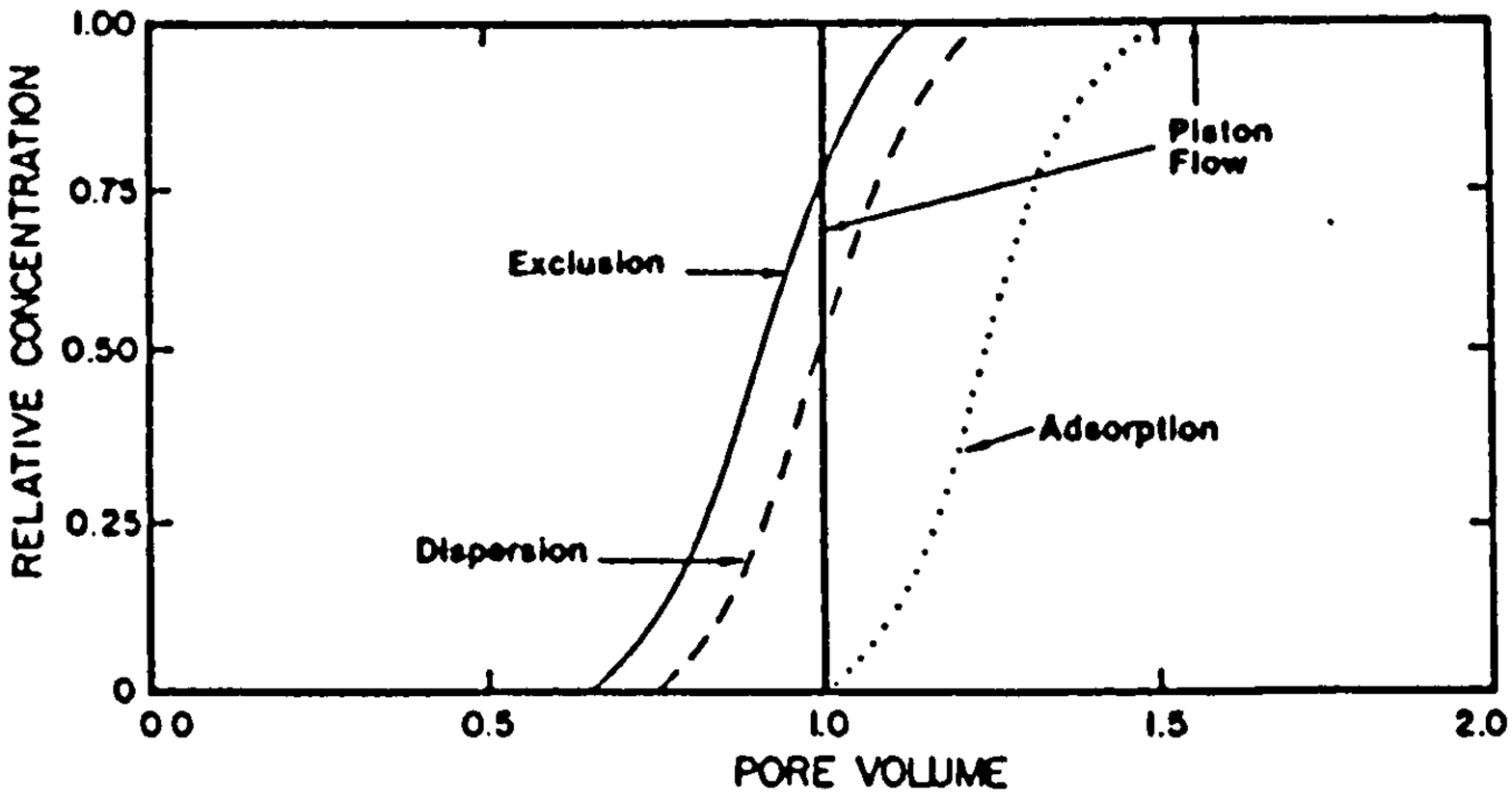

Fig. 2.1: Solute BTC illustrating several patterns of solute elution (after *Wagenet,* 1983)

2.2 Solute transport in soils

2.2.1 Convection - Dispersion equation

According to the previous miscible displacement theory, the total flux of solute is the result of the combined effects of diffusion and convection. That is:

$$J_S = J_D + J_C \tag{2.1}$$

where J is the mass of solute transported through a cross-sectional area in a unit time, and the subscripts S, D, and C represent total solute, solute transported by diffusion , and solute transported by convection, respectively.

2.2.1.1 Solute transport by diffusion

Fick's first equation states that for one-dimensional diffusion in free solution:

$$J_D = -D_0 \frac{dC}{dx} \tag{2.2}$$

where

C = solute concentration,

x = distance and,

D_0 = the ionic diffusion coefficient in free water. (Values of D_0 for major ions can be obtained from *Robinson & Stokes*, 1970.)

In a soil:

Because of the tortuous flow path in the soil matrix, Eq. 2.2 becomes;

$$J_D = -D_e(\theta)\frac{dC}{dx} \tag{2.3}$$

where D_e is the effective diffusion coefficient, which takes into account the tortuosity of the soil matrix.

Estimation of $D_e(\theta)$ has been the subject of a number of studies (*Nye*, 1979). *Bresler* (1973) related $D_e(\theta)$ for any given ion to D_0 by

$$D_e(\theta) = D_0\,\theta\left(\frac{l}{l_e}\right)^2 \zeta\,\gamma \tag{2.4}$$

where θ is volumetric water content, $(l/l_e)^2$ is a tortuosity factor reflecting the tortuosity of pores within the soil matrix (l is the average straight path of diffusion, l_e is the actual tortuous path along which diffusing molecules or ions move) and ζ and γ represent the effects of anion exclusion and the charged soil matrix on water viscosity respectively.

Jury (1991) based his equation on the *Millington & Quirk* (1961) tortuosity model to estimate D_e, i.e.,

$$D_e(\theta) = D_0\, \theta^{10/3} / \varepsilon^2 \qquad (2.5)$$

where ε is soil porosity.

Other equations are empirical. For example it has been found that, in a clay-water system, D_e can be represented as (*Kemper & van Schaik*, 1966):

$$D_e(\theta) = D_0\, a\, e^{b\theta} \qquad (2.6)$$

where a and b are empirical constants. *Olsen & Kemper* (1968) found a good fit for soils of texture ranging from sandy loam to clay, with b=10, and $0.001 < a < 0.005$.

2.2.2.2 Solute transport by convection

Macroscopic convective solute transport is usually described by considering the two components of the convective flow to be :

1) mean pore water velocity,

2) deviations from mean as a result of local variations of the flow velocity in individual pores.

The latter creates a mechanical dispersion effect which is similar to diffusion but the movement is not due to concentration differences but results, as discussed before, from interaction between large and small pores through the connecting local velocity (*Wagenet, 1983*). Its effect can be presented now in the same general form of Fick's equation by using mechanical dispersion instead of molecular diffusion .

Assuming a steady one-dimensional water movement through a homogeneous soil of uniform water content, the total amount of solute transported by convection across a unit area in the flow direction is given by

$$J_c = v\,\theta\, C - \theta\, D_m\left(v\right)\frac{dC}{dz} \qquad (2.7)$$

where

z = is the space co-ordinate (positive downwards)

v = is the average pore water velocity

D_m = is the mechanical dispersion which is given by (*Elrick & Clothier*, 1990)

$$D_m = \lambda v^{\eta} \tag{2.8}$$

where λ and η are empirical constant to be experimentally determined. For saturated homogeneous systems, the exponent η has been shown to be close to one and the above equation is often written as (*Bachmat & Bear*, 1964);

$$D_m = \lambda v \tag{2.9}$$

where λ is the dispersivity, which ranges from about 0.2 to 2 cm for different soils (*Biggar*, 1980).

2.2.2.3 The combined solute transport equation

Combining Eqs. 2.3 and 2.7 with 2.1 gives

$$J_s = -[(\theta D_m(v) + D_e(\theta)]\frac{dC}{dz} + v\ \theta C \tag{2.10}$$

or

$$J_s = -\theta D_S(v, \theta)\frac{dC}{dz} + v\ \theta C \tag{2.11}$$

where D_s is the hydrodynamic dispersion coefficient, given by:

$$D_S(v,\theta) = D_m(v) + \frac{D_e(\theta)}{\theta}\ . \tag{2.12}$$

The continuity equation states that the rate of change of solute within a finite volume element must equal the difference between the fluxes of solute that enter and leave that element (in addition, in some cases, to the gain or loss of solute due to chemical reactions or radioactive decay) (*Freeze & Cherry*, 1979). i.e.,

$$\frac{\partial(\theta C)}{\partial t} = -\frac{\partial J_s}{\partial z}$$

Applying these relationships to Eq. 2.11, and including consideration of ion-soil interaction (i.e., ion adsorption or exclusion) and sources or sinks of solute (i.e., chemical precipitation, adsorption, dissolution reactions), one obtains (*Addiscott & Wagenet,* 1985):

$$\frac{\partial(\theta C)}{\partial t} + \frac{\partial(\rho S)}{\partial t} = -\left\{-\left[\theta D_s(\theta, v)\right]\frac{\partial^2 C}{\partial z^2} + v\,\theta\,\frac{\partial C}{\partial z}\right\} \mp \varphi(z,t) \qquad (2.13)$$

where:

$\varphi(z,t)$ = solute source or sink

ρ = soil bulk density

S = concentration of solute in adsorbed phase, expressed as mass of sorbant adsorbed on the solids per unit bulk dry mass of the soil.

For steady water flow, θ, v and D_s can be taken as constant (*Hillel,* 1980), and the above equation simplifies to (*Selim,* 1992):

$$\frac{\partial C}{\partial t} + \frac{\rho}{\theta}\frac{\partial S}{\partial t} = -\left\{-D_s\frac{\partial^2 C}{\partial z^2} + v\,\frac{\partial C}{\partial z}\right\} \mp \frac{\varphi(z,t)}{\theta} \qquad (2.14)$$

Eq. 2.14 is the historical representation of miscible displacement theory, usually called the convection - dispersion equation **(CDE).**

2.2.2 Modelling approaches for solute transport in soils

Recent years have seen a variety of approaches to describing solute transport in soils. A number of models have been proposed, varying widely in their conceptual approach and degree of complexity. *Addiscott & Wagenet (*1985*)* classified the models for solute transport in soil within this framework :

I. Deterministic models

A- *Mechanistic models*

1- Analytical

2- Numerical

B- *Functional models.*

1- Partially analytical

2- Layer and other simple approach

II. Stochastic models

The key distinction is between *deterministic* models, where individual processes and the interactions between those processes are defined mathematically, with each set of input data leading to a unique and reproducible prediction, and *stochastic* models, which place less emphasis on processes and more on predicting the statistical distribution or probability of a given characteristic (*Tanji*, 1990). These last models are particularly useful for field studies where the soil properties vary spatially, so that solute and water movement also vary (*Addiscott* & *Wagenet*, 1985).

With deterministic models the main distinction is between *mechanistic* models and *functional* models. These two types will be discussed in turn below.

2.2.2.1 Mechanistic models

Mechanistic is taken here to imply that the model incorporates the most fundamental mechanisms of the process. For solute transport, this implies the use of equations derived from Darcy's equation for water flow and the expression of resulting solute transport as a combination of mass flow and diffusion - dispersion (referred to as the convection - dispersion equation, CDE).This is achieved formally in the following way.

- **Transient water flow equation**

One-dimensional water flow in unsaturated soil is given by one of Richards' equations (*Jury,* 1991):

$$\frac{\partial \theta}{\partial t} = \frac{\partial}{\partial z}\left[K(\theta)\frac{\partial h}{\partial z}\right] + W_s\,(z,t) \qquad (2.15)$$

which is termed the water content form of Richards' equation,

or

$$C_w(h)\frac{\partial h}{\partial t} = \frac{\partial}{\partial z}\left[K(h)\frac{\partial h}{\partial z}\right] + W_s\,(z,t) \qquad (2.16)$$

which is termed the matric potential form of Richards' equation.

where :

z = depth

K = hydraulic conductivity [L T^{-1}]

h = hydraulic potential [L]

$C_w(h) = \frac{\partial \theta}{\partial h}$ = water capacity or the slope of soil water retention curve [L^{-1}]

$W_S\,(z,t)$ = water sink or source [$L^3\,L^{-3}\,T^{-1}$]

t = time.

t = time.

- **CDE equation :**

Recalling Eq. 2.13 for unsteady water flow

$$\frac{\partial(\theta C)}{\partial t} + \frac{\partial(\rho S)}{\partial t} = -\left\{-\left[\theta D_s(\theta, v)\right]\frac{\partial^2 C}{\partial z^2} + v\,\theta\,\frac{\partial C}{\partial z}\right\} \mp \varphi(z,t)$$

For saturated, steady flow conditions, these equations are replaced by Eq. 2.14. This equation is soluble analytically for particular initial and boundary conditions (reviewed by e.g. *van Genuchten & Cleary*, 1979), and numerically using finite difference or finite element methods. However, because of the conditions attached to the analytical models, their practical use is greatly limited.

2.2.2.2 Functional models

The second type of deterministic model are functional models. Such models incorporate simplified treatments of solute and water flow and make no claim to fundamentalism. Apart from being mathematically very simple, functional models have the advantage that their requirements for input data are modest. There are two main types of such models:

(i) *Partially analytical models :*

In these models the position of the solute peak is computed by ignoring the effects of dispersion and diffusion (*piston flow*). The computed effects of these factors are then imposed around this peak (e.g. *Rose et al.*, 1982).

(ii) *Layer models:*

In these models the incoming water and salts are assumed to mix with water and salts already present in the layer. If the new water content of the layer exceeds field capacity, the surplus water and the salts it contains are

transferred to the next layer where the process is repeated (e.g. the model of *Burns,* 1974).

Additionally, it is useful to distinguish between models that are primary research tools, developed to aid the testing of hypotheses and exposure of areas of incomplete understanding, and those that are mainly useful as guides to the management of agricultural resources. This distinction again tends to parallel the separation of the models into mechanistic and functional categories (*Addiscott & Wagenet*, 1985) with relatively more complicated mechanistic models serving primarily as research tools, and the less demanding (in terms of input and execution) functional models serving as more widely used management guides.

2.3 Solute transport in structured soils

Soil structure can greatly influence the characteristics of the transport process (*Jury*, 1990). The BTCs of structured soils show an early breakthrough and a long tailing. This part will study the theory and the modelling approaches of solute transport in these soils. But first, what is soil structure?

2.3.1 Soil structure

Soils are commonly described as a three-phase system, composed of solid, liquid, and gaseous phases.

The solids consist mainly of mineral particles; however, these minerals do not occur as loose particles, but are bound together as aggregates (or peds). The arrangement of aggregates and associated pore spaces located between them is known as " *soil structure* " (*Marshall & Holmes*, 1988). This varies from the single-grain structure of sandy soils, in which each particle is separate, through those with well-formed aggregates to those that are compact

and massive. Well structured soils are soils which have durable peds that adhere weakly to one another and consequently readily separate when the soils are disturbed (*White,* 1987).

2.3.1.1 Characterisation of soil structure

The complete description of soil structure includes (*Foth,* 1990):

1) The type, which notes the shape and arrangement of peds: the four basic types are granular, platy, blocky, and prismatic.

2) The class, which indicates the ped size.

3) The grade, which indicates the distinctiveness of the peds: i.e., structureless, weakly, moderately, and strongly distinctive peds.

The sequence followed in combining the three terms to form compound names is first the grade, then the class, and finally the type. An example of soil structural description is "strong fine granular."

Soil structure, can be considered quantitatively in terms of the total porosity and of the pore size distribution of the resulting matrix (*Hillel,* 1980). Soil porosity refers to the proportion of the total soil volume occupied by pores. Porosity is represented by the ratio

$$\textit{Porosity} = \text{volume of pores / total soil volume.}$$

Pore size distribution may be determined from the moisture-tension curve (sometimes called, water release curve) that relates the amount of water in the soil in equilibrium with the tension forces applied. Using the following simplified equation, the size of pores can be calculated from the tension (τ) at which they drain (*Rowell,* 1994);

$$r = \frac{0.15}{\tau}$$

where, r is the pore radius in metres, and (τ) is the tension in pascals.

2.3.1.2 Pore sizes and functions

Greenland (1979) found that clay particles exist in domains up to 5 μm diameter with pores of 0.005- 0.1 μm between them; clusters of domains are conventionally referred as micro-aggregates which are themselves clustered into aggregates 1-5 mm in diameter. Most pores within the aggregates are **storage pores** or **micropores** with diameter 0.1 - 30 μm, and between the aggregates are **transmission pores** or **macropores** with diameters 30-500 μm. However, there is normally no sharp break in size distribution of pores in a soil and the choice of lower size limit for macropores is arbitrary (*White*, 1985). Summarising the literature, *Beven & Germann* (1982) reported the use of the term macropore to describe pores from > 30 to > 3000 μm.

Inter-aggregate pores are larger and straighter than the intra-aggregate pores. Large straight pores conduct water more quickly than do small curved pores (*Singer & Munns,* 1992). This arrangement helps control water movement through the soil by allowing excess water to drain away but retaining moisture in the smaller pores within aggregates (*David,* 1979). In addition to the pore sizes, pore orientation and continuity also play major roles in water movement through the soil.

2.3.1.3 Structure and hydraulic conductivity

Hydraulic conductivity values are related to textural and structural characteristics of a soil. A difference of about ten times in hydraulic conductivity values can be found between coarse granular and platy soil structure (*Landon*, 1984).

2.3.2 Bi-continuum concept

Solute transport in structured soils is, and has been, the focus of a significant research effort. Transport in such systems is often characterised by non-ideal (*White,* 1985) or non-equilibrium transport (*van Genuchten,* 1981). To model

such systems a bi-continuum (or dual porosity) approach is often used, in which the porous medium is considered to comprise two "regions" :

-Mobile water region, where solute transport occurs by convection and dispersion , and

-Immobile water region, where diffusion alone, or with minimal convection, occurs.

The BTCs of these systems (Fig. 2.2) are characterised by "*early*" initial breakthrough and by "*tailing*" or delayed approach to a steady-state relative concentration.

The explanation of this using bi-continuum theory is that in these systems rapid transport in the mobile domain occurs causing the early breakthrough. This is accompanied by a slower, diffusive, transfer of solutes between the mobile and immobile domains which results in the latter behaving as sink / source components and causing tailing (*Passioura,* 1971; *Davidson et al.,* 1980; *Lafolie & Hayot,* 1993).

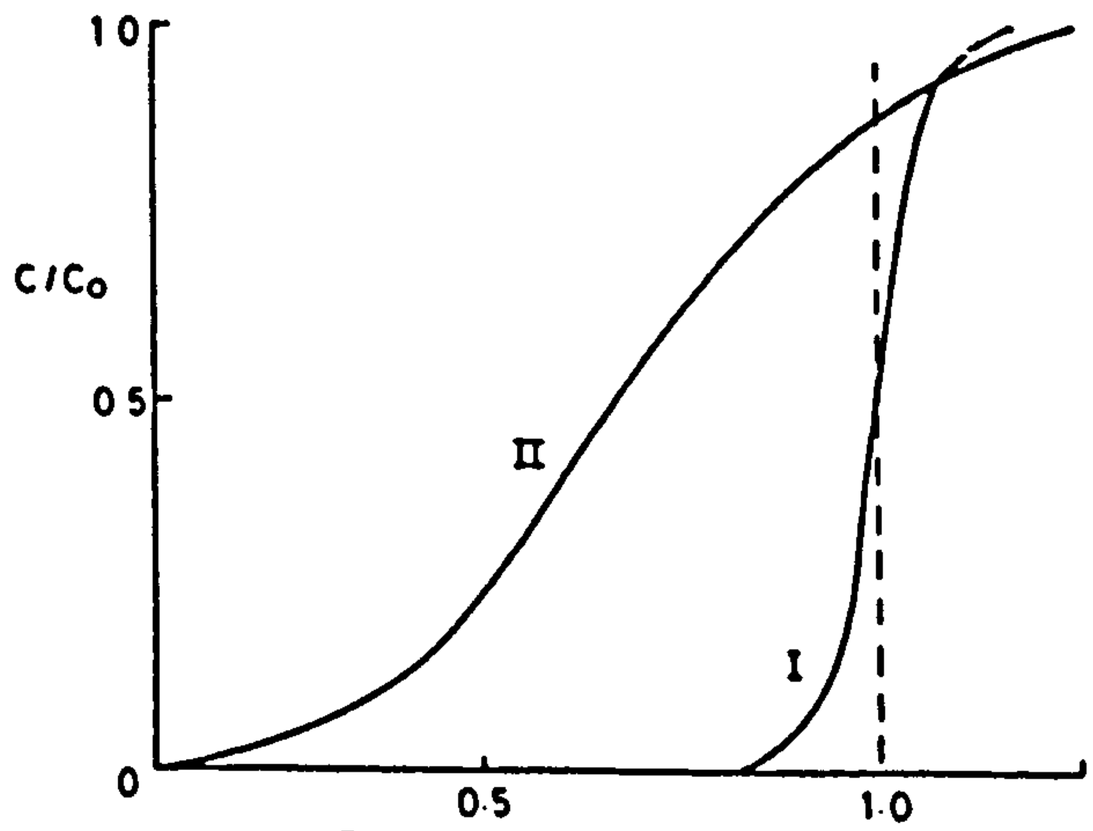

Fig. 2.2: BTC for I- ideal miscible displacement
II- displacement in bi-continuum systems (after *White*, 1985)

This behaviour has been observed in

A)- ***Aggregated soil*** : A bi-modal pore size distribution exists, with macropores between the aggregates as a region of mobile water and micropores within the aggregates as region of immobile water (Fig. 2.3). Flow and mixing of the solute is dominated by the larger pores, while the pores within the aggregates act as a sink or source. In such soils the solute will be transported through the inter-aggregate (mobile water) volume by convection and hydrodynamic dispersion while it will transport through intra-aggregate (immobile water) volume by diffusion alone (*Rose,* 1973*; van Genuchten & Wierenga,* 1976; *De Smedt & Wierenga,* 1979*; Rao et al.,* 1980b*; Tillman et al.,* 1991*).*

Biggar & Nielsen (1962) used three aggregate sizes of Aiken clay loam for chloride and tritium movement under saturated conditions. Tailing increased with an increase in aggregate size. An increase in the proportion of "immobile" water with an increase in aggregate size was suggested as the cause. In the larger aggregates the increase in "immobile" water in the intra-aggregate pores caused diffusion pathways to become longer and thus more tailing.

This approach, as reported by *Wagenet* (1983), is not limited to strongly aggregated media as almost any soil can be envisaged to consist of relatively mobile and immobile water phases.

B)- ***Unsaturated flow*** : here the larger pores are mostly filled with air, leaving only small water films on pore walls. This water has been identified as dead (*Coats & Smith*, 1964), stagnant (*Gaudet et al.,* 1977) or immobile water (*De Smedt & Wierenga,* 1979). A decrease in water content increases the proportion of the air-filled macropores of the mobile region, resulting in the creation of additional dead-end pores (immobile water regions). In unsaturated sand columns *Gaudet et al.* (1977) found as much as 40% of all water was immobile at a water content of 0.20 cm^3/cm^3. *De Smedt & Wierenga* (1979)

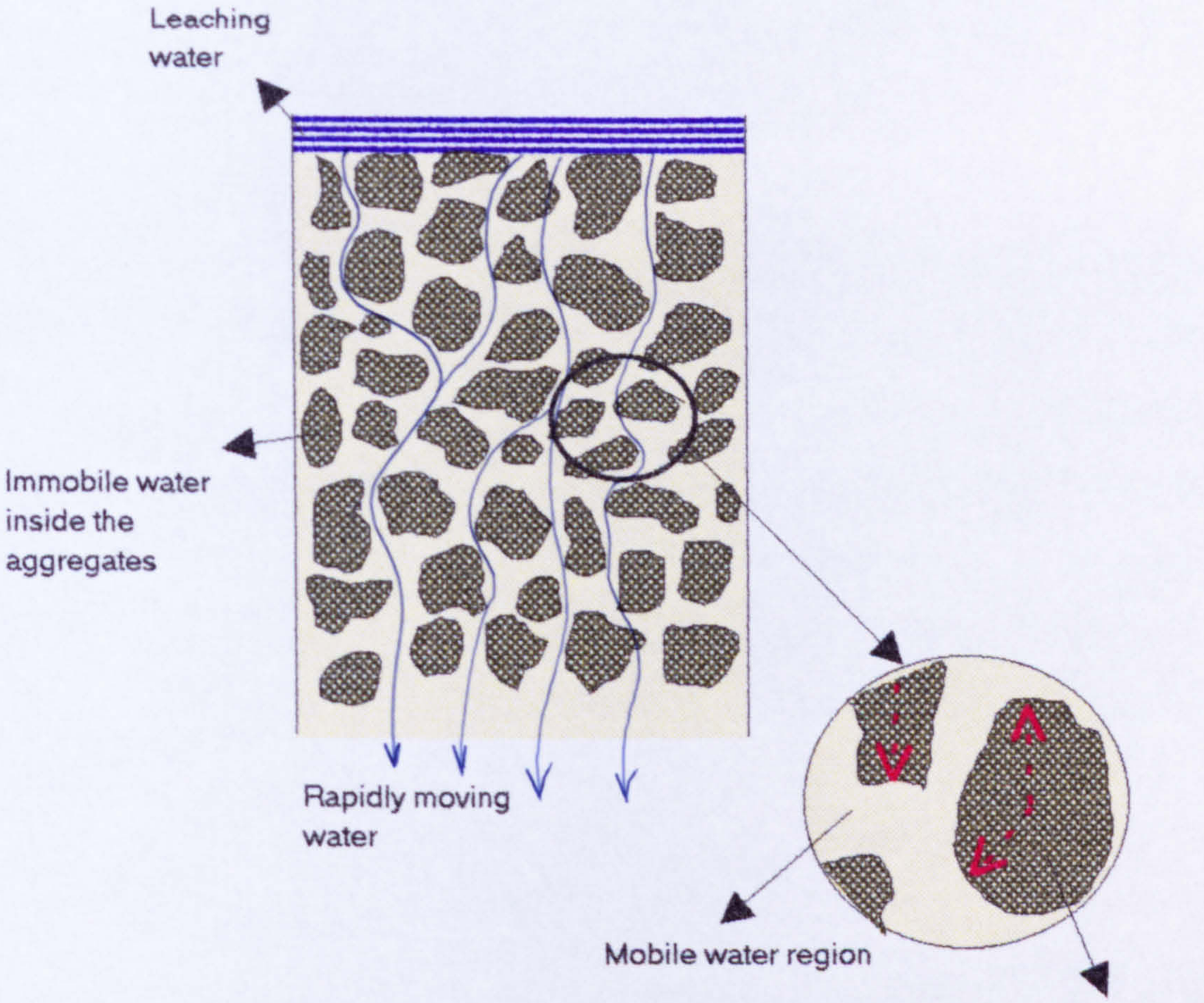

***Fig. 2.3*: Schematic section through a column of aggregated material.**

found that about 16% of all water became immobile when the water content of glass beads columns decreased from 0.367 to 0.276 cm^3/cm^3. *Nielsen & Biggar* (1961) observed increases in tailing with decreasing water content at approximately the same flow velocity.

The bi-continuum concept may also be applied to ***heterogeneous porous media,*** such as aquifers consisting of laminae having different hydraulic conductivities (K). In such cases , the greater K layer(s) correspond(s) to mobile water zones and the low K layer(s) to the immobile water zones (*Gillham et al., 1984*). Transport in ***fractured media*** can also be modelled with a bi-continuum approach. The fractures serve as a mobile water zones, while the inter - fracture matrix act as a diffusion sink/source (*Huyakorn & Pinder, 1983*).

2.3.3 Salt leaching in structured soils

Few papers refer explicitly to salt leaching in structured soils. *White* (1985) produced a comprehensive study about the influence of macropores on the transport of solute through soil. He suggested that further studies were required and found that the amount of salt leached depends on :

1) location of solute

2) the ratio of mobile flow to immobile flow

3) the saturated hydraulic conductivity (K_{sat}) of the soil matrix

4) the antecedent water content of the soil

5) the contact area between the bypass flow and the relatively immobile water of soil matrix ; and

6) the rate of solute diffusion between the mobile and immobile water volumes.

2.3.3.1 Modelling approach

Modelling of solute leaching in structured soils can be treated by simple functional models as well as by mechanistic models.

• *Functional models:*

Addiscott (1977) developed a layer model in which the water in each layer is divided into mobile and immobile phases on the basis of the soil moisture characteristic with division between the phases at a suction of 2 bar (equivalent to a pore size of 0.75 μm). Rainfall causes *piston flow* in the mobile phase during which solute may move just from one layer to the next or, if the fall is large, through several layers. When such piston flow ceases , solute movement between the phases occurs to equalise the concentrations in the soil water between phases. This model was used to simulate the leaching of chloride from Rothamsted drain gauges under an irregular rainfall pattern (*Addiscott et al.,* 1978). Recently the model has been developed so that the pore volume available for mobile water is partitioned to allow for flow through smaller water-filled pores and rapid preferential flow through larger macropores and fissures (*Hall,* 1993).

• *Mechanistic models:*

It has been found that the classical convection-dispersion equation (CDE) (Eq. 2.14) is not sufficient to explain solute transport through such soils (*Biggar & Nielsen,* 1962; *van Genuchten & Wierenga,* 1976; *Dahyia et al.*, 1984).

Several attempts have been made to account for the observed "tailing" in BTCs. The resulting equations which describe the movement of non-interacting solute in such a porous medium, were presented by *Coats & Smith* (1964). The system consists of a classical CDE for the mobile zone, coupled with a term

which describes the sidewards movement of solute in and out the immobile zone:

$$\theta_m \frac{\partial C_m}{\partial t} = \theta_m D_s \frac{\partial^2 C_m}{\partial z^2} - v_d \frac{\partial C_m}{\partial z} - \theta_{im} \frac{\partial C_{im}}{\partial t} \qquad (2.17)$$

where:

z = vertical distance, positive downwards

C_m = solute concentration within the inter-aggregate "mobile water region"

C_{im} = solute concentration within the intra-aggregate "immobile water region"

D_s = hydrodynamic dispersion coefficient for "mobile water "

v_d = Darcy velocity, which is equal to the flux q divided by the column cross-sectional area A, i.e.,

$$v_d = \frac{q}{A}$$

θ_m = ratio of volume of mobile water to total column volume

θ_{im} = ratio of volume of immobile water to total column volume.

Modelling of solute transfer between mobile and immobile water regions:

Solute transfer between the mobile and immobile water regions can be modelled either *explicitly* (mechanistic or functional) or *implicitly* (*Brusseau & Rao,* 1990):

A) - Explicitly:

(i) mechanistic diffusion models : by using Fick's equation to describe the physical mechanism of diffusion transfer (e.g., *Rao et al.,* 1980a; *Huyakorn,* 1983).

For example, for a single sphere the diffusion equation is:

$$\frac{\partial C_{im}(r,t)}{\partial t} = D_e(\theta)\frac{\partial^2 C_{im}(r,t)}{\partial r^2} \qquad (2.18)$$

where:

r = radial distance co-ordinate.

(ii) functional diffusion models: by using an *empirical* first-order mass-transfer expression *(van Genuchten & Wierenga,* 1976*)*

$$\theta_{im}\frac{\partial \overline{C}_{im}}{\partial t} = \alpha\left(C_m - \overline{C}_{im}\right) \qquad (2.19)$$

where:

$\overline{C}_{im}$ = average solute concentration within the immobile water region,

α = mass transfer rate coefficient between the mobile and immobile water region.

B) - Implicitly

This uses an effective or lumped dispersion coefficient that includes the effects of sink or source diffusion ,as well as hydrodynamic dispersion and axial diffusion (*Passioura,* 1971; *Passioura & Rose,* 1971). In this model the pore water is also divided into two regions. However, rather than an explicit description of solute transfer between each *Passioura* (1971) lumped the effect of the sink/source term into the dispersion coefficient. This lumped parameter replaces the usual hydrodynamic dispersion coefficient in the convection - dispersion transport equation for a limiting condition but gives an explicit and experimentally verified analytic expression for the dispersion coefficient. The limiting condition is that,

$$\frac{(1-\Phi)\,D_e\,L}{a^2\,v_o} > 0.3$$

where:

Φ = fraction of total water existing within inter-aggregate region

L = column length

v_o = average pore water velocity on the basis of total volumetric water content ($v_o = \frac{v_d}{\theta}$)

a = aggregate radius.

This model was later developed by *van Genuchten & Dalton* (1986) for sorbed solute.

Mechanistic diffusion models are not usually attempted because the solution processes can be too complicated. The first-order mass transfer model is usually preferred because it provides a good approximation of physical diffusion , and is simpler to use (*Lafolie & Hayot,* 1993). This was concluded also by *Rao et al.* (1980b) who related their models for these kinds of transfer to saturated flow in columns. They obtained good agreement between the measured and calculated BTCs for all pore-water velocities, with the functional model giving better agreement with measured results at low pore-water velocities than the mechanistic model. They concluded that functional diffusion model, which does not require an explicit conceptual "geometric" description of porous medium, may be of more immediate practical use.

2.4 Salt leaching in practice

So far this review has been concerned with the theory and mathematics of solute transport in soils. In this part the practical side of leaching will be reviewed with particular concern to the potential advantage gained by use of the intermittent leaching method.

Leaching is the usual way to reclaim salt-affected soils. Salt leaching involves the dissolution of soluble salts in the soil, the passage of the resulting solution through soil profiles, and the consequent removal of salt from the root

zone. The efficiency of salt leaching can be defined as the quantity of soluble salts leached per unit volume of water applied (*Tanji*, 1990).

Salt leaching has been carried out in the fields by different methods. Table 2.2 summarises the leaching effectiveness of the most common irrigation methods. With micro-irrigation systems, salts move away from each emitter and accumulate at the outer fringes of the soil mass wetted by the emitter. For long-term use they may create a large, irregular zone of salt accumulation (*Tanji*, 1990) which may restrict the use of the land. A sprinkling irrigation system has the advantage of uniformly distributing water over the surface of the soil but is not usually attempted under high evaporative conditions. Continuous ponding of water on the soil surface is the traditional method of leaching and is used extensively in surface-irrigated areas (*Tanji*, 1990). This method is cheaper than other methods, but is less efficient. However, several experiments have showed that by applying the leaching water intermittently the leaching efficiency was increased (*Oster et al.*, 1972; *Dahyia et al.*, 1981; *Meiri & Plaut*, 1985). The principle of intermittent leaching and the main factors affecting its efficiency will be discussed in detail next.

2.4.1 Intermittent and continuous leaching

Several studies have examined leaching methods. One of the first experiments was conducted by *Miller et al.* (1965) to observe chloride displacement in Panoche clay loam. They used three different water treatments: (i) the soil surface continuously ponded with water, (ii) the soil surface intermittently ponded with repeated applications of 15 cm of water and (iii) the soil surface intermittently ponded with repeated applications of 5 cm of water. The intermittent applications were made when the soil water pressure head at 30 cm soil depth reached a value of -150 cm. Of these three treatments, intermittent ponding of the soil with 5 cm increments of water was markedly more efficient

Water application method (1)	Application (2)	Pattern of salt accumulation (3)	Leaching effectiveness (4)	Special considerations (5)
Furrow	Row crops, low to medium infiltration-rate soils.	High in ridges between furrows, may increase in direction of slope if irrigations are nonuniform.	Effective leaching beneath furrow channels, salt left in ridges. Leaching requires more water than for methods with lighter, intermittent applications.	None
Corrugation	Close-growing crops.	Leaves saltier strips between corrugation channels unless entire field surface inundated.	Similar to furrows, above.	None
Border dike	Close-growing crops.	Leaves salt in dikes that separate borders.	Areas between dikes leached uniformly, but more water required than for light, intermittent applications.	None
Sprinkler: set	Most crops, all but very fine-textured soils.	No salt concentrations in root zone, if system designed and managed properly.	Uniform leaching. Can be used to leach salt accumulations left by other irrigation methods.	May encourage disease in sensitive crops, e.g., beans. Salty irrigation water may leave harmful deposits on leaves.
Sprinkler: Mobile	Most crops, except trees, vines. Can be used to irrigate fields on rolling topography.	No salt concentrations in root zone, if system designed and managed well.	Uniform leaching. Same as for set sprinklers.	None
Micro irrigation (drip, trickle, sub-irrigation)	Because of high initial costs, used mostly for high value crops or crops with high irrigation labor costs.	Salt concentrates at outer fringes of the soil mass wetted by each emitter.	Soil mass wetted by each emitter is well-leached. Difficult to leach all soil to depth of root zone.	When automated for light, frequent irrigations, saline water can be used, because low matric stress compensates for osmotic stress.

Table 2.2: Leaching effectiveness of irrigation methods (adopted from *Tanji*, 1990)

in leaching the applied chloride from the profile. In fact, such intermittent ponding produced results comparable with continuous ponding of 90 cm after only a total of 50 cm of water. A saving of one-third of the quantity of water to obtain the same leaching represents a significant reduction in water use. *Dahyia et al.* (1981) cited that "leaching intermittently allows more time for movement of water through the small pores and will improve the leaching efficiency . Also intermittent irrigation may give time for solute to diffuse from less mobile to mobile water in between applications". They concluded that leaching efficiency was considerably higher with intermittent than with continuous ponding.

Furthermore, as the water content decreases, the proportion of water moving in the large pores decreases (*Dahyia et al.,* 1981). With increasing macropore flow the effectiveness of solute removal decreases because a decreasing proportion of flow occurs through micropores (*Oster et al.,* 1972; *Hoffman,* 1980). The leaching experiments of *Nielsen et al.* (1965) indicated that intermittent leaching caused the soil profile to develop a lower water content than continuous and sprinkling leaching. Continuous ponding increased the water content of the soil profile up to almost the saturation content, whereas sprinkling resulted in water contents 0.01 to 0.03 cm^3/cm^3 less than the continuous ponding and intermittent leaching in water contents of $\approx$ 0.07 cm^3/cm^3 lower (Fig. 2.4). Thus intermittent leaching does not just give more time for solutes to diffuse out of immobile regions between applications, but also improves the leaching efficiency by decreasing the proportion of flow in large pores.

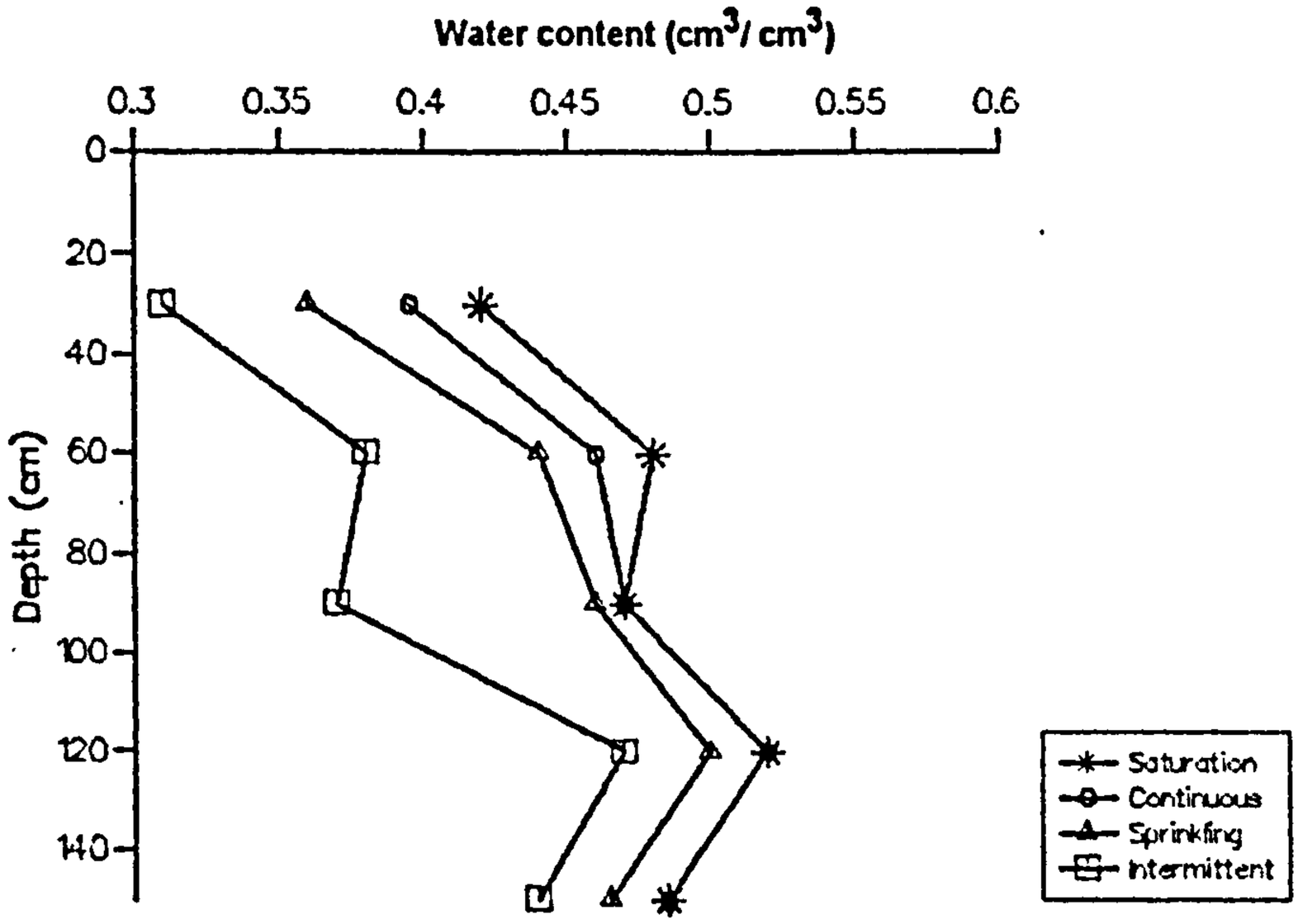

Fig. 2.4: Soil water content profiles developed under steady state flow conditions for three different application, continuously ponding, continuously sprinkling, and 150 cm of intermittently ponding (15 cm applications) (data from *Nielsen et al.*, 1965)

By contrast, *Cameron* (1982) found no significant difference between 80 mm irrigation and 71 mm intermittent net rainfall for silty clay loam soil. Similar results found by *Verma* and *Gupta* (1989). They attributed that to the low hydraulic conductivity of the clay soil which allowed ample time for diffusion even under continuous ponding.

However; as *Kutilek & Nielsen* (1994) stated, different results will no doubt be obtained for different soils, solutes and local conditions. It appears that several various factors are involved and need to be taken into account (*Minhas & Khosla*, 1986).

2.4.2 Factors affecting intermittent leaching

Five important factors affecting intermittent leaching can be deduced from the literature. There are discussed in turn.

2.4.2.1. Effect of evaporation rate

The beneficial effects of intermittent water application in terms of quantity of water required for leaching may be limited to conditions of low evaporativity. When leaching is attempted under high atmospheric evaporativity, the salts which are leached to shallow depths move again towards the surface during each rest period. Also, as a fraction of the subsequently added water increments during intermittent ponding is retained in the upper soil layers to replace the water lost by the evaporation, the quantity of water actually available for salt displacement to lower depth is decreased. *Minhas & Khosla* (1986) found no difference in leaching of chloride when the same amount of water was applied continuously or intermittently (with 10-day intervals between applications) during the periods of high (7.74 mm/day) and medium (4.51 mm/day) evaporation rates. However, when evaporation at the surface remained low (1.52 mm/day), distinctly more chloride was removed from the soil and the salt load was displaced deeper under intermittent as compared to continuous ponding. Using mulches with intermittent leaching decreases the evaporation from soil surface and improves the leaching efficiency. *Carter & Fanning* (1964) demonstrated that combining intermittent ponding with mulching greatly improved the performance over a period of five months. It can be deduced that the greatest efficiency of intermittent leaching is when it is conducted under the lowest evaporation rate environment. Under these conditions the least water will be lost during rest periods.

2.4.2.2 Effect of plot size

The study of the desalinisation of salt-affected soil in plots of different sizes by *Dahyia et al.* (1984) showed that poor levelling of the large plots (6 X 6 m) resulted in water concentrating in localised small depressions randomly distributed in the plots during the rest periods of intermittent leaching. During continuous leaching water was continuously standing over the whole soil

surface. The uniformly distributed water was more effective in leaching salts and the leaching efficiency for large plots was better under continuous than intermittent ponding. However, in the smallest plots (2 x 2 m), the leaching efficiency was significantly greater with intermittent than with continuous ponding, since better levelling was achieved.

2.4.2.3 Effect of soil hydraulic conductivity

A low hydraulic conductivity of the soil will allow ample time for solute to diffuse out of the soil aggregates even under continuous ponding and the solution within the aggregates will be nearer equilibrium with the leaching water (depending on, in addition to the time, effective diffusion coefficient and aggregate size). This will reduce the advantage of using intermittent ponding since this is the main reason for relatively high intermittent leaching efficiency. *Verma & Gupta* (1989) found only a marginal decrease in soil salinity with intermittent application compared with continuous leaching. They attributed this to the low hydraulic conductivity of their clayey soil.

2.4.2.4 Effect of crop

Crops may play three roles;

(i) Changing soil water permeability

Root development may open up channels and improve aggregation in the surface and subsoil, thereby increasing permeability (*Kovda et al.* 1973) and thus increasing the relative advantage using intermittent leaching. *Kanchanasut & Scotter* (1982) came to a similar conclusion when they leached bromide from soil under pasture. They found that rainfall leached bromide more efficiently than did ponded water.

(ii) Reducing soil surface evaporation

Crops also shade the soil and reduce soil evaporation which in turn reduces water loss and the accumulation of salts on the surface (*Kovda et*

al. 1973) albeit that the transpirational losses will result in an increased water movement up to the root zone.

(iii) Removing part of the salts

Another possible advantage of leaching during cropping may be that the crop will remove part of the salt content (*Minhas & Khosla*, 1986). At intermediate levels of salinity, *Chapman* (1966) reported that the salt content of alfalfa, maize, and sorghum was about 3% of the dry tissue mass.

2.4.2.5 Effect of sodicity

Leaching of highly saline-sodic soils with low soil permeability is best accomplished when coupled with the addition of soluble calcium salts (e.g., gypsum) to replace the exchangeable sodium (Na^+) . *Abrol & Bhumbla* (1973) found for high saline-sodic soil, with Na^+ dominating the exchange and solution phase that, without using gypsum, intermittent ponding had no particular advantage over continuous ponding. They ascribed this to the low permeability of sodic soils. When gypsum was added, the leaching efficiency improved, but there was no particular advantage gained from intermittent ponding. They suggested that this was because the surface layer in these soils remained limiting to water penetration even after the addition of gypsum. However, with greater soil permeability, the benefit of using intermittent leaching was increased as found by *Dahiya et al.* (1981). They found that for highly saline-sodic, moderately permeable soil, with Na^+, Ca^{2+}, and Mg^{2+} being the dominant cations, there was no need to apply any amendment (like gypsum) in reclamation, and that leaching efficiency was considerably higher with intermittent than with continuous ponding.

2.4.3 Management advantage of Intermittent leaching

Other advantages may result from leaching intermittently. The farmer may be able to leach by ponding intermittently without major revision of the existing field layout. Pre-irrigating a soil each season before a crop is planted provides a source of water for the emerging crop and also reduces the salinity of the topsoil. It is not uncommon to pre-irrigate Panoche soils with 30 cm of water before planting. If water continuously were ponded on the soil surface until 30 cm entered the profile *Miller et al.* (1965) found a major part of the chloride originally at the surface would collect in the upper 60 cm, with a maximum concentration occurring at 30 cm depth. A strikingly different distribution is obtained by leaching with the same total amount of water in 5-cm increments. Not only did most of the chloride collect below 60 cm, but the topsoil from which the seedlings emerged had a chloride concentration 4 times less than the topsoil under the ponded condition. *Oster et al.* (1972) showed in their study that salinity can be maintained at low levels by several large irrigations prior to planting the crop instead of by conventional leaching with long periods of continuous ponding.

2.5 Proposed programme of the study

From Section 2.4.1, it is clear that intermittent leaching (IL) has the potential to increase the leaching efficiency in terms of saving leaching water. However, many of the variables affecting this efficiency are still not well defined, and the extent of their influence is not fully understood. The main variables which may still need more investigation are: the soil aggregate size and aggregate size distribution, the interstitial water velocities, the duration of water application periods, the duration of rest periods between the applications, the adsorption/desorption properties of the solute, and the soil water content. No model has been found in the literature which is able to simulate solute transport

under such intermittent conditions. This study attempts to fill this gap and produce a model which can be used to simulate and optimise leaching using intermittent applications of water.

The investigation starts using a bi-continuum medium (Section 2.3.2) created by packing porous ceramic spheres in cylindrical columns. This medium is a simple analogue of aggregated soils with the ceramic spheres acting as aggregates (Section 3.1 and 3.2). Using such ceramic spheres (which are physically and chemically inert) as a start has the advantage of removing any confounding effects of the swelling, shrinkage, and dispersion of soil aggregates or of solute adsorption/desorption on the clay surfaces. The investigation includes leaching under continuously saturated conditions (Chapter three) and a situation where the interstitial pore spaces drain during the *off* time ("drained" conditions) (Chapter eleven).

After establishing the advantage of IL for leaching ceramic spheres, the study becomes more realistic by using soil aggregates (Chapter eight). These were chosen to be physically inert (with little swelling and no clay dispersion) but chemically reactive (with solute adsorption and desorption). The effect of adsorption/desorption is studied by simultaneously tracing two ions during leaching, potassium and bromide. These were continuously monitored using two ion-selective electrodes (ISE) connected to a computer *via* a data logger.

2.5.1 Leaching under saturated conditions

IL will be described by several cycles, each cycle consisting of two periods:

A)- water application period: during this period the water is continuously ponded on the column surface. The column is saturated and the flow is steady. This is a case of miscible displacement. Therefore this period will be called the displacement period or, briefly, "*On time*" ;

B)- rest period : this period follows the water application period. During this period the column is saturated but the flow is stopped for a predetermined time. No convective transport will occur and the solute transfers only by diffusion from the immobile region within the spheres or aggregates to the mobile region between them. Therefore this period will be called the diffusion period or, briefly, "*Off time*".

The effect of sphere diameter, interstitial velocities, the *On* time, and the *Off* time, were investigated separately. A model was developed to simulate the results and to produce a group of graphs relating these parameters together.

2.5.2 Leaching under drained conditions

Section (2.4.1) showed that, as the water content decreases, the effectiveness of solute removal improves due to the decreasing proportion of flow occurring through macropores. This gives an idea about what is happening during the infiltration of the leaching water. However, it is not clear what is happening during the rest periods when no (or minimum) flow occurs. The amount of solute diffusing out of the spheres will be decreased because there is less water in the mobile water regions around the spheres. The study will tackle this by applying different meanings for *on/off* cycles. The saturated columns will be drained at the end of the *on* time and remain like this during the whole *off* time. In this case the mobile water region will be almost empty during this diffusion period.

The thesis has been divided into three main parts. The first part will study solute transport through columns of saturated porous ceramic spheres. The second will study solute transport through columns of saturated soil aggregates. The last part will consider solute transport through columns of porous spheres when drained during the *off* times.

PART ONE

Solute transport through columns of ceramic spheres under saturated condition

Chapter Three

Experimental work

The experimental work was divided into four main experiments: for each, the aim, material and method, and the results are discussed. The experiments were:

1) Accessory experiments

2) Diffusion from porous ceramic spheres

3) Continuous leaching experiments

4) Intermittent leaching experiments.

3.1 Accessory experiments

3.1.1 Aim of the experiments

These experiments were designed to measure some independent physical and chemical properties of the porous media for use in the later models.

The porous medium used was created by packing porous ceramic spheres (D99 balls, Denston Inert Support Products; *NORTON* [1] *Chemical Process Products Corporation*), composed mainly of Al_2O_3 (99%) (see Appendix F). Spheres of three sizes were used, 3, 6, or 13 mm diameter respectively.

3.1.2 Particle density

The standard procedure described by *Avery & Bascomb* (1982) was used to

[1] *NORTON* Chemical Process Products Corporation. P.O. Box 350, Arkon, OH 44309-0350.

determine average particle density of the ceramic spheres by displacement of water in specific gravity bottles. The average particle density was found to be $\rho_p = 3.97 \pm 0.01$ g cm^{-3} , for the three sizes of the spheres, which is in the range quoted in *International Critical Tables* (1927) for Al_2O_3 materials (3.93 - 4.00 g cm^{-3}).

3.1.3 Porosity of the ceramic porous spheres

The ceramic spheres were washed, cleaned and oven dried, and then saturated under vacuum with de-aired distilled water. They were then removed from the water, wiped clean of surplus surface water, weighed (W_{ws}) and oven dried for 24 h and weighed again (W_s). The spheres were assumed to be initially saturated and the volume of pores within the spheres was assumed to be equal to the water content (V_{ws}). The sphere porosity was calculated as follows:

$V_{ws} = (W_{ws} - W_s)/\rho_w$ (the water density at experiment temperature (20° C) is ρ_w = 0.998 g cm^{-3}),

volume of the dry solid matrix (V_d)

$V_d = W_s / \rho_p$.

Therefore volume of the spheres (V_s) is given by:

$V_s = V_{ws} + V_d$,

and sphere porosity (θ_{sp}) by:

$$\theta_{sp} = \frac{V_{ws}}{V_s} .$$

The average sphere porosity was 0.45 ± 0.02 cm^{3}cm^{-3} with no difference between the three sizes of spheres.

3.2 Diffusion from porous ceramic spheres experiment

3.2.1 Material and method

The experiments were aimed to determine the effective diffusion coefficient of a non adsorbed solute (KCl) through the porous ceramic spheres. This involved

experimental observation of diffusion out of the spheres (reported here) and development of a mathematical model describing the diffusion process (reported in Section 4.1). The effective diffusion coefficient could then be determined by optimisation (Section 5.1).

The ceramic spheres were first washed, cleaned and oven dried. They were then saturated under vacuum with de-aired distilled water and left immersed overnight in excess water (to allow any possible resident solute to diffuse out), oven dried and again saturated under vacuum with de-aired solution of 7.455 g dm^{-3} KCl (0.1 M) and left immersed for at least one day.

For each diffusion experiment a known number of spheres (n_s) (Table 3.1) were removed from solution, wiped clean of surplus solution, weighed and placed on a nylon screen, and then placed inside a vessel similar to that used by *Addiscott* (1982) (Fig. 3.1).

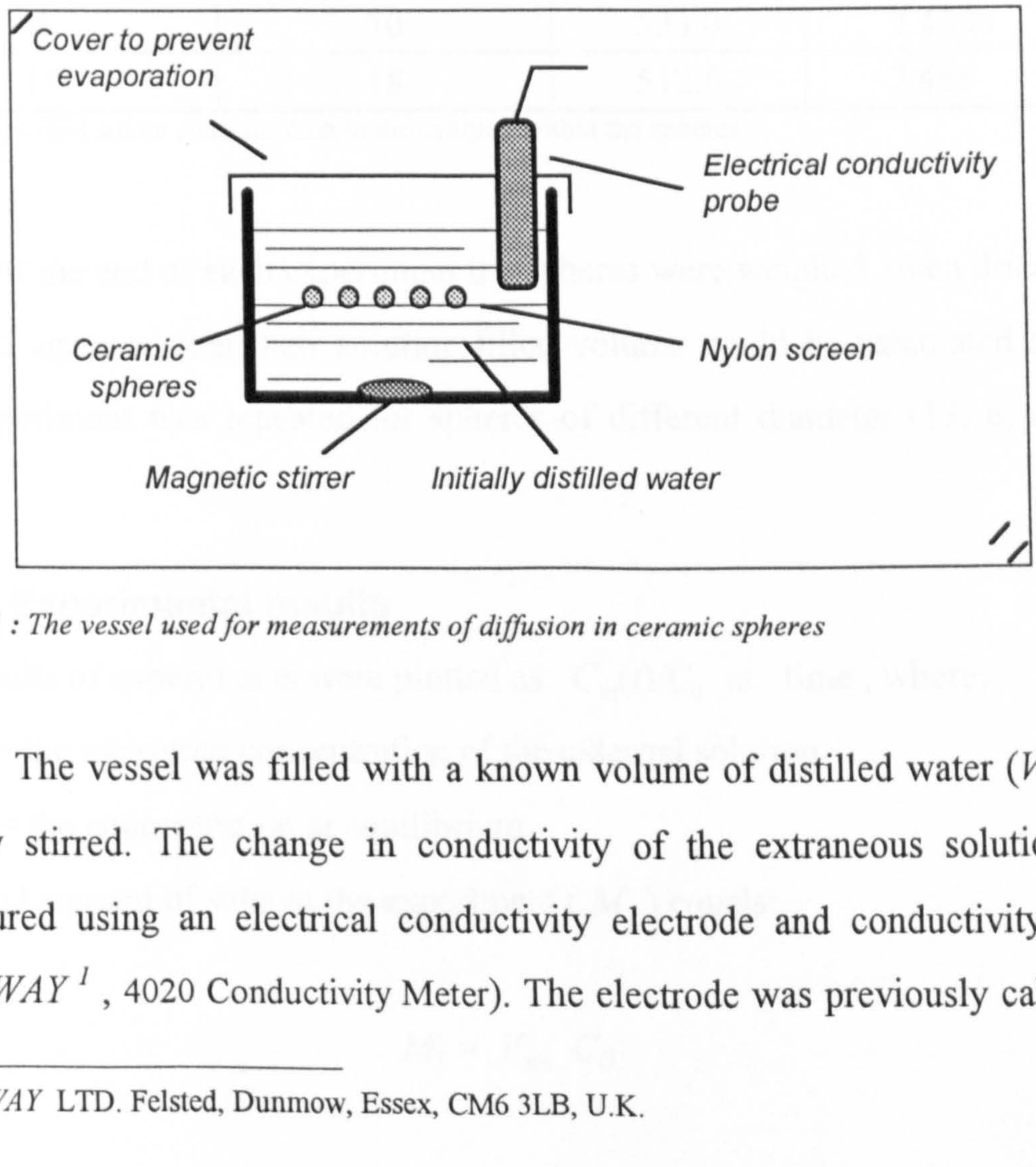

***Fig. 3.1** : The vessel used for measurements of diffusion in ceramic spheres*

The vessel was filled with a known volume of distilled water (V_e) and gently stirred. The change in conductivity of the extraneous solution was measured using an electrical conductivity electrode and conductivity meter (*JENWAY* [1], 4020 Conductivity Meter). The electrode was previously calibrated

[1] *JENWAY* LTD. Felsted, Dunmow, Essex, CM6 3LB, U.K.

against known concentrations solutions of KCl. Temperature was kept constant (20 ± 0.5°C) during the whole experiment as the molecular diffusion rate increases with temperature according to Nernst-Einsten equation for molecular diffusion coefficient at infinite dilution (i.e., sufficient dilution such that solutes ions/molecules do not interact with each other in solution):

$$D_0 = \frac{uRT}{N}$$

where R = the universal gas constant (8.134 J mol^{-1} K^{-1}), T = the absolute temperature, N = Avogadro's number (6.022 x 10^{23} mol^{-1}), and u = the absolute mobility of a particle (*Robinson & Stokes,* 1970; *Shackelford & Daniel*, 1991).

Table 3.1: Diffusion experiment conditions.

Sphere diameter (d) (mm)	**No. of spheres (n_s)**	V_e (cm^3)	C_0 * ($g\ dm^{-3}$)
3	635	524.3	7.455
6	70	523.0	7.455
13	18	512.6	7.455

* C_0 is the initial solute concentration in the solution within the spheres

At the end of each experiment the spheres were weighed, oven dried and weighed again so that their solution-filled volume could be calculated (V_{ws}). The experiment was repeated for spheres of different diameter (13, 6, and 3 mm).

3.2.2 Experimental results

The results of experiments were plotted as $C_m(t)/C_e$ *vs.* time , where;

$C_m(t)$ = the measured concentration of the external solution

C_e = the concentration at equilibrium.

The total amount of salts in the experiment (M_T) equals:

$$M_T = V_{ws}\ C_0 .$$

Thus the equilibrium concentration can be calculated from:

$$C_e = \frac{M_T}{V_e + V_{ws}} \quad .$$

Fig. 3.2 shows a plot of $C_m(t)\,/C_e$ against the diffusion time (t) for sphere diameters 3, 6, and 13 mm. An initial rapid increase in the external solution concentration (and so in $C_m(t)\,/C_e$) was observed due to the initially large solute concentration gradient between intra-spheres and external solution. This was followed by a more gradual approach to an equilibrium concentration for all spheres. However, as the smaller spheres have a shorter diffusion path, the initial gradient of the curve was higher and they reached the equilibrium much faster than the larger spheres. It took about 5, 50 and 120 min for 90% of the initial amount of solute in the spheres to diffuse out of the 3, 6 and 13 mm sphere diameters respectively. Similar shapes of the curves have also been observed by *Rao et al.* (1980a) for porous ceramic spheres and by *Addiscott* (1982) for chalk cubes.

3.3 Continuous leaching experiments

3.3.1 Aim of the experiments

These experiments were designed to investigate the leaching dynamics from a column of porous ceramic spheres by monitoring the concentration of the outflow when distilled water displaced a 0.1 M KCl solution out of the column. The experimental results would then be used to test the continuous leaching model in Section 5.2.1.

3.3.2 Materials and methods

The ceramic spheres were initially saturated with 0.1 M KCl solution as in Section 3.2.2. They were then carefully poured into 30-cm long glass cylinders (which had previously been filled with 0.1 M KCl solution) such that no air

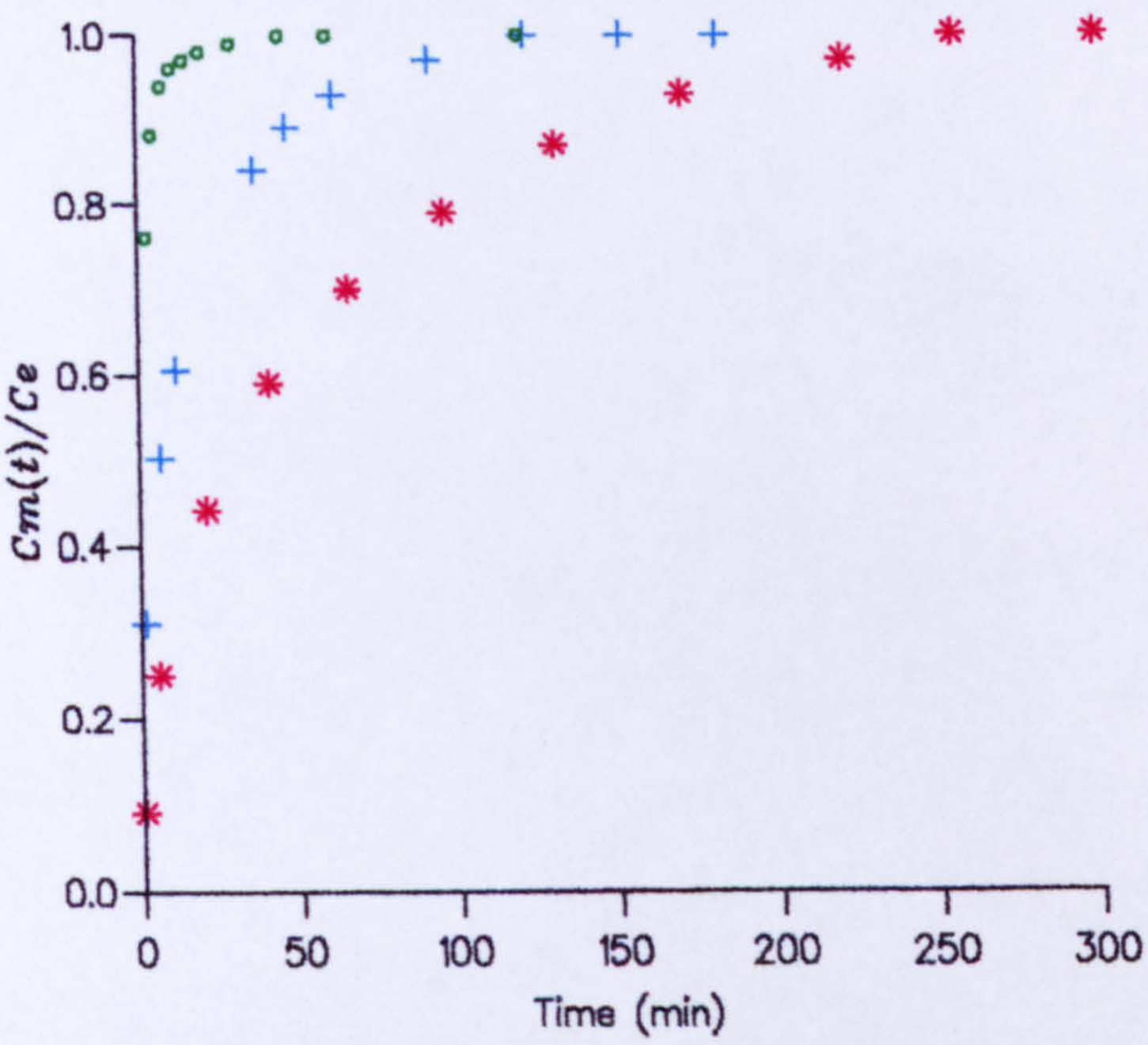

Fig. 3.2: $C_m(t)/C_e$ against diffusion time for spheres of three diameters. o, d= 3 mm; +, d = 6 mm; and *, d = 13 mm.

bubbles were trapped in the columns (Fig. 3.3). The column was subjected to vibration for 10 min to pack to a maximum density. Where a mixture of sphere diameters was used, the column was packed following the method of *McGeary* (1961). The column was first packed with the largest diameter spheres, then the smaller spheres were slowly poured in while the column was vibrated (with a weight of 250 g resting on the surface to prevent the surface rising and so eliminate or minimise volume expansion). This method gave a homogeneous and reproducible mixture.

A Mariotte bottle filled with distilled water and connected to the upper surface of the porous media, was used to provide the leaching water during the experiment.

Effluent was passed through an in-line conductivity probe (connected to a data logger *via* conductivity meter) and flux was controlled by a peristaltic pump downstream. The effluent was finally collected in a container placed on a balance for measuring the outflow mass.

When all was ready the inflow and outflow were simultaneously started and the conductivity and mass were recorded. The experiments were performed at 20±1°C. Table 3.2 shows the experimental conditions.

***Table 3.2*:** Continuous leaching experiment conditions.

	Sphere diameter (mm)	v_d (mm/min)	**Interstitial porosity** # ($cm^3\ cm^{-3}$)	L_r (mm)
Exp. 1C	13	2.31	0.486	185
Exp. 2C	13+3 *	0.96	0.320	140
Exp. 3C	6	5.47	0.404	185

* the mass proportions of sphere diameters 13 & 3 were 0.727 g g^{-1} & 0.273 g g^{-1} respectively.

$\text{interstitial porosity} = \dfrac{\text{inter spheres pore space}}{\text{total volume of column}}$

L_r = the length of the porous column.

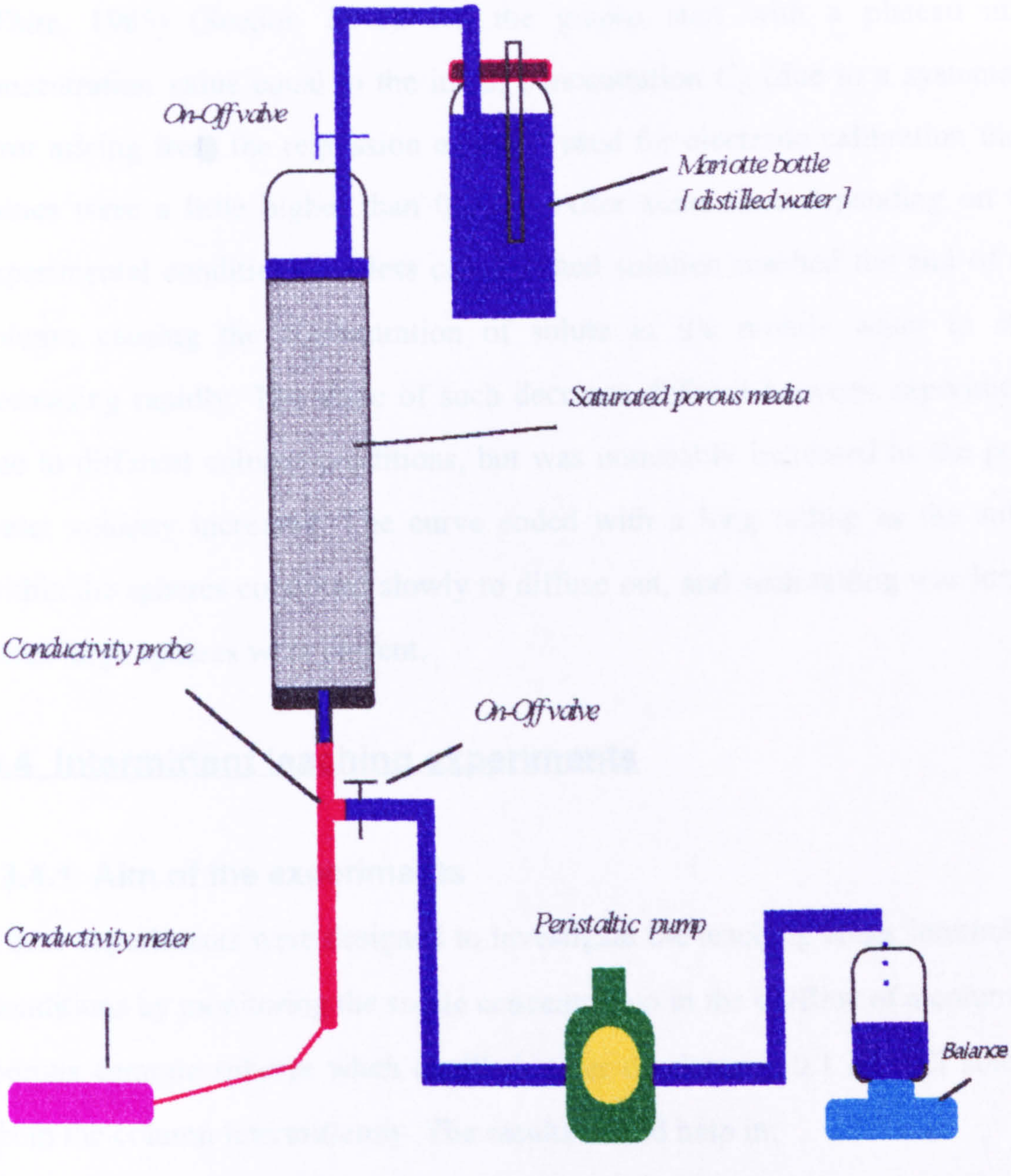

Fig. 3.3: Experiment set-up for continuous leaching .

3.3.3 Experimental results

Fig. 3.4 shows the results as a graph of effluent concentration *vs.* time for experiments 1C, 2C and 3C. The three resulting curves are asymmetric, with early breakthrough and long tailing, which characterise bi-continuum systems (*White*, 1985) (Section 2.3.2). All the graphs start with a plateau at a concentration value equal to the initial concentration C_0 (due to a systematic error arising from the regression equation used for electrode calibration these values were a little higher than 0.1 M). After some time depending on the experimental conditions the less concentrated solution reached the end of the column causing the concentration of solute in the mobile water to start decreasing rapidly. The slope of such decrease differed between experiments due to different column conditions, but was noticeably increased as the pore-water velocity increased. The curve ended with a long tailing as the solute within the spheres continued slowly to diffuse out, and such tailing was longer when large spheres were present.

3.4 Intermittent leaching experiments

3.4.1 Aim of the experiments

These experiments were designed to investigate the leaching under intermittent conditions by monitoring the solute concentration in the outflow of a column of porous ceramic spheres when distilled water displaced a 0.1 M KCl solution from the column intermittently. The results would help in:

(i) illustrating the advantage of intermittent over continuous leaching

(ii) testing a mathematical model (Section 5.2.2) .

3.4.2 Materials and methods

Similar columns to those used in the continuous leaching experiments (Section 3.3) were prepared, and the same procedures were followed, except that the outflow was regularly interrupted (using the on-off valves (Fig. 3.3)) during the

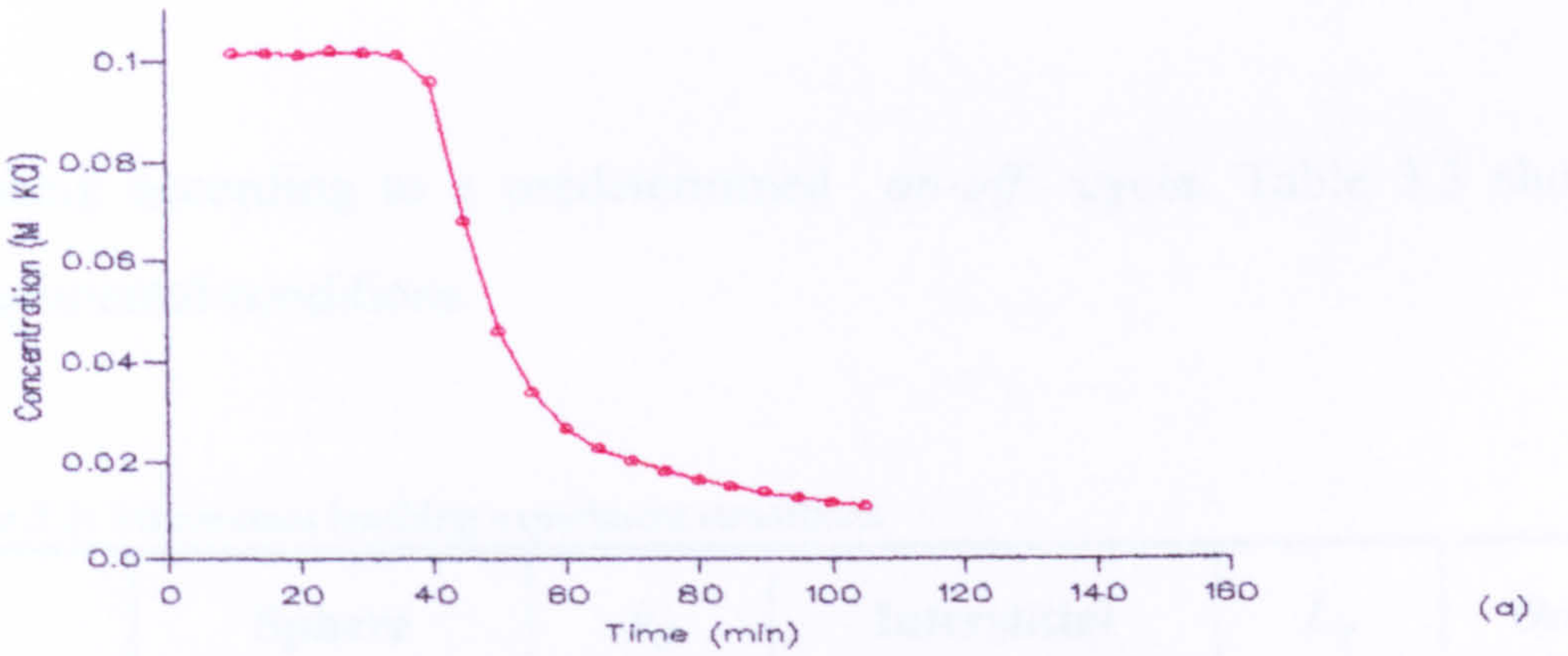

Fig. 3.4: Graphs of effluent concentration against time for continuous leaching experiments 1C, 2C, and 3C (see Table 3.2 for experimental conditions).

leaching according to a predetermined *on-off* cycle. Table 3.3 shows the experimental conditions.

***Table 3.3*: Intermittent leaching experiment conditions**

	Sphere diameter (mm)	v_d (mm/min)	**Interstitial porosity** ($cm^3\ cm^{-3}$)	L_r (mm)	***On/Off periods*** (min)
Exp. 1I	13	2.31	0.486 [a]	185	45/60
Exp. 2I	13+3 *	0.93	0.300 [b]	140	20/20
Exp. 3I	6	5.97	0.400 [b]	185	30/30

* the mass proportions of sphere diameters 13 & 3 were 0.733 g g^{-1} & 0.267 g g^{-1} respectively

[a] same value of Exp. 1C, because the same column was used with both experiments

[b] different values from those of Exp. 2C and 3C; because different column were used and the shaker was not able to produce exactly the same interstitial porosity, in addition the sphere shape was not exactly spherical. However, the difference is too small to affect the experimental objects.

3.4.3 Experimental results and discussion

Fig. 3.5 shows the results as effluent concentration against time for experiments 1I, 2I and 3I. The curves followed the same basic pattern as in the earlier continuous leaching experiment with a decrease in effluent concentration after an interval. The concentration was initially equal to C_0 then it decreased rapidly until the end of the first *on* time. After each *off* time the solute concentration in the effluent increased proving the proposed hypothesis that, during *off* times, the immobile solution within the spheres has a chance to equilibrate with the less concentrated mobile solution causing an increase in the solute concentration of the latter. The increase in mobile solution concentration after each *off* time means solute is lost from the column more quickly, i.e., there is a greater efficiency in leaching. The amplitude of these peaks, which occurred after each *off* time, decreased as leaching proceeded, because the concentration gradient between mobile and immobile volumes decreased with a consequent decrease in diffusion flux.

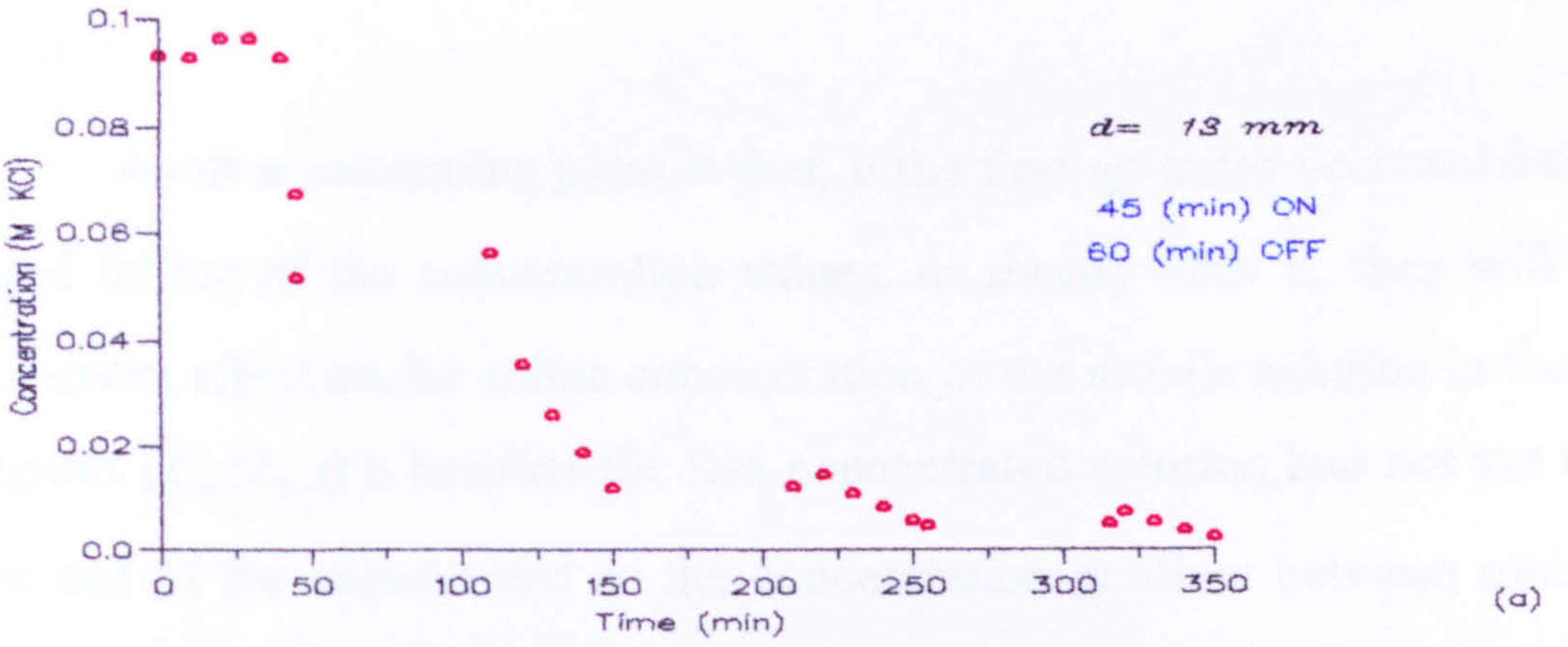

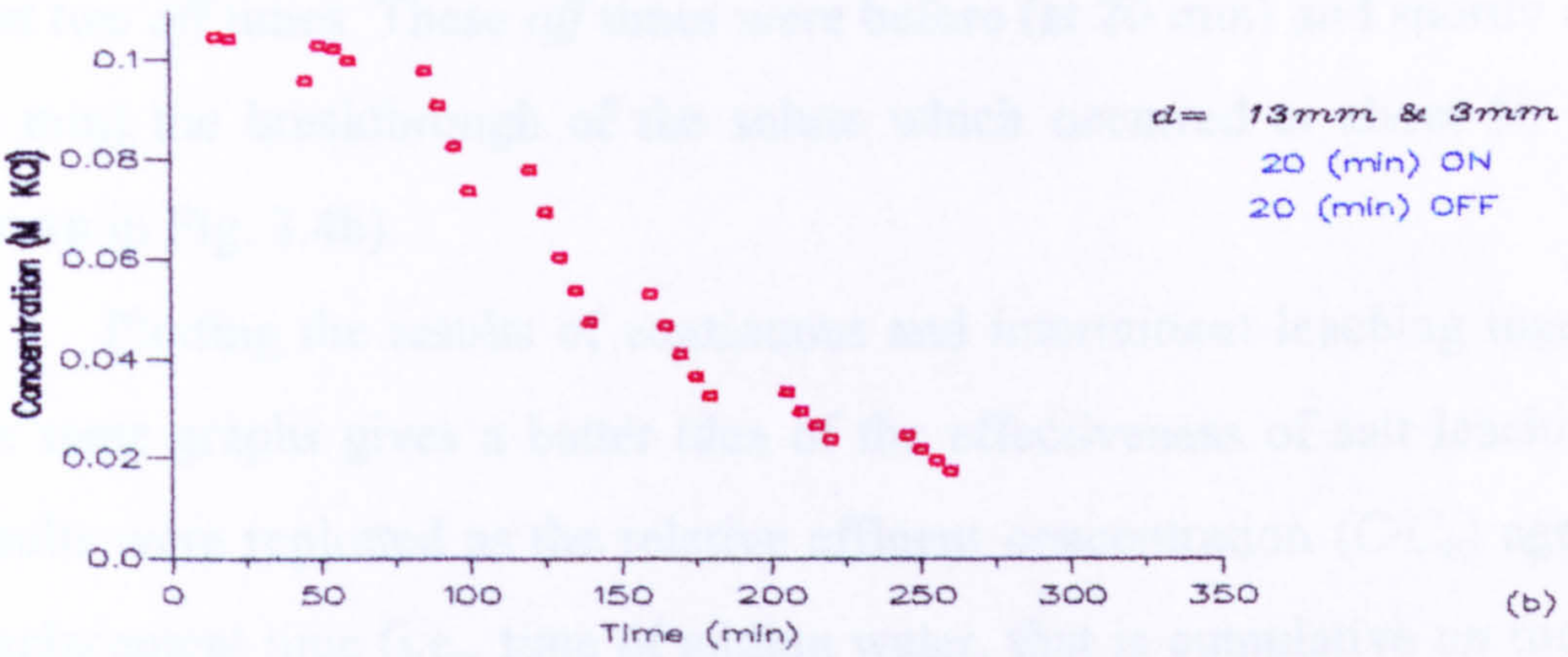

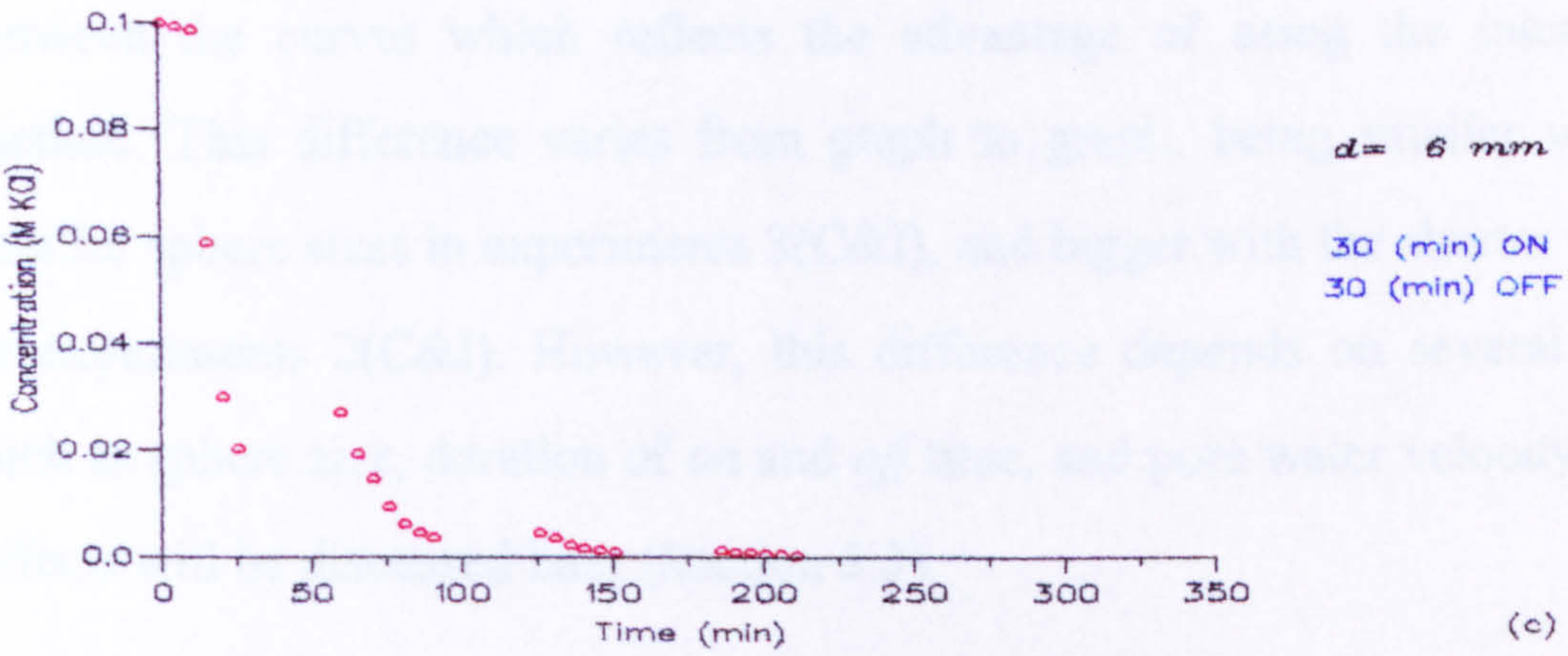

***Fig. 3.5*: Graphs of effluent concentration against time for intermittent leaching experiments 1I, 2I, and 3I (see Table 3.3 for experimental conditions).**

Another interesting point is that, if the first *off* times occurred before the rapid falling of the concentration values, or shortly after it, they will have a minimum effect on the solute concentration of the mobile solution in the lowest regions ($C_m(L_r,t)$), because the less concentrated solution had not yet reached the end of the column and so the concentration gradient between mobile and immobile solutions is zero (or still very small). This is the reason why only a very small change in effluent concentration occurred in experiment 2I at the first two *off* times. These *off* times were before (at 20 min) and shortly after (at 60 min) the breakthrough of the solute which occurred at about 50 min (as shown in Fig. 3.4b).

Plotting the results of continuous and intermittent leaching together on the same graphs gives a better idea of the effectiveness of salt leaching. The results were replotted as the relative effluent concentration (C/C_0) against the displacement time (i.e., time of adding water, that is cumulative *on* time) (Fig. 3.6). The graphs show that both BTCs started changing together, then after the first *off* period, there was a greater effluent concentration for intermittent leaching, i.e., more solute was being leached. In fact, it is this difference between the curves which reflects the advantage of using the intermittent method. This difference varies from graph to graph, being smaller with the smaller sphere sizes in experiments 3(C&I), and bigger with the shorter *on* time of experiments 2(C&I). However, this difference depends on several factors such as sphere size, duration of *on* and *off* time, and pore water velocity. These effects will be discussed later (Section 5.3).

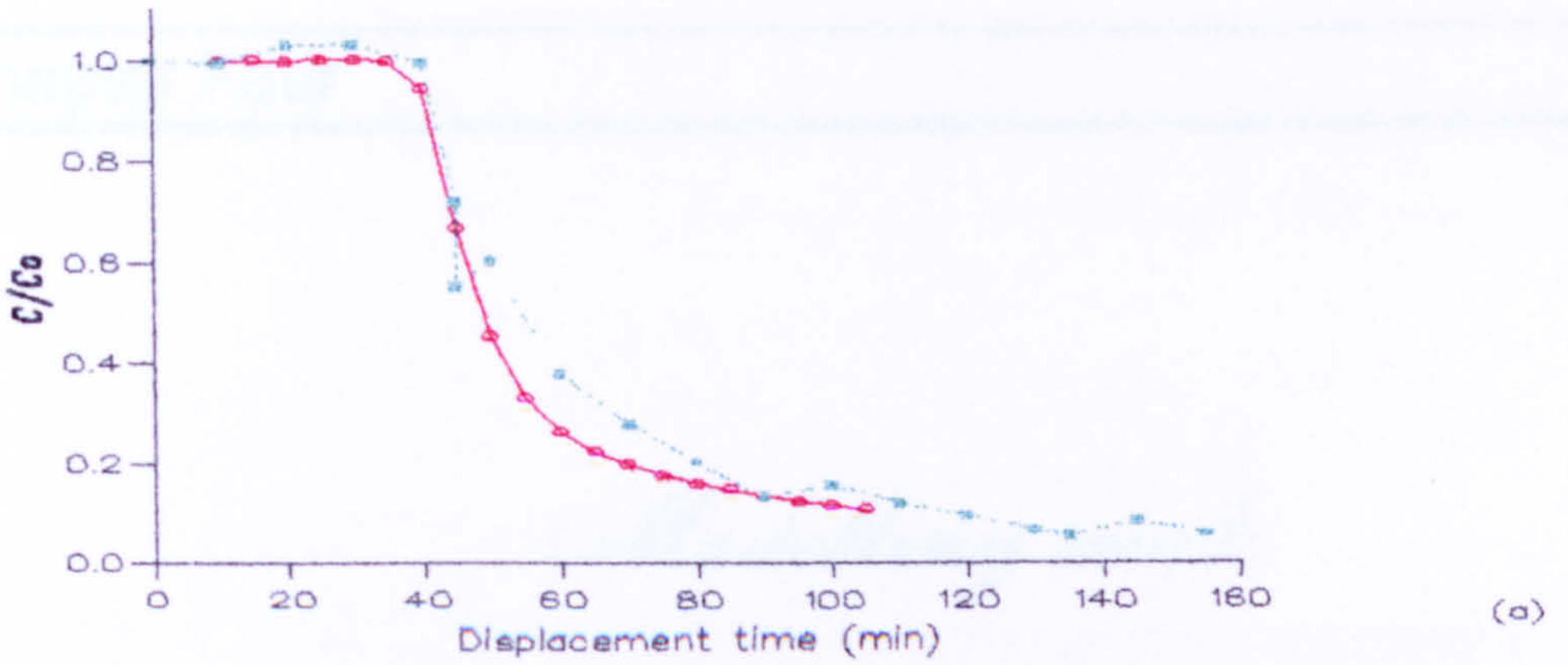

***Fig. 3.6*: Relative effluent concentration against displacement time for intermittent (--o--) and continuous (—o—) leaching experiments 1C&I, 2C&I, and 3C&I.**

Chapter Four

Modelling work

The aim of the modelling work was to write a computer code able to simulate the solute transport in a bi-continuum system during intermittent leaching. This chapter consists of four parts. The first, dealing with diffusion out of inert spheres, and the resulting spread-sheet programme, will be useful later to estimate the effective diffusion coefficient D_e . In the second part the SIL (Saturated Intermittent Leaching) model is constructed; this model is tested for continuous leaching against an analytical solution in the third part, and the validation of the model is discussed in the fourth part.

4.1 Diffusion from porous spheres

4.1.1 Introduction

Diffusion is the process by which matter is transported from one part of a system to another down a concentration gradient as a result of random molecular motion.

The transfer of heat by conduction is also due to random molecular motion, and there is an obvious analogy between the two processes. This was recognised by Fick (1855), who first put diffusion on a quantitative basis by adopting the mathematical theory derived some years earlier by Fourier. The mathematical theory of diffusion in an *isotropic* substance is therefore based on

the hypothesis that the rate of transfer of diffusible substance through unit area of cross-section is proportional to the concentration gradient measured normal to the area, i.e. for one-dimensional transfer:

$$F = -D_0 \frac{dC}{dx} \tag{4.1}$$

where F is the rate of transfer per unit area of cross-section, C the concentration of diffusing substance, x the space co-ordinate measured normal to the cross-sectional area, and D_0 is the molecular diffusion coefficient. Eq. 4.1 is often called Fick's first equation of diffusion.

The second Fick's equation for one-dimensional diffusion (i.e., if there is a gradient of concentration only along the x-axis) can be derived by combining equation 4.1 with the equation of continuity, i.e.,

$$\frac{\partial C}{\partial t} = -\frac{\partial F}{\partial x} = -\frac{\partial}{\partial x}\left[-D_0 \frac{\partial C}{\partial x}\right] .$$

If D_0 is constant, i.e. not a function of concentration, then

$$\frac{\partial C}{\partial t} = D_0 \frac{\partial^2 C}{\partial x^2} \quad . \tag{4.2}$$

Other forms of this equation follow by transformation of co-ordinates, or by considering elements of volume of different shape . *Crank* (1975) gave, in his comprehensive study on the mathematics of diffusion, the following equation for diffusion in a sphere

$$\frac{\partial C(r,t)}{\partial t} = D_0 \left\{ \frac{\partial^2 C}{\partial r^2} + \frac{2}{r} \frac{\partial C}{\partial r} \right\} \tag{4.3}$$

where

r = radial co-ordinate.

4.1.2 Aim of the model

The model aims to simulate the diffusion of a non-adsorbed solute (e.g. KCl) out of inert porous spheres into a continuously stirred volume of dilute solution. From this, the diffusion coefficient of the solute within the spheres may be determined.

4.1.3 Governing equations

A mechanistic model was developed based on Fick's second equation of diffusion (Eq. 4.2 and 4.3) , where the rate of solute transfer is described by:

$$\frac{\partial C_{im}(r,t)}{\partial t} = D_e\left\{\frac{\partial^2 C_{im}}{\partial r^2} + \frac{2}{r}\frac{\partial C_{im}}{\partial r}\right\} \qquad (4.4)$$

where

t = time

$C_{im}(r,t)$ = concentration of solute in the solution within the sphere

D_e = effective diffusion coefficient in porous spheres.

D_e replaces the molecular diffusion coefficient, D_0, in order to account for the tortuous path followed by ions within the complex matrix in the porous spheres.

The total mass of solute (M_T) in the system (in the saturated spheres plus the external solution, Fig. 4.1) is given by :

$$M_T = V_{ws}\,\overline{C_{im}}(t) + V_e\,C_m(t) = V_{ws}\;C_0 \qquad (4.5)$$

where

V_{ws} = volume of solution inside the spheres

V_e = volume of external solution

$C_m(t)$ = concentration of solute in the external solution

C_0 = initial concentration of solute within the spheres.

The average concentration in the sphere, $\overline{C_{im}}(t)$, is calculated as (*Rao et al.*, 1980a):

$$\overline{C_{im}}(t) = \frac{3}{a^2}\int_0^a r^2 C_{im}(r,t)\ \mathrm{d}r \qquad (4.6)$$

where

a = sphere radius.

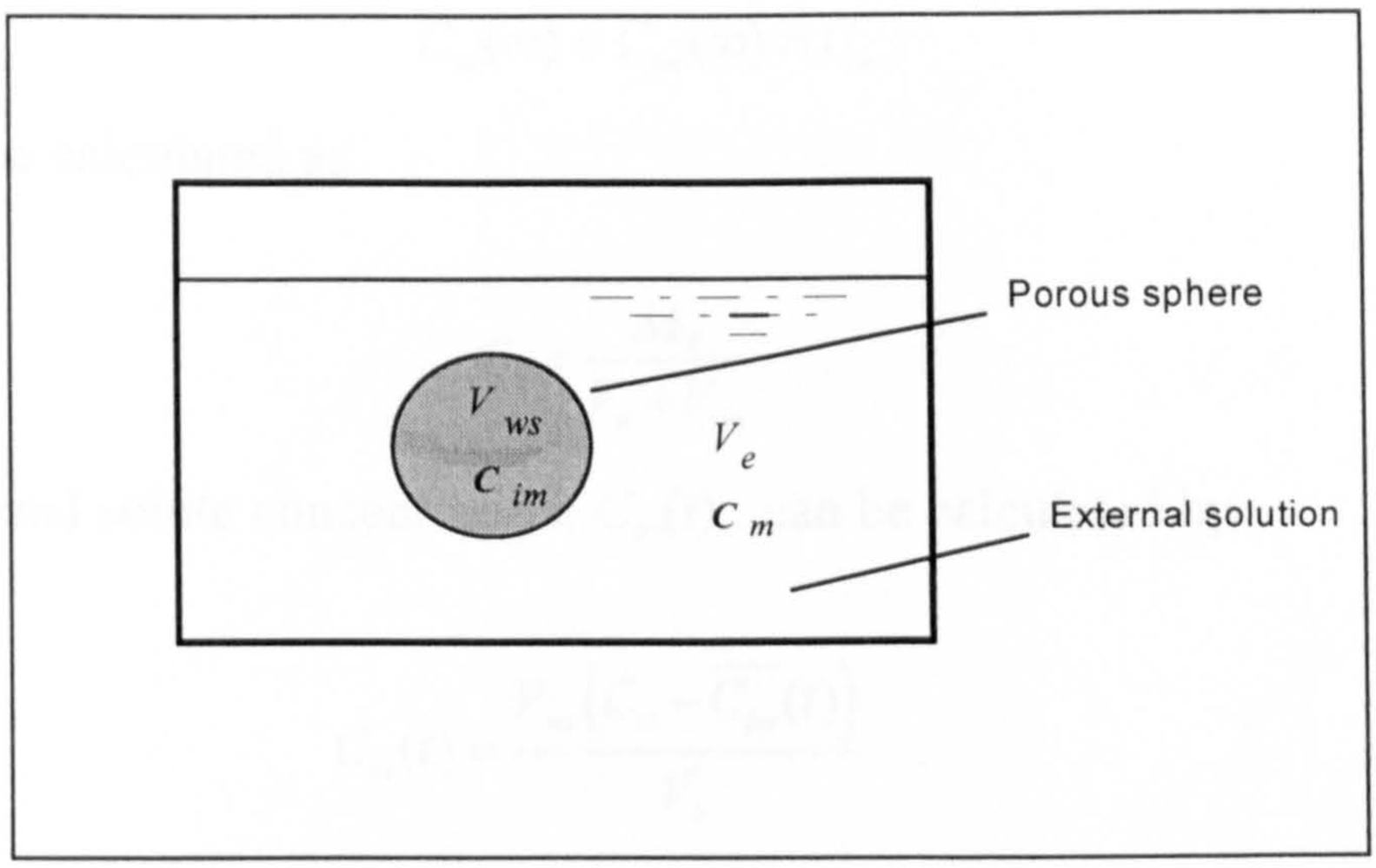

Fig. 4.1 : Simple diagram showing diffusion model parameters

The initial and boundary conditions are:

$$C_{im}(a,t) = C_m(t); \qquad t \geq 0 \qquad (4.7a)$$

$$C_{im}(r,t) = C_0 \quad ; \qquad 0 \leq r \leq a\,, \ \ t = 0 \qquad (4.7b)$$

$$C_m(t) = 0 \quad ; \qquad t = 0 \qquad (4.7c)$$

$\overline{C_{im}}(t)$ can be calculated from the solution of Eqs. 4.4 to 4.6 under conditions (4.7a,b,c), given by *Crank* (1975):

$$\frac{M_t}{M_\infty} = \frac{C_0 - \overline{C}_{im}(t)}{C_0 - C_e} = 1 - \sum_{n=1}^{\infty} \frac{6\gamma\ (\gamma+1)\exp(-\dfrac{D_e q_n^2 t}{a^2})}{9 + 9\gamma + q_n^2\gamma^2} \qquad (4.8)$$

where

M_t, M_∞ are the amount of solute in the sphere at times t and ∞ respectively,

$\gamma = \dfrac{V_e}{V_{ws}}$ and

q_n are the non-zero roots of $\tan q_n = \frac{3q_n}{3+\gamma q_n^2}$.

A table of q_n values can be found in *Crank* (1975).

At equilibrium (i.e., as $t \rightarrow \infty$), the solute concentration (C_e) will be the same inside and outside the porous sphere, i.e.

$$C_m(\infty) = C_{im}(\infty) = C_e \qquad \text{(at } t \rightarrow \infty\text{)}$$

and can be calculated as

$$C_e = \frac{M_T}{V_e + V_{ws}} \quad . \tag{4.9}$$

The external solute concentration, $C_m(t)$, can be calculated by

$$C_m(t) = \frac{V_{ws}\left(C_0 - \overline{C_{im}}(t)\right)}{V_e} \quad . \tag{4.10}$$

4.1.4 Testing the diffusion model

An "Excel" spreadsheet was used to calculate $C_m(t)$ and C_e using Eqs. 4.8, 4.9 and 4.10 at different time steps. For each time, t, the ratio $C_m(t)/C_e$ was calculated and plotted against time. Fig. 4.2 shows such results compared with the data of *Rao et al.* (1980a) (for $CaCl_2$ diffusion out of ceramic spheres into a continuously stirred volume of water).

The model successfully simulated the measured results ($R^2 = 0.985$).

4.2 Solute transport through a column of saturated porous spheres

4.2.1 Aim of the model

The **SIL** (Saturated Intermittent Leaching) model was aimed to simulate the solute transport, under steady flow conditions, through a saturated column of inert porous spheres containing both mobile (inter-spheres) and immobile water (intra-spheres) and for continuous or intermittent water application.

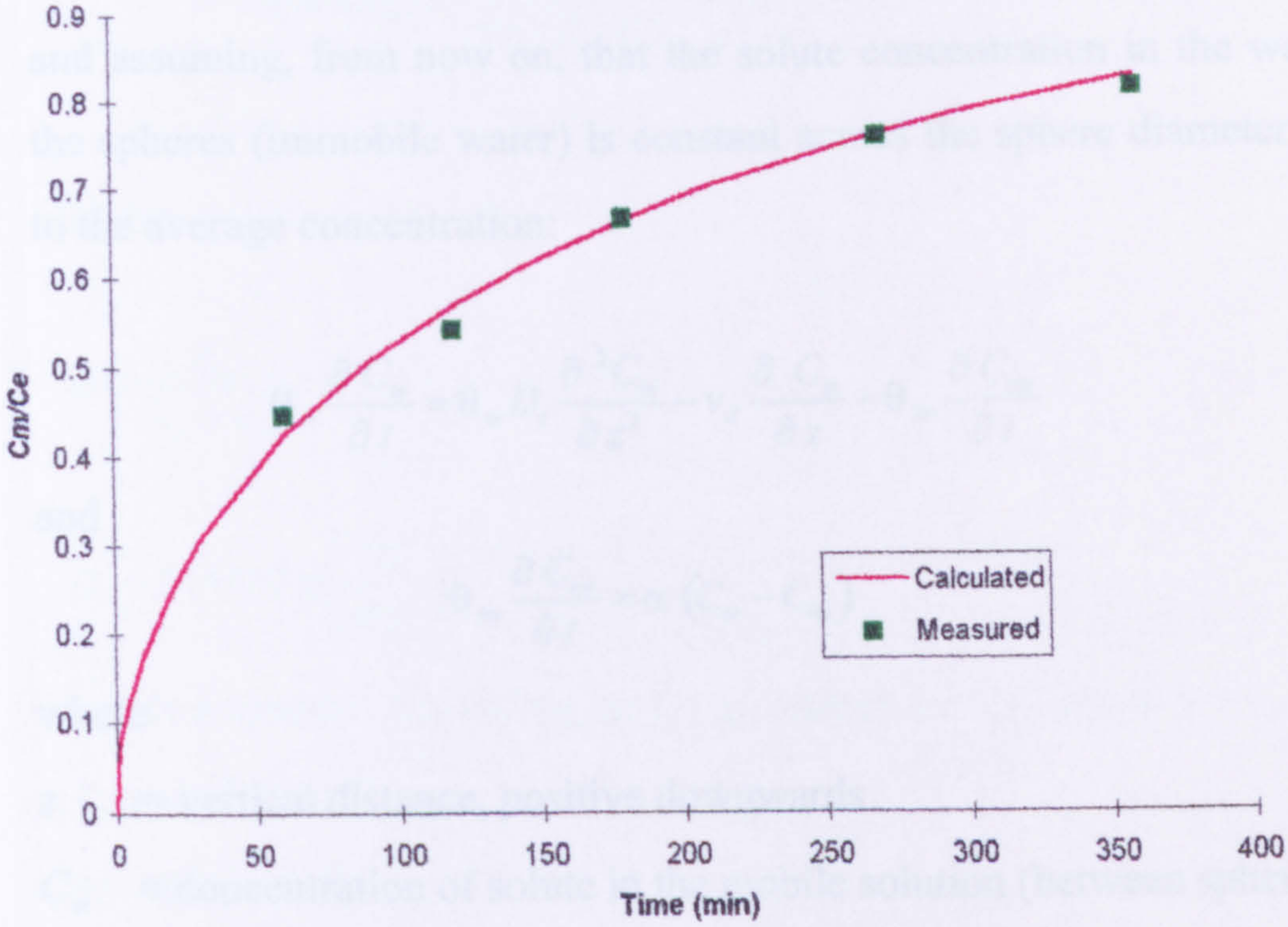

D_e = 0.012 cm^2 h^{-1}, C_o = 0.01 N $CaCl_2$, a = 0.75 cm, V_e = 100 cm^3, V_{ws} = 14.83 cm^3.

$C_m(t)$ = concentration of solute in the external solution

C_e = concentration of solute at equilibrium

Fig. 4.2: A plot of $C_m(t)/C_e(t)$ against diffusion time (measured data from *Rao et al.*, 1980a).

4.2.2 Continuous leaching

In this case the water is continuously ponded on the surface of the porous medium. The leaching here is similar to the miscible displacement process (Section 2.1).

4.2.2.1 Governing equations

Recalling Eqs. 2.17 and 2.19 for solute transport through bi-continuum media, and assuming, from now on, that the solute concentration in the water within the spheres (immobile water) is constant across the sphere diameter and equal to the average concentration:

$$\theta_m \frac{\partial C_m}{\partial t} = \theta_m D_s \frac{\partial^2 C_m}{\partial z^2} - v_d \frac{\partial C_m}{\partial z} - \theta_{im} \frac{\partial C_{im}}{\partial t} \tag{4.11}$$

and

$$\theta_{im} \frac{\partial C_{im}}{\partial t} = \alpha \left(C_m - C_{im} \right) \tag{4.12}$$

where

z = vertical distance, positive downwards

C_m = concentration of solute in the mobile solution (between spheres)

C_{im} = concentration in of solute in the immobile solution (within spheres)

D_s = hydrodynamic dispersion coefficient for mobile solution

v_d = Darcy velocity

θ_m = volume of mobile solution as a proportion of the total column volume

θ_{im} = volume of immobile solution as a proportion of the total column volume

α = mass transfer rate coefficient from immobile to mobile solution.

Rao et al. (1980a) showed experimentally that the mass transfer rate coefficient, α , is not constant but changes with time. They introduced the

averaged mass transfer coefficient which can be calculated independently for porous spheres from the equation:

$$\alpha = \frac{\Phi q_1^2}{1-B_1}\left(\frac{0.1}{T}\right)^{B_1}\left(\frac{D_e\theta_{im}}{a^2}\right) \qquad 0.0001 < T \le 0.1 \qquad (4.13a)$$

or

$$\alpha = \Phi q_1^2\left(1+\frac{0.1B_1}{(1-B_1)T}\right)\left(\frac{D_e\theta_{im}}{a^2}\right) \qquad T \ge 0.1 \qquad (4.13b)$$

where

$$\Phi = \frac{\theta_m}{\theta_m+\theta_{im}}$$

$$B_1 = 0.14472\,ln\left(\frac{167}{\Phi q_1^2}\right)$$

q_1= is a constant depending on Φ, q_1 values for various Φ values are given in *Rao et al.* (1980),

a = sphere radius,

and the dimensionless time, T, is given by

$$T = \frac{D_e\,\Delta t}{a^2} \quad . \qquad (4.14)$$

Δt is the time period over which α is calculated. For a displacement experiment it is considered to be the mean column residence time (i.e. $\Delta t = \frac{L_r}{v_d/\theta_m}$) which has been shown to give the best result (*Rao et al.*, 1980b).

4.2.2.2 Initial and boundary conditions

The initial condition for the solute concentration of the mobile and immobile solutions is given by:

$$C_{im}(z,t) = C_m(z,t) = C_0 \qquad (t = 0) \qquad (4.15)$$

where

C_0 = the initial solute concentration of both mobile and immobile solutions.

For the upper boundary condition ($z = 0$), three possibilities are available (*Javandel et al.*, 1984):

1) Dirichlet boundary condition: which prescribes concentration along the boundary,

2) Neumann boundary condition: which prescribes the normal gradient of concentration over the boundary, and

3) Cauchy boundary condition or prescribed flux boundary condition: which prescribes concentration and its gradient.

Van Genuchten & Parker (1984) showed that a prescribed flux boundary condition is a better representation of the physical reality than the others, since it gives a better prediction of the mass balance by allowing for dispersion in the column at $z = 0$. With this boundary condition the mass flux of the solute at the upper boundary at any time is equivalent to the total flux of that solute carried out by dispersion and convection (*Javandel et al.*, 1984), i.e.

at $z = 0$, $t \geq 0$

$$v_d C_{inp} = v_d C_m - \theta_m D_S \frac{\partial C_m}{\partial z} \qquad (4.16)$$

where

C_{inp} = is the concentration of solute in the added water.

For a finite column of length L_r, a frequently used lower boundary condition is

$$\frac{\partial C}{\partial z}(L_r,t) = 0 \ .$$

Brenner (1962) gave the analytical solution for CDE under these two conditions. However, accommodating the presence of a boundary layer at $z=L_r$ leads to a discontinuous concentration distribution across the lower boundary,

and thus to a gradient in the concentration interior to the transition zone that is not constrained to be zero (*Parker & van Genuchten*, 1984). Therefore, it is often more convenient to solve the CDE equation for an "effectively" semi-infinite column rather than for a finite column (*Selim*, 1992). For a column assumed to be semi-infinite, the lower boundary condition is written as :

at $z = \infty$, $t \geq 0$

$$C_{im}(\infty, t) = C_m(\infty, t) = C_0 \ . \tag{4.17}$$

Even though this condition does not exactly represent the physical reality (since the column is finite), it can be used if the length of the column is extended as shown in Fig. 4.3. *Parker* (1984) stated that " so long as back mixing at the exit boundary is negligible (which normally is the case), Eq. 4.17 for a semi-infinite case can be used with impunity and the resulting solution applied to the finite region $0 \leq z \leq L_r$ as well". Accordingly, this boundary condition was used.

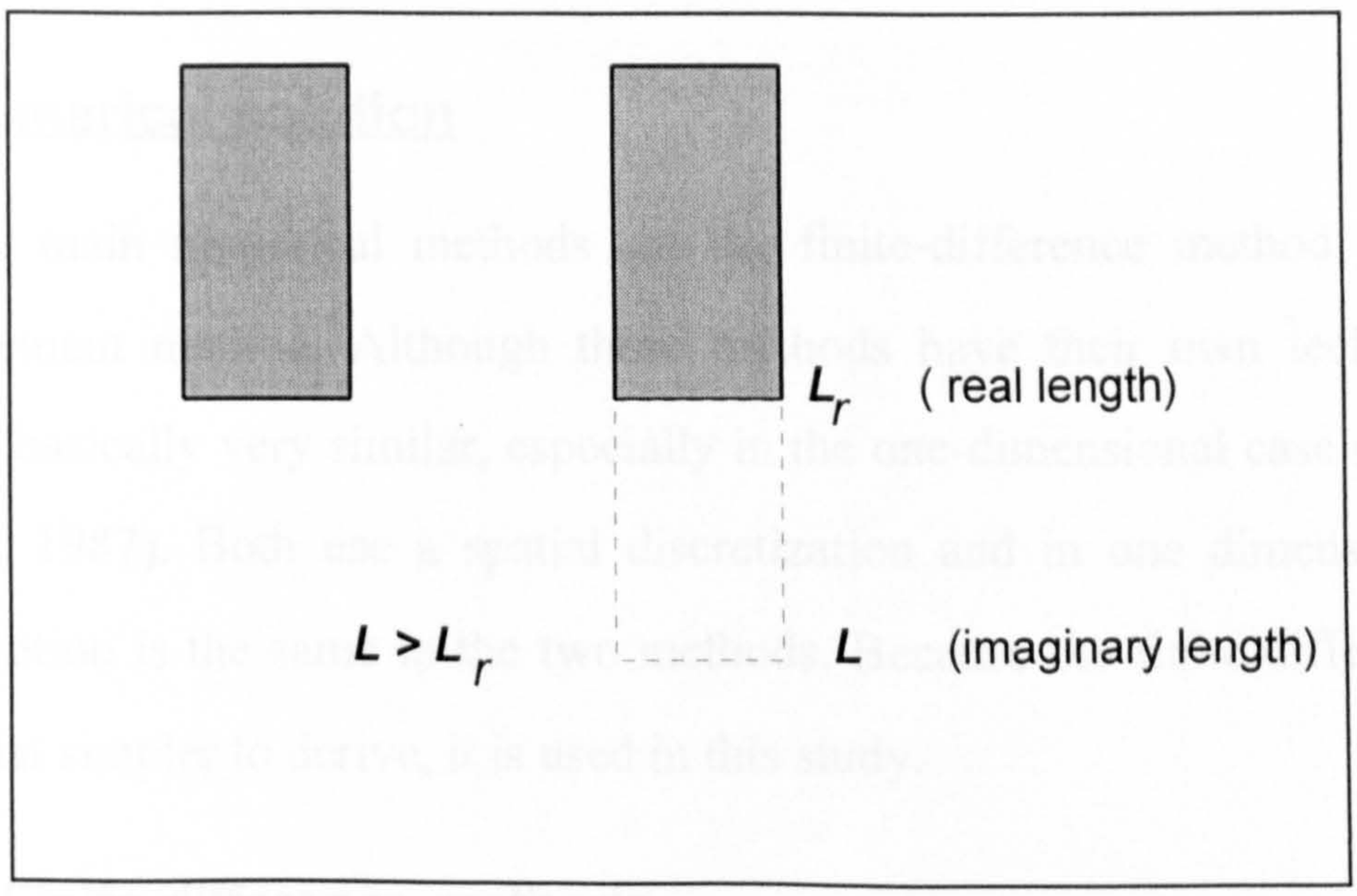

Fig. 4.3: *Hypothetical expansion of the column.*

4.2.3 Intermittent leaching

4.2.3.1 Governing equations

I) During the displacement period, "*On* Time" :

The governing equations are same as in the continuous leaching, i.e., Eqs. 4.11 & 4.12.

II) During the rest period "*Off* Time" :

The governing equations can be obtained from Eqs. 4.11 and 4.12, by assuming that there is no mass flow, and that solute is only transferred by diffusion (i.e., $v_d = D_s = 0$). Thus, from Eq. 4.11:

$$\theta_m \frac{\partial C_m}{\partial t} = \theta_{im} \frac{\partial C_{im}}{\partial t} \tag{4.18}$$

where

$$\theta_{im} \frac{\partial C_{im}}{\partial t} = \alpha \left(C_m - C_{im} \right).$$

In calculating α during the "*on*" time, the Δt in Eq. 4.14 is the same as for the continuous case; however, for the "*off*" time , it is equal to the period of the "*off*" phase, since this is the real time of the diffusion .

4.3 Numerical solution

The two main numerical methods are the finite-difference method and the finite-element method. Although these methods have their own techniques, they are basically very similar, especially in the one-dimensional case (*Bear & Verruijt*, 1987). Both use a spatial discretization and in one dimension this discretization is the same in the two methods. Because the finite difference is somewhat simpler to derive, it is used in this study.

4.3.1 Finite-difference methods

In most numerical methods of solving differential equations (such as Eqs. 4.11 & 4.12), the first step is to replace the latter by algebraic *finite-difference equations*. These are relationships between values of the dependent variable (here, concentration values) at neighbouring points in z,t space. The numerical

solution of the series of simultaneous equations thus obtained gives the values of dependent variables at a predetermined number of discrete points (grid points) through the domain investigated .

There are many possible ways of writing Eqs. 4.11 & 4.12 in a finite-difference form, according to the choice of the approximation of the terms. Usually the time and space domain is divided into a grid, where Δt represents the time increment and Δz the space increment (Fig. 4.4). Time and space can be expressed as multiples of Δt and Δz :

$t = j.\ \Delta t \qquad \{ j = 0,1,2,.....n \}$

$z = i.\Delta z \qquad \{ i = 0,1,2,.....m \}.$

So a z,t function $f(z,t)$ is written as $F(i.\Delta z\ ,\ j.\Delta t\ ) = {}_i^jF$, where ${}_i^jF$ is the approximate solution of $f(z,t)$ at the discrete point ($i.\Delta z$, $j.\Delta t$) of the defined domain.

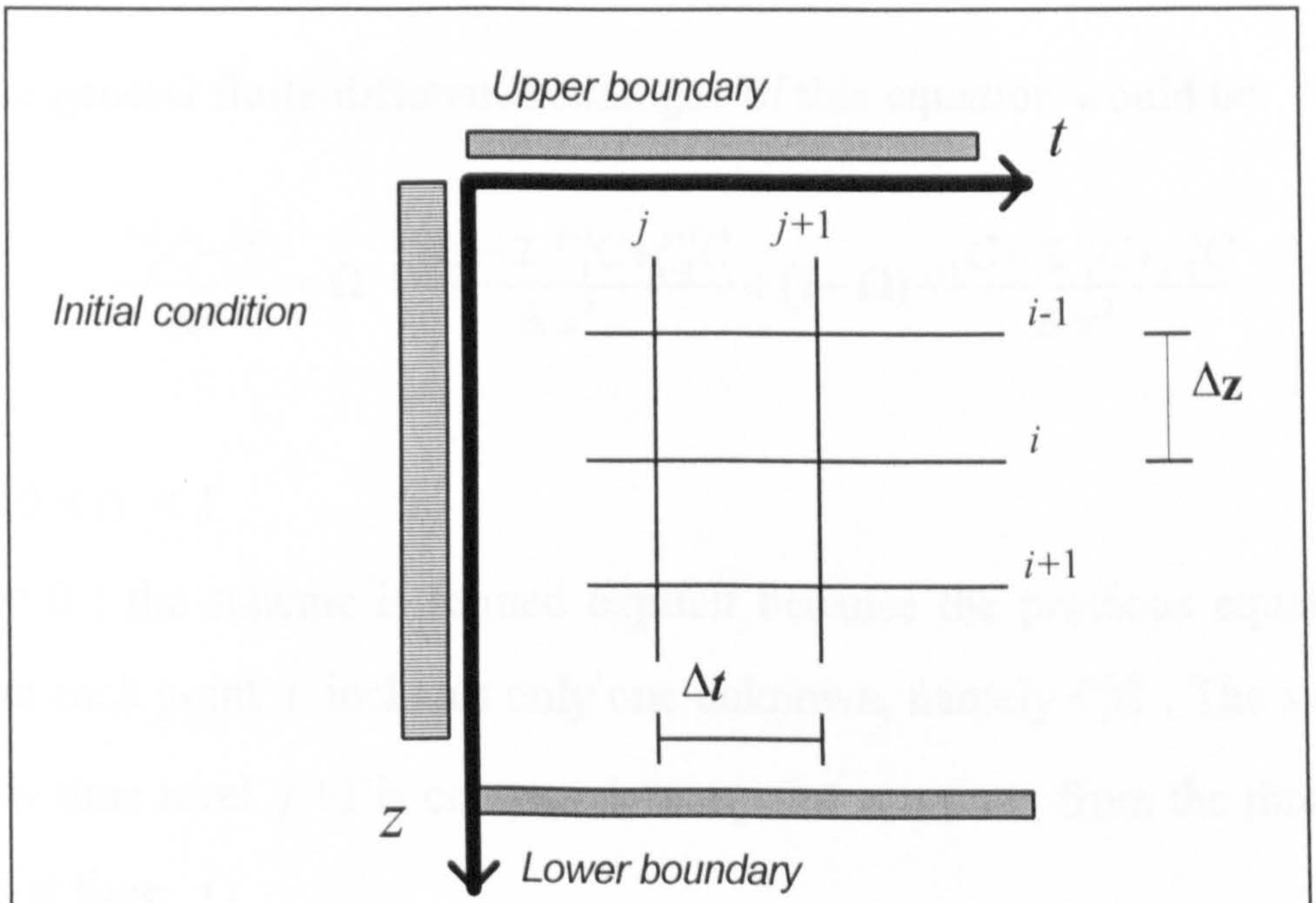

Fig. 4.4: *A grid of the numerical solution with initial and boundary conditions.*

The differential equation is replaced by a finite-difference equation written in terms of the values of the dependent variable at the grid points. The solution of the difference equation, or set of difference equations, is carried out numerically. Denoting the exact solution of the differential equations by *S*, the exact solution of the difference equations by *D*, and the numerical solution of difference equations by N ,the term $|S-D|$ is called the *truncation error* and $|D-N|$ the *numerical*, or the *round-off error* .The condition for *convergence* of the solution is that $|S-D| \to 0$ everywhere in the solution domain. The condition for *stability* is that everywhere in the solution domain $|D-N| \to 0$ (*Bear*, 1972).

For example, if the partial differential equation was of the style:

$$\frac{\partial C}{\partial t} = \frac{\partial^2 C}{\partial^2 x}$$

then the general finite-difference analogue of this equation would be:

$$\frac{{}_i^{j+1}C - {}_i^{j}C}{\Delta t} = \Omega \frac{{}_{i+1}^{j+1}C - 2\,{}_i^{j+1}C + {}_{i-1}^{j+1}C}{\Delta x^2} + (1-\Omega)\frac{{}_{i+1}^{j}C - 2\,{}_i^{j}C + {}_{i-1}^{j}C}{\Delta x^2} \qquad (4.19)$$

where $0 < \Omega < 1$.

If $\Omega = 0$: the scheme is termed explicit because the previous equation (Eq. 4.19) at each point i includes only one unknown, namely ${}_i^{j+1}C$. The solution at the new time level $j+1$ is computed, one point at a time, from the three known values at time j.

If $\Omega = 1$: the scheme is called full implicit, and there will be three unknowns in Eq. 4.19 for each i . The equation is written for all values of i and the resulting set of equations is solved simultaneously. This scheme is superior in efficiency to the explicit scheme and is unconditionally stable.

If $\Omega = 0.5$: this is called the Crank-Nicolson approximation or central finite difference. This scheme is the most natural, and the most accurate, approximation of the second-order derivative (*Bear & Verruijt*, 1987).

A complete detailed discussion about writing the differential equations in a finite-difference analogue can be found in most textbooks on numerical integration (such as *Smith*, 1978).

4.3.1.1 Crank-Nicolson method

The Crank-Nicolson implicit method is a finite-difference approximation to a differential equation which is unconditionally stable (*Peaceman*, 1977; *Smith*, 1978) and has a truncation error of second order in both space and time dimensions. By applying this method Eq. 4.11 becomes :

I- For continuous displacement:

$$\frac{{}_{i}^{j+1}C_m - {}_{i}^{j}C_m}{\Delta t} = \frac{D_s}{2}\left(\frac{{}_{i+1}^{j+1}C_m - 2\,{}_{i}^{j+1}C_m + {}_{i-1}^{j+1}C_m}{\Delta z^2} + \frac{{}_{i+1}^{j}C_m - 2\,{}_{i}^{j}C_m + {}_{i-1}^{j}C_m}{\Delta z^2}\right)$$
$$-\frac{v_d}{2\theta_m}\left(\frac{{}_{i+1}^{j+1}C_m - {}_{i-1}^{j+1}C_m}{2\Delta z} + \frac{{}_{i+1}^{j}C_m - {}_{i-1}^{j}C_m}{2\Delta z}\right) - \frac{\theta_{im}}{\theta_m}\left(\frac{{}_{i}^{j+1}C_{im} - {}_{i}^{j}C_{im}}{\Delta t}\right). \qquad (4.20)$$

Rearranging Eq. 4.20 and taking all the unknowns to the left-hand side gives

$${}_{i}^{j+1}C_m - \frac{D_s\Delta t}{2}\left(\frac{{}_{i+1}^{j+1}C_m - 2\,{}_{i}^{j+1}C_m + {}_{i-1}^{j+1}C_m}{\Delta z^2}\right) + \frac{v_d\Delta t}{2\theta_m}\left(\frac{{}_{i+1}^{j+1}C_m - {}_{i-1}^{j+1}C_m}{2\Delta z}\right) =$$
$${}_{i}^{j}C_m + \frac{D_s\Delta t}{2}\left(\frac{{}_{i+1}^{j}C_m - 2\,{}_{i}^{j}C_m + {}_{i-1}^{j}C_m}{\Delta z^2}\right) - \frac{v_d\Delta t}{2\theta_m}\left(\frac{{}_{i+1}^{j}C_m - {}_{i-1}^{j}C_m}{2\Delta z}\right) - \frac{\theta_{im}\Delta t}{\theta_m}\left(\frac{{}_{i}^{j+1}C_{im} - {}_{i}^{j}C_{im}}{\Delta t}\right) \qquad (4.21)$$

i.e.

$${}_{i}^{j+1}RHS = {}_{i}^{j}C_m + \frac{D_s\Delta t}{2}\left(\frac{{}_{i+1}^{j}C_m - 2\,{}_{i}^{j}C_m + {}_{i-1}^{j}C_m}{\Delta z^2}\right)$$
$$-\frac{v_d\Delta t}{2\theta_m}\left(\frac{{}_{i+1}^{j}C_m - {}_{i-1}^{j}C_m}{2\Delta z}\right) - \frac{\theta_{im}\Delta t}{\theta_m}\left(\frac{{}_{i}^{j+1}C_{im} - {}_{i}^{j}C_{im}}{\Delta t}\right). \qquad (4.22)$$

Choosing coefficients A, B, C, E, F and G as:

$$E = \frac{D_S \Delta t}{2\Delta z^2} + \frac{v_d \Delta t}{4\theta_m \Delta z} \tag{4.23}$$

$$F = 1 - \frac{D_S . \Delta t}{\Delta z^2} \tag{4.24}$$

$$G = \frac{D_S \Delta t}{2\Delta z^2} - \frac{v_d \Delta t}{4\theta_m \Delta z} \tag{4.25}$$

$$A = E \tag{4.26}$$

$$B = 1 + \frac{D_S . \Delta t}{\Delta z^2} \tag{4.27}$$

$$C = G \tag{4.28}$$

then , Eqs. 4.21 & 4.22 become respectively:

$$A\ {}^{j+1}_{i-1}C_m + B\ {}^{j+1}_{i}C_m + C\ {}^{j+1}_{i+1}C_m = E\ {}^{j}_{i-1}C_m + F\ {}^{j}_{i}C_m + G\ {}^{j}_{i+1}C_m - \frac{\theta_{im}}{\theta_m}\left({}^{j+1}_{i}C_{im} - {}^{j}_{i}C_{im}\right) \tag{4.29}$$

$${}^{j+1}_{i}RHS = E\ {}^{j}_{i-1}C_m + F\ {}^{j}_{i}C_m + G\ {}^{j}_{i+1}C_m - \frac{\theta_{im}}{\theta_m}\left({}^{j+1}_{i}C_{im} - {}^{j}_{i}C_{im}\right) \tag{4.30}$$

where

RHS is the right-hand side of Eq. 4.29

${}^{j+1}_{i}C_{im}$ can be derived from Eq. 4.12 as:

$$\theta_{im} \frac{{}^{j+1}_{i}C_{im} - {}^{j}_{i}C_{im}}{\Delta t} = \alpha \left(\frac{{}^{j+1}_{i}C_m + {}^{j}_{i}C_m}{2} - \frac{{}^{j+1}_{i}C_{im} + {}^{j}_{i}C_{im}}{2} \right)$$

$$\theta_{im}\,{}_i^{j+1}C_{im} = \theta_{im}\,{}_i^{j}C_{im} + \frac{\alpha\Delta t}{2}\left({}_i^{j+1}C_m + {}_i^{j}C_m - {}_i^{j+1}C_m - {}_i^{j}C_m\right)$$

$${}_i^{j+1}C_{im} + \frac{\alpha\Delta t}{2\theta_{im}}\,{}_i^{j+1}C_{im} = {}_i^{j}C_{im} - \frac{\alpha\Delta t}{2\theta_{im}}\,{}_i^{j}C_{im} + \frac{\alpha\Delta t}{2\theta_{im}}\left({}_i^{j+1}C_m + {}_i^{j}C_m\right)$$

$${}_i^{j+1}C_{im}\left(1+\frac{\alpha\Delta t}{2\theta_{im}}\right) = {}_i^{j}C_{im}\left(1-\frac{\alpha\Delta t}{2\theta_{im}}\right) + \frac{\alpha\Delta t}{2\theta_{im}}\left({}_i^{j+1}C_m + {}_i^{j}C_m\right)$$

$${}_i^{j+1}C_{im} = \left[\ {}_i^{j}C_{im}\left(1-\frac{\alpha\,\Delta t}{2\theta_{im}}\right) + \frac{\alpha\,\Delta t}{2\theta_{im}}\left({}_i^{j+1}C_m + {}_i^{j}C_m\right)\ \right] / \left(1+\frac{\alpha\,\Delta t}{2\theta_{im}}\right) \quad . \qquad (4.31)$$

Eq. 4.30 can be written in matrix form as:

{M} [C_m] = [RHS]

where the coefficient matrix **{M}** is tridiagonal and therefore the simultaneous equations can easily be solved for each time step by using one of the algorithms based on Gaussian elimination (*James & Poole,* 1981).

II- For intermittent leaching

- *On Time*

As in the continuous leaching case.

- *Off Time*

Eq. 4.18 becomes:

$$\frac{{}_i^{j+1}C_m - {}_i^{j}C_m}{\Delta t} = \frac{\theta_{im}}{\theta_m}\left(\frac{{}_i^{j+1}C_{im} - {}_i^{j}C_{im}}{\Delta t}\right)$$

$${}_i^{j+1}C_m - {}_i^{j}C_m = \frac{\theta_{im}}{\theta_m}\left({}_i^{j+1}C_{im} - {}_i^{j}C_{im}\right)$$

$${}_i^{j+1}C_m = {}_i^{j}C_m + \frac{\theta_{im}}{\theta_m}\left({}_i^{j+1}C_{im} - {}_i^{j}C_{im}\right) \quad . \qquad (4.32)$$

The SIL model is written in FORTRAN-77. The following diagram (Fig. 4.5) represents the flow chart of the model. The computer program is printed in Appendix A.

III- For a column filled with a mixture of spheres

In this case the model will require the mass proportions of each size of sphere. The mass transfer coefficient is calculated for each diameter by Eqs. 4.13a,b using the relevant D_e value. The concentration within the spheres (C_{im}) is also separately calculated for each diameter using Eq. 4.31. The "overall" C_{im} at each (z,t) is obtained by solution of the equation :

$$ {}^{j+1}_{i}C_{im} = \sum_{n=1}^{n_p} ({}^{j+1}_{i}C_{im})_n \, P_n \qquad (4.33) $$

where

n_p = the number of different diameters in the mixture.

P_n = the mass proportion for spheres of diameters (n).

The SIL model then continues as previously. The FORTRAN-77 code for this case is presented in Appendix B.

4.4 Model stability and convergence

It is desirable to control the stability and convergence of finite-difference schemes by comparison with an analytical "exact" solution, if such a solution exists. Analytical solutions for continuous saturated displacement (Eqs. 4.11 & 4.12) have been derived for a variety of initial and boundary conditions (*De Smedt & Wierenga* (1979), *van Genuchten* (1980, 1981), and *Parker & van Genuchten* (1984)).

Rao et al. (1980b) performed miscible displacement experiments on columns of inert porous spheres. Using the values of parameters of one of their experiments (Table 4.1), both analytical and SIL models were run. The results

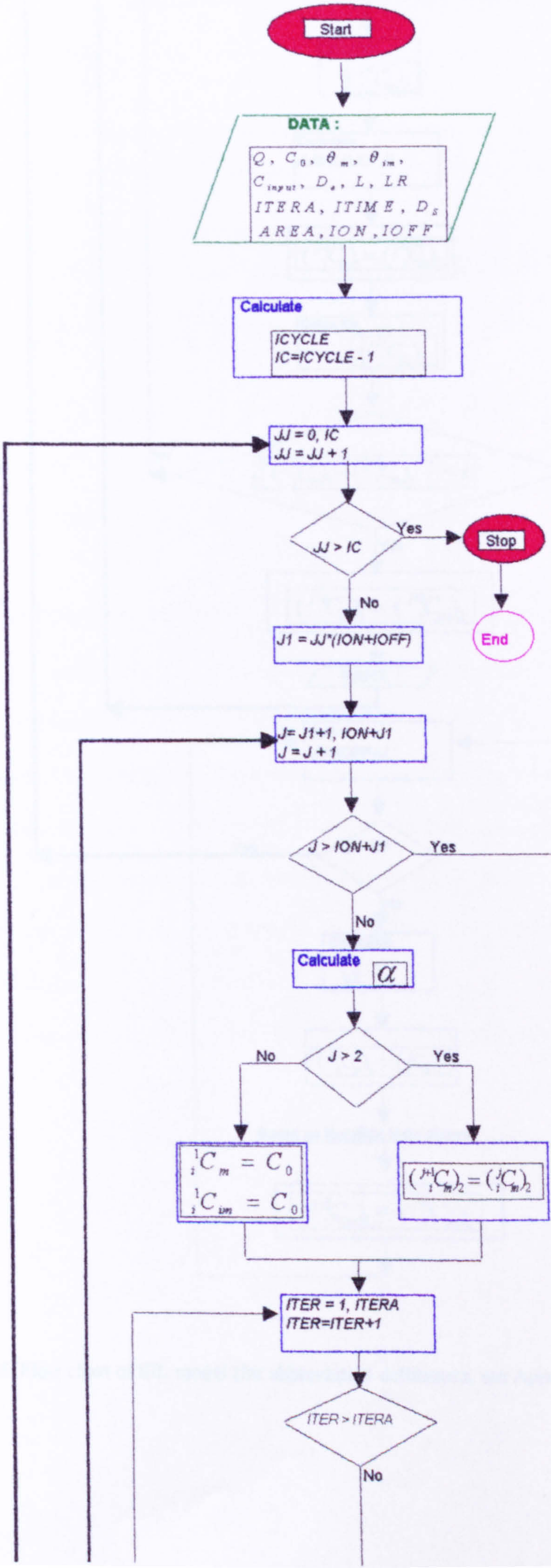
Start
DATA :
Q, C_0, θ_m, θ_{im},
C_{input}, D_a, L, LR
$ITERA$, $ITIME$, D_s
$AREA$, ION, $IOFF$
Calculate
ICYCLE
IC=ICYCLE - 1
JJ = 0, IC
JJ = JJ + 1
JJ > IC
Yes
Stop
End
No
J1 = JJ*(ION+IOFF)
J= J1+1, ION+J1
J = J + 1
J > ION+J1
Yes
No
Calculate α
J > 2
No
Yes
${}_i^1C_m = C_0$
${}_i^1C_{im} = C_0$
$({}_i^{j+1}C_m)_2 = ({}_i^jC_m)_2$
ITER = 1, ITERA
ITER=ITER+1
ITER > ITERA
No

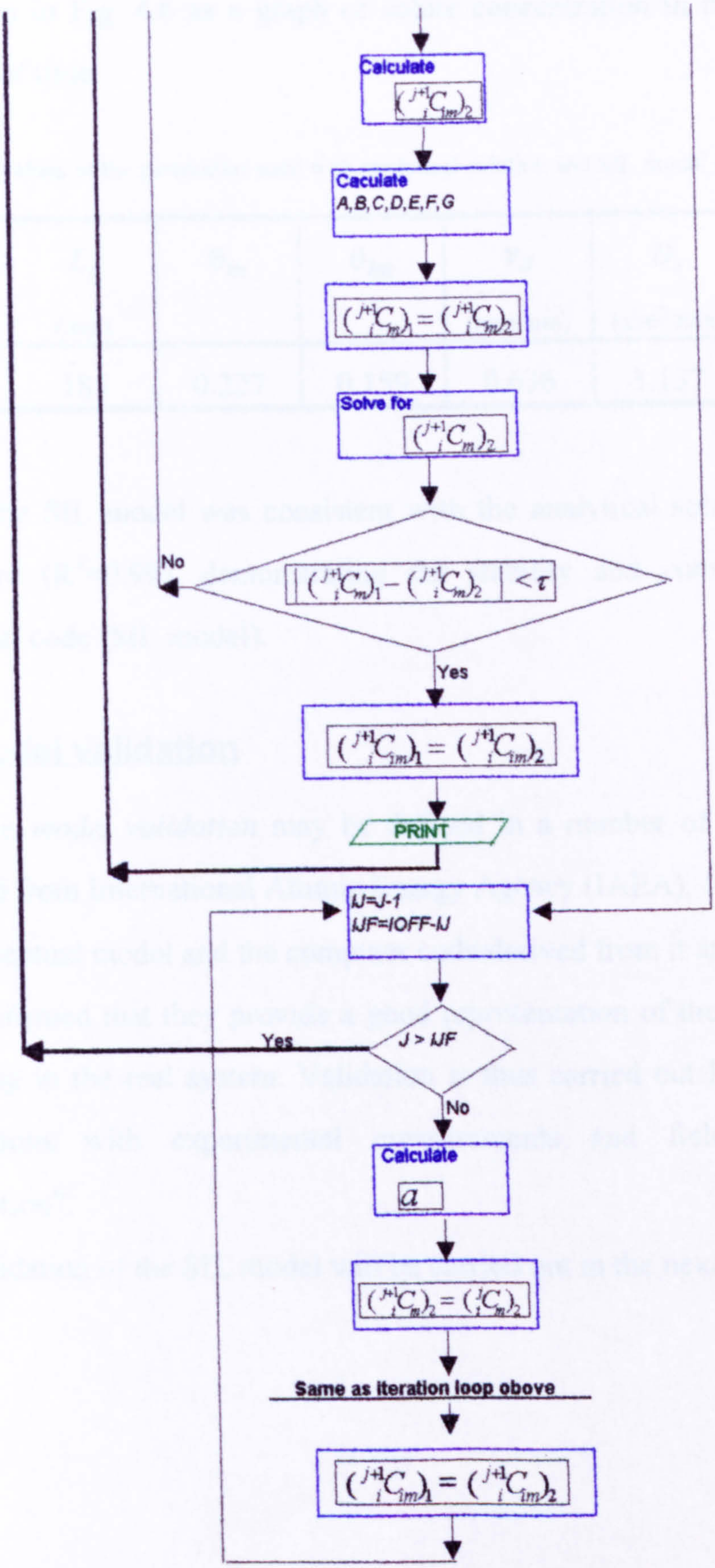

Fig. 4.5: Flow chart of SIL model (for abbreviation definitions, see Appendixes)

are shown in Fig. 4.6 as a graph of solute concentration in the effluent as a function of time.

Table 4.1 :Values of the parameters used with analytical solution and SIL model (data from *Rao et al.* ,1980b).

d (mm)	L_r (mm)	θ_m	θ_{im}	v_d (mm/min)	D_s (mm^2/min)	α (min^{-1})
55	185	0.227	0.159	0.636	3.137	0.00168

The SIL model was consistent with the analytical solution throughout the curve (R^2=0.99), demonstrating the stability and convergence of the numerical code (SIL model).

4.5 Model validation

The term *model validation* may be defined in a number of ways. One such (adopted from International Atomic Energy Agency (IAEA), 1982) is:

"A conceptual model and the computer code derived from it are validated when it is confirmed that they provide a good representation of the actual processes occurring in the real system. Validation is thus carried out by comparison of calculations with experimental measurements and field or laboratory observation".

The validation of the SIL model will be carried out in the next chapter.

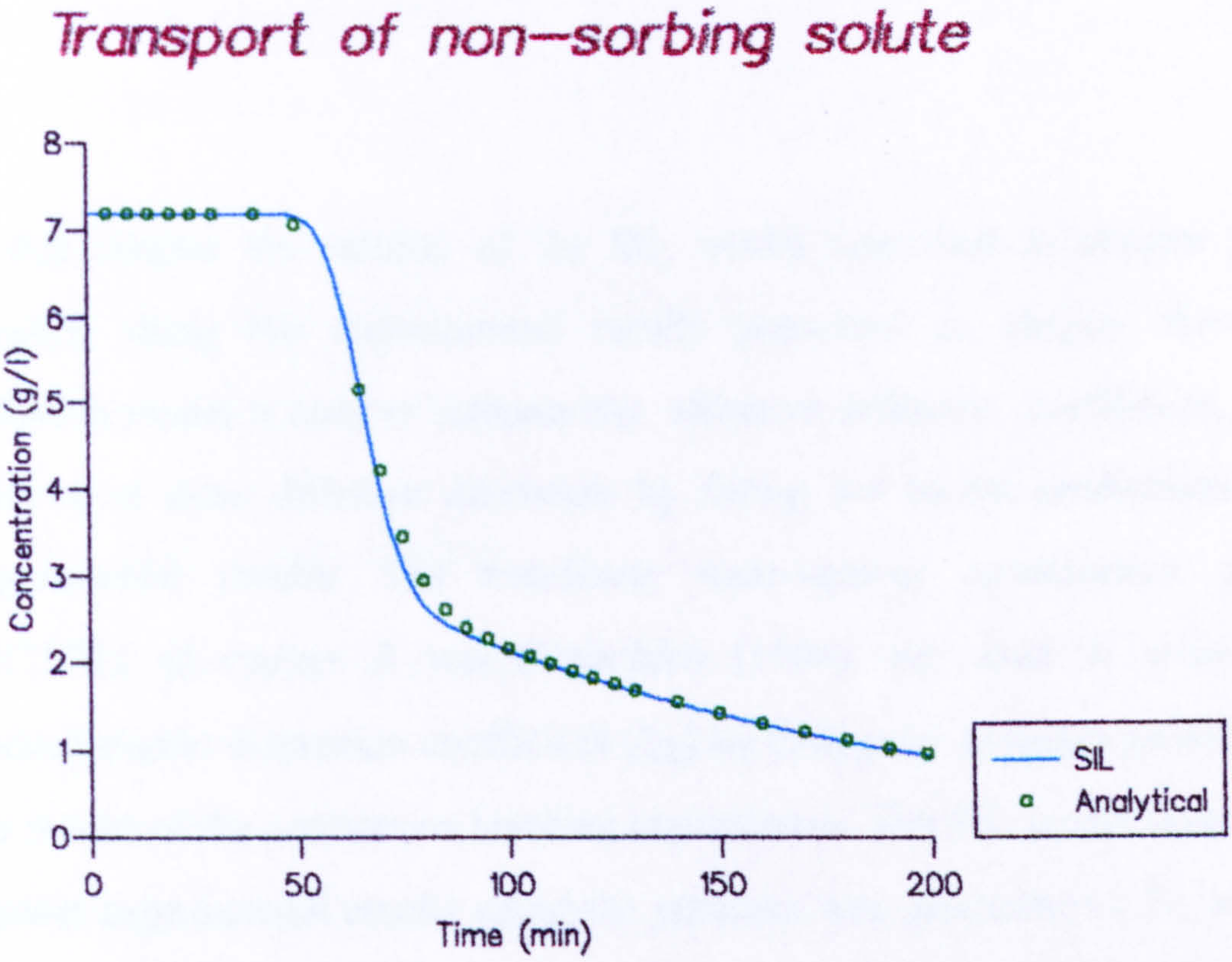

***Fig. 4.6*:** A plot of effluent concentration against time for SIL model and analytical solution results (data from *Rao et al.* (1980b) for leaching of $^{36}Cl^-$ out of column of inert porous ceramic spheres randomly distributed through glass beads (125 μm in diameter)).

Chapter Five

Simulation work

In this chapter the validity of the SIL model described in chapter four is checked using the experimental results presented in chapter three. The diffusion model is used to estimate the effective diffusion coefficient, D_e , of spheres of three different diameters by fitting the model predictions to the experimental results. The non-linear least-squares optimisation program CXTFIT1 of *Parker & van Genuchten* (1984) was used to estimate the hydrodynamic dispersion coefficient (D_s) by fitting the program predictions to the results of the continuous leaching experiments. The SIL model was checked against experimental results using the previous two parameters (D_e and D_s). After establishing the validity of the SIL model, the model was used to explore the behaviour of IL under different conditions.

5.1 Estimating of effective diffusion coefficient D_e

All the parameters required in the diffusion model (Eqs. 4.8, 4.9, and 4.10), except D_e , can be calculated from the experimental data (Table 3.1). D_e was found by optimising the fit with the experimental results using the values of the coefficient of determination as an indication of the goodness of the fit (*Hogg & Ledolter*, 1992).

Fig. 5.1 shows a plot between $C_m(t)/C_e$ against time for experimental and numerical results. Experiment and theory agree closely with all values of R^2 larger than 0.95. The optimised values of effective diffusion coefficient are shown in Table 5.1. The values changed slightly with sphere diameter, perhaps due to something related to the manufacturing process.

Table 5.1: Parameters of diffusion model.

Sphere diameter (mm)	No. of spheres	Ve (cm^3)	D_e* (mm^2/min)	D_e/D_0#	R^2
3	635	524.3	0.0528	0.525	0.955
6	70	523.0	0.0422	0.420	0.996
13	18	512.6	0.0575	0.572	0.996

* values are obtained by optimisation using diffusion model
R^2 = coefficient of determination
$D_0 = 0.101\ mm^2\ min^{-1}$ for KCl @ 20° C.

5.2 SIL model simulation

5.2.1 Continuous leaching

The results recorded from continuous leaching experiments (Section 3.3) were used to test the SIL model for continuous conditions. The model parameters were estimated independently before conducting the test as follows.

5.2.1.1 Estimating the SIL model parameters

The main parameters required by the SIL model are:

1) θ_m : The ratio of volume of mobile water (within the inter-sphere region) to total column volume

The total volume of the column occupied by the spheres is

$$V_T = L_r A$$

where

L_r = the height filled with spheres

A = cross-sectional area of the column.

The volume occupied by the spheres is

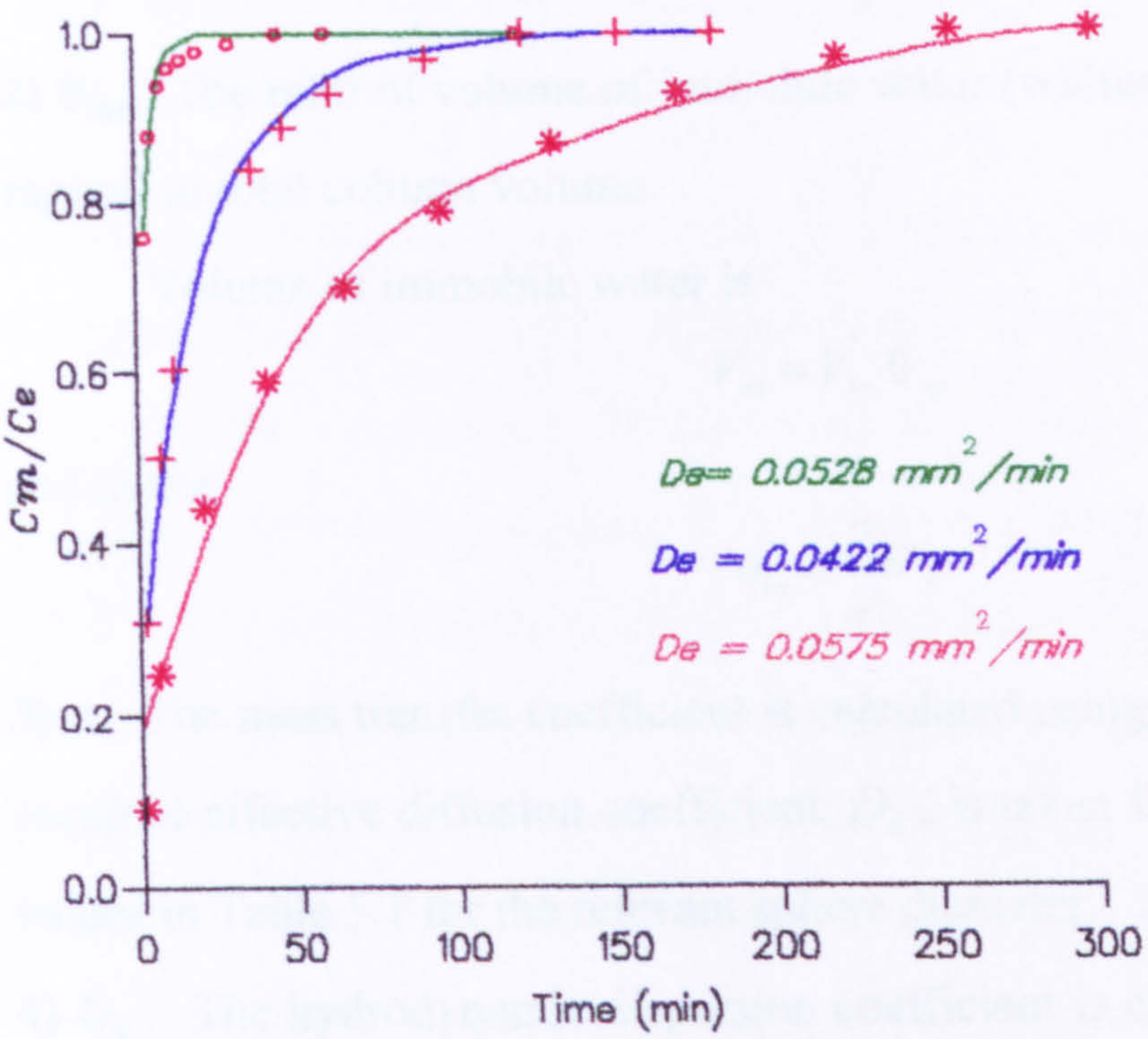

$C_m(t)$ = concentration of solute in the external solution

C_e = concentration of solute at equilibrium

***Fig. 5.1*:** A plot between $C_m(t)/C_e$ against time for experimental data and simulation results for each of three sphere diameters: o, 3 mm; +, 6 mm; *, 13 mm.

$$V_{sp} = \frac{W_S / \rho_p}{1-\theta_{sp}}$$

where

W_S = mass of oven-dried spheres

ρ_p = average particle density of the spheres

θ_{sp} = sphere porosity.

Thus the mobile water volume is

$$V_m = V_T - V_{sp} \quad .$$

and

$$\theta_m = \frac{V_m}{V_T} \quad .$$

2) θ_{im} : The ratio of volume of immobile water (within the intra-spheres region) to total column volume.

Volume of immobile water is

$$V_{im} = V_{sp}\ \theta_{sp}$$

and hence

$$\theta_{im} = \frac{V_{im}}{V_T} \quad .$$

3) α : The mass transfer coefficient is calculated using Eqs. 4.13a,b. The required effective diffusion coefficient, D_e , is taken from the optimised values in Table 5.1 for the relevant sphere diameter.

4) D_s : The hydrodynamic dispersion coefficient is estimated using the non-linear least-squares optimisation program CXTFIT1 of *Parker & van Genuchten* (1984). The parameters used in CXTFIT1 program for inert media are (in addition to D_s) v_d , β, and ω where

$$\beta = \frac{\theta_m}{\theta_m + \theta_{im}}$$

$$\omega = \frac{\alpha\ L_r}{v_d} \quad .$$

The only unknown parameter is D_s . The program optimises the value of D_s by fitting the predictions to the experimental results. Fig. 5.2a,c shows the results as a plot between effluent concentration and time. All the curves start with a plateau followed by a rapid decrease in the effluent concentration, when the less concentrated water reached the end of the column, and end with long tailing caused by the slow diffusion of solute from the spheres. The results from the optimisation program fit the experimental data throughout the curve with a value of $R^2 > 0.95$. However, the CXTFIT1 program slightly underestimated the effluent concentration at early stages and overestimated it at late stages. This may be ascribed to an underestimation of the value of Φ ($=\frac{\theta_m}{\theta_m+\theta_{im}}$).

Underestimating the Φ value resulted in similar early breakthrough and long tailing as observed by *van Genuchten & Wierenga* (1976).

The CXTFIT1 program is not applicable to a column containing mixture of sphere diameters (i.e., Exp. 2C) because it uses only one value for α. It is therefore necessary to optimise an "average" α, in addition to D_s . The SIL model is able to deal with different sphere diameters (and/or different effective diffusion coefficients) using Eq. 4.33 (Section 4.3.1.1) . The SIL model optimised the value of D_s by subsequently altering it until the model predictions best fitted the experimental data (Fig. 5.2b).

The SIL model was then run with all the determined parameters (Table 5.2) and assuming that the *off* time equals zero and that the *on* time equals the experiment times. The results are shown in Fig. 5.3 as graphs between effluent concentration and time. There is close agreement between the SIL model

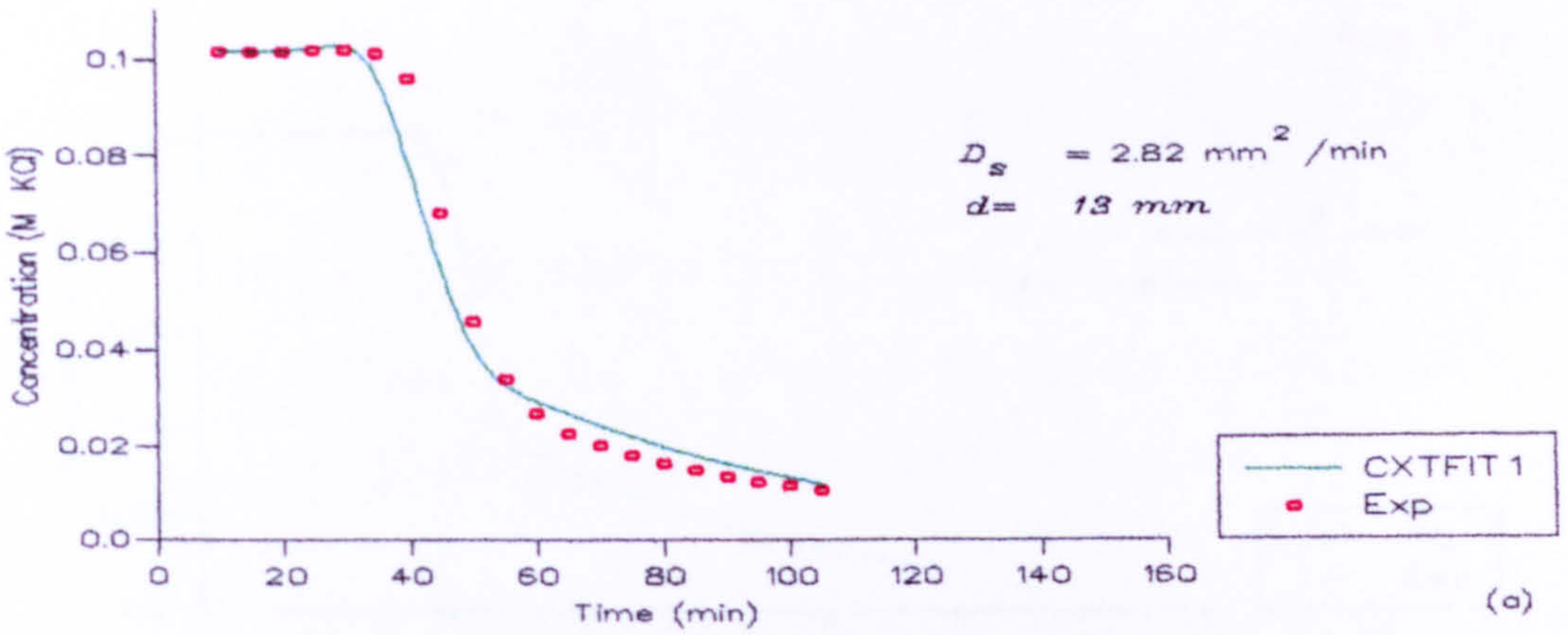

Fig. 5.2 : Plot of effluent concentration *vs.* time for optimising and experimental results for Exp. 1C, 2C, and 3C.

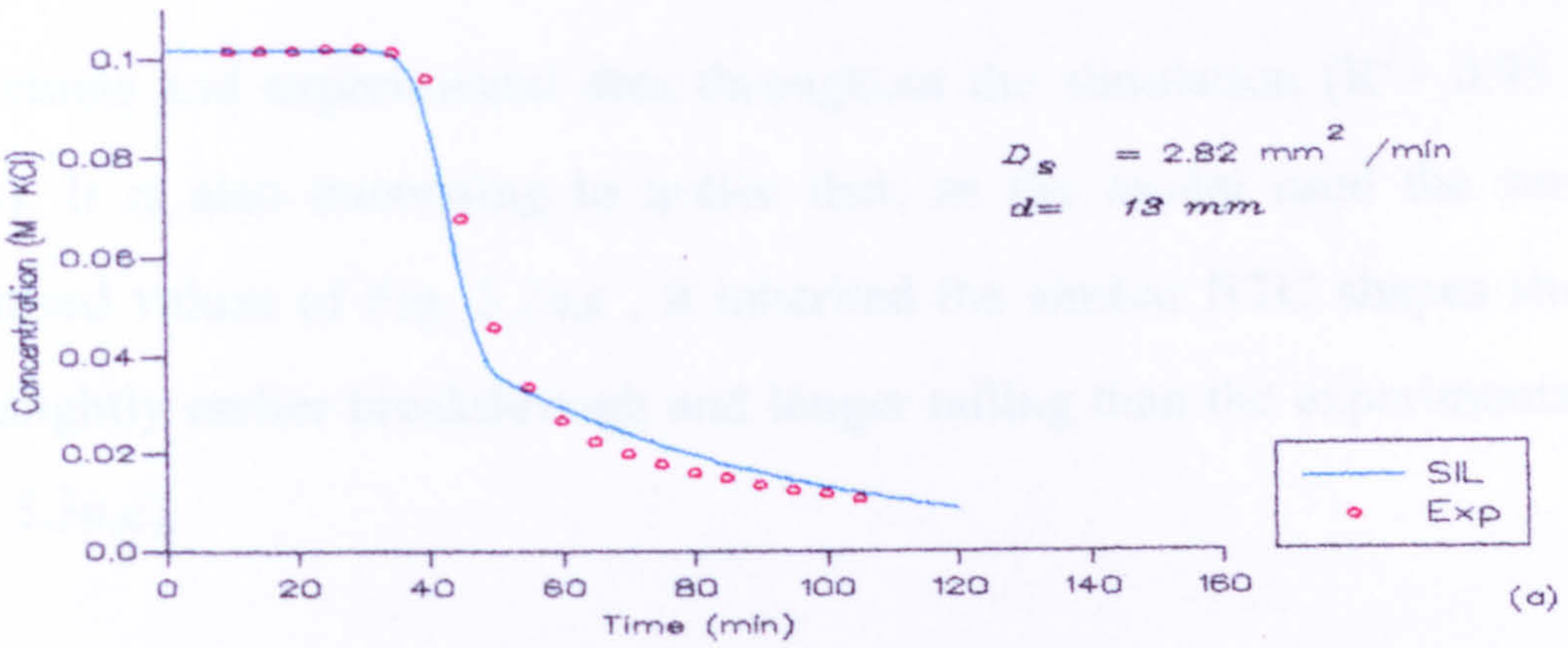

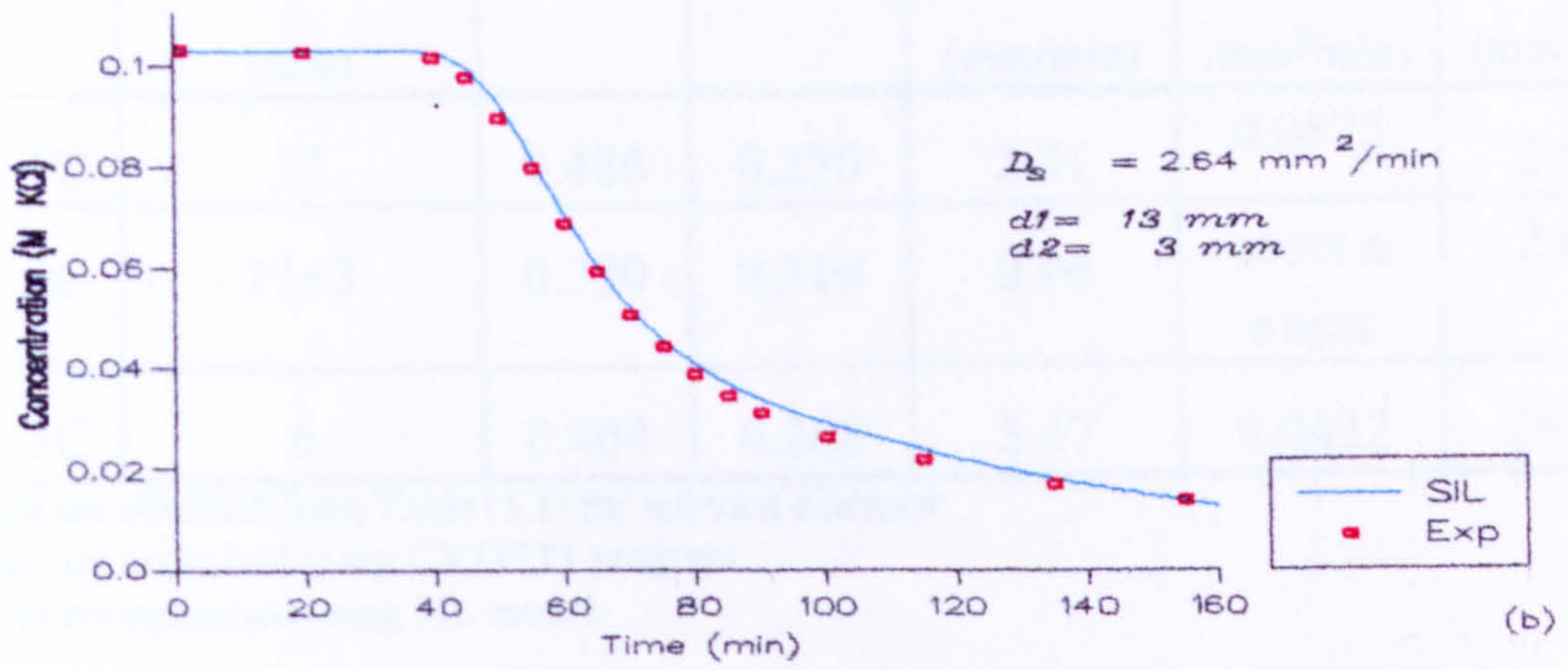

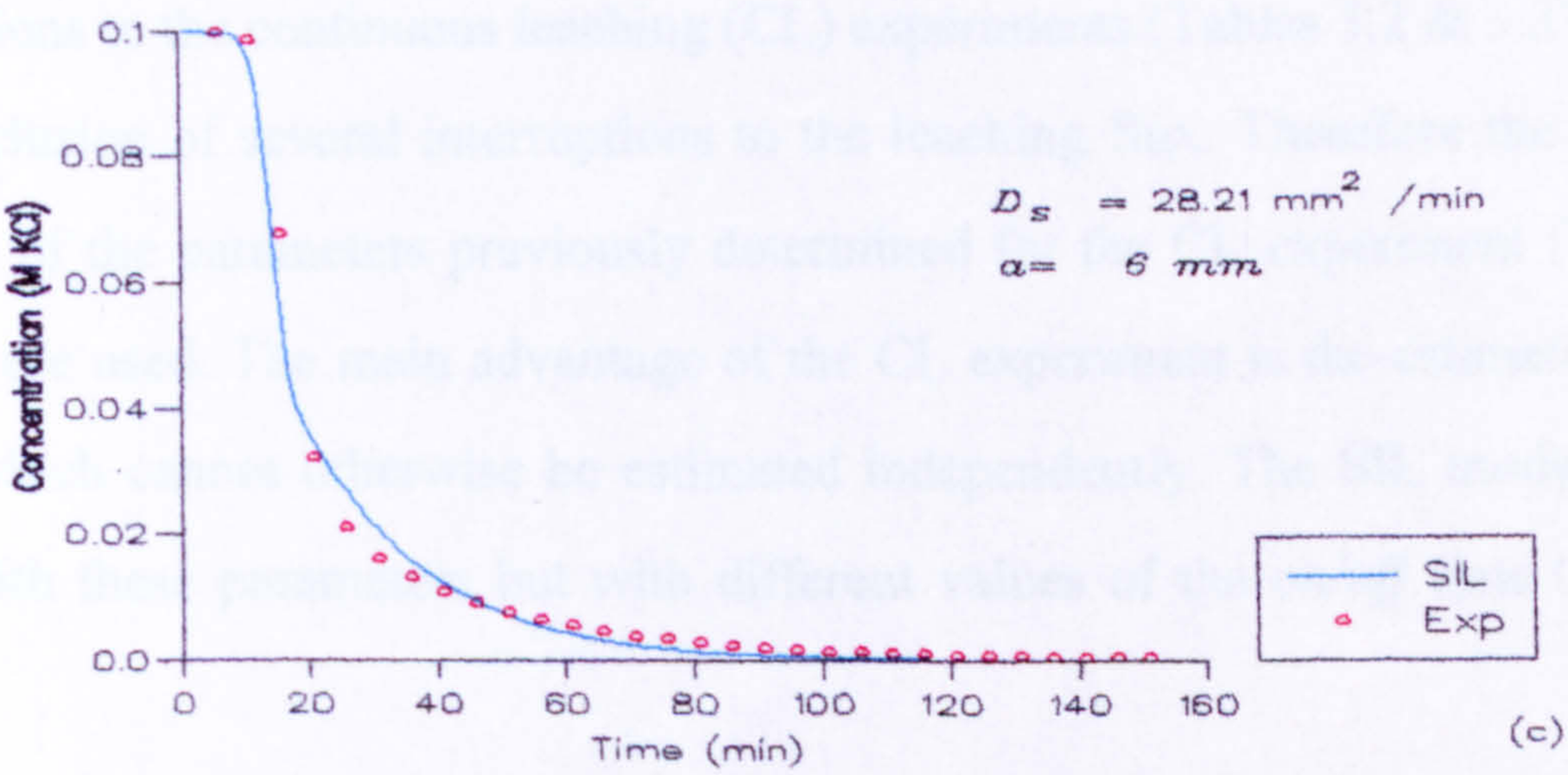

Fig. 5.3 **: Plot of effluent concentration *vs.* time for SIL model and experimental results for Exp. 1C, 2C, and 3C.**

predictions and experimental data throughout the simulation (R^2> 0.95 in all cases). It is also interesting to notice that, as the model used the same D_s optimised values of Fig. 5.2a,c , it inherited the similar BTC shapes showing also slightly earlier breakthrough and longer tailing than the experimental data (Fig. 5.3a,c).

Table 5.2: Parameter values for SIL model.

	Sphere diameter (mm)	θ_m	θ_{im}	v_d (mm/min)	D_e * (mm²/min)	D_s (mm²/min)
Exp. 1C	13	0.486	0.230	2.31	0.0575	2.82 #
Exp. 2C	13+3	0.320	0.310	0.96	0.0575 & 0.0528	2.64 !
Exp. 3C	6	0.404	0.268	5.47	0.0422	28.21 #

* values are obtained from Table (5.1) for relevant diameter
# values are optimised using CXTFIT1 program
! values are optimised using SIL model.

5.2.2 Intermittent leaching

The intermittent leaching (IL) experiments were performed under similar conditions to the continuous leaching (CL) experiments (Tables 3.2 & 3.3) with the inclusion of several interruptions to the leaching flux. Therefore the same values of the parameters previously determined for the CL experiment (Table 5.2) were used. The main advantage of the CL experiment is the estimation of D_s , which cannot otherwise be estimated independently. The SIL model will run with these parameters but with different values of the *on/off* time (Table 5.3).

Fig. 5.4 shows the results as plots between effluent concentration and time. Experimental data points follow the same general pattern as for the continuous leaching experiments (Fig. 5.3) with a decrease in effluent concentration after a certain time. Superimposed on this pattern are successive

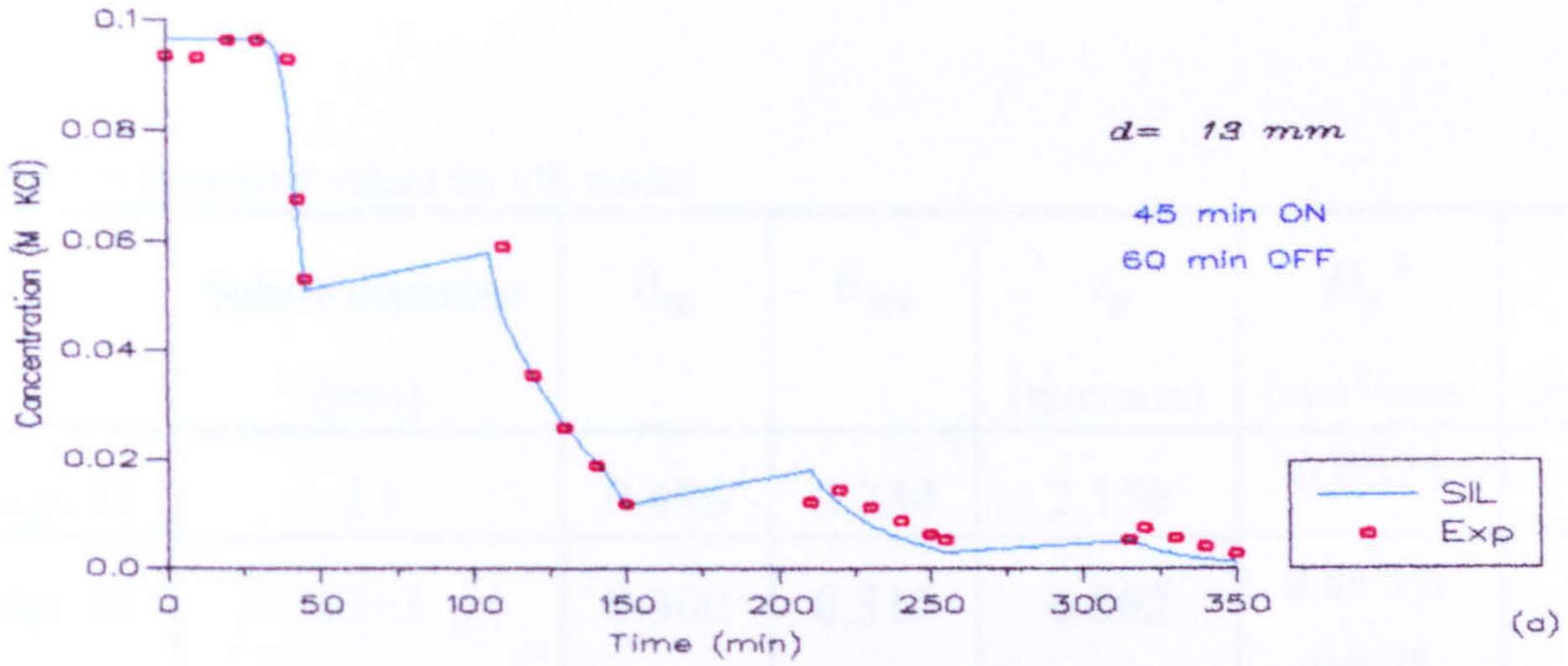

***Fig. 5.4*:** Plot of effluent concentration *vs.* time for SIL model and experimental results for Exps. 1I,2I, and 3I

Table 5.3: Parameter values for SIL model.

	Sphere diameters (mm)	θ_m	θ_{im}	v_d (mm/min)	D_e * (mm²/min)	D_s # (mm²/min)
Exp. 1I	13	0.486	0.230	2.150	0.0575	2.82
Exp. 2I	13+3	0.300	0.316	0.862	0.0575 & 0.0528	2.64
Exp. 3I	6	0.398	0.271	5.240	0.0422	28.21

* values are obtained from Table (5.1) for relevant diameter
\# values are taken from Table (5.2) of continuous leaching simulations.

short increases in concentration corresponding to measurements made after the end of each *off* period. The amplitudes of these peaks progressively decrease with successive *off* periods with the most rapid such decrease in Exp. 3I and the least rapid in Exp. 2I. These reflect the temporary increase in concentration of the mobile water during the *off* time due to continuing diffusion out of the spheres.

The model simulated the IL experimental data (Section 3.4) **without** any optimisation and excellent agreement between the model and experimental results for all the three cases was obtained ($R^2 > 0.95$). The small differences between the model predictions and experimental data could be because of some small differences between the experimental conditions of CL and IL (Table 5.3 & 5.2). The model was able to simulate the increase in effluent concentration at each *off* time using Eq. 4.18 for uni-sphere and mixed-sphere columns.

Using the parameters of Exp. 1I the model was run with two different conditions: 1) with different *on/off* times

2) with different inflow concentrations.

5.2.2.1 Running the SIL model with different on/off times

The model was run for different combinations of *on/off* times (5/15, 15/25, and 25/15 min). The results of the model were plotted as C/C_0 (relative concentration) *vs.* V/V_0 (pore volumes) (Fig. 5.5), where

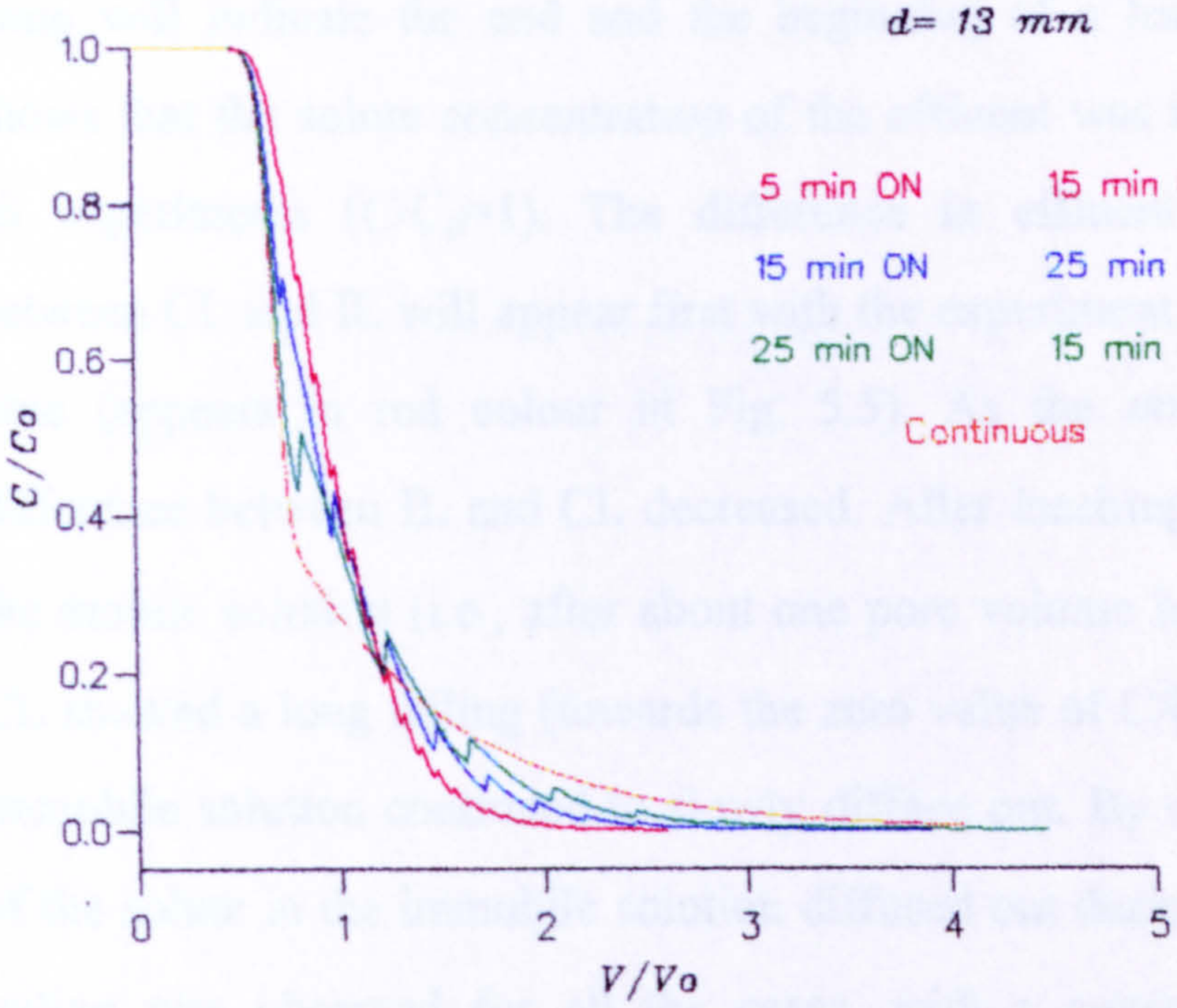

***Fig. 5.5*: Plot of C/C_0 *vs.* V/V_0 for different *on/off* times and under Exp. 1I conditions.**

C = the concentration of solute in the effluent

C_0 = the initial concentration of solute in both the mobile and immobile solution

V = the outflow volume

V_0 = the total volume of mobile and immobile water in the column (i.e., 1 pore volume).

With this dimensionless unit on *x*-axis, the *off* times will appear as an instantaneous increase in concentration because no flow occurred. Every such jump will indicate the end and the beginning of a leaching cycle. Fig. 5.5 shows that the solute concentration of the effluent was initially equal to C_0 in all experiments (C/C_0=1). The difference in effluent solute concentration between CL and IL will appear first with the experiment having the shortest *on* time (appears in red colour in Fig. 5.5). As the *on* time increased such difference between IL and CL decreased. After leaching most of the solute in the mobile solution (i.e., after about one pore volume has passed) the BTC of CL showed a long tailing (towards the zero value of C/C_0) as the solute in the immobile solution continued to slowly diffuse out. By contrast, in IL, as most of the solute in the immobile solution diffused out during the *off* times, shorter tailing was observed for all the cases, with a consequent greater effluent concentration at the beginning and a shorter tailing. More discussion about the effect of *on* and *off* times will come in Section 5.3.

However, this is not the whole story since the previous results showed only the effluent concentration and gave no information about how the solute concentration in the immobile solution was changing. Fig. 5.6 is a plot of simulated solute concentrations of the mobile, $C_m(z,t)$, and immobile, $C_{im}(z,t)$, solutions *vs.* depth for both CL and IL (with 5/15 min *on/off* cycles) at two values of V/V_0 (0.5 and 1.8). The concentration of both mobile and immobile solutions increased with depth, with the concentration of the immobile solution

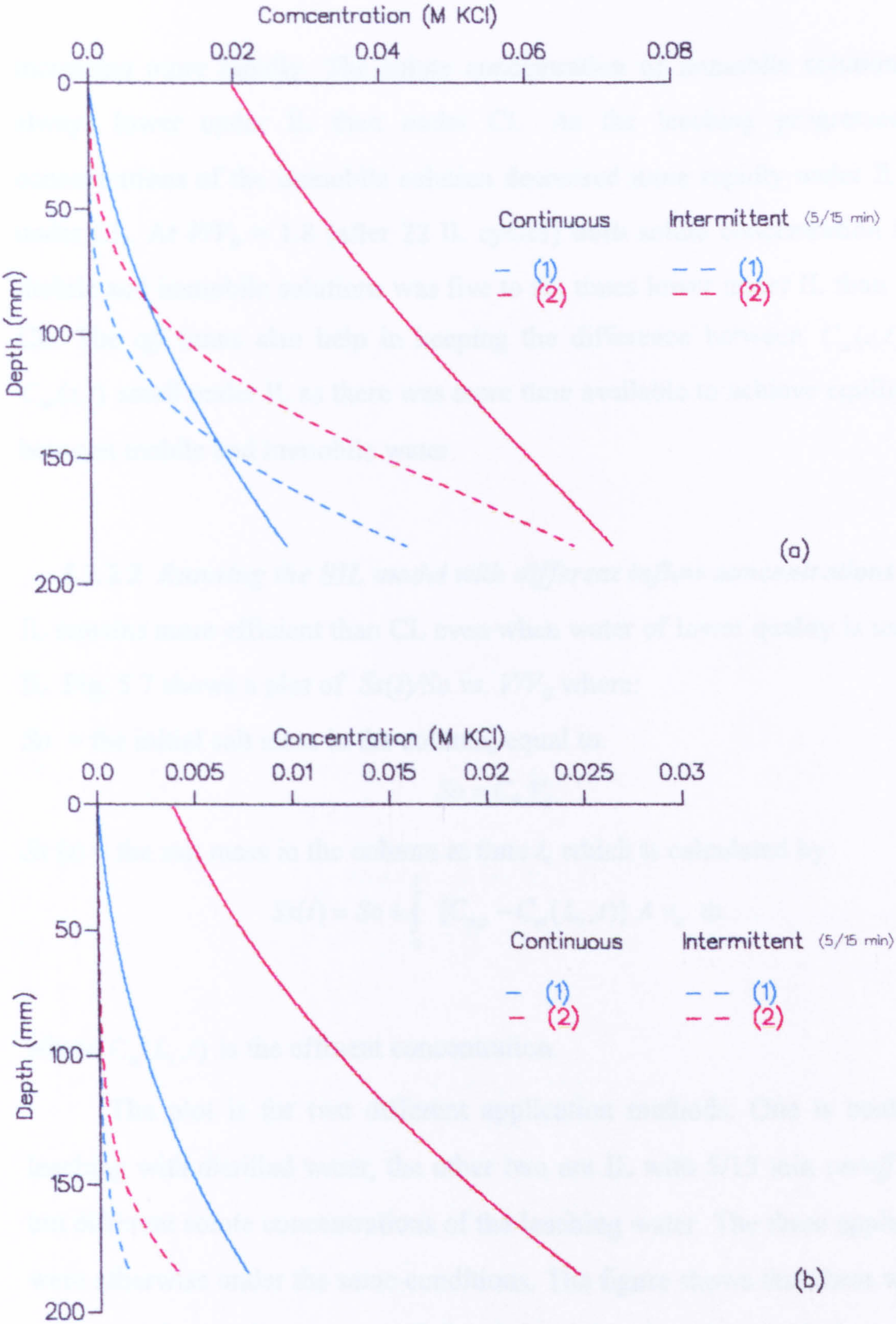

(1) $C_m(z,t)$
(2) $C_{im}(z,t)$

***Fig. 5.6*:** Concentration profile of solute in mobile (blue) and immobile (red) water at V/V_0 equal to (a) 0.5 (6 IL cycles) and (b)1.8 (22 IL cycles) respectively for intermittent and continuous leaching. Note different scales for the *x*-axis.

increasing more rapidly. The solute concentration of immobile solution was always lower under IL than under CL. As the leaching progressed the concentrations of the immobile solution decreased more rapidly under IL than under CL. At V/V_0 = 1.8 (after 22 IL cycles) both solute concentration in the mobile and immobile solutions was five to six times lower under IL than under CL. The *off* times also help in keeping the difference between $C_m(z,t)$ and $C_{im}(z,t)$ small under IL as there was more time available to achieve equilibrium between mobile and immobile water.

5.2.2.2 Running the SIL model with different inflow concentrations

IL remains more efficient than CL even when water of lower quality is used for IL. Fig. 5.7 shows a plot of $Ss(t)/So$ *vs.* V/V_0 where:

So = the initial salt mass in the column, equal to:

$$So = C_0 V_0$$

$Ss\ (t)$ = the salt mass in the column at time t, which is calculated by:

$$Ss(t) = So + \int_0^t \{C_{inp} - C_m(L_r,t)\}\, A\, v_d \ \mathrm{d}t$$

where $C_m(L_r,t)$ is the effluent concentration.

The plot is for two different application methods. One is continuous leaching with distilled water, the other two are IL with 5/15 min *on/off* cycles but different solute concentrations of the leaching water. The three applications were otherwise under the same conditions. The figure shows that there was less salt remaining in the column, all the time, under CL with distilled water than under IL with water containing 1 g solute /l. However, leaching of about 80% of solute ($Ss(t)/So$ = 0.2, requiring $V/V_0 \approx 1.2$) can be achieved with the same quantity of water by continuously leaching with distilled water or intermittently with water containing 1 g solute /l (point B in the graph).

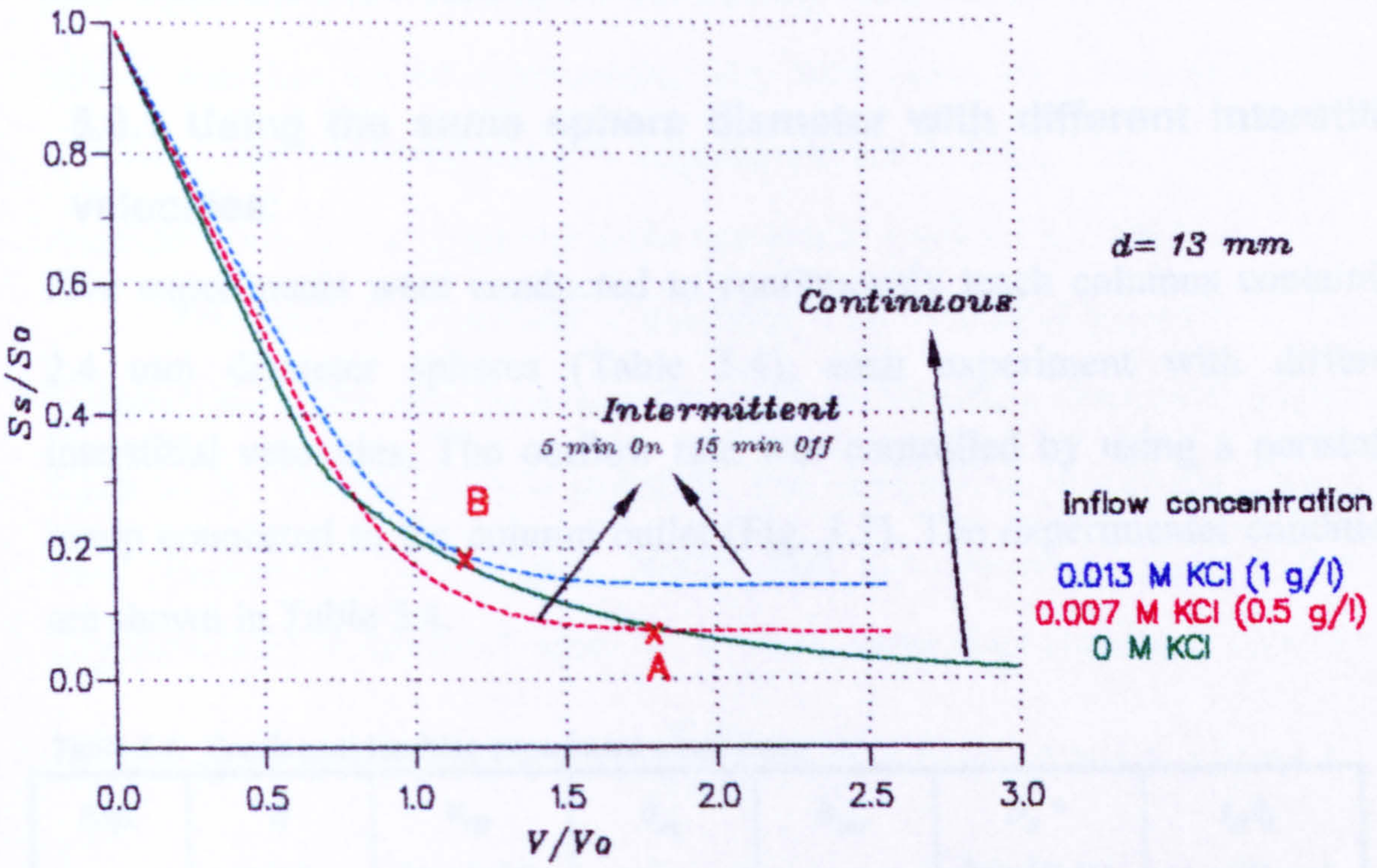

***Fig. 5.7*:** Plot between the relative amount of solute remaining in the column *vs.* the number of pore volumes for leaching continuously with distilled water and intermittently with low quality water (see text for point A and B).

When the column was intermittently leached with water containing 0.5 g solute /l, IL was more effective in leaching than CL after about 0.8 pore volumes, and remained so until about 90% of solute leached ($Ss(t)/So$ = 0.1 and $V/V_0 \approx 1.8$, point A in the graph). The salt load in the column remained constant under IL as solute kept entering with the inflow water.

Leaching salt-affected soil with low quality water will be of particular importance in arid and semi-arid areas where water of good quality is frequently unavailable.

5.3 Effect of *On/Off* time on intermittent salt leaching

5.3.1 Using the same sphere diameter with different interstitial velocities:

Five experiments were conducted to continuously leach columns containing 2.4 mm diameter spheres (Table 5.4), each experiment with different interstitial velocities. The outflow rate was controlled by using a peristaltic pump connected to the column outlet (Fig. 3.3). The experimental conditions are shown in Table 5.4.

Table 5.4: Continuous leaching experiment conditions.

Exp.	d (mm)	v_m (mm/min)	θ_m	θ_{im}	D_s * (mm^2/min)	t_o/t_l (L_r=250 mm)
1	2.4	1.89	0.498	0.226	1.61	73.98
2	"	5.56	0.484	0.232	7.70	25.15
3	"	22.78	0.486	0.231	90.30	6.13
4	"	48.11	0.514	0.190	256.70	2.90
5	"	101.00	0.496	0.227	294.50	1.38

v_m is mobile water velocity ($v_m = v_d / \theta_m$)
* The values are optimised using CXTFIT1 program.

These experiments were aimed both to test the SIL model at different velocities and to determine the hydrodynamic dispersion coefficients (D_s) for these experimental conditions (in the same manner as in Section 5.2.1). The estimated D_s values will be used later with intermittent leaching simulations.

Fig. 5.8 shows the results of SIL, CXTFIT1, and experimental data as effluent concentration against time for Exps. 1,2,3,4, and 5. The experimental data points follow the same general pattern for all the experiments with a rapid decrease in effluent concentration after a certain time depending, for these experiments, on the interstitial velocities. As the interstitial velocity increases, the less concentrated water reaches the column end sooner and the effluent concentration decreases earlier. The experiment with the highest interstitial velocity showed a longer tailing in its BTCs, because the solute of the mobile water leached out much faster than the solute of the immobile water, which then continued to slowly diffuse out causing such tailing. The SIL model was able to simulate all the experiments very well using the parameters in Table 5.4. However, when the velocity became extremely high (i.e., Exp. 5), some oscillatory behaviour occurred in the numerical results (Fig. 5.8e).

This oscillation (usually in the form of an overshoot) is typical of many higher-order difference equations designed to eliminate numerical dispersion (such as the Crank-Nicolson method). The oscillations slowly die away with time (*Peaceman* ,1977; *Smith,* 1985) and were found to occur when the displacement " residence " time ($t_o = \frac{L_r}{v_m}$) became very small and close to the characteristic diffusion time ($t_l = \frac{a^2}{15D_e}$) as shown in Table 5.4. However , by decreasing the time steps this problem disappeared (Fig. 5.8f).

5.3.1.1 SIL model predictions for IL

The SIL model was run with each experimental set of parameters (Table 5.4) but with different *on/off* time combinations. Twelve different intermittent leaching cycles were used to explore the effect of different *on* and *off* times and pore-water velocities on the water required to leach 90% of the initial salt

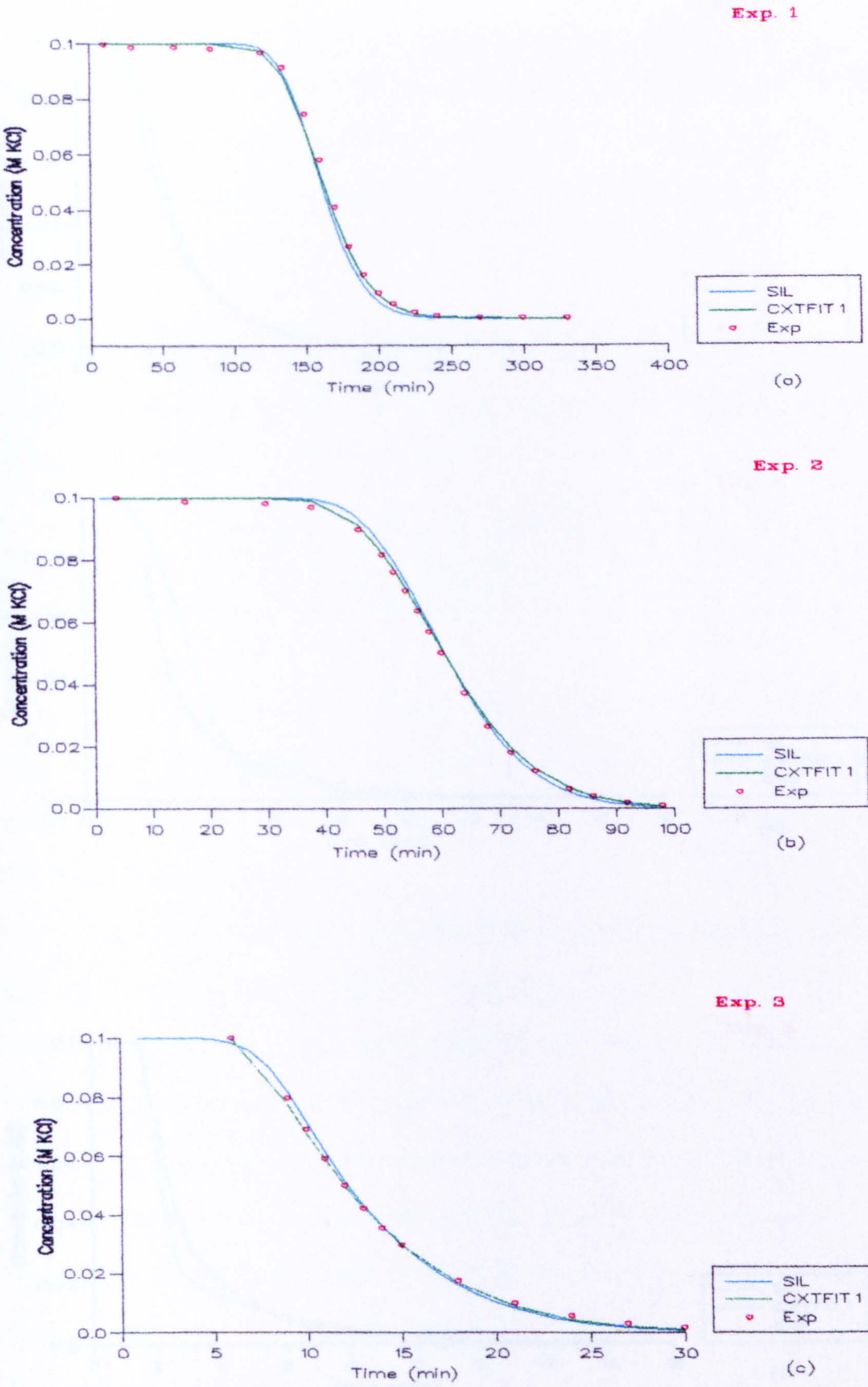

***Fig. 5.8*: A plots of effluent concentrations against time for experiments 1,2,3,4 and 5. Note (e) and (f) corresponed to the same experimental data set but having time steps of 1 min (SIL, e) or 1 s (SIL1, f) in the numerical integrations in the simulations. Note also the different *x*-axis scales.**

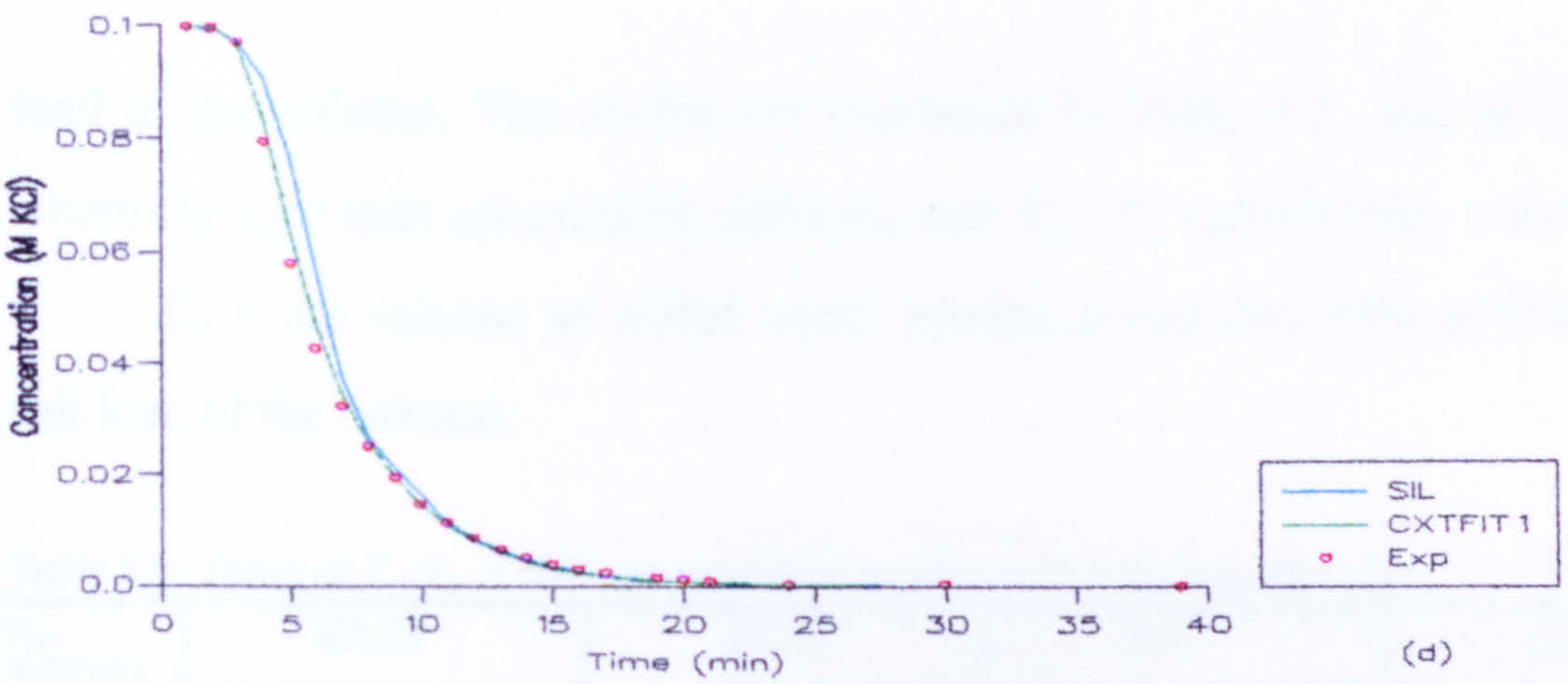
Exp. 4
Concentration (M KCl)
0.1
0.08
0.06
0.04
0.02
0.0
0
5
10
15
20
25
30
35
40
Time (min)
SIL
CXTFIT 1
Exp

(d)

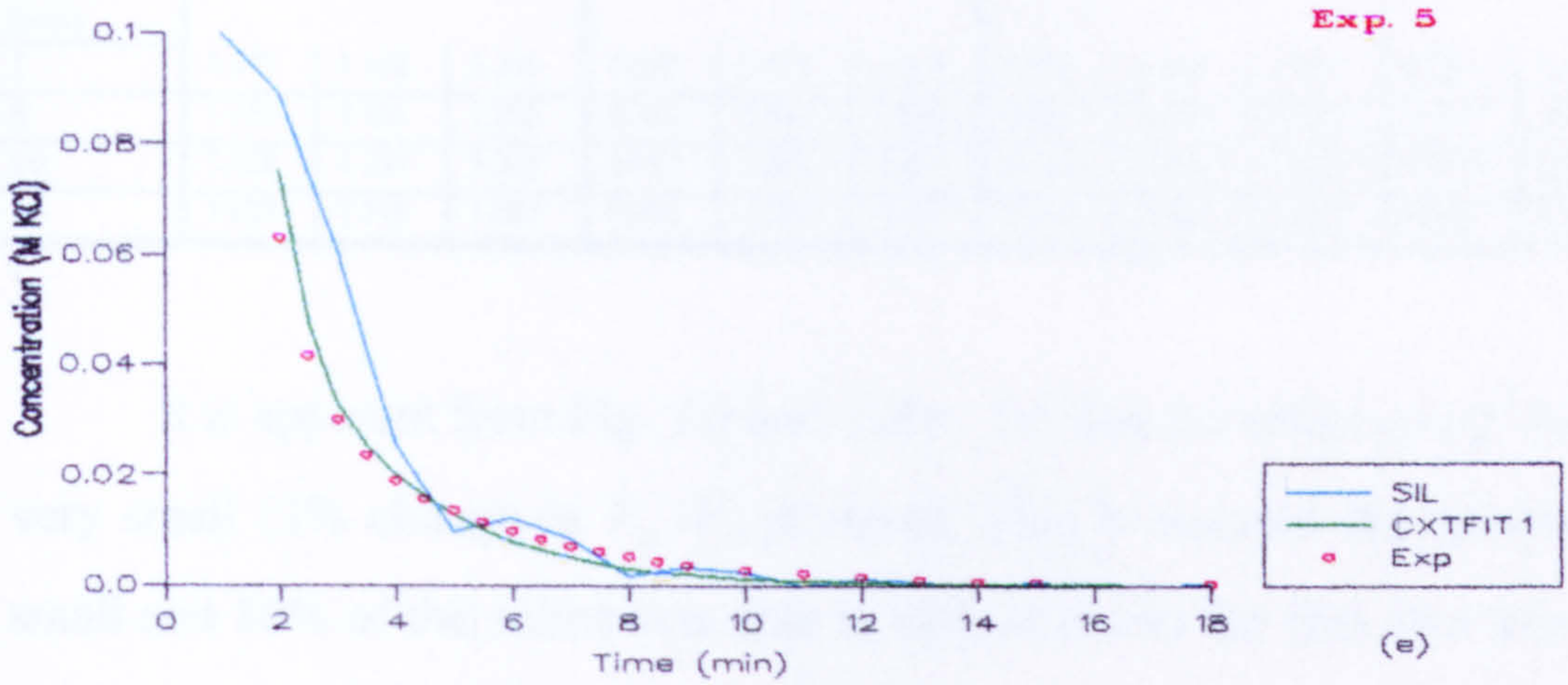
Exp. 5
Concentration (M KCl)
0.1
0.08
0.06
0.04
0.02
0.0
0
2
4
6
8
10
12
14
16
18
Time (min)
SIL
CXTFIT 1
Exp

(e)

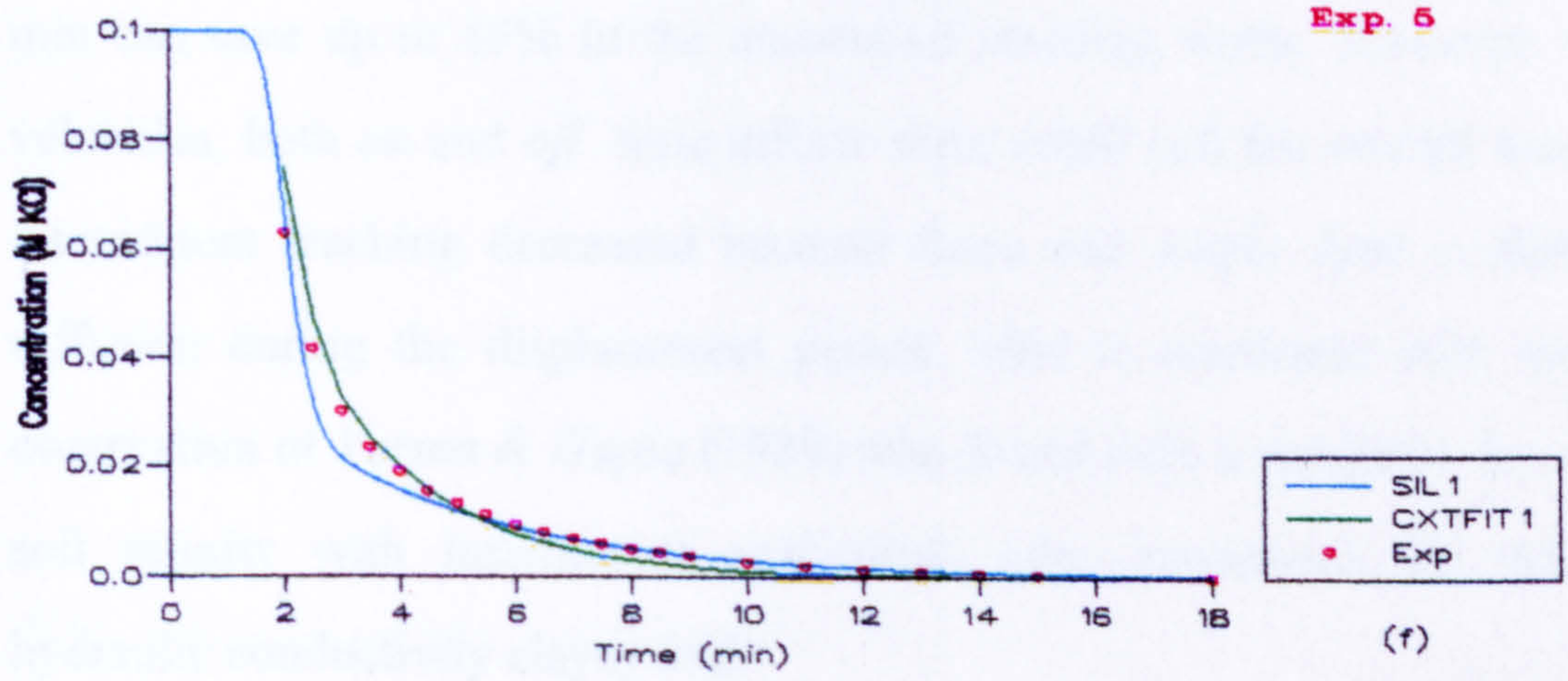
Exp. 6
Concentration (M KCl)
0.1
0.08
0.06
0.04
0.02
0.0
0
2
4
6
8
10
12
14
16
18
Time (min)
SIL 1
CXTFIT 1
Exp

(f)

load of the column. The results are presented in Table 5.5 and in Fig. 5.9 where the *x,y,z* axes are *on* time, *off* time, and V_a / V_o respectively, where

V_a = the volume of added water needed to remove 90% of the initial salt load of the column.

Table 5.5: Values of V_a/V_o at different velocities for spheres of diameter d=2.4 mm.

v_m (mm/min)	*48.11*			*22.78*			*5.56*			*1.89*		
On Time (min)	1	5	10	1	5	10	1	5	10	1	5	10
Off Time (min)												
1	1.047	1.162	1.206	0.995	1.070	1.087	0.924	0.945	0.951	0.909	0.915	0.917
5	1.030	1.151	1.205	0.985	1.064	1.084	0.921	0.942	0.950	0.907	0.914	0.917
10	1.028	1.149	1.205	0.983	1.063	1.083	0.920	0.941	0.950	0.907	0.914	0.917
15	1.028	1.149	1.205	0.983	1.063	1.083	0.920	0.941	0.950	0.907	0.914	0.917

It is apparent from Fig. 5.9 and Table 5.5 that the effect of *off* time was very small (2% change in V_a / V_o at most). This is because the spheres were small and 80% of the solute was able to diffuse out in the first five minutes of the rest period (Fig. 5.1).

The effect of *on* time was more distinct especially at high velocities. At v_m= 48.11 mm/min and *off* time =1 min, using 1 min *on* time rather than 15 min can save up to 15% in the amount of leaching water. However, at low velocities, both *on* and *off* time effects were small and the overall benefit of intermittent leaching decreased because there was ample time available for diffusion during the displacement period. This is consistent with the field observation of *Verma & Gupta* (1989) who found only a marginal decrease in soil salinity with intermittent application over continuous for their low hydraulic conductivity clayey soil.

5.3.2 Using different sphere diameters with the same interstitial velocity

Three continuous leaching experiments were performed (Table 5.6) with almost the same interstitial velocity but with different sphere diameters. A

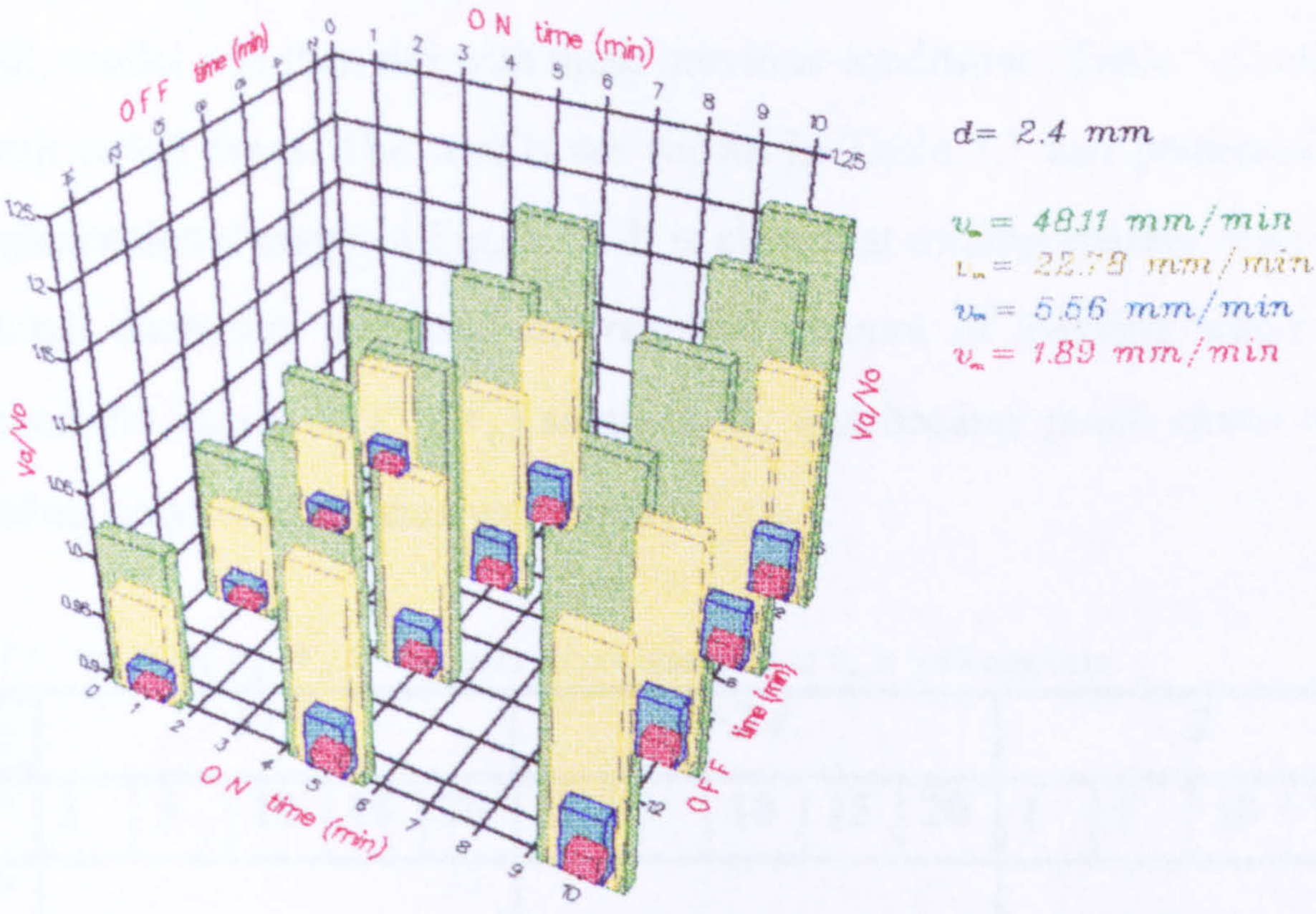

V_a/V_o = is number of pore volumes needed to remove 90% of the initial salt load of the column.

***Fig. 5.9*: Relationship between V_a/V_o, and *on* and *off* times for Exps. 1 to 4.**

mixture of 13 and 2.4 mm diameter spheres was used in Exp. 7 with mass proportions of 0.56 and 0.44 g g^{-1} respectively.

Table 5.6: Continuous leaching experiment conditions.

Exp.	d (mm)	v_m (mm/min)	θ_m	θ_{im}	D_s (mm^2/min)
6	13	4.18	0.425	0.259	3.2*
7	13+2.4 #	3.83	0.337	0.298	3.7
8	2	3.94	0.485	0.232	3.7*

* The values are optimised using CXTFIT1 program
# the mass proportions of sphere diameters 13 & 3 were 0.56 & 0.44 g g^{-1} respectively.

5.3.2.2 SIL model predictions for IL

The SIL model was then run with these previous conditions (Table 5.6) and for different *on/off* times. The results are shown in Table 5.7 and presented as a three-dimensional graph in Fig. 5.10. It is clear that mixing spheres with large and small diameters increased the required amount of leaching water (i.e., increased the values of V_a / V_o) significantly and became much closer to the case when only large spheres were used.

Table 5.7: Values of V_a / V_o for different sphere diameters at $v_m \cong 3.89$ mm/min.

d (mm)	*13*					*13+2.4*					*2*				
On Time (min)	1	5	10	15	20	1	5	10	15	20	1	5	10	15	20
Off Time (min)															
5	.948	1.07	1.17	1.23	1.28	.932	1.02	1.08	1.12	1.15	.912	.923	.976	.927	.928
10	.931	1.03	1.11	1.18	1.28	.926	.994	1.05	1.09	1.12	.912	.923	.976	.927	.928
20	.923	.996	1.07	1.13	1.18	.922	.978	1.03	1.06	1.09	.912	.923	.976	.927	.928
40	.918	.969	1.04	1.09	1.13	.919	.967	1.01	1.04	1.06	.912	.923	.976	.927	.928

The effect of changing *on /off* times on a column of small spheres (d=2 mm) was small as the velocity is low which allowed sufficient time for diffusion. With large spheres, the effect is clearer.

The effect of *On* time was found to be much greater than *off* time. For *off* time =5 min, the largest spheres (13 mm) would require 26% less leaching

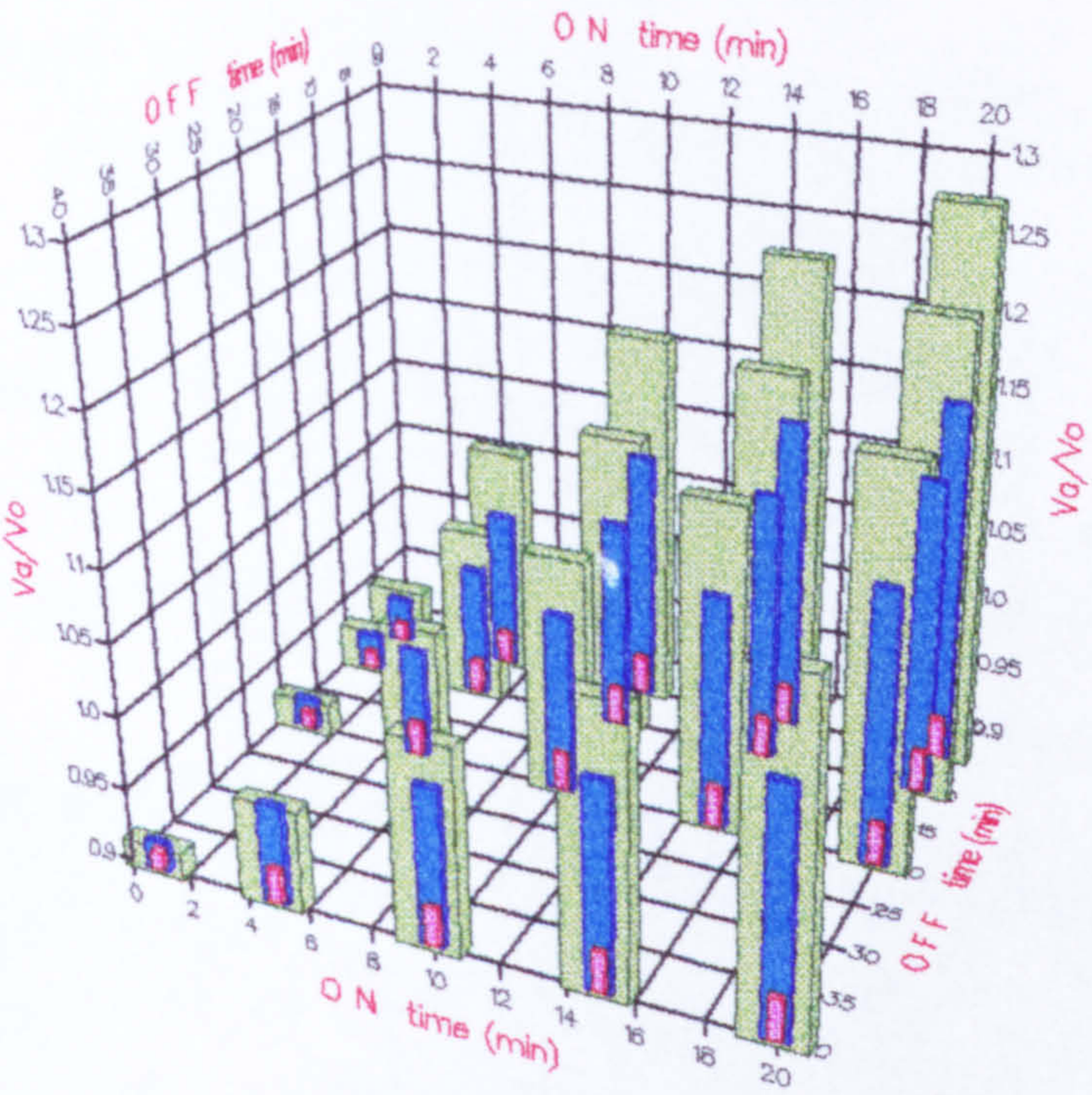

$v_m = 3.98\ mm/min$

$d = 13\ mm$

$d = (13\ \&\ 2.4)\ mm$

$d = 2\ mm$

V_a/V_o = is number of pore volumes needed to remove 90% of the initial salt load of the column.

***Fig. 5.10*:** Relationship between V_a/V_o, and *on* and *off* times for Exps. 6 to 8.

water if the 1 min *on* time had been used than if the 20 min *on* time had been used, and up to 19% less leaching water in the case of a mixture of spheres.

The effect of *Off* time was very small for the smallest spheres (almost no change was noticed in V_a/V_o values when the *off* time varied for sphere diameter = 2 mm). This effect was clearer for large spheres, though it was still smaller than the effect of *on* time. For the "best" case (largest diameter, longest *on* time) 13% of the leaching water could be saved if an *off* time of 40 min had been used instead of 5 min.

Fig. 5.10 also can be transformed to show the effect of *on/off* times on the total leaching time needed to remove the 90% of the initial salt load of the column (TT). Fig. 5.11 and Table 5.8 demonstrates these results. Comparing Fig. 5.11 with Fig. 5.10 shows that saving water is always accompanied by longer leaching times.

Table 5.8: Values of total leaching time (min) for different sphere diameters at $v_m \cong 3.89$ mm/min.

d (mm	*13*				*13+2.4*				*2*			
On Time (min)	5	10	15	20	5	10	15	20	5	10	15	20
Off Time (min)												
5	215	177	167	162	205	164	151	146	187	140	125	117
10	311	225	198	186	302	212	184	170	280	187	156	141
20	504	324	266	238	495	311	251	221	467	281	219	188
40	882	526	405	344	880	509	385	323	840	468	344	281

Tables 5.7 & 5.8 show that for the largest spheres at 20/5 min *on/off* time combination, the number of pore volumes required to leach 90% of solute was 1.28, and the time taken for leaching was 162 min. With a 5/40 *on/off* time combination the number of pore volumes was 0.918, and the leaching time was 882 min. This means that, to save 28% of the leaching water, the total duration of leaching increased 5.4 times. Using the same argument with the same *on/off* time combinations it can be shown that, for the mixture of spheres, increasing the total leaching time six-fold saved 20% of water. For the smallest spheres,

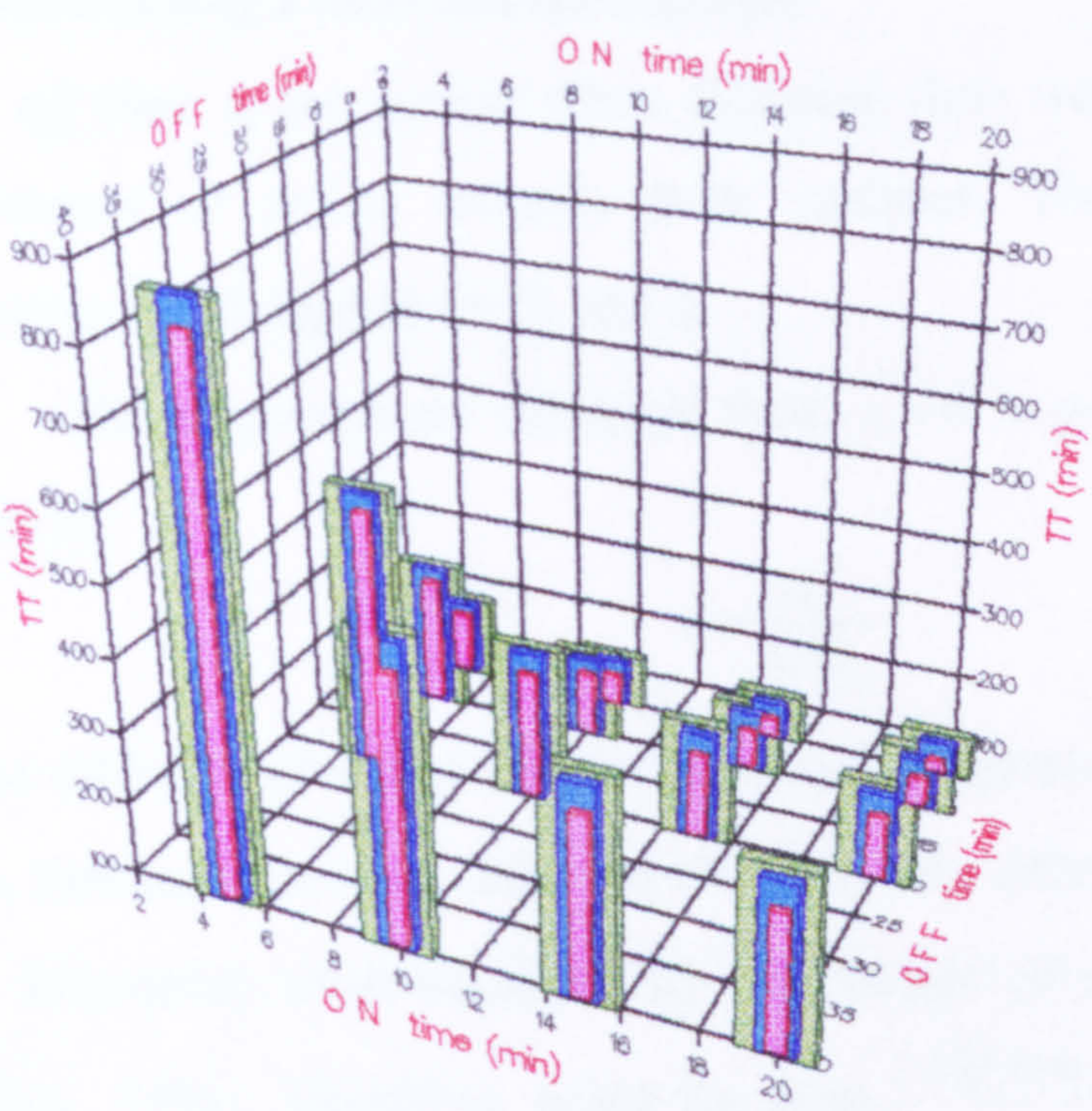

$v_m = 3.98\ mm/min$

$d = 13\ mm$

$d = (13\ \&\ 2.4)\ mm$

$d = 2\ mm$

TT **= is the total time needed to remove 90% of the initial salt load of the column.**

Fig. 5.11: Relationship between time to remove 90% of the initial salt load and *on* and *off* times, Exps. 6 - 8.

increasing the leaching time by 718% saved only 1.7% of water. It can be concluded that using IL is much more worthwhile if the proportion of large aggregates in the soil is high. However, the time taken by IL is still very large and is the main disadvantage of this method.

• Constructing a dimensionless graph:

The *off* time is the period when diffusive flow within the spheres allows a movement of solute towards their surfaces. The total amount of such movement will depend on D_e and a.

The characteristic diffusion time, t_i, of a sphere is given (*Passioura*, 1971) by:

$$t_i = \frac{a^2}{15D_e} \quad .$$

If the diffusion of solute within the sphere is assumed to be well approximated by a first-order process, then the characteristic diffusion time is the inverse of the first-order mass-transfer rate coefficient (*Passioura*, 1971; *Hayot* & *Lafolie*, 1993). Therefore, using the ratio $\left(\frac{Off\ time}{t_i}\right)$ as a dimensionless unit instead of *off* time might be more appropriate because the effects of D_e and a on diffusion results will be minimised.

The mobile phase "residence" time is the average time required for the displacing fluid to reach the column end (assuming *piston* flow in the mobile phase) and is calculated by:

$$t_o = \frac{L_r}{v_m} \quad .$$

It also might be more appropriate to use the ratio $\left(\frac{On\ time}{t_o}\right)$ as a dimensionless unit instead of *on* time.

To calculate the characteristic diffusion time ($t_i = \frac{a^2}{15D_e}$) the sphere radius, a, should be known. For a mixture of spheres, a is taken as the *mean radius* of mixture.

Estimating a mean radius for a mixture of sphere diameters:

Five different estimates of mean radii have been used in the literature to model the diffusion out of mixed sizes of spherical aggregates:

1) *MSR*= the mean square radius for the mixture (*Passioura*, 1971)

$MSR = \sqrt{(\sum a_i^2 P_i)}$

where

a_i = the radius of sphere i

P_i = the mass proportion of spheres of radius a_i

2) *MVR*= mean sphere volume radius (*Han et al.*, 1985)

$MVR = \left(\sum a_i^3 P_i\right) / \left(\sum a_i^2 P_i\right)$

3) *MER*= mean exchange area radius (*Hayot & Lafolie*, 1993)

$MER = 3 / \left(\sum S_i . P_i\right)$

S_i is the surface to volume ratio , for spheres $S = 3 / a$.

4) *WAR*= weighted-average radius (*Rao et al.*, 1982)

$WAR = \left(\sum P_i \frac{1}{a_i^2}\right)^{-\frac{1}{2}}$

5) *VWR*= volume-weighted average radius (*Rao et al.*, 1982)

$VWR = \sum a_i . P_i$.

To ascertain which mean radius is the best to average a mixture of sphere diameters, a FORTRAN-77 computer code depending on Eqs. 4.8 & 4.10, for diffusion of solute out of inert spheres into a fixed volume of solution, was developed (Appendix C). The equations were:

$$\frac{M_t}{M_\infty}=\frac{C_0-\overline{C}_{im}(t)}{C_0-C_e}=1-\sum_{n=1}^{\infty}\frac{6\gamma(\gamma+1)\exp(-\frac{D_e q_n^2 t}{a^2})}{9+9\gamma+q_n^2\gamma^2}$$

and

$$C_m(t)=\frac{V_{ws}\left(C_0-\overline{C_{im}}(t)\right)}{V_e}$$

where V_{ws} is the total volume of water inside the spheres.

The code was used in two different ways :

A)- The code was run with the real medium which consisted of a mixture of sphere diameters. At each time step, Eqs. 4.8, and 4.10 will be solved for each diameter.

B)- The code was run assuming a "simpler" medium consisting only of one mean radius. The model was run with each of the five definitions of mean radii above.

The values V_{ws} , C_0 , and V_e were kept the same in each case. Case A is considered as the reference to compare the utility of the results of case B.

Six tests were done with these two cases:

Test 1 (T1): Assuming two spheres of diameter 13 mm, and 177 spheres of diameter 2.4 mm (giving a mass proportion for large spheres P_1=0.727, and for small spheres P_2=0.273).

Test 2 (T2): Assuming two spheres of diameter 13 mm, and 370 spheres of diameter 2.4 mm (giving a mass proportion for large spheres P_1=0.56, and for small spheres P_2=0.44).

Test 3 (T3): Assuming 12 spheres with diameters normally distributed around a mean value of 5 mm, and a value of standard deviation $\sigma = 0.05$.

Test 4 (T4): Assuming 12 spheres with diameters normally distributed around a mean value of 5 mm, and a value of $\sigma = 0.1$

Test 5 (T5): Assuming 12 spheres with diameters log-normally distributed around a mean value of 5 mm, and a value of $\sigma = 1$.

Test 6 (T6): Assuming 12 spheres with diameters log-normally distributed around a mean value of 5 mm, and a value of $\sigma = 1.5$.

For each test, the code was run as A and B above and values of the coefficient of determination between the result of case A and case B are given. The results are shown numerically in Table 5.9 and as an example the results of first test are shown as a plot of external concentration against time in Fig. 5.12.

It is clear from the values of coefficient of determination (Table 5.9) that, for the case of diffusion from spheres, the mean square radius (*Passioura*, 1971) , *MSR*, was the best to average the mixture of radii for tests 1,2,3 and 4. However, for the last two tests (5&6) the volume-weighted average radius, *VWR*, was slightly better to average the mixture.

The mixture in Exp. 7 was similar to that of test T2, thus the best average radius is *MSR*. i.e.,

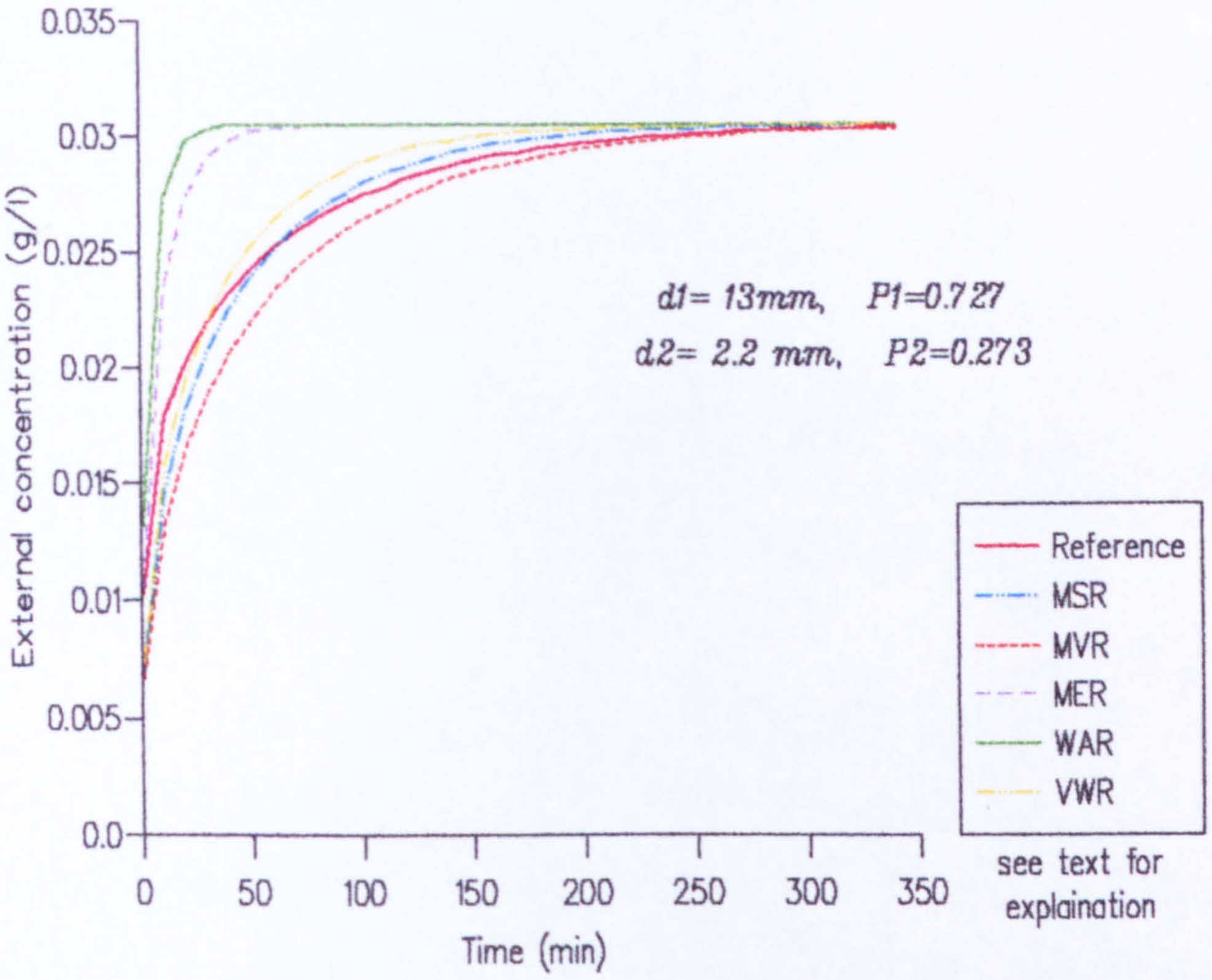

d_i = the diameter of sphere *i*

P_i = the mass proportion of spheres of diameter d_i

Fig. 5.12: A plot between the external solution concentration and diffusion time.

Table 5.9: Values of different average radii and their R^2.

		*MSR**	*MVR**	*MER**	*WAR**	*VWR**
T1	*Mean radius* (mm)	5.83	6.74	2.82	2.04	5.25
	R^2	0.958	0.881	0.536	0.326	0.952
T2	*Mean radius* (mm)	5.14	6.68	2.08	1.63	4.29
	R^2	0.811	0.352	0.219	0.048	0.810
T3	*Mean radius* (mm)	6.03	6.22	5.70	5.54	5.95
	R^2	0.998	0.994	0.993	0.983	0.998
T4	*Mean radius* (mm)	7.37	7.47	6.98	6.59	7.31
	R^2	0.999	0.998	0.991	0.962	0.999
T5	*Mean radius* (mm)	29.93	32.60	26.19	24.02	28.88
	R^2	0.991	0.957	0.970	0.922	0.993
T6	*Mean radius* (mm)	25.98	28.21	21.95	19.95	24.98
	R^2	0.990	0.962	0.952	0.892	0.991

* see text for explanation.

$$MSR = \sqrt{(\sum a_i^2 P_i)} = \sqrt{\left(6.5^2\ 0.56 + 1.2^2\ 0.44\right)} = 4.93 \text{ mm.}$$

The mean radius value calculated above was then used to calculate the characteristic diffusion time, t_l, value for the mixture of sphere diameters of Exp. 7. However, using a mean radius to predict the BTCs from miscible displacement experiments, instead of the real size distribution, was shown by *Hayot & Lafolie* (1993) to give a very different result. They stated that an average radius cannot be found such that this "homogeneous" medium behaves similarly to the porous medium presenting an aggregate size distribution, and that the possibility of finding an average radius depends not only on the characteristics of the size distribution but also on the velocity. Therefore, the previously calculated mean radius was used only to calculate the value of t_l.

The SIL model was run again with the same conditions of Exps. 6, 7, and 8, but for new *on/off* times as shown in Table 5.10. The new *on/off* times were chosen so that all the experiments would have the same dimensionless values on the *x,y* axes. The results are shown in Fig. 5.13 where the *x* and *y* axes become $\left(\frac{On\ time}{t_o}\right)$ and $\left(\frac{Off\ time}{t_i}\right)$ respectively.

Table 5.10: Values of ($On\ time / t_o$) and ($Off\ time / t_i$) for Fig. 5.13.

d (mm)	*13*				*13+2.4*				*2*		
On Time (min)	5	10	20		5	10	20		5	10	20
On Time/t_o	0.083	0.167	0.334		0.077	0.153	0.306		0.078	0.157	0.315
Off Time (min)	14	38	76	114	8	23	46	69	1	2	3
Off Time/t_i	0.262	0.712	1.425	2.137	0.261	0.749	1.499	2.248	0.792	1.584	2.376

Representing the results on this dimensionless graph did not eliminate the differences between the results of the experiments as was expected. It can be noted that the number of pore volumes hardly changed for small diameter spheres, while it changed almost in the same manner for the mixture and large spheres. This is mainly because the graph used residence time rather than using other "characteristic displacement" times similar to the characteristic diffusion time where the influence of hydrodynamic dispersion and the lateral diffusion from the spheres are taken into account. Such a characteristic time is out of reach because the amount of solute leached during time *t* is in a very complicated mathematical form, especially with the existence of *off* times and different sphere sizes, and will include the integral of the analytical solution of Eq. 2.17 with time.

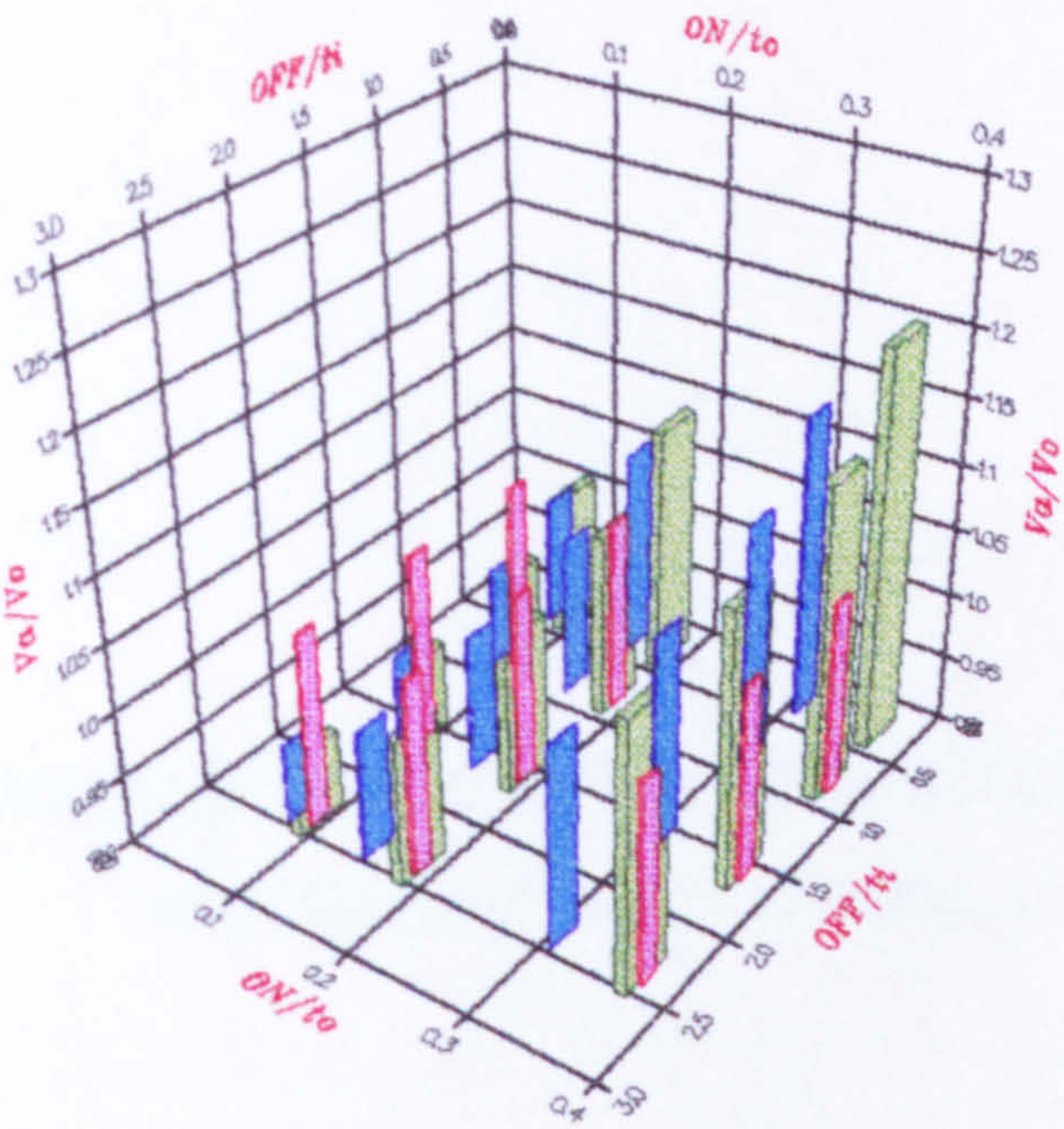

v_a = 3.98 mm/min

d= 13 mm
d= (13 & 2.4) mm
d= 2 mm

V_a/V_o = is number of pore volumes needed to remove 90% of the initial salt load of the column.

Fig. 5.13: Relationship between $\left(\frac{On\ time}{t_o}\right)$, $\left(\frac{Off\ time}{t_i}\right)$, and V_a/V_o for Exps. 6 to 8.

PART TWO

Solute transport through columns of soil aggregates under saturated condition

Chapter Six

Transport of sorbing solutes through soils

This chapter introduces the theory of solute adsorption/desorption from soil surfaces. Equilibrium and kinetic adsorption models are introduced and the different principles of modelling transport of sorbed solute through the soils are explored.

6.1 Definitions

Adsorption is the net accumulation of matter at the interface between a solid phase and an aqueous solution phase (*Sposito*, 1989). It differs from precipitation because it does not include the development of a three-dimensional molecular structure. The material accumulating in such a two-dimensional molecular arrangement at an interface is the *adsorbate*. The solid surface on which it accumulates is the *adsorbent*. A molecule or an ion in the soil solution that can potentially be adsorbed is termed an *adsorptive* (*Sposito*, 1989).

The processes of adsorption involve changes in the composition of the bulk phase from which the amount adsorbed can be described. It is necessary to distinguish between changes of bulk phase composition brought by *ab*sorption, when a given chemical substance is partitioned between two bulk phases, and

by *ad*sorbtion at an interface (*Burchill et al.*, 1981). Desorption refers to the reverse of the process of adsorption.

A general term *sorption* (or sometimes retention) is used when it is not desired, or is experimentally impossible, to distinguish between adsorption and absorption.

6.2 Equilibrium adsorption isotherms

The partitioning of solutes between liquid and solid phases in a porous medium as determined by laboratory experiments is commonly expressed in two-ordinate graphical form where the mass adsorbed per unit mass of dry solids "adsorbent" (S) is plotted against the concentration of solute in solution (C). This graphical relation of S *versus* C and the equivalent mathematical description are known as *isotherms*. This term derives from the fact that adsorption experiments are normally conducted at constant temperature (*Freeze et al.*, 1979).

Solute sorption-desorption processes in soils have been quantified by several scientists along two different lines. One represents equilibrium reactions and the second represents kinetic or time-dependent types of reactions. A comprehensive survey of sorption relationships for reactive solutes in soil has been undertaken by *Travis & Etnier* (1981). Table 6.1 shows some selected equilibrium and kinetic-type isotherms.

Equilibrium isotherms are those for which solute reaction is assumed to be fast or instantaneous. The *Langmuir* and *Freundlich* isotherms are perhaps the most commonly used equilibrium isotherms (*Rubin & Mercer*, 1981). Kinetic isotherms represent slow reactions in which the amount of solute sorption is function of contact time. Most common is the first-order kinetic reaction (*Selim*, 1992).

Table 6.1: Selected equilibrium and kinetic-type models (from *Selim*, 1992).

Model	Formulation[b]
Equilibrium type	
Linear	$S = K.C$
Freundlich (nonlinear)	$S = K.C^b$
Langmuir	$S = \omega C S_{max}/(1 + \omega C)$
Langmuir with sigmoidicity	$S = \omega C S_{max}/(1 + \omega C + \sigma/C)$
Kinetic type	
First order	$\partial S/\partial t = k_f(\Theta/\rho)C - k_b S$
n-th order	$\partial S/\partial t = k_f(\Theta/\rho)C^n - k_b S$
Irreversible (sink/source)	$\partial S/\partial t = k_s(\Theta/\rho)(C - C_p)$
Langmuir kinetic	$\partial S/\partial t = k_f(\Theta/\rho)C(S_{max} - S) - k_b S$
Elovich	$\partial S/\partial t = A \exp(-BS)$
Power	$\partial S/\partial t = \hat{K}(\Theta/\rho)C^n S^m$
Mass transfer	$\partial S/\partial t = \hat{K}(\Theta/\rho)(C - C^*)$

[b] A, B, b, C^*, C_p, $\hat{K}$, K_d, k_b, k_f, k_s, n, m, S_{max}, ω, and σ are adjustable model parameters.

6.2.1 Langmuir equilibrium isotherm

Langmuir (1918) described the relationship between S and C as:

$$S = \frac{K_1 C}{1 + K_2 C} \tag{6.1}$$

where K_1 and K_2 are constants,

S = is the mass of adsorbate per mass of dry adsorbent, and

C = is the equilibrium concentration of solute in the solution after adsorption has occurred.

This isotherm was developed to describe the adsorption of gases by solids assumming that the surface of a solid possesses a finite number of adsorption sites. If the gas molecule strikes an unoccupied site, it is adsorbed, otherwise it is reflected back. The derivation of this equation can be found in most Physical chemistry textbooks (e.g., *Adamson*, 1976; *Rubin & Mercer*, 1981).

This isotherm has been used extensively in the literature (see *Travis & Etnier* , 1981) e.g., for sorption of Pb, Cd, Zn and P among other elements.

6.2.2 Freundlich equilibrium isotherm

Freundlich (1926) suggested the following empirical equation for describing the sorption of ions or molecules from a liquid onto a solid surface:

$$S = K C^b \tag{6.2}$$

where

K = is the distribution coefficient, found by *Baes & Sharp* (1983) to be a very variable and unpredictable parameter, which may range from 1 dm^3 g^{-1} to many orders of magnitude greater depending on solute and soil characteristics, including pH.

b = is a constant, typically having a value of $b < 1$ (*Selim*, 1992).

The Freundlich equation has been used widely to describe the sorption of solutes by soils and numerous examples exist in the literature. *Travis & Etnier* (1981) mentioned thirty cases where the Freudlich equation has been used, including sulphate, Cd, Zn, Cu and P.

The resulting curve of the Freundlich equation is normally parabolic. However, in the especial case of a *linear isotherm* where b=1 (as for many pesticides at dilute concentrations (*Tan*, 1982)), the S versus C data will plot as a straight line, i.e.:

$$S = K C \tag{6.3}$$

and so

$$\frac{\mathrm{d}S}{\mathrm{d}C} = K \quad .$$

The difference between Freundlich and Langmuir isotherms is shown in Fig. 6.1. At very high concentrations, $K_2 C$ in the Langmuir equation reaches such a value that the factor 1 (Eq. 6.1) can be neglected and S approaches a constant (K_1 / K_2),whereas, in the Freundlich equation, S continues to increase as C increases. In other words, the Langmuir equation describes a system

where, at high values of C, the surface of adsorbents becomes saturated and adsorption reaches a maximum (*Tan*, 1982). This makes it more appropriate in soils which have a finite adsorption capacity (*Jury et al.*, 1991). However, in practice, since the adsorption maximum is rarely observed, the Freundlich equation is used more often than the Langmuir (*Hinz et al.*, 1994).

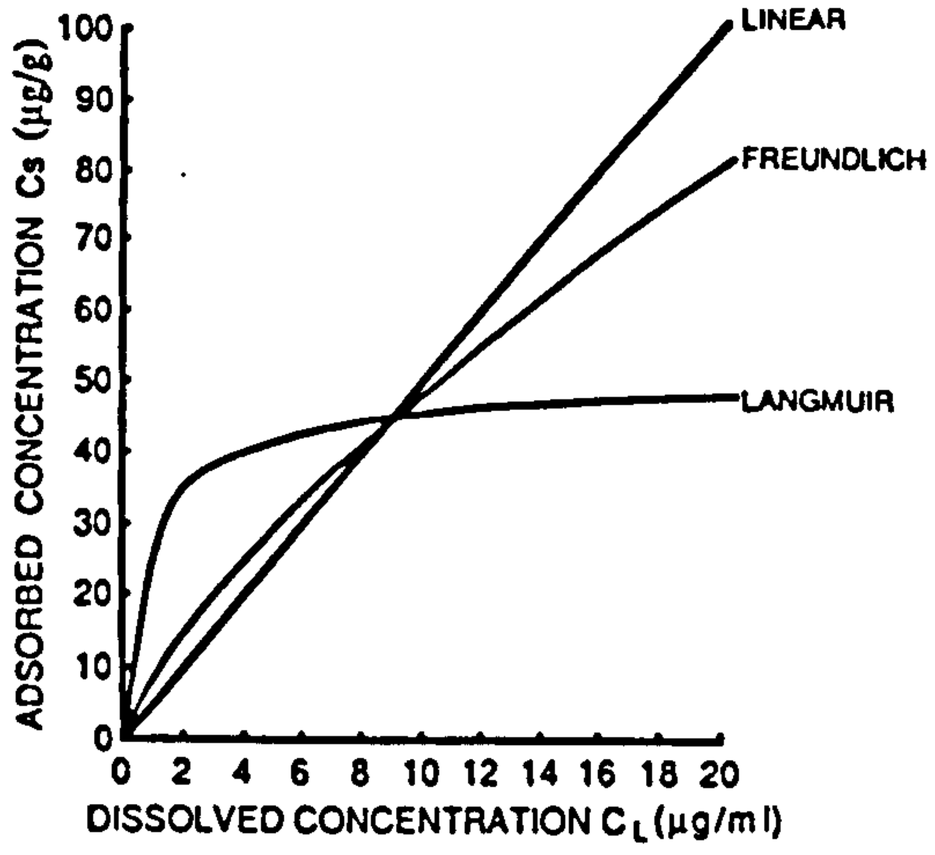

Fig. 6.1: Adsorption isotherm shapes. (from *Jury*, 1991)

6.2.3 First-order kinetic isotherm

A number of empirical models have been proposed to describe kinetic sorption reactions of solute. The earliest one is the first-order kinetic reaction (*Selim*, 1992):

$$\frac{\partial S}{\partial t} = k_f(\theta/\rho)\,C - k_b S \qquad (6.4)$$

where

k_f, k_b = the forward and backward rates of reactions,

θ = volumetric water content, and

ρ = soil bulk density.

Eq. 6.4 assumes that the rate of solute sorption by the soil matrix is related to the difference between what can be adsorbed at some concentration (C) and what has already been adsorbed (*Travis & Etnier*, 1981). For small

values of k_f and k_b , the rate of sorption is slow and strong kinetic dependence is anticipated. In contrast, for large values of k_f and k_b , the sorption reaction is a rapid one (*Selim*, 1992). At large times ($t \rightarrow \infty$), when the rate of sorption approaches zero, the above equation yields

$$S = \frac{\theta\, k_f}{\rho\, k_b} C = K\, C$$

which results in a linear equation similar to that for linear isotherms (Eq. 6.3) in which equilibrium conditions were assumed.

Eq. 6.4 has been used frequently to describe the sorption kinetics of several different organic chemicals, some heavy metals and more frequently the sorption kinetics of P in soils (*Travis & Etnier*, 1981).

6.3 Modelling transport of sorbing solutes through soils

Adsorption reactions are important processes governing the fate of dissolved solutes. Models of solute transport must therefore incorporate a mathematical description of the chemical processes of adsorption as well as the physical processes of convection and dispersion . The classical equation that describes one-dimensional solute transport by saturated flow (with no solute source or sink) is (Eq. 2.14):

$$\frac{\partial C}{\partial t} + \frac{\rho}{\theta}\frac{\partial S}{\partial t} = D_s \frac{\partial^2 C}{\partial z^2} - v \frac{\partial C}{\partial z} \qquad (6.5)$$

where

v = is the average pore water velocity

C = is solute concentration

D_S = is the hydrodynamic dispersion coefficient

z = the space co-ordinate (positive downwards).

The transport of reactive solute through the soil is dependent on the rate of adsorption-desorption between the soil solution and the solid phase. In a general sense, this reaction can be either a kinetic one, in which the relative amount of solute in soil solution and in soil matrix is changing with time, or it can be an equilibrium situation in which the above relationship is attained rapidly and thereafter remains constant (*Travis & Etnier*, 1981).

The modelling of adsorption within the transport models therefore takes one of two directions depending on the acceptance or not of the *local equilibrium assumption* "LEA", defined by *Valocchi* (1985) as: "If the microscopic processes are "fast enough" with respect to the bulk fluid flow rate, then reversible sorption reaction can be assumed to be in the state of local chemical equilibrium". In other words, an equilibrium situation is one in which the rate of adsorption between the soil solution and solid phase is much faster than the rate of change in concentration of solute in the soil solution because of any other cause (*Travis & Etnier*, 1981).

6.3.1 Equilibrium model

If the LEA is accepted, the adsorption reaction is considered to be instantaneous, and may be described by one of the equilibrium adsorption isotherms.

The most common approach for modelling the adsorption term $\frac{\partial S}{\partial t}$ (in Eq. 6.4) has been to assume instantaneous adsorption and a simple linear relation between S and C (*Parker et al.*, 1984; *Nielsen et al.*, 1986). i.e.;

$$S = K\,C$$

so that

$$\frac{\partial S}{\partial t} = \frac{\partial S}{\partial C}\frac{\partial C}{\partial t} = K\,\frac{\partial C}{\partial t}$$

and Eq. 6.4 becomes:

$$R\frac{\partial C}{\partial t} = D_s\frac{\partial^2 C}{\partial z^2} - v\ \frac{\partial C}{\partial z} \qquad (6.6)$$

where R is the retardation factor, given by;

$$R = 1 + \frac{\rho K}{\theta} \quad .$$

The validity of LEA is found to depend upon a complex interplay between macroscopic transport properties (flow velocity, hydrodynamic dispersion, time variation of mass input) and microscopic properties (e.g. effective diffusion coefficient, aggregate size, distribution coefficient) (*Valocchi*, 1985). *Nielsen et al.* (1986) found that the equilibrium model did not perform well with aggregated soils. For these soils it is likely that chemical transport is not at equilibrium and the equilibrium model fails. Various kinetic and diffusion-limited rate laws (i.e., non-equilibrium models) have consequently been proposed to describe this non-equilibrium transport.

6.3.2 Non-equilibrium models

As reviewed by *van Genuchten & Cleary* (1979), most models of non-equilibrium adsorption of solutes flowing through soils and aquifers have been based upon the assumption that only one of the microscopic mechanisms is rate limiting. These models are usually grouped in two classes :

1- chemical non-equilibrium models, or

2- physical non-equilibrium models.

6.3.2.1 Chemical non-equilibrium models

A chemical non-equilibrium model that did lead to improved transport description is the **two- site** model (*Selim et al.*, 1976). The model assumes that adsorption sites can be divided into two fractions; adsorption on one fraction (type 1 site) is assumed to be instantaneous (linear Freundlich isotherm), while

adsorption on the other fraction (type 2 site) is assumed to be time-dependent. This leads to the following equation (*Nkedi-Kizza et al.,* 1984; *Parker et al.*, 1984);

$$\left(1+\frac{F\rho K}{\theta}\right)\frac{\partial C}{\partial t}+\frac{\rho}{\theta}\frac{\partial S_2}{\partial t}=D_s\frac{\partial^2 C}{\partial z^2}-v\frac{\partial C}{\partial z} \qquad (6.7)$$

and, assuming first-order kinetic reaction in site 2 similarly to Eq. 6.3, one obtains:

$$\frac{\partial S_2}{\partial t}=\alpha_k\left[(1-F)KC-S_2\right] \qquad (6.8)$$

where

α_k = first-order kinetic rate coefficient

F = is the mass fraction of type 1 "equilibrium" sites

S_2 = is the adsorption on type 2 "kinetic" sites.

The parameters F and α_k were found in most studies to be functions of pore-water velocity, and generally could not be derived independently from batch equilibrium studies. They usually needed to be adjusted for different experiments carried out on the same soil column (*Nielsen et al.*, 1986).

6.3.2.2 Physical non-equilibrium models

These are sometimes also called **two-region** models. In such models fluid inside the porous aggregate is assumed to be stagnant, and thus the total liquid phase is partitioned into mobile (inter-aggregate) and immobile (intra-aggregate) water regions. The soil also is divided into two regions (*van Genuchten & Wierenga*, 1976):

a) the mobile water soil region, located sufficiently close to the mobile water phase for equilibrium (assumed) between solute in the mobile liquid and that adsorbed by this part of the soil mass, and

b) the immobile water soil region, located mainly around the immobile water inside the aggregates. Adsorption occurs here only after the chemical has diffused through the liquid barrier of the immobile liquid phase (diffusion controlled).

Transport models are based on first-order exchange of solute between the mobile and immobile water regions. *Van Genuchten & Wierenga* (1976) extended this concept of mobile-immobile water to include Freundlich-type equilibrium adsorption processes. Their equations are of the form;

$$\theta_m R_m \frac{\partial C_m}{\partial t} = \theta_m D_s \frac{\partial^2 C_m}{\partial z^2} - v_m \theta_m \frac{\partial C_m}{\partial z} - \theta_{im} R_{im} \frac{\partial C_{im}}{\partial t} \qquad (6.9)$$

$$\theta_{im} R_{im} \frac{\partial C_{im}}{\partial t} = \alpha \left(C_m - C_{im} \right) \qquad (6.10)$$

where

α = mass transfer rate coefficient between the mobile and immobile water regions

C_m = solute concentration in the mobile water (within the inter-aggregate region)

C_{im} = solute concentration in the immobile water (within the intra-aggregate region)

θ_m = volume of mobile water as a proportion of total column volume

θ_{im} = volume of immobile water as a proportion of total column volume.

R_m and R_{im} = retardation factors, which account for equilibrium-type adsorption processes in the mobile and immobile water regions, respectively. For a Freundlich adsorption isotherm, they are given by:

$$R_m = 1 + \frac{f\rho K\, bC_m^{\,b-1}}{\theta_m}$$
$$R_{im} = 1 + \frac{(1-f)\rho K\, bC_{im}^{\,b-1}}{\theta_{im}} \qquad (6.11)$$

where f represents the fraction of adsorption sites that equilibrate with the mobile liquid phase. As f increases, more adsorption occurs in the mobile water region and relatively less inside the aggregates, the total adsorption remaining the same, and the chemical will appear later in the effluent (Fig. 6.2). When $f = 1$, adsorption takes place only in the mobile water soil region. The influence of all the model parameters on the shape of the breakthrough curves (BTCs) was comprehensively studied by *van Genuchten & Wierenga* (1976).

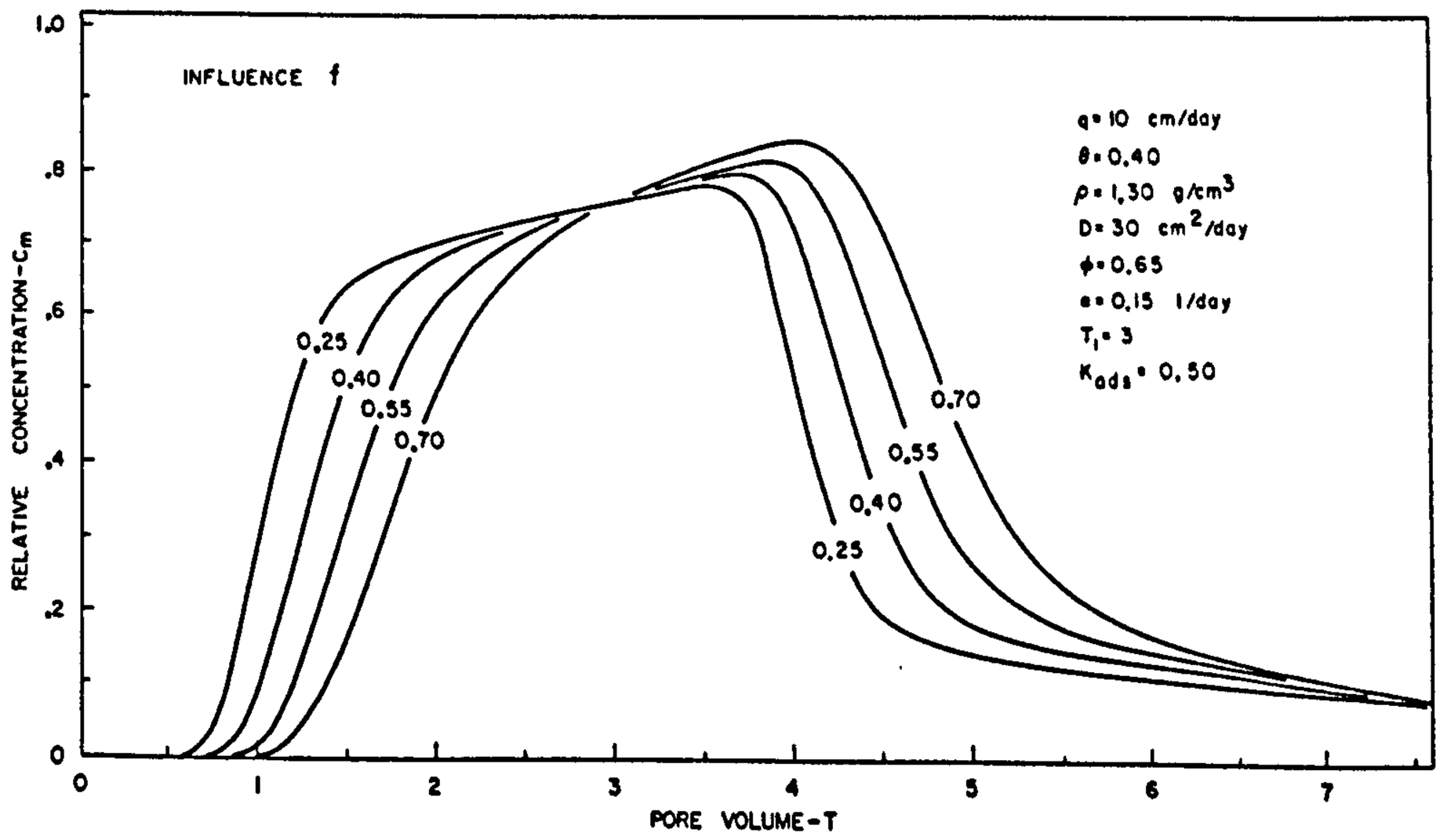

Fig. 6.2: Influence of f values on the BTCs (from *van Genuchten & Wierenga*, 1976).

Comparison of the two types of non-equilibrium model (Section 6.3.2.1 & 6.3.2.2) shows that they have the same mathematical structure and can be put into the same dimensionless form by means of model-specific dimensionless parameters (*Nkedi-Kizza et al.*, 1984; *Parker et al.*, 1984). Thus Eqs. 6.7 and 6.9 may both be expressed as

$$\beta R\frac{\partial C_1}{\partial T}+(1-\beta)\frac{\partial C_2}{\partial T}=\frac{1}{P}\frac{\partial^2 C_1}{\partial Z^2}-\frac{\partial C_1}{\partial Z} \qquad (6.12)$$

where

$$(1-\beta)R\frac{\partial C_2}{\partial T}=\omega\,(C_1-C_2) \quad . \qquad (6.13)$$

The relations between these parameters and those of the previous two models are given in Table 6.2.

Table 6.2 **:** The relations between the dimensionless parameters and the physical and chemical non equilibrium models parameters

Parameter	Non equilibrium chemical model	Non equilibrium physical model
Z	z/L	z/L
T	$\frac{v_m t}{L}$	$\frac{v_m t\Phi}{L}$
P	$\frac{v_m L}{D_s}$	$\frac{v_m L}{D_s}$
β	$\frac{\theta+F\rho K}{\theta+\rho K}$	$\frac{\theta_m+f\rho K}{\theta+\rho K}$
ω	$\frac{\alpha_k(1-\beta)RL}{v_m}$	$\frac{\alpha L}{v_m\theta_m}$
C_1	$\frac{C-C_0}{C_{inp}-C_0}$	$\frac{C_m-C_0}{C_{inp}-C_0}$
C_2	$\frac{S_2-(1-F)K\,C_0}{(1-F)K\,(C_{inp}-C_0)}$	$\frac{C_{im}-C_0}{C_{inp}-C_0}$

C_{inp} is the solute concentration in the input water.

$$\Phi=\frac{\theta_m}{\theta_m+\theta_{im}}$$

The retardation factor R describes the effects of adsorption during transport through the soils ($R < 1.0$ means ion exclusion or negative adsorption). The parameter β is directly related to the value of f or F, and reflects the fraction of adsorption occurring in the mobile liquid phase or in site 1 for physical and chemical non-equilibrium models respectively. Finally, the mass-transfer coefficient ω describes the rate at which equilibrium is attained from an initial non-equilibrium situation; the larger is ω, the sooner is equilibrium obtained (*Nkedi-Kizza et al.*, 1984).

Because both models can be described in exactly the same dimensionless transport equation (Eq. 6.12 & 6.13), and the BTC curve in both models could be described by the same dependent variable (C_1), it follows that the two models are equivalent with respect to their BTCs. Therefore both models were equally successful in describing measured BTCs (*Nkedi-Kizza et al.*, 1984). However, the two dependent variables define conceptually different quantities in the two models. For example, C_2 in the physical non-equilibrium model describes the average solution concentration of the immobile water region, whereas C_2 in the chemical non-equilibrium model defines the adsorbed concentration associated with type 2 (kinetic) non-equilibrium sites.

Anamosa et al. (1990) modelled displacement of ^3H_2O from an undisturbed soil column of a structured soil consisting of a gravelley Oxisol (with aggregate diameters <2, 2-12 and 12-75 mm with mass fractions of 0.37, 0.42 and 0.21 respectively). They found that the equilibrium model couldn't fit the observed BTC at a large flux (q =111 cm/day = 0.77 mm/min), but performed better for a small flux (q = 2.71 cm/day = 0.018 mm/min) (Fig. 6.3). They attributed this to immobile water regions that were not in physical equilibrium at the greater flux. However, at the smaller flux, there was enough time to allow diffusion to bring the concentration of ^3H in the mobile and immobile water regions closer to physical equilibrium and the fit was better.

Using the physical non-equilibrium model they obtained closer agreement with the observed BTCs at both the greatest and smallest fluxes (Fig. 6.4). They concluded that the equilibrium model was inadequate in describing solute transport through such soils but the physical non-equilibrium model adequately described solute transport at all flow rates. The equilibrium model was unable to account for diffusive mass transfer of solute into immobile water regions. For such soils, with a well-defined aggregate geometry, most of the physical non-equilibrium model parameters seem easier to define and estimate (notably, θ_{im} and θ_{m}) than those of the chemical-non equilibrium model (i.e., F and α_{k}). For this reason, the physical-non equilibrium model will be used in this study.

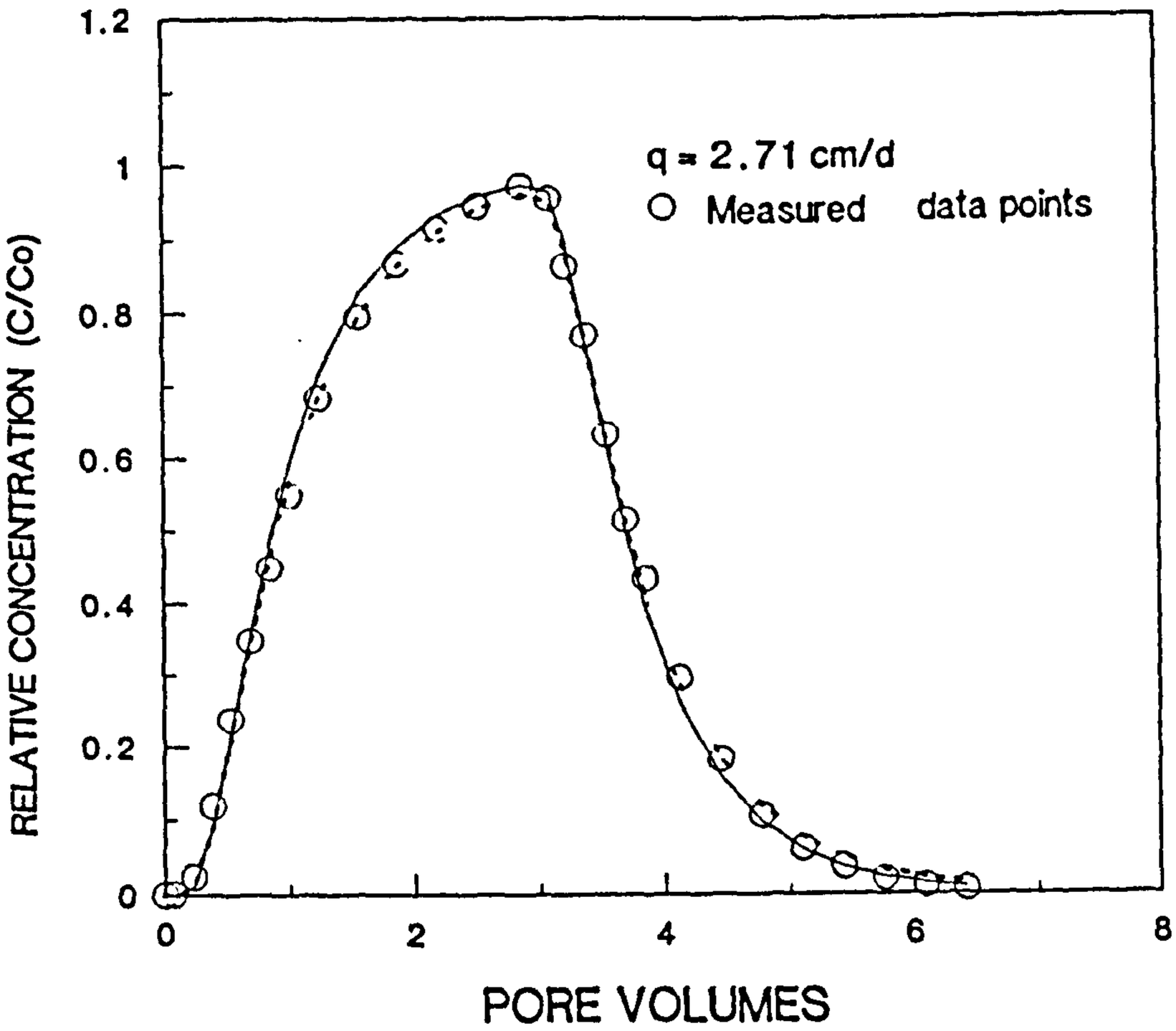

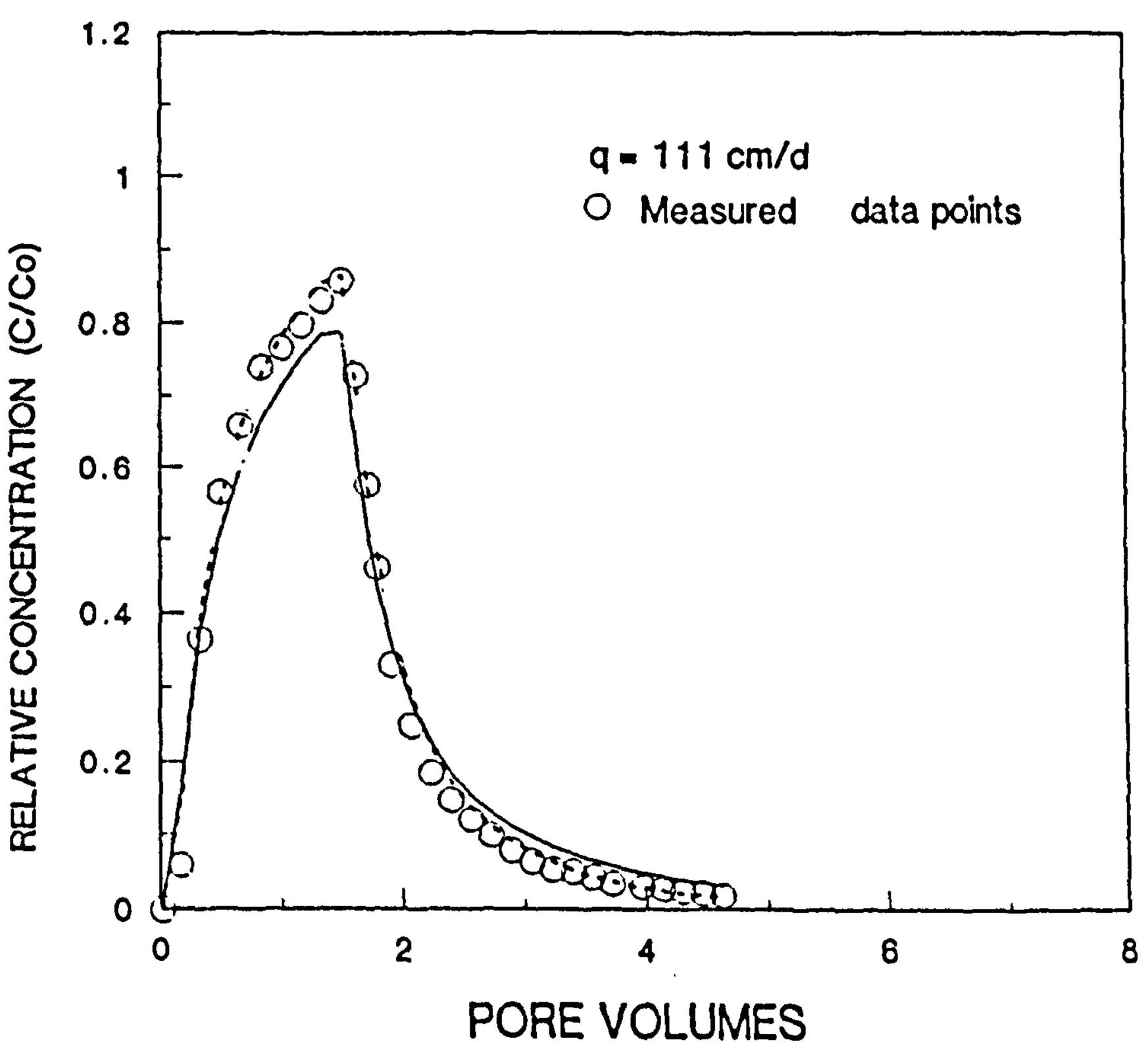

Fig. 6.3: Measured (o) and equilibrium model (solid line) BTCs at two different fluxes (adopted from *Anamosa et al.*, 1990).

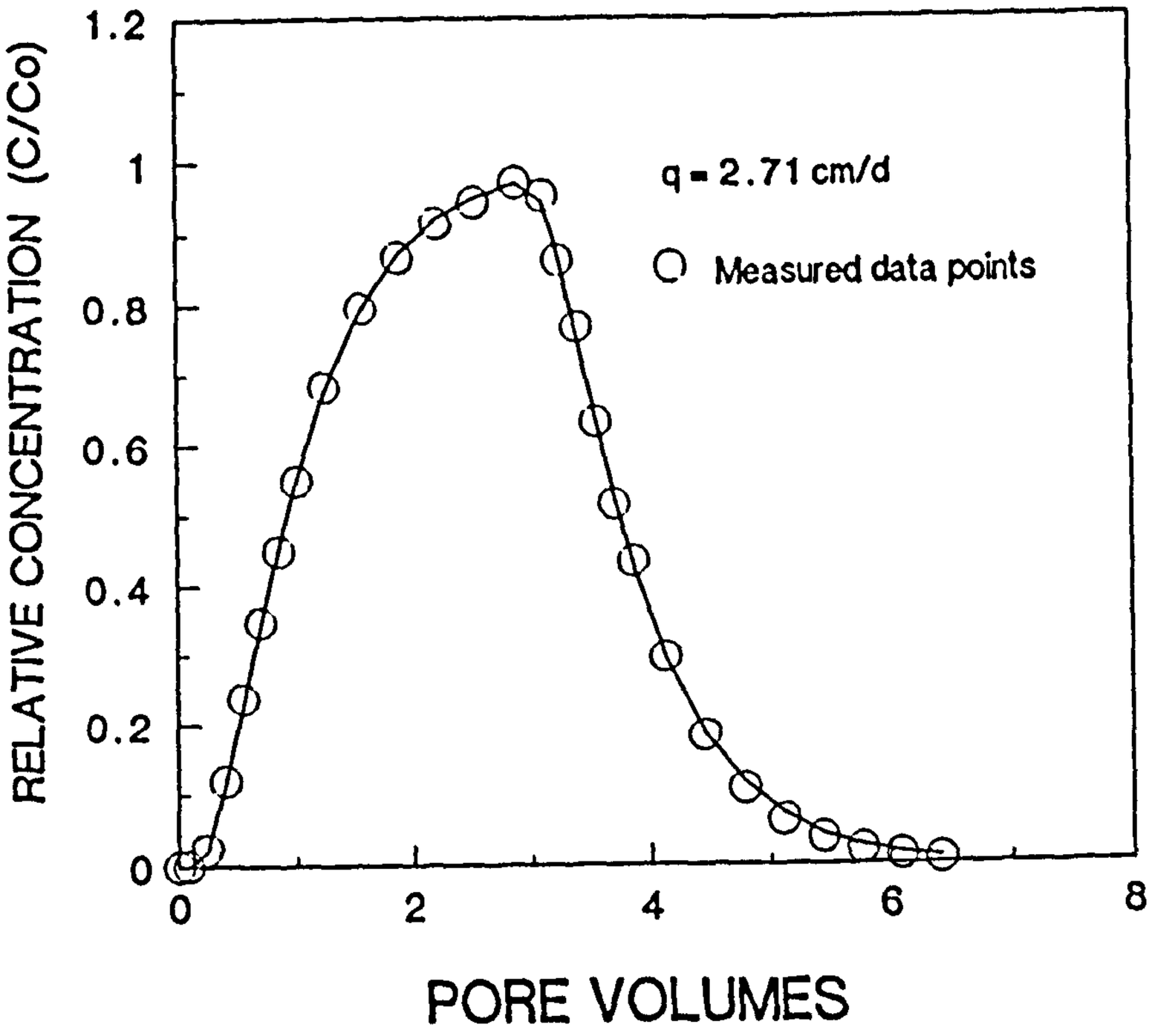

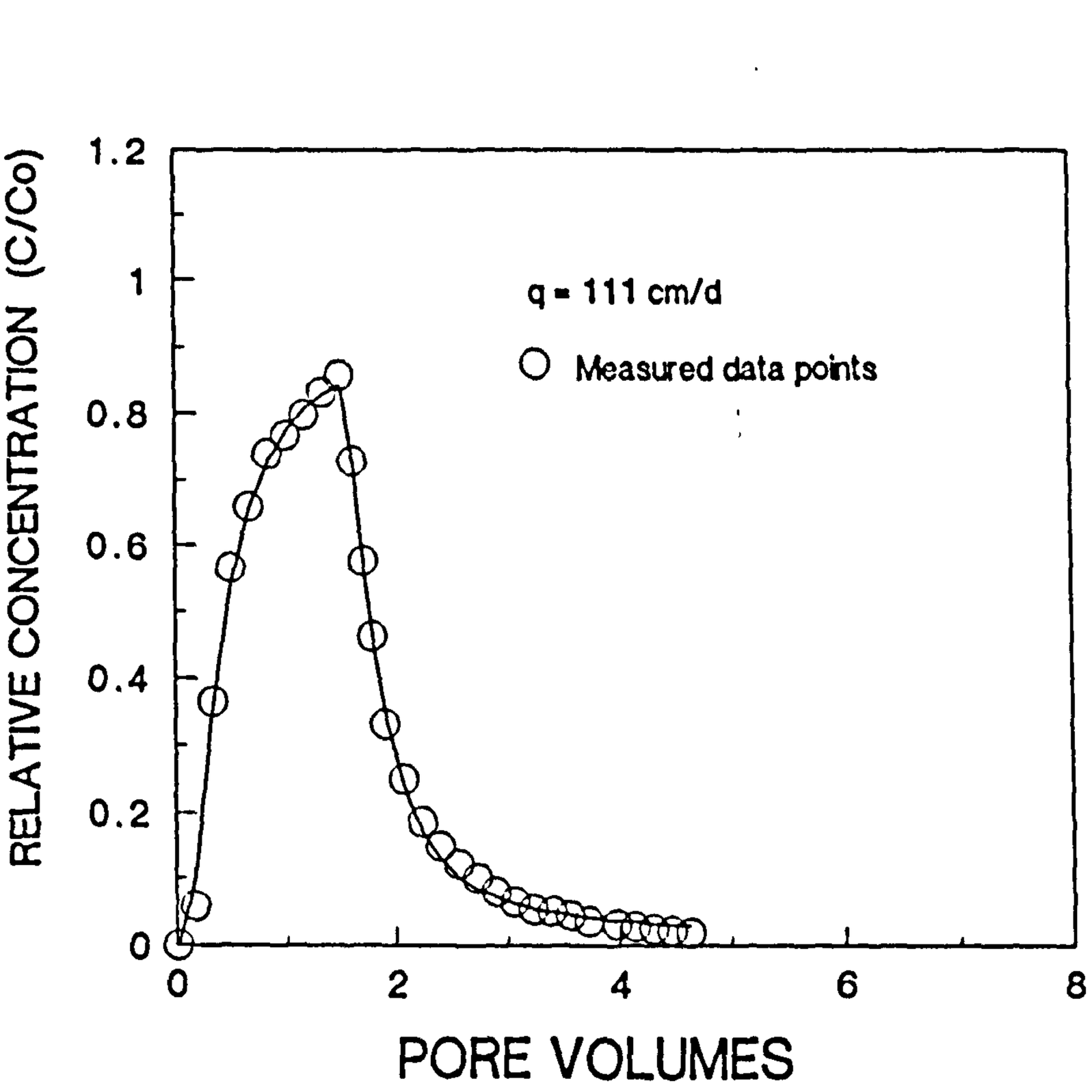

Fig. 6.4: Measured (o) and physical non-equilibrium model (solid line) BTCs at two different fluxes (adopted from *Anamosa et al.*, 1990).

Chapter Seven

Ion- selective electrodes

Ion-selective electrodes were used in this research for continuous monitoring of tracers in the soil column effluent. This chapter introduces the theory, principles, and characteristics of ion-selective electrodes, and the possibility of using them in continuous flow measurements.

7.1 Introduction

The term ion-selective electrode (ISE) is applied to a range of membrane electrodes which respond selectively towards one (or several) ion species in the presence of others (*Covington,* 1979).

The first ISE was invented in the first decade of this century. The active component was a glass membrane sensitive to hydrogen ions, and the electrode forms the basis of the modern pH glass electrode. Since then much attention has been given to crystalline and liquid membranes sensitive to a wide range of cations and anions. This has resulted in the availability of membranes of high ion specificity and robustness under appropriate environmental conditions (*Talibudeen,* 1991).

7.2 Essential components

Regardless of sample conditions, the essential components of an ISE measuring system are (*ATI Orion,* 1995) :

- a sensing electrode (half cell)
- a reference electrode (half cell)
- a readout device
- a solution containing the ion to be measured.

When a sensing electrode is exposed to a solution of ions for which it is selective, an electrical potential develops across the sensing membrane surface. This membrane potential varies with the concentration of the ion being measured, the magnitude may thus be related to concentration.

To make a measurement, a second unvarying potential, against which the membrane potential may be compared, is required. The reference electrode provides this. A filling solution completes the electrical circuit between the sample and the internal cell of the reference electrode. The point of contact between the sample and the filling solution is known as the liquid junction. (Fig. 7.1)

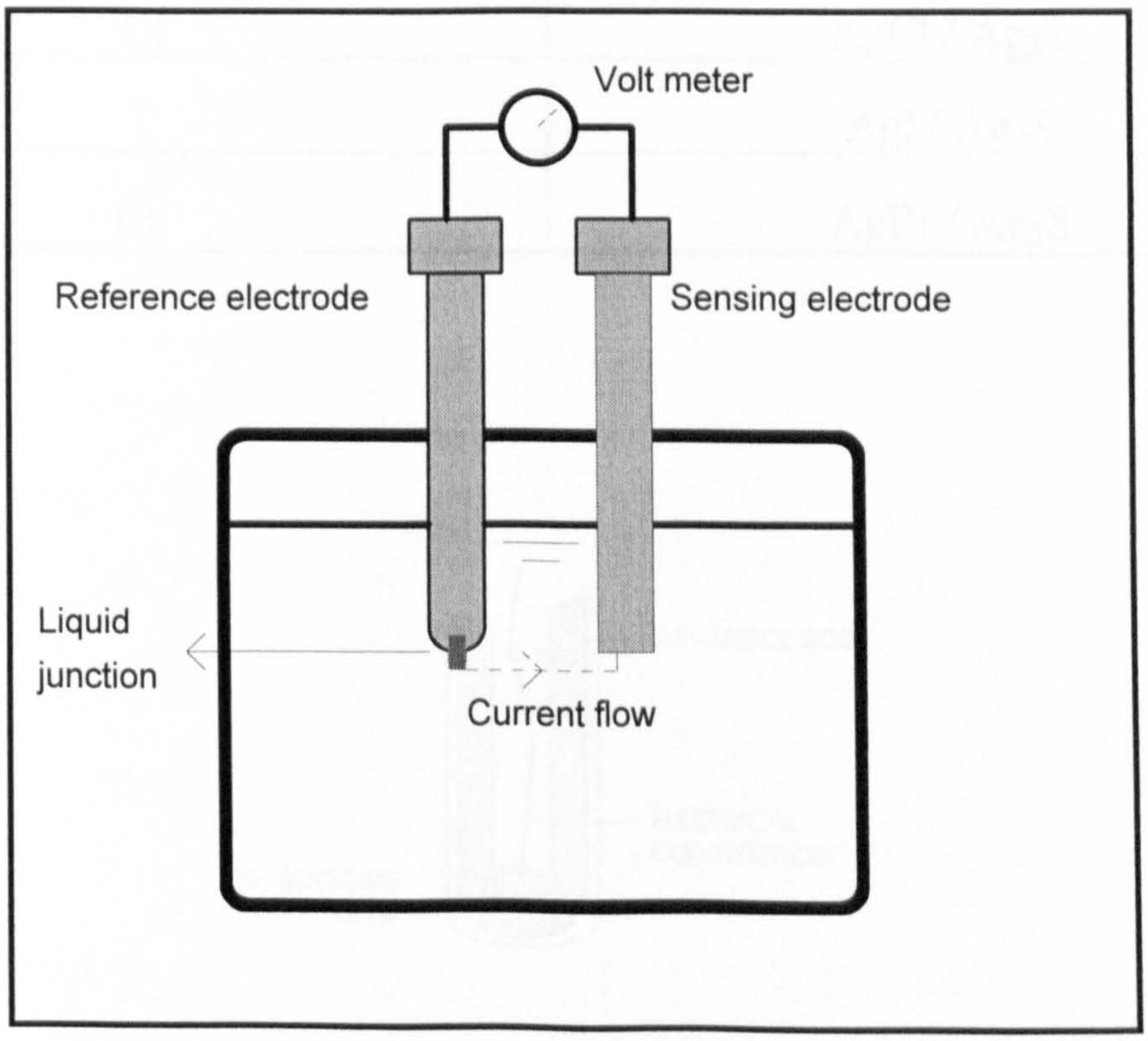

Fig. 7.1 :Ion-selective electrode measuring system (adapted from *ATI Orion*, 1995)

7.2.1 Ion-selective electrode types

There are four major types of ISEs classified by their membrane materials (*Skoog et al.*, 1992):

7.2.1.1 Glass membrane electrodes

This is the most familiar type of sensing electrode. A glass membrane is routinely used for measuring pH and some ions, such as sodium.

7.2.1.2 Solid-state membrane electrodes

The membrane is made of a uniform or homogeneous solid substance (Fig. 7.2). Examples of this types of electrode and their membrane materials are shown in Table 7.1.

Table 7.1: Solid-state membrane electrodes (adapted from *James & Ross*, 1969)

Ion determined	Membrane composition
F^-, L^{3+}	LaF_3
Cl^-	$AgCl / Ag_2S$
I^-	AgI / Ag_2S
Br^-	$AgBr / Ag_2S$

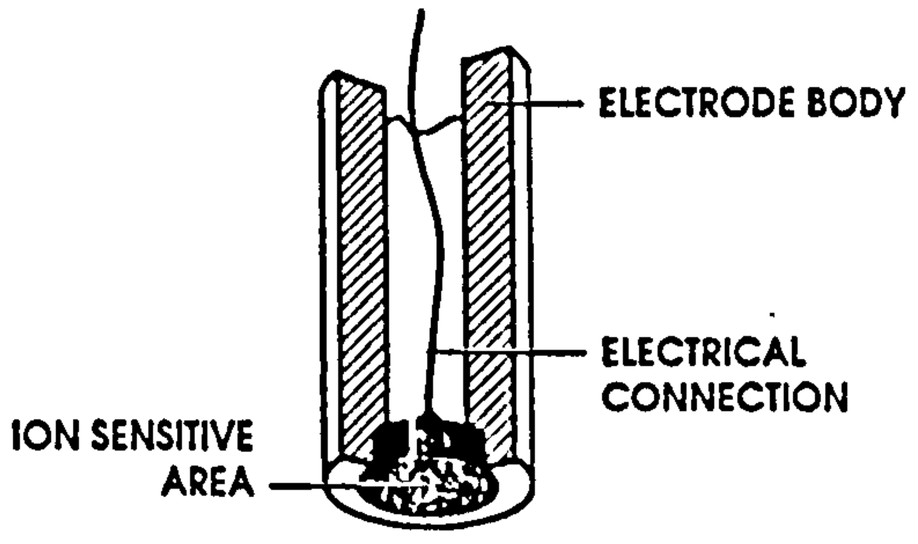

Fig. 7.2: Solid-state electrode (from *ATI Orion*, 1995)

7.2.1.3 Plastic membrane electrodes

This type of electrode has an ion-exchange material contained in a solid plastic membrane. The sensed ion is exchanged across the membrane, creating the potential. These electrodes are used to measure calcium, potassium and nitrate among other ions (Fig. 7.3).

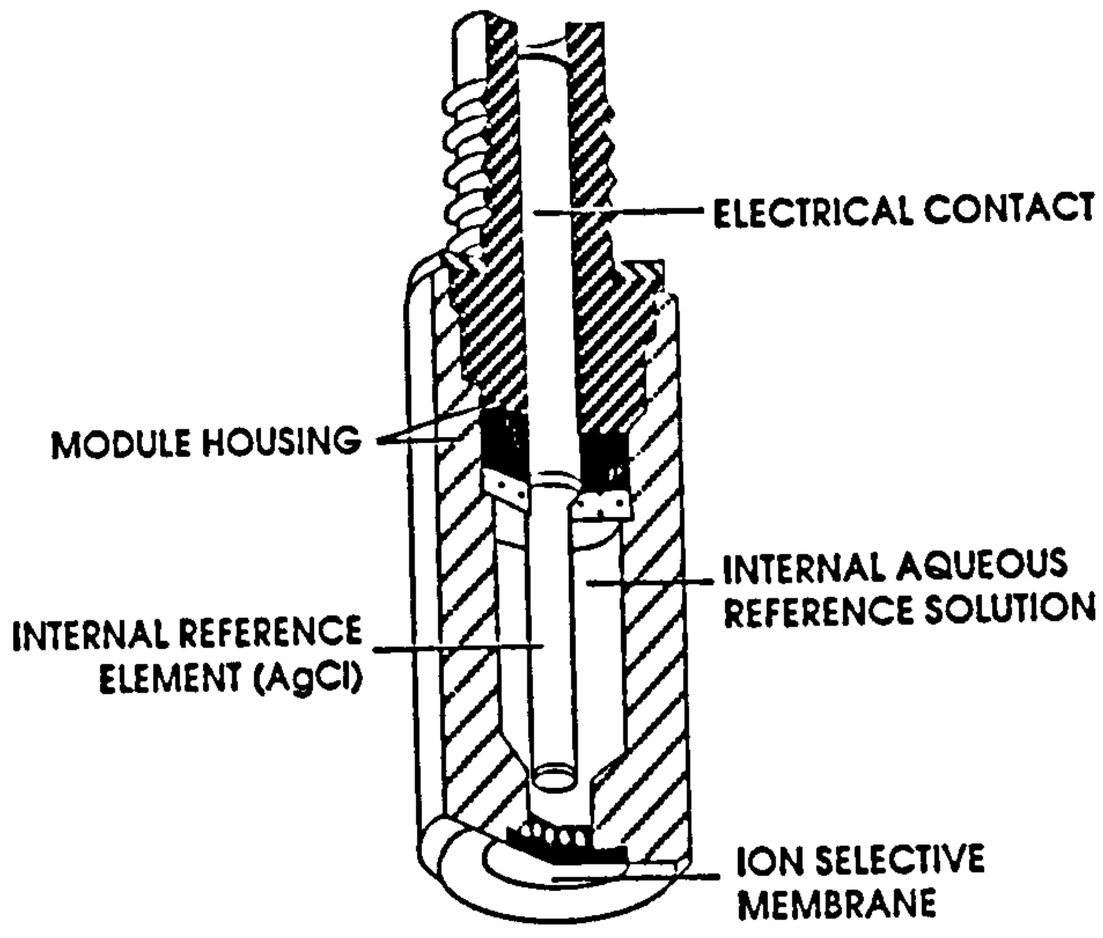

Fig. 7.3: Plastic membrane electrode (module) (from *ATI Orion*, 1995)

7.2.1.4 Gas sensing electrodes

This electrode responds to dissolved gases in solution.

7.2.2 Reference electrodes

The measurements of ion activity require the ISE to be coupled to an external reference electrode. The composition of the reference solution in the latter must, however, be chosen such that it does not affect the concentration of the specific ion in the sample or introduce significant concentrations of interfering ions. It is also essential that the liquid junction potential (LJP) between the reference electrode and the calibrating and test solutions of the specific ion be invariant . A reference electrode must be stable, have a high exchange current to maintain its constant potential under high-current demand , and be reproducible so that the temperature and concentration dependence of its

electrostatic potential difference is not subject to hysteresis (*Talibudeen*, 1991).

They are two main types of reference electrodes: single-junction and double-junction reference electrodes (Fig. 7.4). In the first, the filling solution is in contact with the sample by means of one liquid junction (usually consisting of a porous plug). In double-junction reference electrodes , the filling solution makes contact with a "bridge" solution by means of the first liquid junction. A second liquid junction enables contact to be made between the bridge solution and the sample. The latter electrodes are useful when it is essential that contamination of the sample by the inner filling solution must be kept at a very low level (*Simpson*, 1979).

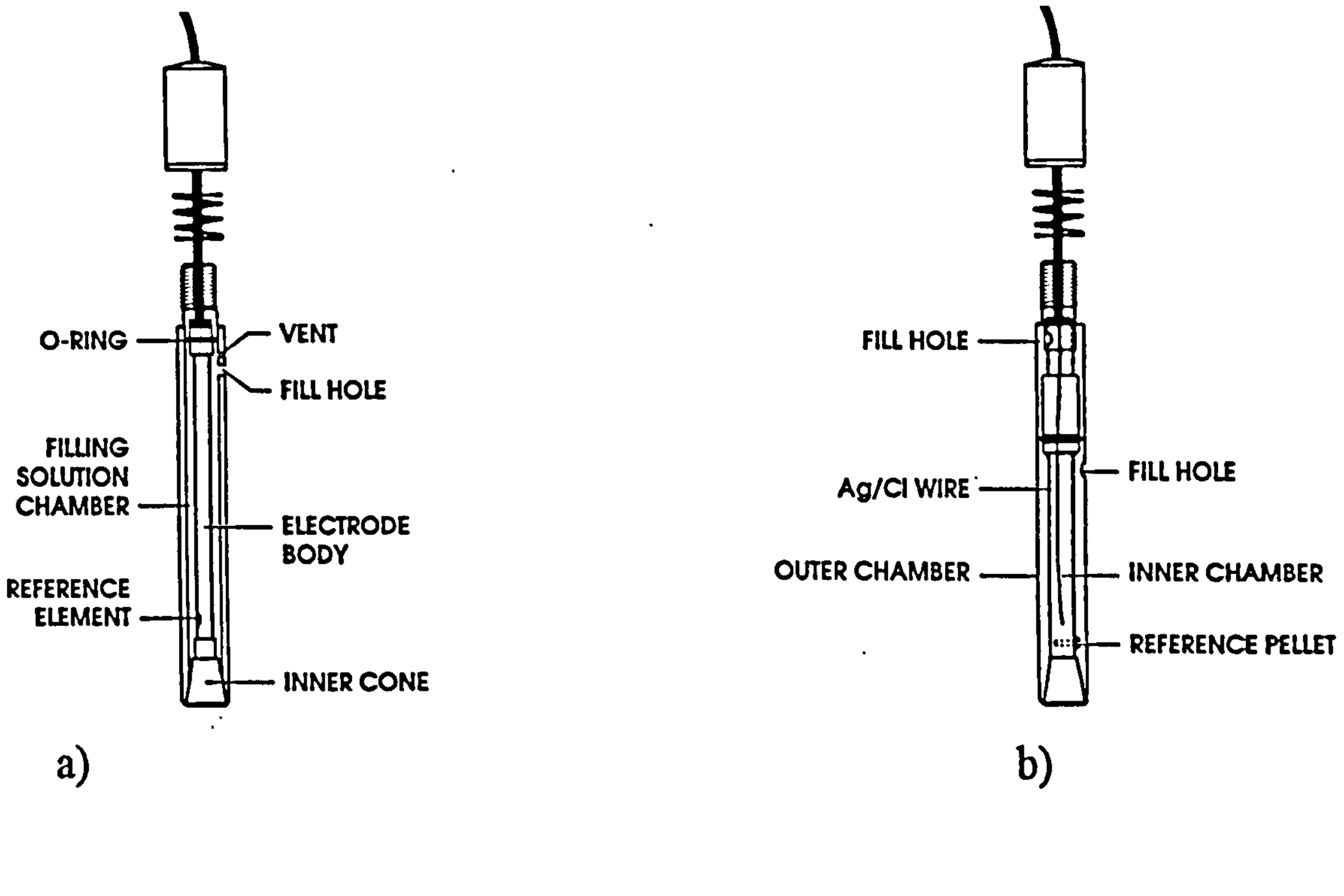

Fig. 7.4: Reference electrodes: a) single junction, b) double junction (from *ATI Orion*, 1995).

7.3 Operation principles

The electrical potential E of an ion selective electrode is a function of the logarithm of the activity of the ion to be measured. The relationship is given by the Nernst equation:

$$E = E^o \pm \frac{2.303RT}{z_i F} \log A_i$$

where

E = a measured electrical potential (mV)

E^o = a constant characteristic of the electrode

T = the absolute temperature

z_i = the charge of the ion

F = the Faraday constant (96485.3 C mol^{-1})

R = the universal gas constant (8.3144 J K^{-1} mol^{-1})

A_i = the activity of the measured ions.

The sign in the equation is positive when i is a cation and negative when it is an anion.

This equation can be simplified to:

$$E = \text{Constant} \pm S_c \log A_i$$

where S_c is the slope of the calibration curve of the electrode.

For a dilute solution of non-electrolytes it is generally safe to make the approximation that solute activity can be replaced by molality. However, in ionic solutions, the interactions between ions are so strong that this approximation is valid only in very dilute solution (less than 10^{-3} mol/kg total ion concentration) and, in precise work, activities themselves must be used (*Atkins*, 1994). The activity of the ion of interest is related to molality by

$$A_i = C_i f_i^o$$

where

C_i = is the concentration of species i expressed in molality (moles of i per kg of solvent). However, in analytical work, it is usual to measure concentration on the molar scale (moles of i per litre of solution) or related units (mg of i per litre of solution, i.e., ppm). Concentrations in either of the

molal or the molar scales are virtually identical except in very strong solutions. Thus the concentration can be considered on the molar scale.

f_i^o = is the activity coefficient of the ion, which depends upon the ionic strength of the solution. The ionic strength of the solution (I) can be calculated from the formula:

$$I = \frac{1}{2}\sum_i C_i z_i^2 \quad .$$

The single-ion activity coefficient, f_i^o, is related to the ionic strength of the solution by the Debye-Huckel equation applicable to a dilute solution:

$$-\log f_i^o = \frac{B_1 z_i^2 \sqrt{I}}{1 + d_i^o B_2 \sqrt{I}}$$

where d_i^o is the mean diameter of the ion (m), and

B_1, B_2 are constants of the solvent at a specified temperature and pressure. Table 7.1 gives the values of B_1 and B_2 for water as a function of temperature at 1 atm pressure.

Table 7.1 : Values of B_1 and B_2 constants for water (*Tan*, 1993)

Temperature °C	B_1 (kg/mol)$^{-1/2}$	$B_2 \times 10^8$ (kg/mol)$^{-1/2}$ m^{-1}
0	0.4883	0.3241
10	0.4960	0.3258
20	0.5042	0.3273
30	0.5130	0.3290
40	0.5221	0.3305

Tabulated data for estimated single ion and mean ionic activity coefficients in solutions of various ionic strength are usually provided with the electrode manual.

7.4 Calibration

The purpose of calibration is to enable the response of the electrodes in standard solutions to be compared with the response in samples. In order for the comparison to be valid, both standards and samples must be treated identically (*Bailey*, 1976), i.e. the concentration standards as presented to the electrode should be as similar as possible in all respects to the samples, and the determined concentration in the standards should closely bracket the expected range in the samples.

Most often it is desired to measure the concentration of a species rather than activity. At fixed ionic strength, activity is proportional to concentration, and the Nernst equation may be rewritten to describe electrode response to the concentration under these conditions:

$$E = E^{o} \pm S_c \log C \ .$$

However, if there are differences in activities between standards and samples , adding a few millilitres of a recommended *ionic strength adjuster* (ISA) to both of them will eliminate these differences. The ISA "swamps" differences in ionic strength and fixes the ionic strength at a constant level.

7.5 Selectivity and interference

No electrode is entirely selective towards the ion specified (*Covington*, 1979), although it is more responsive to the primary ion than to others.

The degree of selectivity of the electrode for the primary ion, i , with respect to an interfering ion , j, is expressed by the selectivity coefficient k_{ij} . When an electrode is very selective for i in comparison with j , then k_{ij} will be much less than unity. Conversely, if the electrode responds preferentially to j than to i , k_{ij} will be greater than unity (*Bailey*, 1976). For example, the selectivity coefficient of the calcium electrode for barium ions, $k_{Ca\ Ba}$, is 0.01; thus, the electrode is 100 times more responsive to calcium ions than to barium

ions. Every manufacturer usually gives the values of selectivity coefficients for the most important interfering ions.

7.6 Using ISE in continuous flow measurements

Most of the ISEs can be used in continuous flow measurements to monitor the concentration of ions in a flowing solution because of their rapid response times (which range from few seconds to about one and half minutes, depending on the membrane type and material) (*Talibudeen,* 1991). A higher precision is normally attainable with continuous flow systems when using ISEs than with manual methods, because of the greater standardisation of the conditions in which the sample is presented to the electrode (*Smith & Scott,* 1991). Different analytical methods and industrial modes for using ISEs in continuous processes for monitoring or control purposes are presented by *Light* (1969), *Toth et al.* (1979) and *Smith & Scott* (1991). They found the technique to be promising for the industrial analytical field.

During continuous flow measurement, the ion-selective electrodes are usually mounted in a flow cell through which the sample is passed. The ISE and reference electrode may be mounted together in the cell, and sometimes more than one ISE are mounted together (Fig. 7.5).

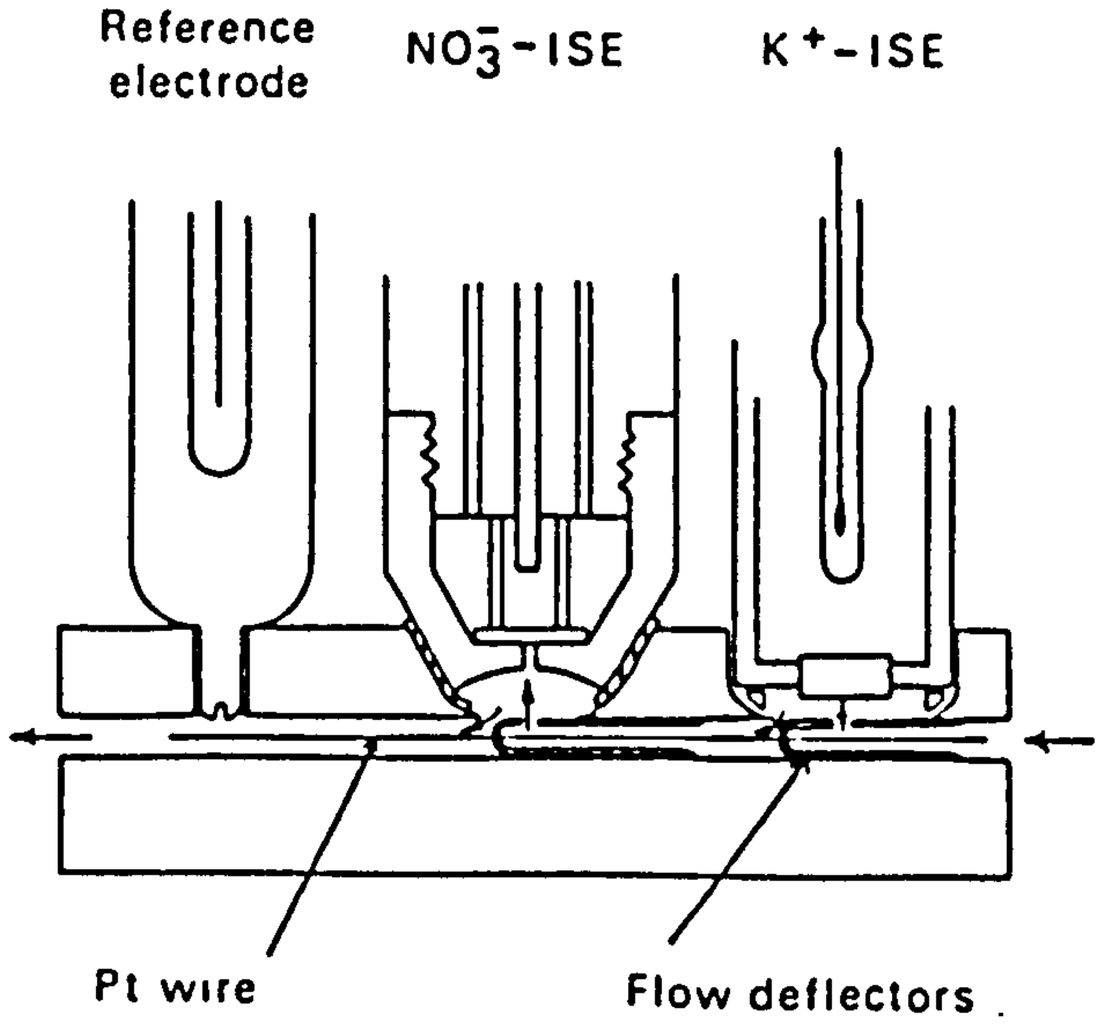

Fig. 7.5: Details of a flow cell with two ion-selective electrodes (from *Smith & Scott*, 1991).

Some caution must be taken because the reference electrode can affect the reading if there is leakage of filling solution. In this case the reference electrode could be mounted in a separate cell (*Simpson,* 1979). For this reason it is always good practice to locate the reference electrode downstream from the ISE.

7.6.1 Continuous flow measurements of soil leachate

The only paper found where ISEs were used to monitor continuously the concentration of a tracer in soil column outflow was by *Mansell & Elezeftawy* (1971). They used a lucite flow cell with a combination reference and chloride electrode (Fig. 7.6) to monitor chloride in aqueous effluent for the range of effluent flow velocities frequently encountered in soils, and found that the electrode-flow cell system gave realistic measurements of chloride concentrations in the column effluent.

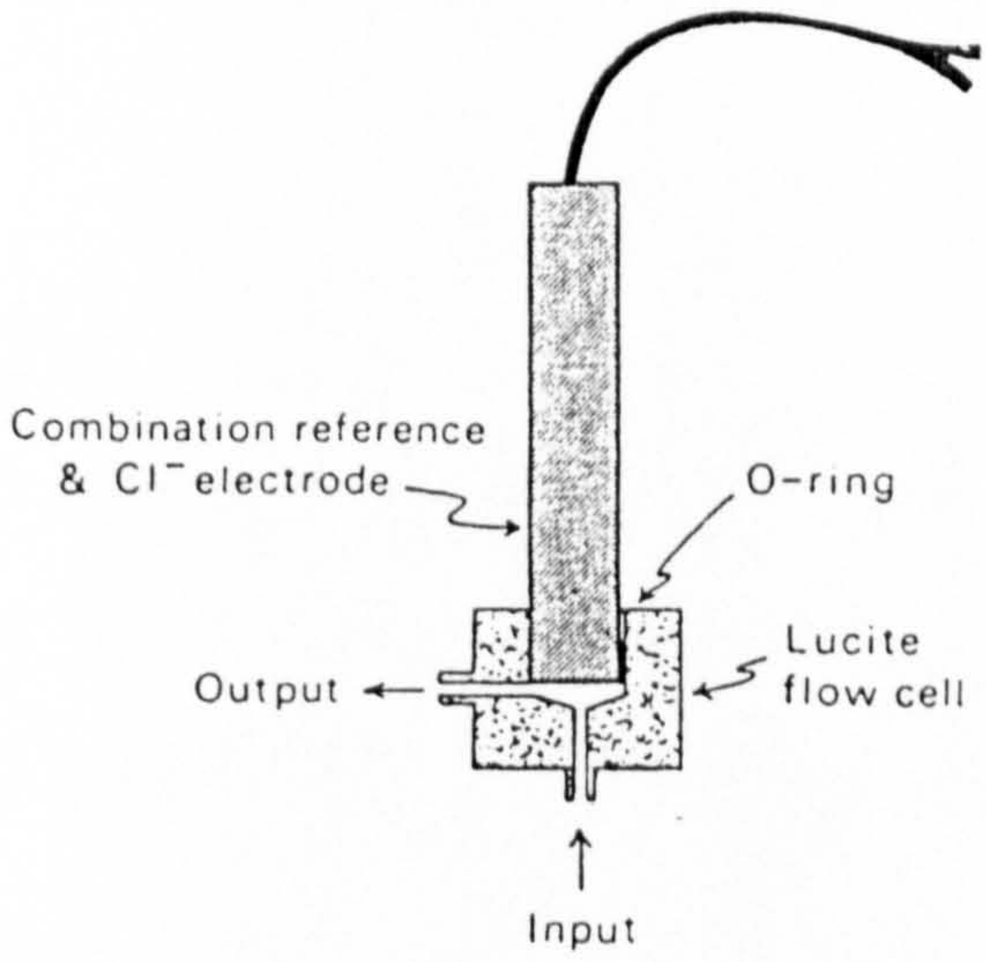

Fig. 7.6: Details of continuos flow cell (from *Mansell & Elezeftawy,* 1971)

7.7 Conclusion

The previous review of the theory and applications of ISEs shows that they have potential for use in the continuous monitoring of solute in the effluent from soil columns. The main advantages are the standardisation of the

measuring conditions, and the ability of ISEs to be connected to a data logger. The main disadvantages are the possible confounding effect of the changing ionic strength of the effluent during leaching, and the interference by other ions if they exist at relatively high concentrations. The first disadvantage may be overcome by calibrating the ISEs with actual samples of effluent solutions. The interference of other ions can be minimised by ensuring that the observed ions are always the dominant ions. In the next chapter these processes will be discussed in detail.

Chapter Eight

Experimental work

The aim of the work described in this chapter was to obtain experimental data from columns of soil aggregates leached either continuously or intermittently.

Two ions were selected as tracers and their interactions with the soil studied. These two ions were monitored simultaneously in the leachate by means of two ion-selective electrodes. The chapter begins with the analysis of the soil used.

8.1 Soil analysis

Experiments were performed using a strongly aggregated soil taken from the University farm of Cockle Park (Hallsworth Series, *Jarvis et al.*, 1984). The soil had been under pasture for the last five years.

8.1.1 Soil texture

The soil texture was determined by the standard method mentioned by *Avery & Bascomb* (1982). In brief, organic matter was destroyed by hydrogen peroxide and the remaining mineral soil dispersed by shaking in the presence of sodium hexametaphosphate. The soil was analysed by sieving and sedimentation, with sand separated from the soil by a 63-μm mesh and silt and clay sampled from the remaining suspension after appropriate sedimentation.

The experiments show that the soil texture is **clay loam** (with 33% clay, 30% silt, and 37% sand).

8.1.2 Soil pH

Soil pH was measured in water and 0.01 M calcium chloride solution using 10 g soil (< 2 mm) mixed with 25 cm^3 of solution (or water). The results were:

pH_w= 5.98 in water, and

pH_s= 5.29 in $CaCl_2$ solution.

The higher value of pH_w indicates that the soil has a net negative charge (*Rowell*, 1994).

8.1.3 Aggregate stability

The stability of the soil aggregates is expressed as the ratio of the proportion of < 20 μm material in suspension after mild dispersion to that after complete dispersion (*Brown,* 1991 (adapted from *Puri et al.,* 1925 and *Quirk* , 1950)).

Mild dispersion involved wetting 10 g of air dried aggregates (1-2 mm) and submerging them in 500 cm^3 distilled water and gently shaking end over end (24 rev/min) in a stoppered bottle for exactly 2 minutes, then sampling 20 cm^3 of the suspension < 20 μm after an appropriate sedimentation time (Stokes' law) using a pipette. Complete dispersion involved destroying the organic matter with hydrogen peroxide and dispersing the soil by shaking it (in the presence of sodium hexametaphosphate) overnight. Aggregate stability, *AS*, was calculated as follows;

$$AS = \left[1 - \frac{<20\mu m\ (mild\ dispersion)}{<20\mu m\ (complete\ dispersion)}\right] \times 100\%$$

where 100% indicates complete stability.

The *AS* of the soil used in the experiment was 98 ± 1 % indicating very stable aggregates (*Brown*, 1991).

8.1.4 Cation exchange capacity CEC

The cations adsorbed on the surface of charged clay minerals can be replaced by other cations in the surrounding soil solution (*Jury et al.*, 1991). Therefore, they are often called "exchangeable cations". The total number of exchangeable cations that the surface will adsorb (generally expressed as meq/g or $mmol_c$/kg of soil) is called the cation exchange capacity (CEC).

The method used to measure CEC involved saturating the exchange sites with NH_4^+ solution at pH 7 and then displacing the excess solution with ethanol. Acidified potassium chloride (pH = 2.5) then displaced the exchangeable ammonium which was measured, by determining the nitrogen of the ammonium using a nitrogen analyzer, to give the CEC (Fig. 8.1).

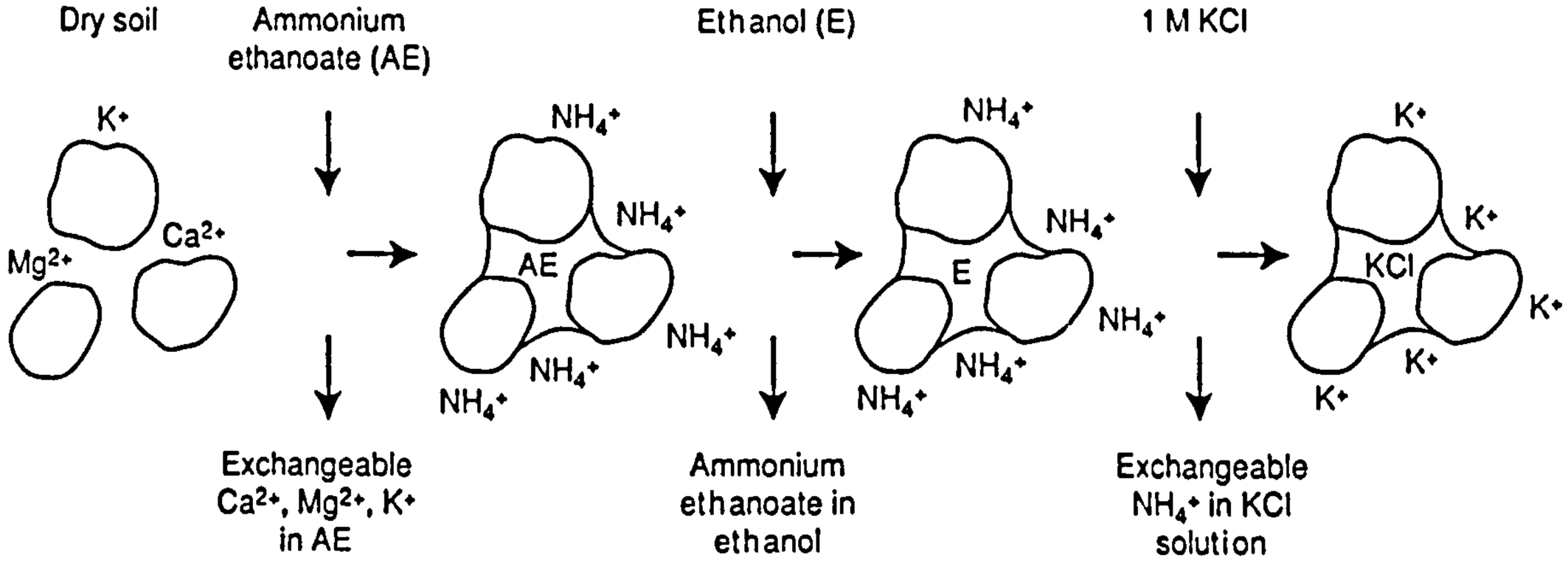

Fig. 8.1 : The determination of exchangeable cations and cation exchange capacity (*Rowell*, 1994).

The CEC of the soil was equal to 240 $mmol_c$ / kg.

8.1.5 Linear shrinkage of the soil

The method used was adapted from *Head* (1992), in which a smooth homogeneous paste was placed in a standard mould and dried in an oven by progressively increasing the temperature from room temperature up to 105°C.

The linear shrinkage, L_s ,is calculated as a percentage of the original length of the specimen from equation;

$$L_s = \left(1 - \frac{L_d}{L_o}\right) \times 100\%$$

where L_o = original length (140 mm),and L_d = length of dry specimen.

The result was L_s = 5.84 % ≅ 6 %.

8.2 Selected tracers

Two ions were selected as a tracers. One was the potassium ion which is adsorbed onto soil particle surfaces, the other was bromide which is weakly adsorbed. By simultaneously detecting both ions in the soil column effluent, the desorption effect on solute leaching can be distinguished. Some of the chemical interaction properties between these ions and soil particles are now described.

8.2.1 Potassium in soils

Selim et al. (1976a) divided potassium in soils into four phases: solution, exchangeable, non-exchangeable, and primary mineral (Fig. 8.2).

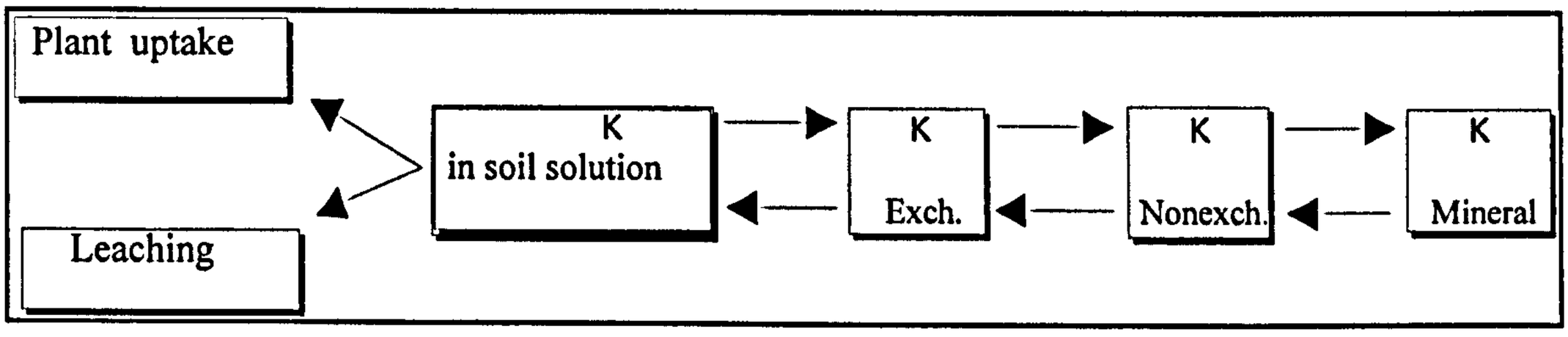

Fig. 8.2: Schematic representation of the reactions of potassium in solution ,exchangeable, non exchangeable, and primary mineral phases in soil (*Selim et al.*, 1976a)

The reactions between the exchangeable and solution phase are rapid enough to provide equilibrium or quasi-equilibrium conditions at all times as found by *Wood & DeTurk* (1940) and *Malcolm & Kennedy* (1969). In contrast,

contrast, the transformation between the exchangeable and non-exchangeable phases is slow (*Wood & DeTurk,* 1940; *McLean & Simon,* 1958).

8.2.1.1 Potassium fixation

Under certain conditions, the adsorbed potassium cations are held so strongly by clays that they cannot be recovered by exchange reactions. These cations are called fixed potassium cations. Among the several reasons reported for fixation, the most important is the entrapment of the ions in the interlayer regions of the clays (e.g., micas, illites, montmorillonites, and vermiculites) (*Tan*, 1993).

8.2.1.2 Release of potassium

Extensive studies (*Mortland et al.*, 1957; *Cook & Hutcheson*, 1960) have been aimed at measuring the rates of transformation and release of potassium from various minerals such as biotite, illite, etc. These studies suggest that potassium release from soil minerals is extremely slow in comparison to transformations between soluble and exchangeable phases. In addition, the release of mineral potassium is relatively more rapid than mineral fixation. *Martine & Sparks* (1983) found that the equilibrium in K^+ release was attained in 40 days for their sandy loam and loamy sand soils.

This preview indicates that using potassium as a tracer should not cause any problem either due to its fixation or to its release, especially for the relatively much shorter time of laboratory leaching experiments. Over this time scale the primary exchange will be between the soil solution and (non-fixed) exchange sites (*Jensen*, 1984).

8.2.2 Potassium adsorption-desorption isotherms

The method used to determine potassium adsorption-desorption isotherms is that used by *van Genuchten et al.* (1977), *Rao & Dividson* (1979) and *Peek & Volk* (1985). Duplicate samples of 5 g of dry soil ($d < 0.5$ mm) were mixed

with 30 cm^3 of KBr solutions of eight different concentrations from 11.9 to 0.476 g KBr/l (3.91 to 0.156 g K/l, i.e. 0.1 to 0.004 M) in 50-cm^3 test tubes and shaken for 36 h (preliminary experiments showed that there were no real increases in the adsorption beyond this time), and then centrifuged at 17000 ***g*** for 20 min. 20 cm^3 of supernatant was then removed and analysed for potassium concentration by means of a flame photometer (previously calibrated). The experiments were done at constant temperature (20 ±1° C). The results are shown in Fig. 8.3 as adsorbed potassium per dry mass of the soil against the potassium concentration in the sample at equilibrium. The amount of adsorbed potassium sharply increased at very low concentrations then increased almost linearly with solution concentration similar to the shape of a Freundlich isotherm (Fig. 6.1). The experimental results were fitted very well (R^2= 0.982) with a Freundlich isotherm:

$$S = 0.0024C^{0.404} \qquad (8.1)$$

where S is in g/g, and C is in g/l.

To determine whether the adsorption - desorption process is reversible (i.e., whether or not there is hysteresis), the 20 cm^3 removed previously from the samples was immediately replaced by 20 cm^3 of distilled water. The soils were loosened from the tubes by vigorous hand shaking and the same procedures were followed (shaking, centrifuging). Again 20 cm^3 removed from the supernatant and analysed to measure the amount of potassium desorbed from the soil. The results shown in Fig. 8.4 indicate that there is hysteresis. Thus the desorption curve will depend on the initial potassium concentration of the sample.

For the desorption isotherm curve, the initial concentration will be taken as 0.1 M KBr (since this is the value chosen later as the initial concentration of soil solution in the leaching experiments). The curve was obtained using 5 g soil to 30 cm^3 of 0.1 M KBr solution. After following the same process of

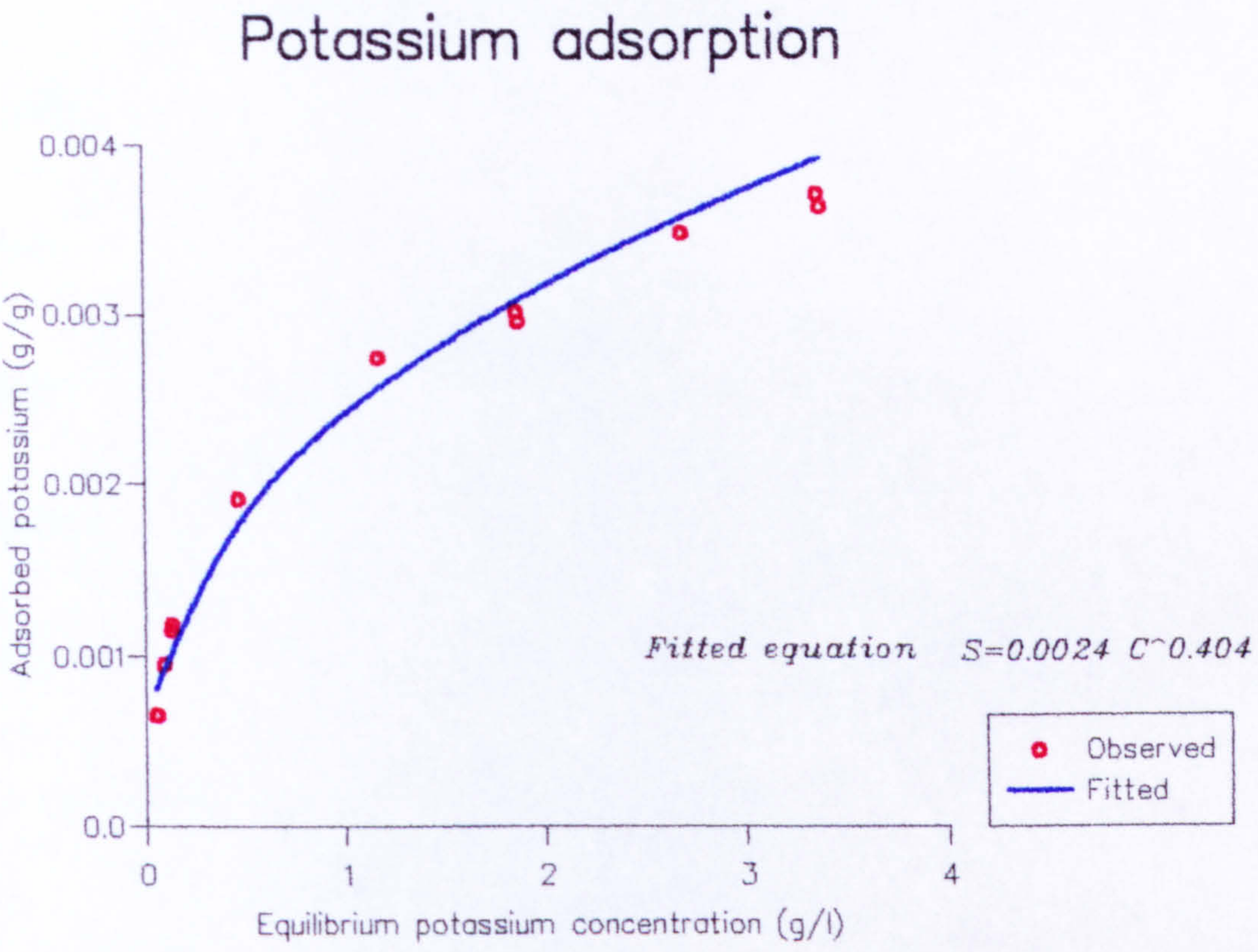

Fig. 8.3 : Adsorbed potassium per unit dry mass of soil as a function of solution potassium concentration during adsorption (for observed and fitted results).

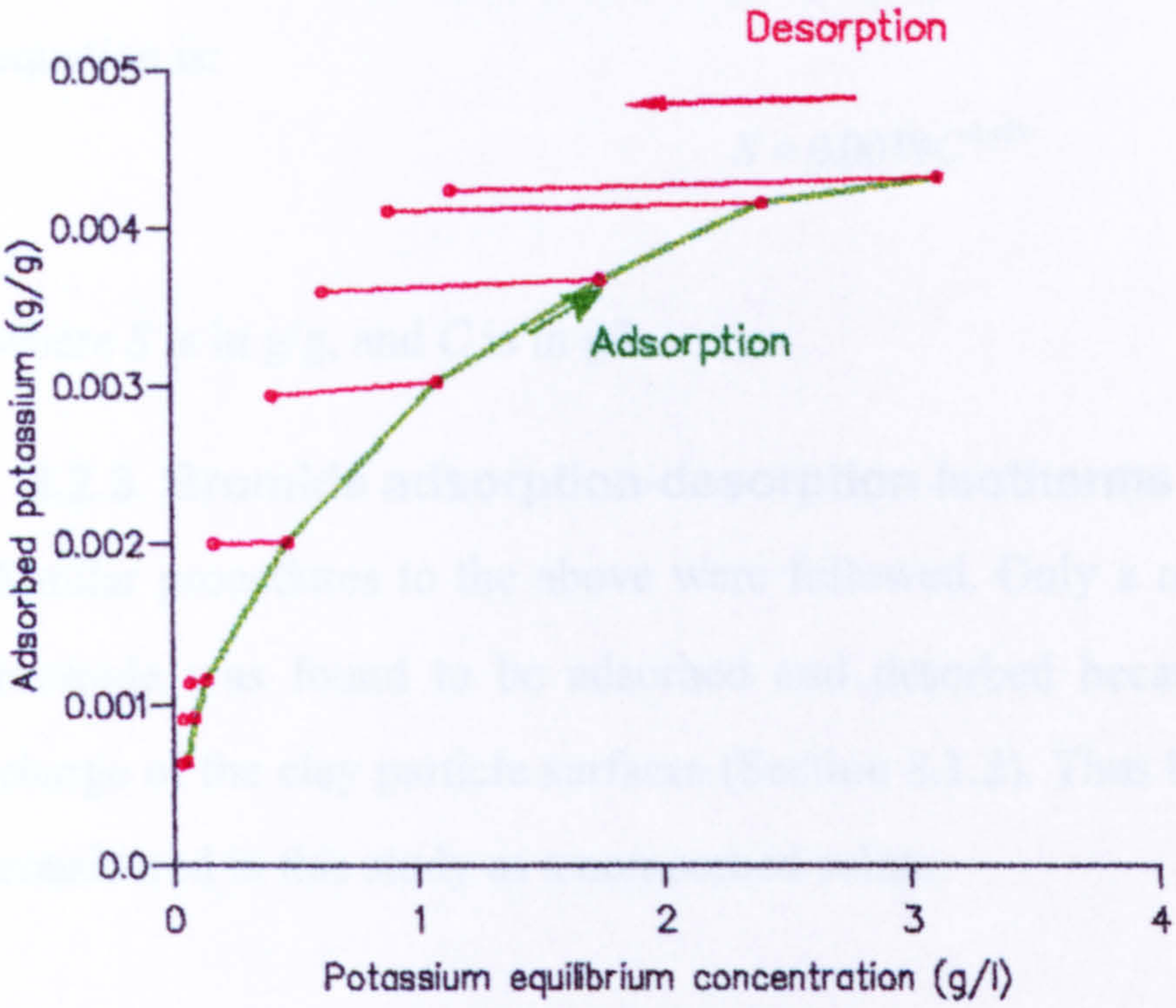

Fig. 8.4 **:** Adsorbed potassium per unit dry mass of soil as a function of potassium concentration (for adsorption-desorption results).

shaking and centrifuging, 20 cm^3 of the supernatant was removed to determine the initial adsorption, then replaced by 20 cm^3 of distilled water and continued as before. This procedure was repeated each successive desorption step. The results are shown in Fig. 8.5 as adsorbed potassium per dry mass of the soil against the potassium concentration in the sample at equilibrium. The potassium was desorbing slowly at high concentrations. However, at low concentrations (<1 g/l), the potassium started to desorb sharply as the potassium concentration in the solution decreased. The best equation fitting the experimental results was a Freundlich equation with R^2= 0.930. The fitted equation is:

$$S = 0.0039C^{0.105} \tag{8.2}$$

where S is in g/g, and C is in g/l.

8.2.3 Bromide adsorption-desorption isotherms

Similar procedures to the above were followed. Only a negligible amount of bromide was found to be adsorbed and desorbed because of the negative charge of the clay particle surfaces (Section 8.1.2). Thus bromide ions will be considered in this study as a non-sorbed solute.

8.3 Electrode characteristics

As discussed in Chapter seven, ISEs have potential for use in the continuous monitoring of solute in the effluent from soil columns, with the main advantage of the standardisation of the measuring process. This section will present some of the characteristics of the two ISEs used. These two electrodes were used to detect potassium and bromide ions in the soil column effluent. Both potassium and bromide electrodes were made by SENTEK[1] . Finally, the

[1] **SENTEK Ltd.**, Unit 6-7 Crittall Court, Crittall Drive, Springwood Industrial Estate, Braintree, Essex CM7 7RT, England.

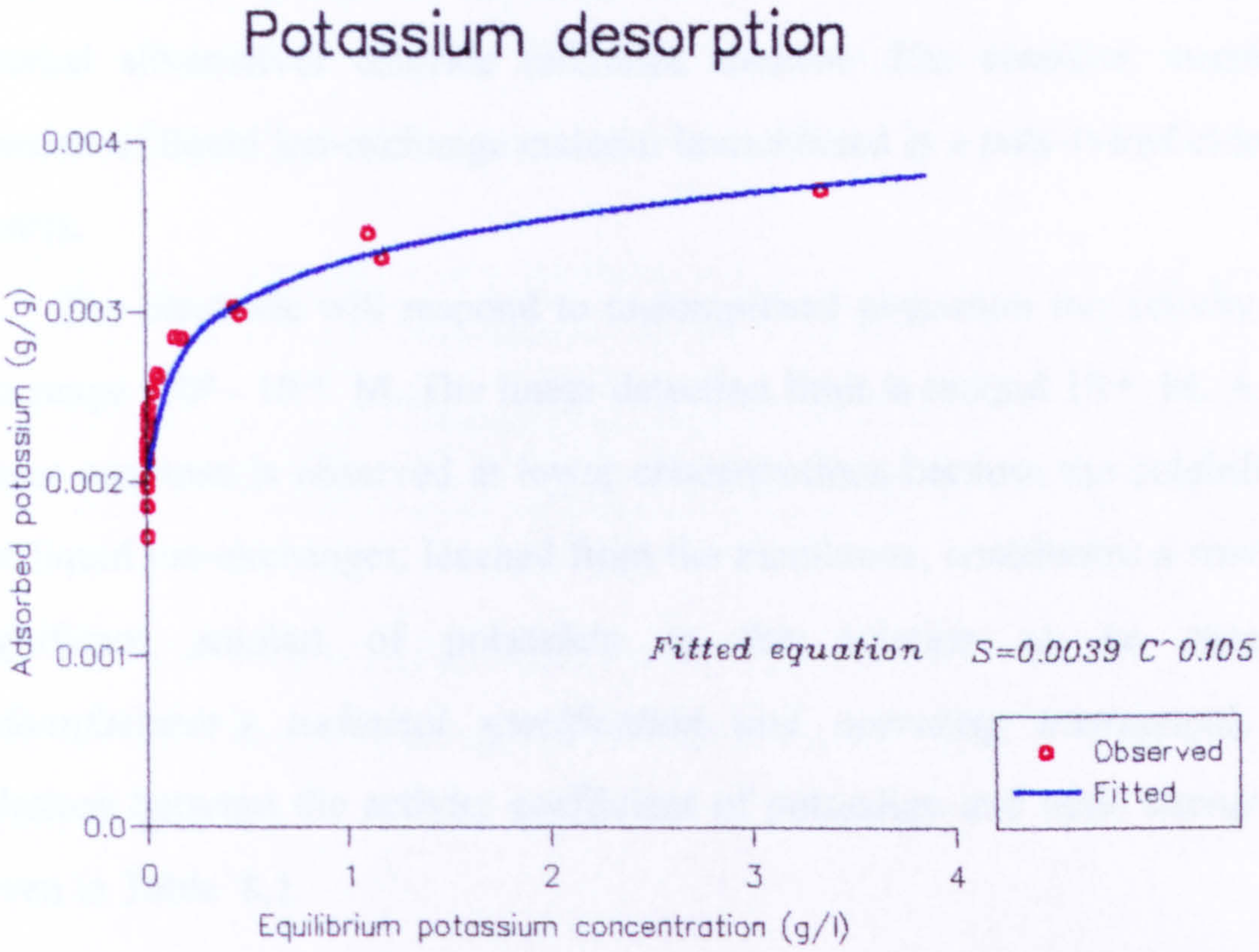

Fig. 8.5 : Adsorbed potassium per unit dry mass of soil as a function of potassium concentration during desorption (for observed and fitted results).

section will examine the system of flow-through cells used in the continuous in-line monitoring and the response time of the electrodes will be checked to ensure that in-line sensors are adequate for both bromide and potassium.

8.3.1 Potassium ISE

The potassium ISE is a plastic-membrane electrode type (Section 7.2.1.3), and consists of an inert fluorocarbon body with a detachable PVC membrane, on the end of which is glued the ion-selective membrane. Inside the membrane unit, an internal filling solution makes contact between the membrane and the internal silver/silver chloride reference element. The sensitive membrane consists of liquid ion-exchange material immobilised in a poly-(vinyl chloride) matrix.

The electrode will respond to uncomplexed potassium ion activity over the range 10^0 - 10^{-4} M. The linear detection limit is around 10^{-4} M. A non-linear response is observed at lower concentrations because the solubility of the liquid ion-exchanger, leached from the membrane, contributes a small but significant amount of potassium to the solution to be measured (*Manufacturer's technical specification and operating instruction*). The relations between the activity coefficient of potassium and ionic strength are given in Table 8.1.

Table 8.1 :Values of potassium activity coefficients and ionic strength, (data from *Manufacturer's manual*).

Ionic strength	0.001	0.005	0.01	0.05	0.1	0.2
Activity coeff. (K^+)	0.975	0.945	0.925	0.85	0.805	0.755

The electrode membrane is chosen to give the greatest possible selectivity for potassium against other ions. The main interfering ions and the selectivity coefficients of the electrode for these ions (Section 7.5), given by the manufacturer, are:

Ca^{++}: 2.8 x 10^{-3} Mg^{++}: 1.9 x 10^{-3} Na^{+}: 2.6 x 10^{-3}.

8.3.2 Bromide ISE

The bromide ISE was a solid-state electrode (Section 7.2.1.2), consisting of an inert polymer body on the end of which is mounted the sensitive membrane. All connections in the electrode are solid-state contacts, there being no liquids of any type inside the body.

The electrode responds to uncomplexed bromide ion activity over the range 10^{0} - 10^{-5} M. The linear detection limit is around 5 x 10^{-5} M. The relation between the activity coefficient of bromide and ionic strength are given in Table 8.2.

Table 8.2 :Values of bromide activity coefficients and ionic strength, (data from *Manufacturer's manual*).

Ionic strength	0.001	0.005	0.01	0.05	0.1	0.2
Activity coeff. (Br^{-})	0.975	0.946	0.926	0.853	0.808	0.755

The electrode is highly selective for bromide. The main interfering ions and the selectivity coefficients of the electrode for these ions, given by the manufacturer, are:

OH^{-}: 3 x 10^{-5} Cl^{-}: 2.5 x 10^{-3}.

8.3.3 Reference electrodes

The reference electrodes are of the double junction type (Section 7.2.2) filled with 3.0 M KCl saturated with AgCl.

8.3.4 Calibration of ISEs

Potassium and bromide electrodes were calibrated by using eight different solutions of KBr (0.004, 0.006, 0.008, 0.02, 0.04, 0.06, 0.08, and 0.1 M) without using any ionic strength adjuster (ISA). Fig. 8.6 shows the results as

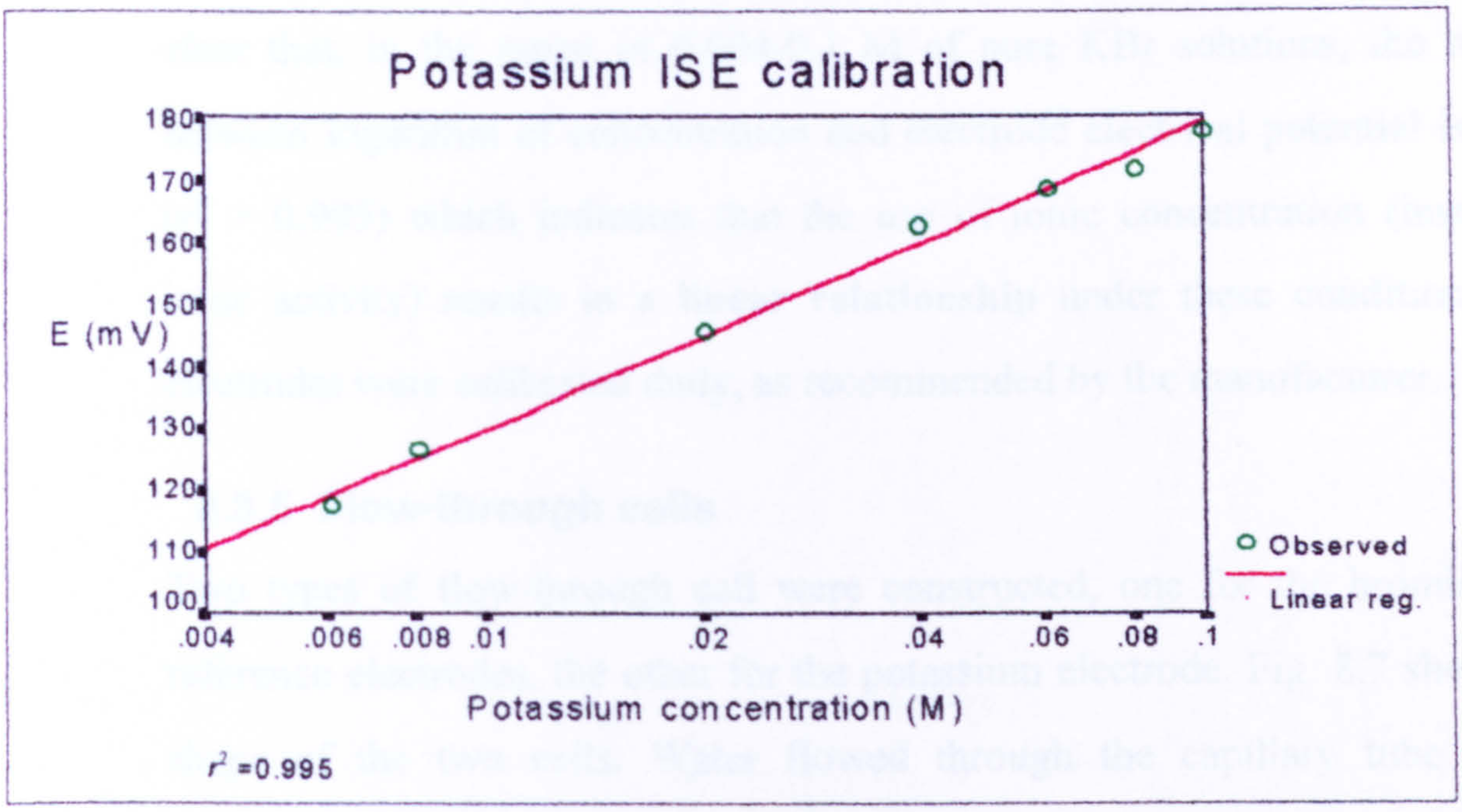

(a)

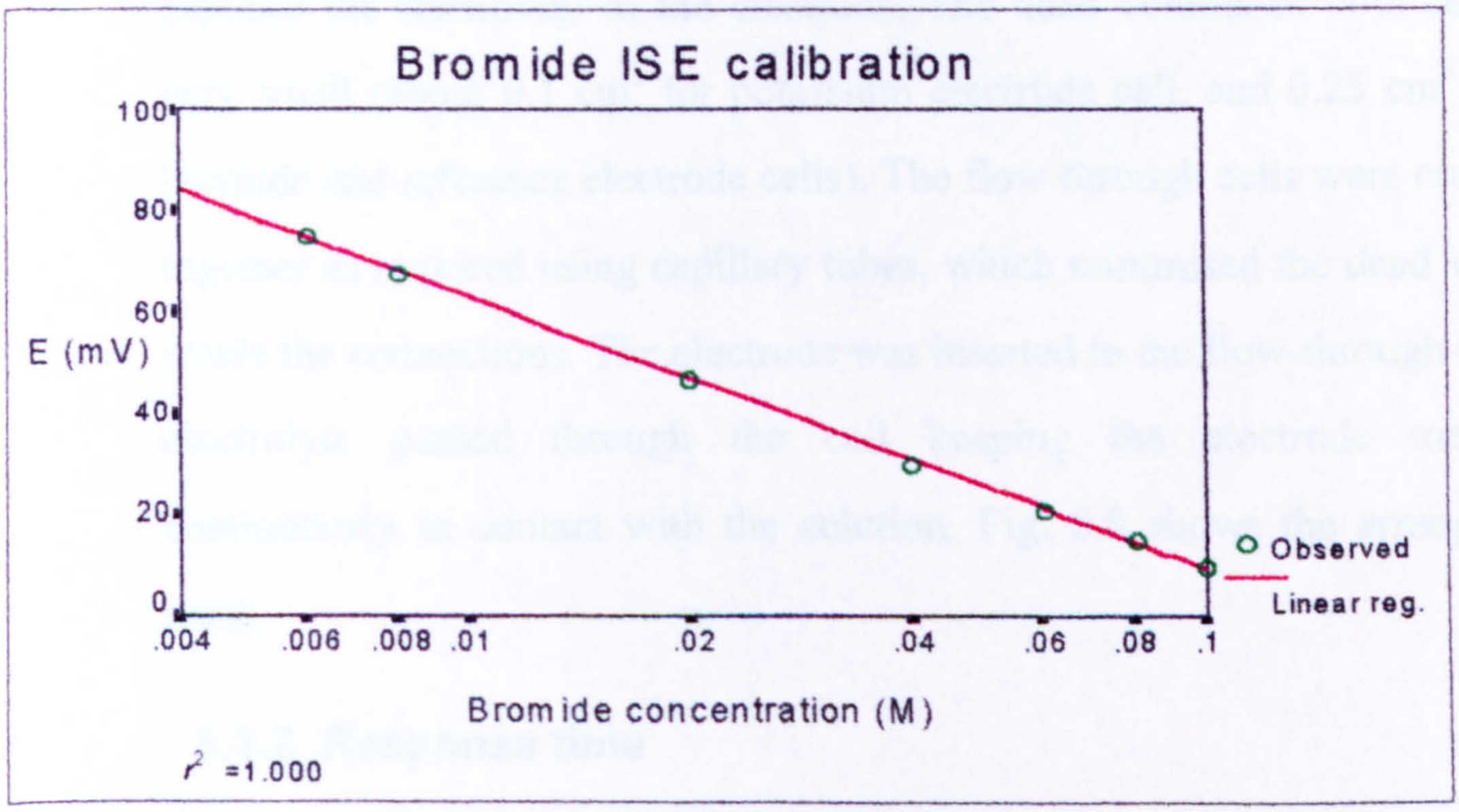

(b)

Fig. 8.6 : Calibration curve of : (a) Potassium (b) Bromide

electrode potential, *E*, against sample concentration on a semi-log scale. It is clear that, in the range of 0.004-0.1 M of pure KBr solutions, the relation between logarithm of concentration and electrode electrical potential is linear ($r^2 > 0.995$) which indicates that the use of ionic concentration (instead of ionic activity) results in a **linear relationship** under these conditions. The electrodes were calibrated daily, as recommended by the manufacturer.

8.3.5 Flow-through cells

Two types of flow-through cell were constructed, one for the bromide and reference electrodes, the other for the potassium electrode. Fig. 8.7 shows the shape of the two cells. Water flowed through the capillary tube of the potassium flow-through cell at a high velocity enabling it to displace the solution in the volume just beneath the electrode's membrane and thus enhance the sensitivity of the electrode. The dead volume in both cells was very small (about 0.1 cm^3 for potassium electrode cell, and 0.25 cm^3 for the bromide and reference electrode cells). The flow-through cells were connected together as required using capillary tubes, which minimised the dead volumes inside the connections. The electrode was inserted in the flow-through cell and electrolyte passed through the cell keeping the electrode membrane continuously in contact with the solution. Fig. 8.8 shows the arrangements used.

8.3.6 Response time

When placing the electrodes in a solution, the electrodes will respond rapidly to the ionic activity in the solution. Equilibrium was reached by the bromide electrode in less than two seconds and by the potassium electrode in less than one minute. To test the transient response of the flow-cell system a 0.1 M KBr solution in a column of 1 mm glass beads was displaced by a 0.004 M KBr solution.

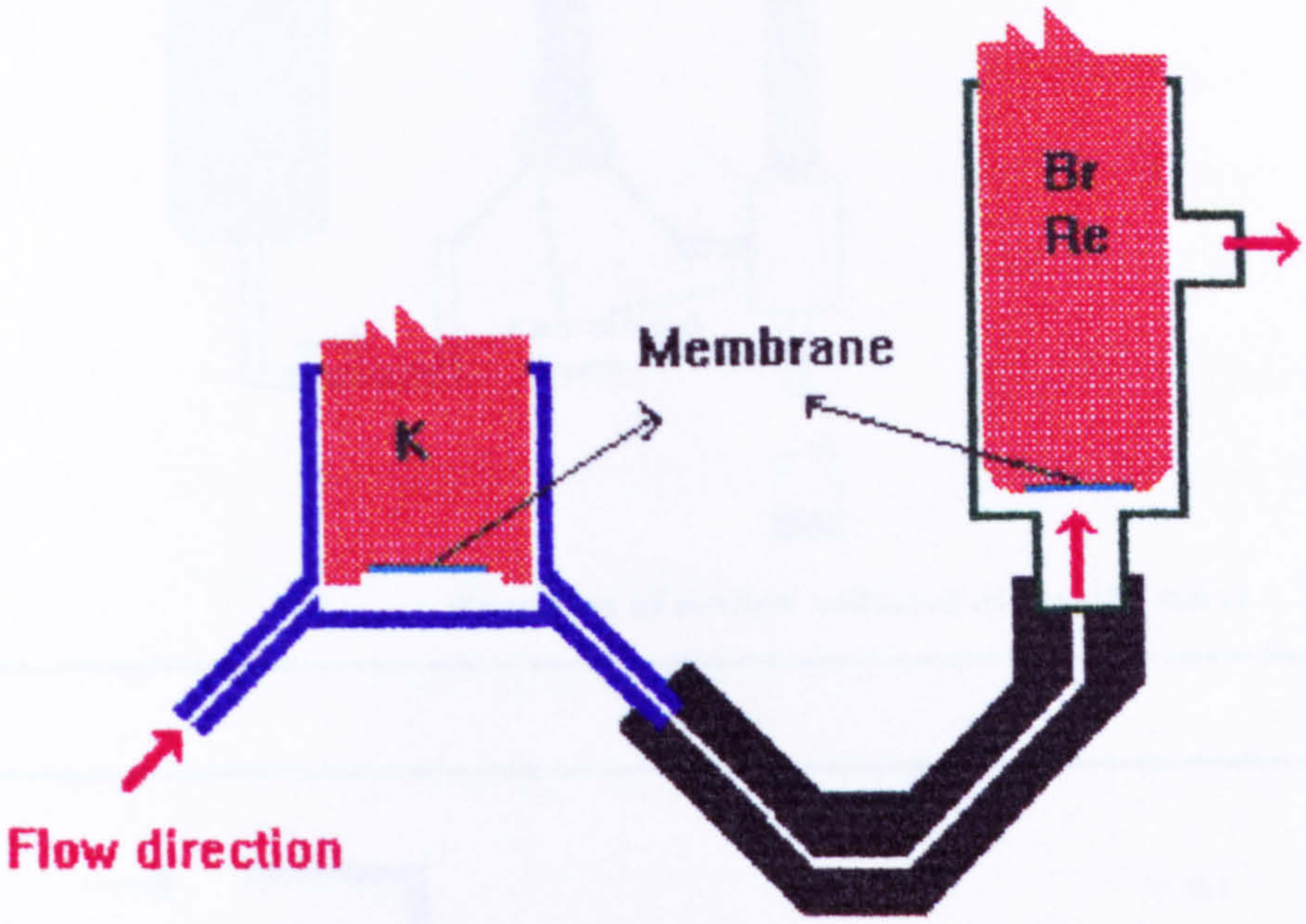

Fig. 8.7 : Flow-through cells

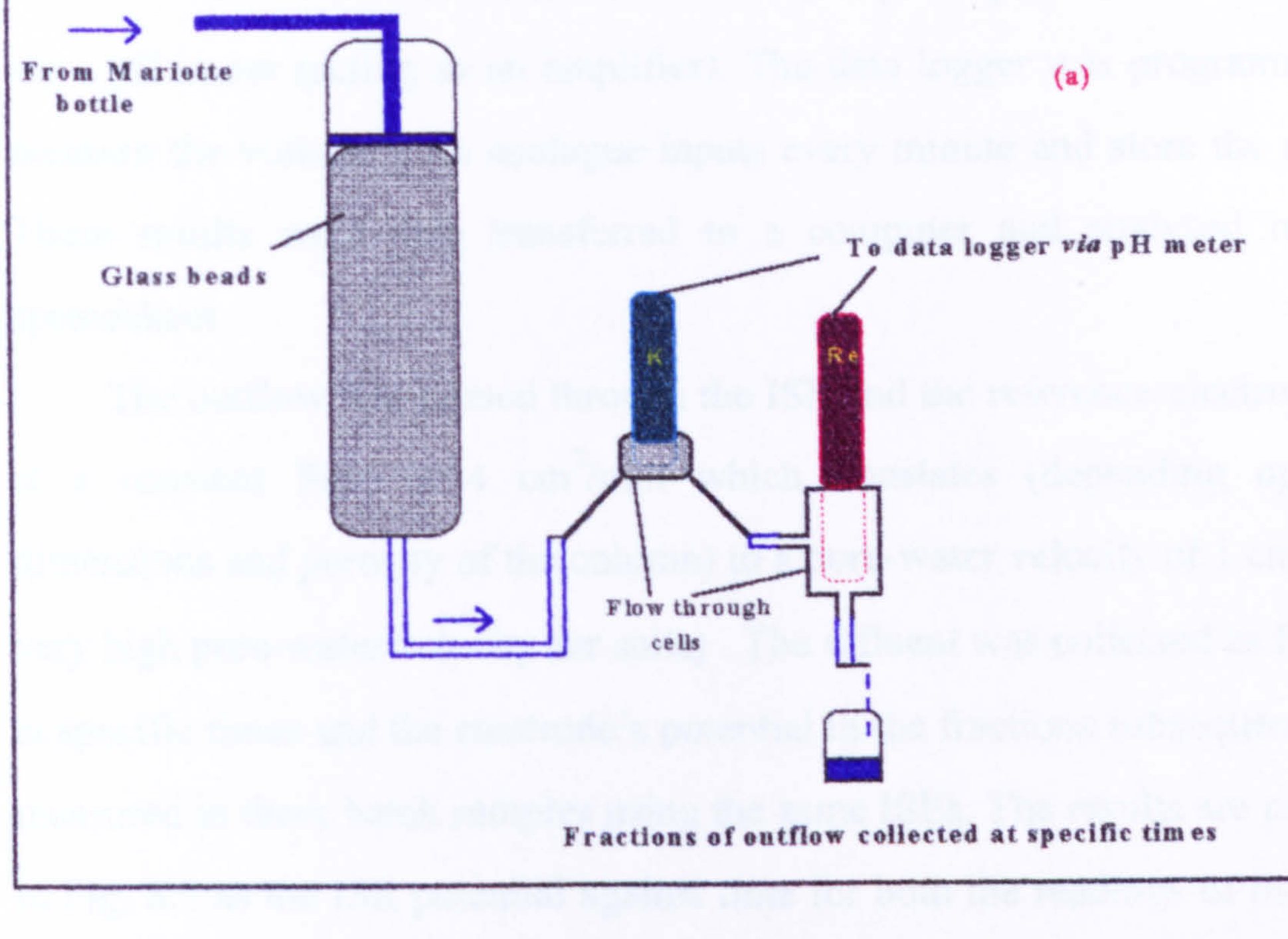

Fig. 8.8: Experimental set-up for continuous monitoring of : (a) Potassium, (b) Bromide.

With the reference electrode installed downstream (Fig. 8.8), both the reference and ISEs were connected to the analogue inputs of the data logger *via* a pH meter (acting as an amplifier). The data logger was programmed to measure the voltage at its analogue inputs every minute and store the results. These results were then transferred to a computer and analysed using a spreadsheet.

The outflow was passed through the ISE and the reference-electrode cells at a constant flow of 4 cm^3/min which translates (depending upon the dimensions and porosity of the column) to a pore-water velocity of 1 cm/min (a very high pore-water velocity for soils) . The effluent was collected as fractions at specific times and the electrode's potential in the fractions subsequently later measured in these batch samples using the same ISEs. The results are presented in Fig. 8.9 as the ISE potential against time for both the readings of the in-line (flow-through cell) system and the batch fractions. The fit between the two methods was very good (R^2 = 0.997 and 0.994 for bromide and potassium electrode respectively) with a closer fit between batch and in-line readings for bromide due to the faster response time of the ISE. However, it is clear from the results that in-line sensors for the range of effluent flow velocities that may encountered in soils would be adequate for both bromide and potassium.

8.4 Using ISEs with soil columns

After establishing the success of the in-line monitoring of the bromide and potassium in the leachate from the glass-bead column, the two ions will be monitored in the leachate from soil-aggregate columns. Firstly the soil columns will be prepared and the flow-through system will be set up. The potassium, bromide and common reference electrodes will be installed in the system and the leaching experiments will then be carried out. The resulting electrical potential will be recorded and, by calibrating the ISEs with soil solution

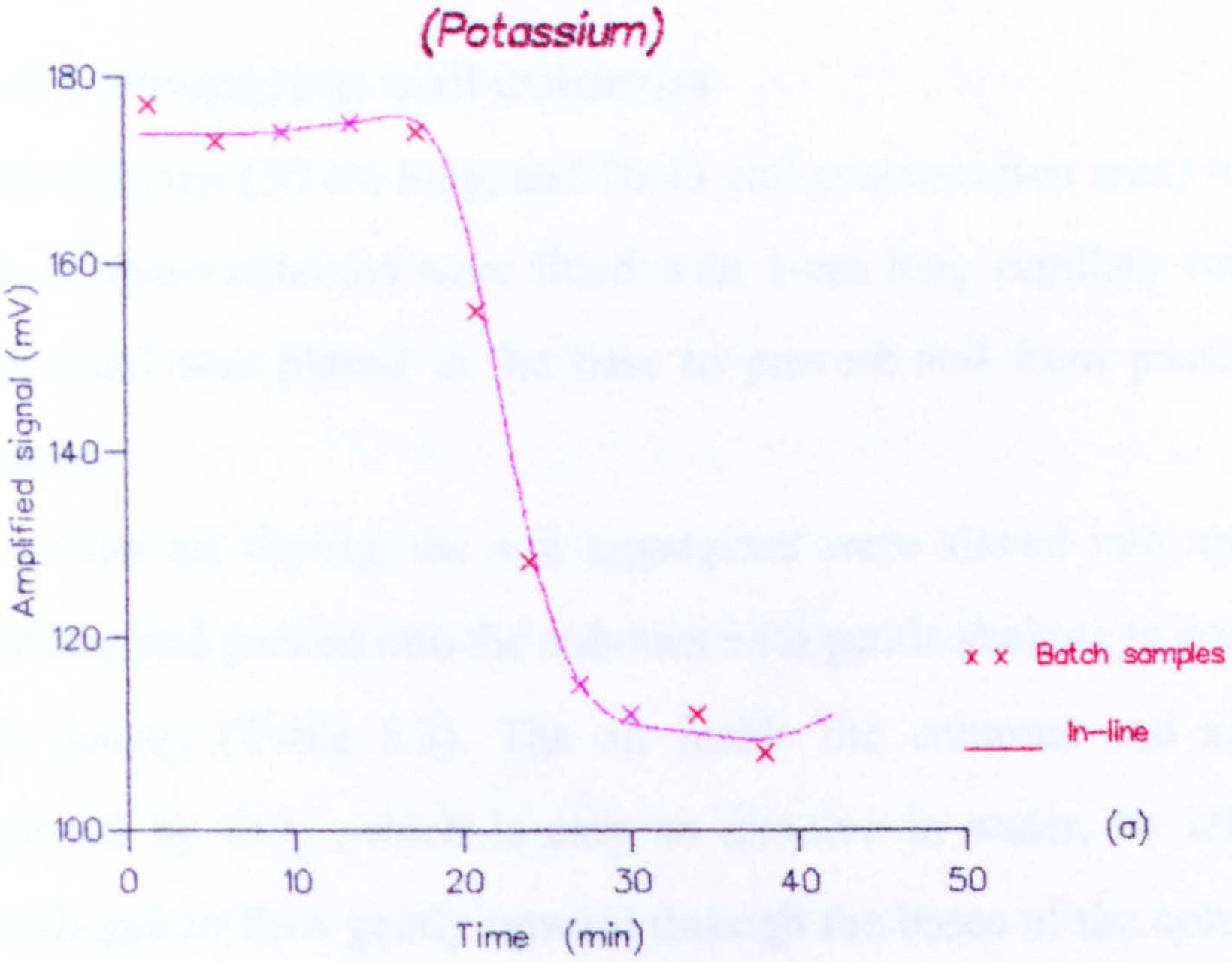

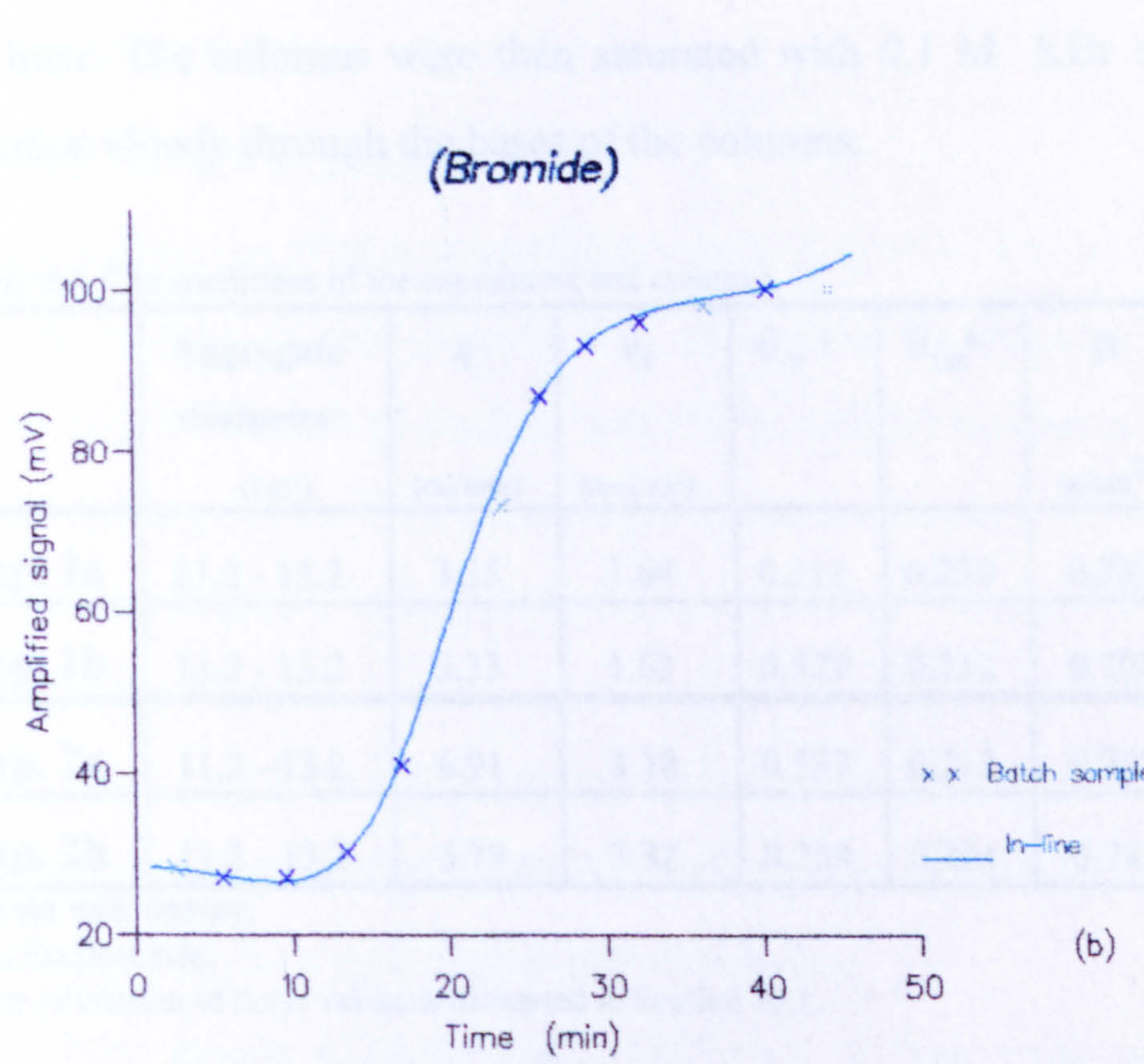

Fig. 8.9 **: Electrode potential against time for continuous monitoring (in-line) and sampling results: (a) Potassium, (b) Bromide.**

samples, such results can be converted to concentration units. These procedures are discussed in turn.

8.4.1 Preparing soil columns

Glass columns (30 cm long, and 20.43 cm^2 cross-section area) were used. The ends of these columns were fitted with 1-cm long capillary tubes. A pad of glass wool was placed at the base to prevent soil from passing out of the columns.

After air drying, the soil aggregates were sieved into appropriate size fractions, and packed into the columns with gentle shaking to ensure a uniform bulk density (Table 8.3). The air inside the columns and aggregates was displaced by CO_2 ,which is easy to dissolve in water, by allowing carbon dioxide gas to flow gently upward through the bases of the columns for about an hour. The columns were then saturated with 0.1 M KBr by passing the solution slowly through the bases of the columns.

Table 8.3: The conditions of the experiment soil columns.

	Aggregate diameter (mm)	q (ml/min)	v_d (mm/min)	θ_m*	θ_{im}*	ρ (g/cm^3)	*On/Off* periods (min)
Exp. 1a	11.2 - 13.2	3.35	1.64	0.311	0.220	0.732	Cont.
Exp. 1b	11.2 - 13.2	3.33	1.63	0.329	0.212	0.708	50/50
Exp. 2a	11.2 - 13.2	6.91	3.38	0.337	0.212	0.708	Cont.
Exp. 2b	11.2 - 13.2	6.79	3.32	0.258	0.224	0.747	25/50

ρ is the bulk density,
q is the flow rate,
* the estimation of these values is discussed in Section 10.1.

The solution inside the column was then displaced slowly with at least two pore volumes of fresh 0.1 M KBr every day for three days so that most of other ions in the soil solution were leached out. The column was then left for another two days in a constant temperature room (20±1°C) to complete the

equilibrium between soil aggregates and soil solution.

8.4.2 The ISEs' connections

The ISEs were connected to two of the analogue inputs of the data logger *via* two pH meters (acting as amplifiers). Connecting the ISEs without using pH meters gave unstable results. One reference electrode was installed downstream as a common reference for both K^+ and Br^- electrodes, and connected to both of the pH meters. The data logger was programmed to measure the voltage at these two analogue inputs every minute and store the results, which were then transferred to a computer to be analysed. Fig. 8.10 shows a simple description of these connections.

The flow was controlled by a peristaltic pump downstream and was finally collected in a container placed on a balance for measurement of the outflow (Fig. 8.11).

8.4.3 Leaching experiment

The leaching experiment procedures were the same as for the leaching of the porous ceramic spheres (Section 3.3), except that the displacing solution was 0.004 M KBr instead of distilled water. This was for two reasons:

1) the readings of the ISEs are unstable at concentrations < 0.004 M;

2) the interference of other ions will be greater at very low concentrations of the monitored ions.

The 0.1 M KBr was displaced from the columns of saturated aggregates by the displacing solution (0.004 M KBr), and the effluent was passed through the ISE set-up for continuous in-line monitoring.

Two groups of experiments (differing in flow rate) were carried out using the same aggregate size and same column dimensions. Each group consisted of two experiments differing only in the leaching method. One was leached continuously and the other intermittently. Table 8.3 shows the conditions.

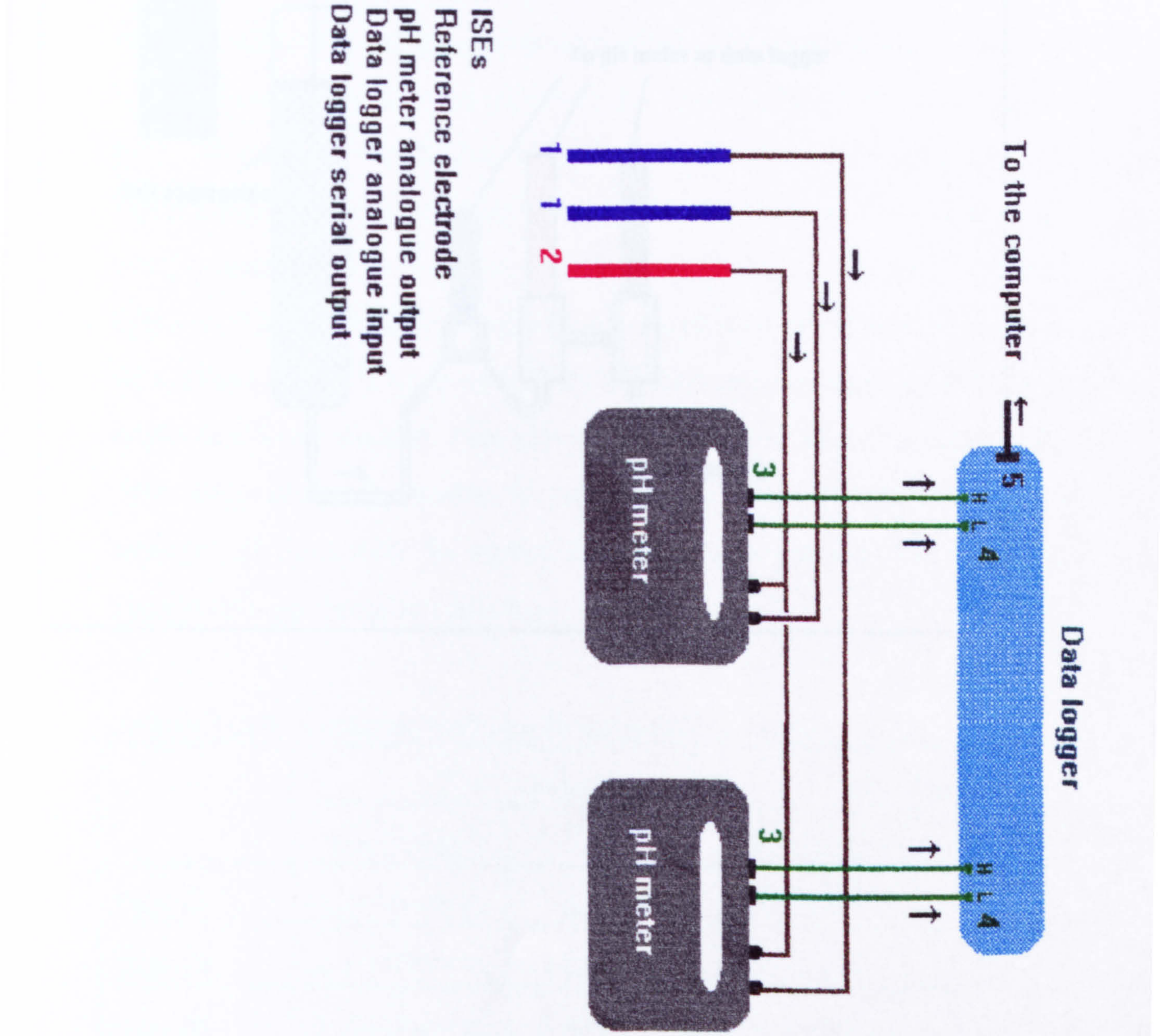

Fig. 8.10: Connections of the ISEs and reference electrode to a data logger *via* two pH meters.

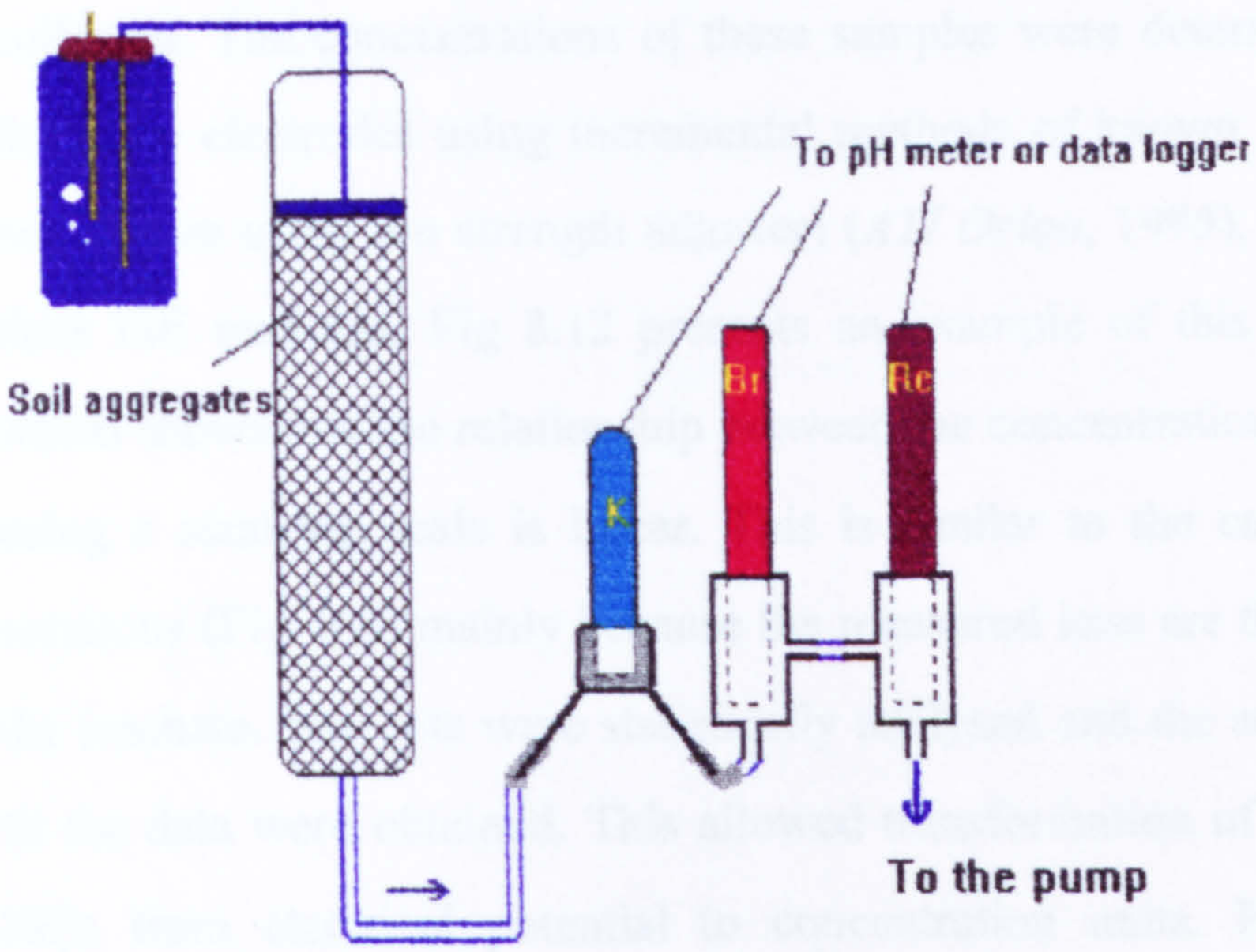

Fig. 8.11: Displacement experiment set-up, showing the connection of ISEs with the soil column.

8.4.4 Calibrating ISEs with soil solution

To transfer the readings of the ISEs to concentration units, the ISEs should be calibrated, but using actual soil solutions instead of the pure KBr solutions so that the effect of interference by any other ions is included.

During the experiment a few samples (five to six) of the effluent were collected. The concentrations of these samples were determined by means of the same electrodes using incremental methods of known addition (which do not require using ion strength adjuster) (*ATI Orion*, 1995), and plotted against their ISE readings. Fig 8.12 presents an example of this plot (for Exp. 1a) which shows that the relationship between the concentrations and ISE readings using a semi-log scale is linear. This is similar to the calibration with pure solutions (Fig. 8.6) mainly because the measured ions are the dominant ions in the leachate. The data were statistically analysed and the equations which best fit the data were obtained. This allowed transformation of the readings of the ISEs from electrical potential to concentration units. Fig. 8.13 shows an example of these best fit curves for Exp. 1a while the results for all experiments are shown in Table 8.4.

Table 8.4: Best-fit equations which relate the ISE reading with concentration.

	For potassium		For bromide	
	Best fit Eqs.	R^2	Best fit Eqs.	R^2
Exp. 1a	$C = e^{(-11.43+0.054\,Y)}$	0.999	$C = e^{(0.496-0.043\,Y)}$	0.997
Exp. 1b	$C = e^{(-11.44+0.052\,Y)}$	0.999	$C = e^{(0.747-0.044\,Y)}$	0.992
Exp. 2a	$C = e^{(-11.46+0.054\,Y)}$	0.998	$C = e^{(1.306-0.042\,Y)}$	0.999
Exp. 2b	$C = e^{(-11.87+0.057\,Y)}$	0.997	$C = e^{(1.125-0.042\,Y)}$	0.999

R^2 is coefficient of determination,
Y is the ISE readings (mV),
C is the solute concentration (mol/l).

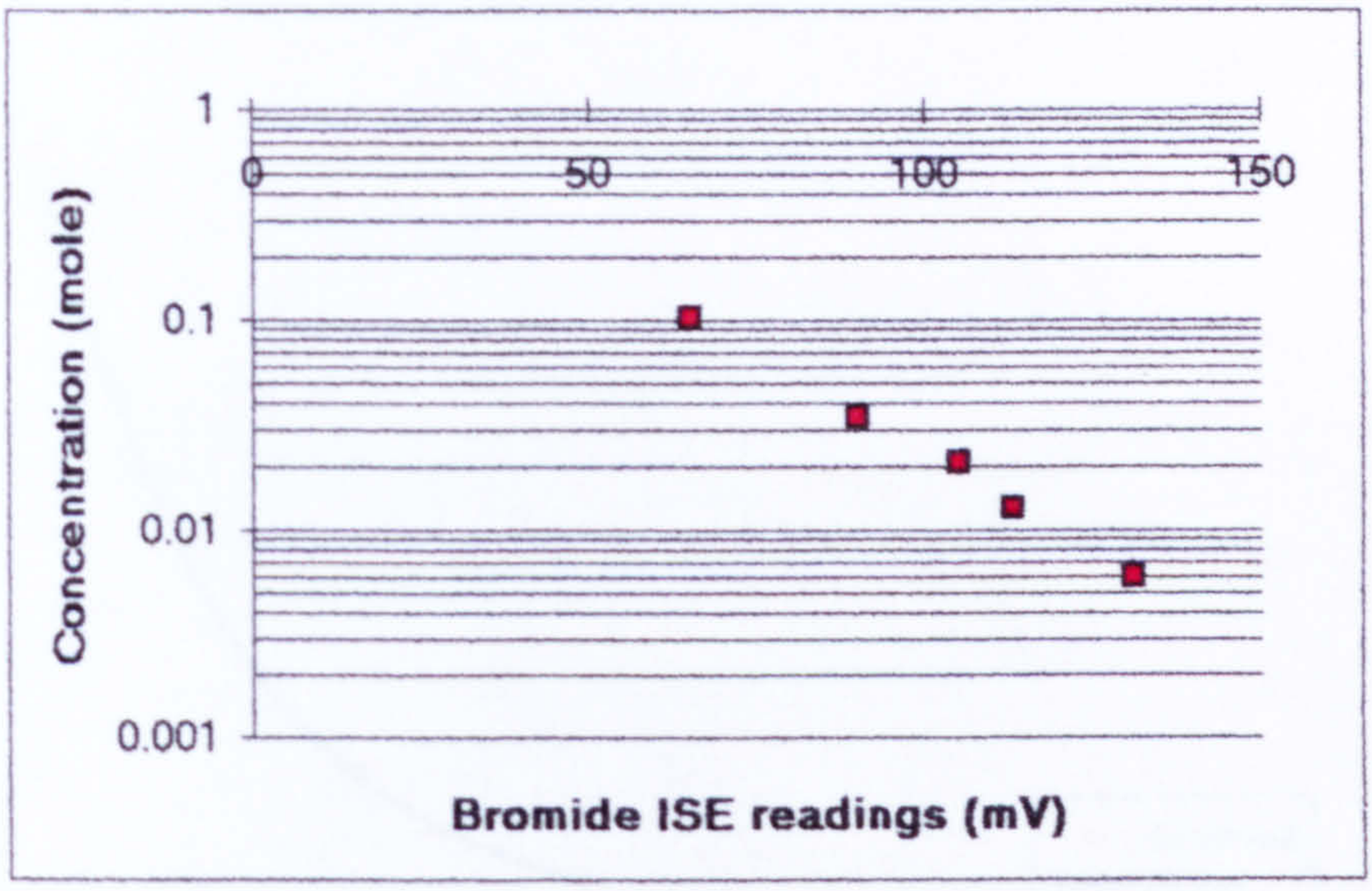

(a)

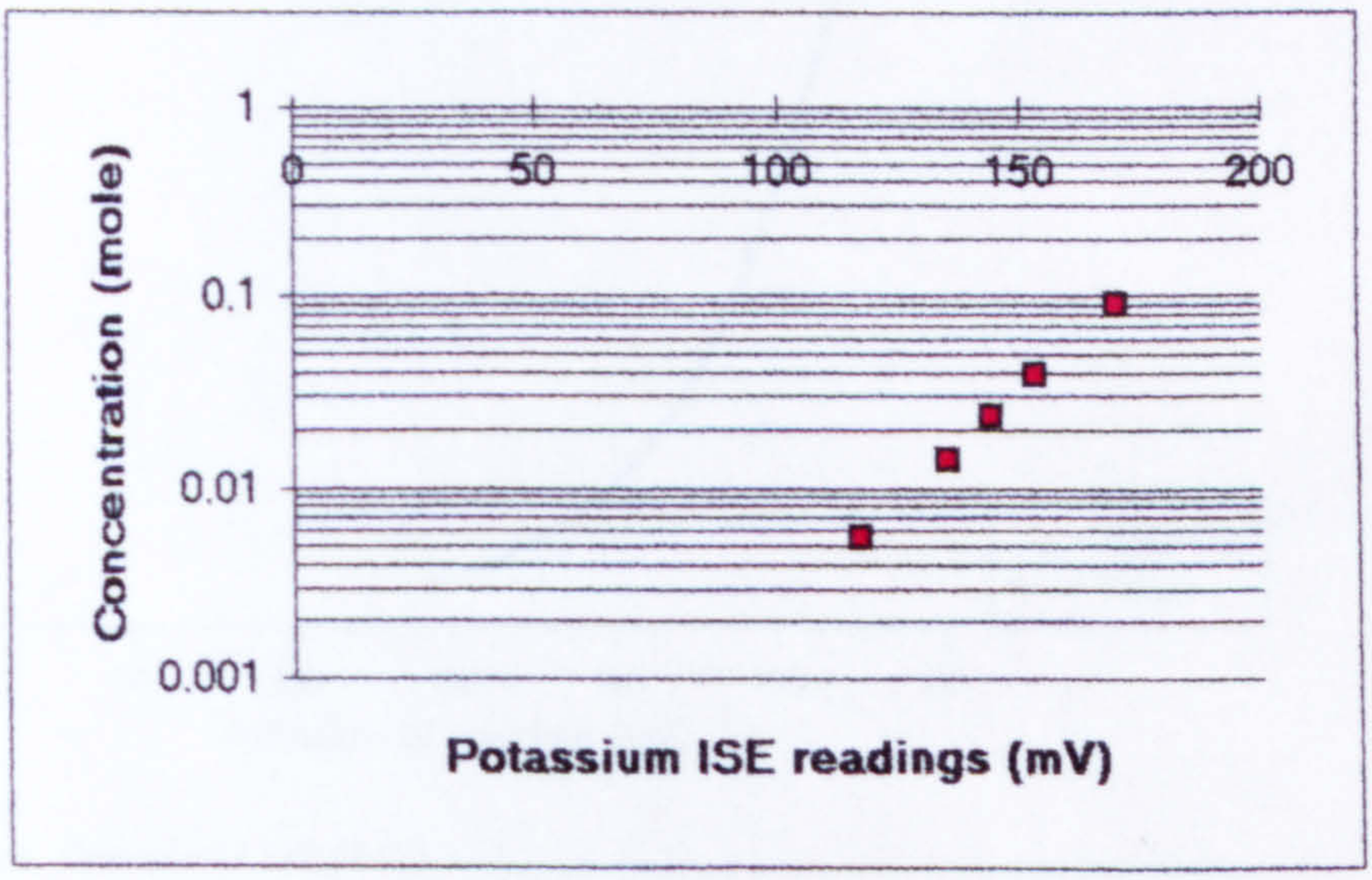

(b)

Fig. 8.12: Concentrations of soil solution samples against their ISE readings for Exp. 1a: (a) Bromide, (b) Potassium.

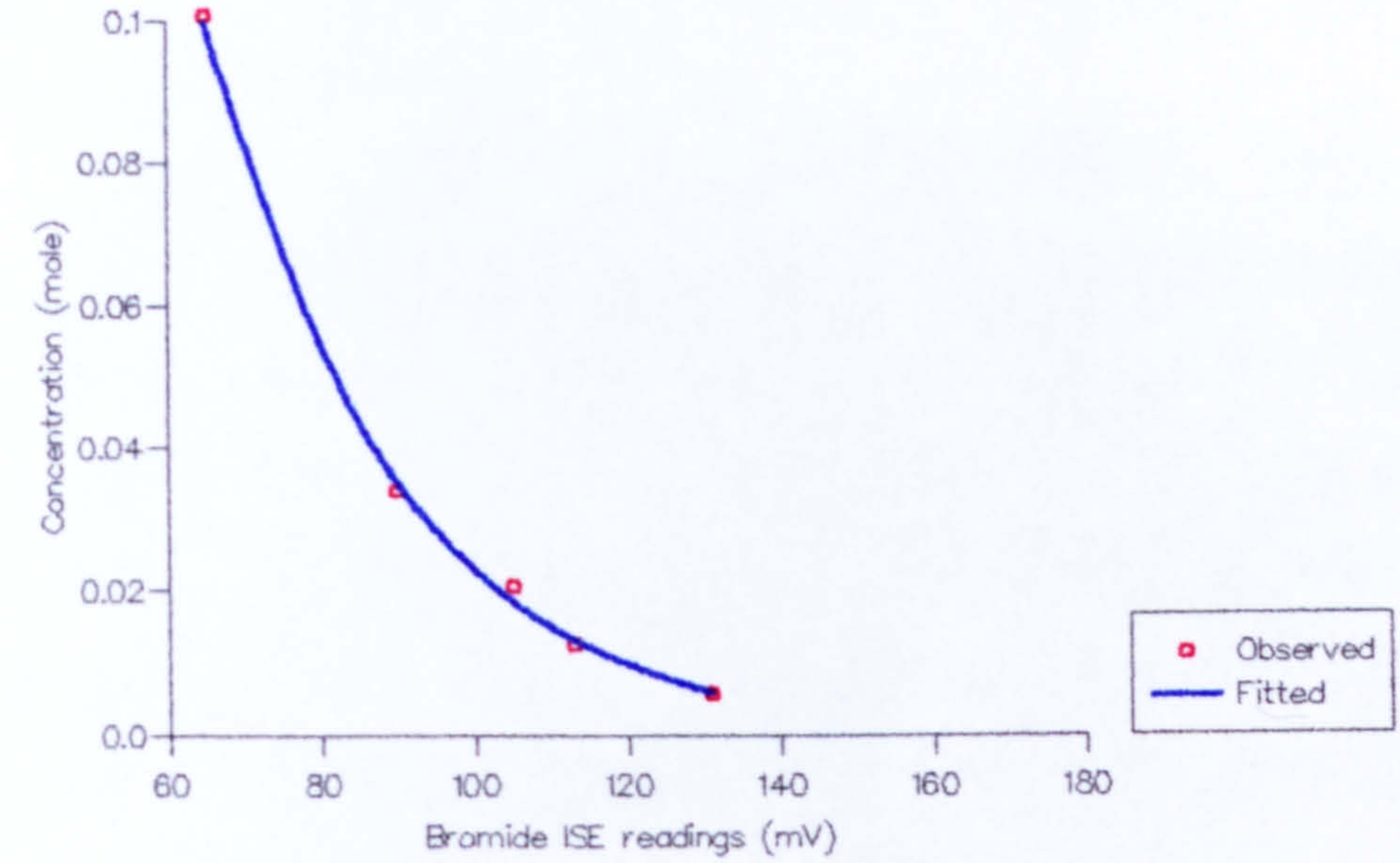

Fitted equation C=exp(0.496−0.043Y)

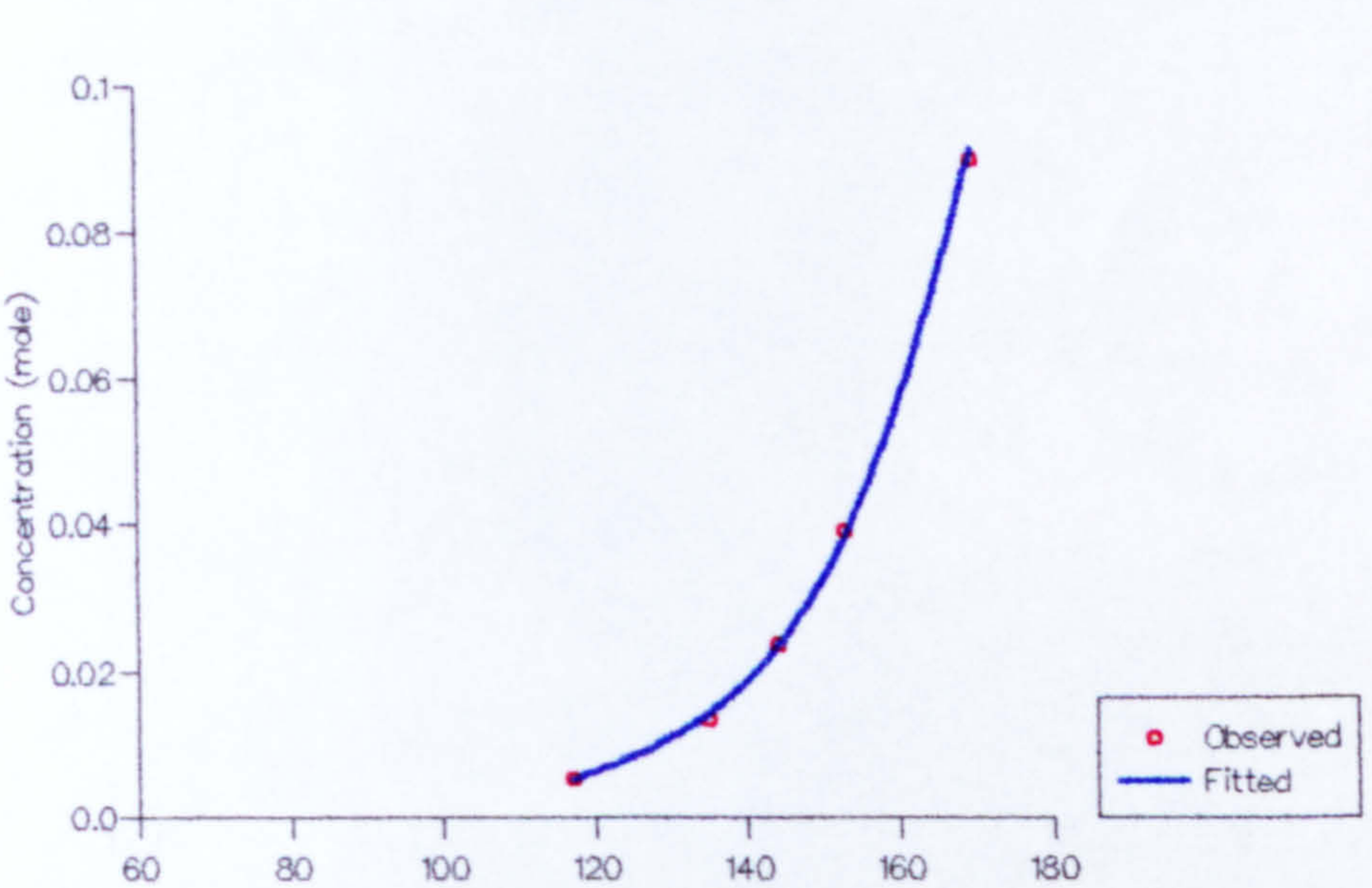

Fitted equation C=exp(−11.43+0.054Y)

***Fig. 8.13*: Concentrations of soil solution samples against their ISE readings for Exp. 1a (observed and fitted results): (a)Bromide, (b) Potassium .**

8.4.5 Experimental results and discussion

Figs. 8.14 & 8.15 show the results of the leaching experiments as ISE readings against the displacement time (i.e., the cumulative *on* time), for experiments 1a,b and 2a,b respectively.

The BTCs show, as expected, a long tailing because of the slow transfer of solute out of the aggregates. During intermittent leaching experiments (Exps. 1b, 2b), the electrode potential changed after each rest period, showing that there was solute diffusion out of aggregates during such periods (note that a decrease of bromide electrode potential means an increase in bromide concentration). These changes were slightly smaller with potassium than with bromide. This is because potassium ions are retarded within the aggregates much more than bromide ions.

Such results will be more informative if the graph uses concentration units instead of the electrical potential. The fitted equations of Table 8.4 were applied to the previous ISE readings. Figs. 8.14 & 8.15 can be represented now as $\frac{C - C_{inp}}{C_o - C_{inp}}$ *vs.* pore volumes where

C = is solute concentration in the effluent,

C_{inp} = is solute concentration in the input,

C_o = is initial solute concentration.

The results are shown in Figs. 8.16 & 8.17 for Exps. 1 & 2, respectively. The figures show that potassium concentration was greater than bromide concentration almost all the time. This is because of the desorption of some of the adsorbed potassium on the soil particle surfaces. Eventually, the two ions reached the same concentration when most of the adsorbed potassium was desorbed. However, with intermittent leaching, the rest periods resulted in more time available for equilibration between the solute in mobile and immobile water causing more potassium to desorb. Thus the two ions reached

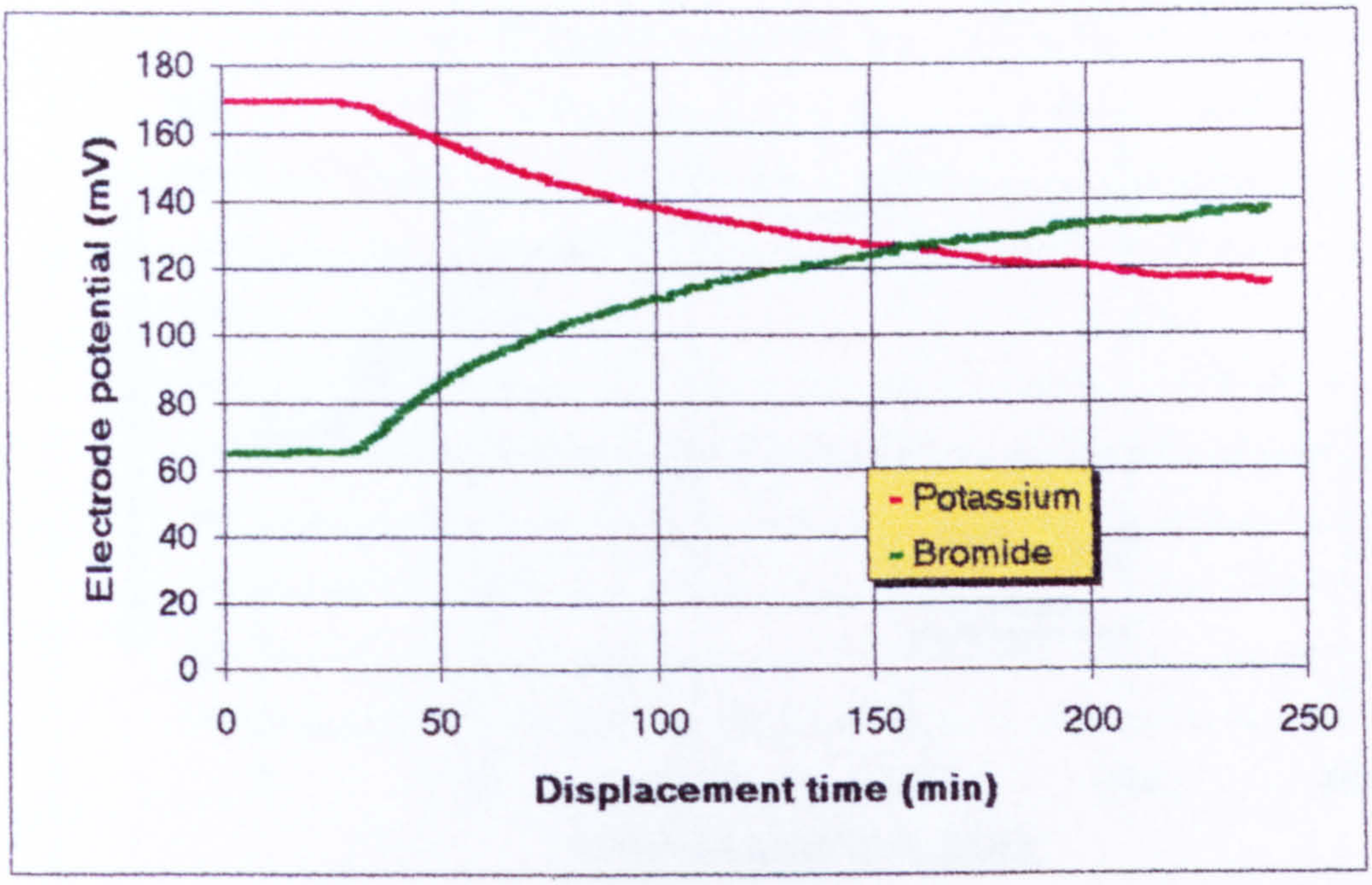

(a)

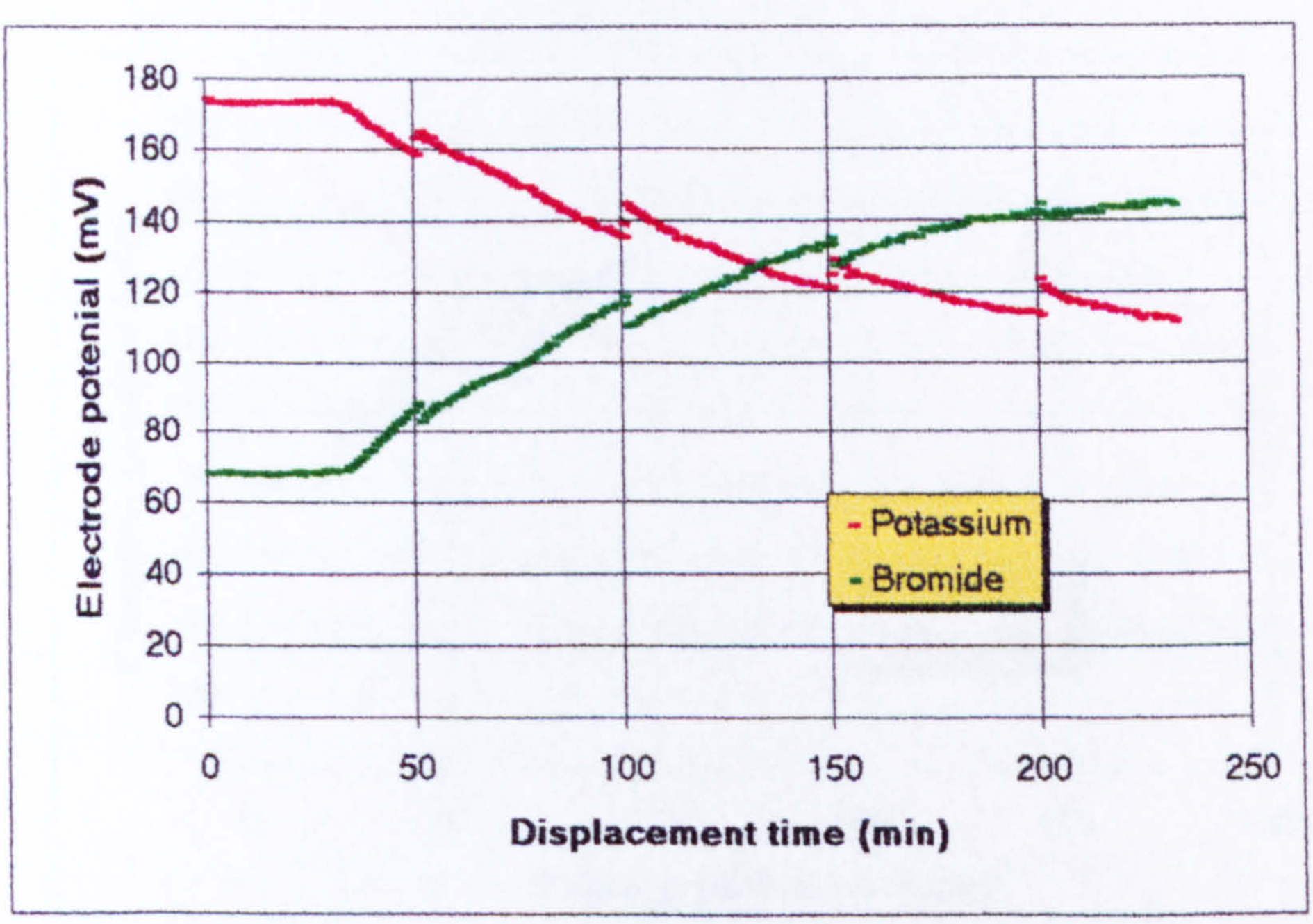

(b)

Fig. 8.14: Electrode potential readings against displacement time for (a) Exp. 1a, (b) Exp. 1b.

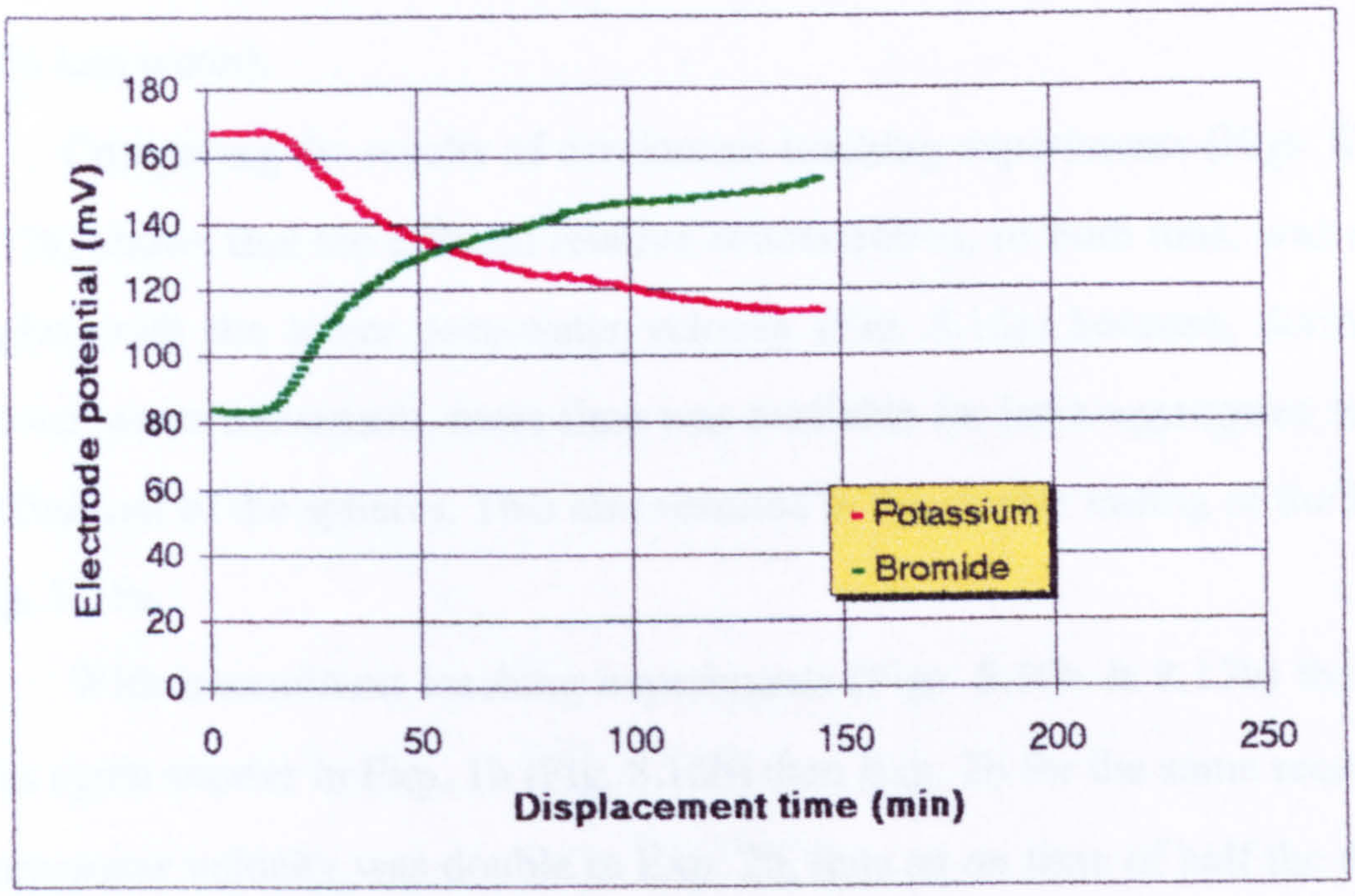

(a)

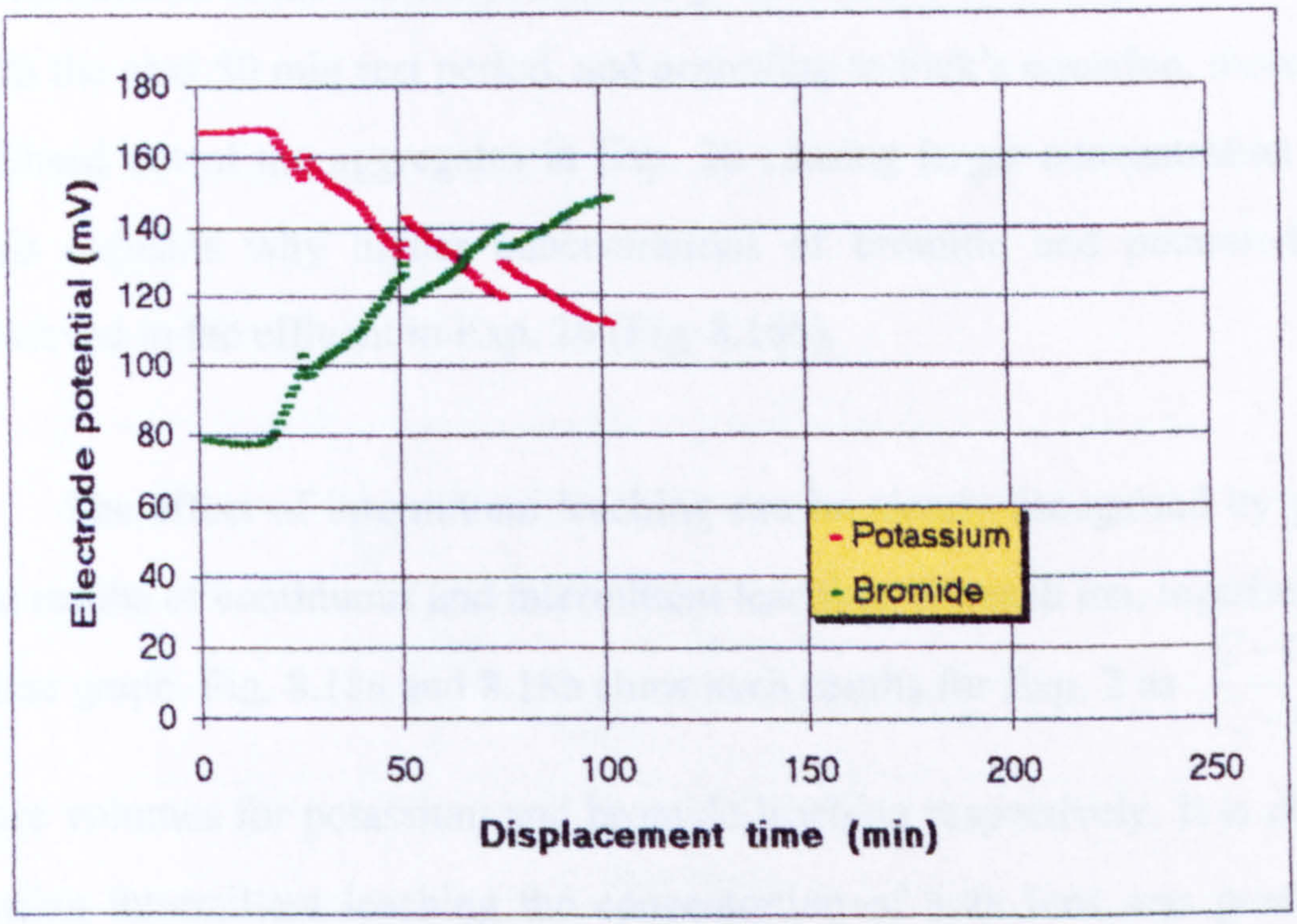

(b)

Fig. 8.15: Electrode potential readings against displacement time for (a) Exp. 2a, (b) Exp. 2b.

the same concentration earlier than with continuous leaching (and used about 25% less water).

Comparing the results of continuous leaching experiments (Figs. 8.16a & 8.17a) shows that the effluent relative concentration, of both ions, was slightly higher with the lower pore-water velocity (Fig. 8.16a) because, during such slower water movement, more time was available for intra-aggregates solute to diffuse out of the spheres. This also resulted in the shorter tailing of the BTC of Fig. 8.16a.

With intermittent leaching experiments (Figs. 8.16b & 8.17b) the tailing was again shorter in Exp. 1b (Fig. 8.16b) than Exp. 2b for the same reason. The pore-water velocity was double in Exp. 2b, thus an *on* time of half the duration of Exp. 2a was required to pass the same amount of leaching water. Consequently less solute diffused out of the aggregates, which left the concentration in the immobile solution greater than that of Exp. 2a. Therefore, with the next 50 min rest period, and according to Fick's equation, more solute diffused out of the aggregates in Exp. 2b causing larger concentration peaks. This explains why higher concentrations of bromide and potassium were observed in the effluent in Exp. 2b (Fig. 8.16b).

The effect of intermittent leaching can be clearly recognised by plotting the results of continuous and intermittent leaching, for each ion, together on the same graph. Fig. 8.18a and 8.18b show such results for Exp. 2 as $\frac{C - C_{inp}}{C_o - C_{inp}}$ *vs.* pore volumes for potassium and bromide leaching respectively. It is clear that during intermittent leaching the concentration of both ions was greater than during continuous leaching, as with the leaching of porous spheres (Fig. 3.6). This demonstrates that solute was leached more quickly during intermittent leaching. The difference between the two methods was, however, smaller for the lower velocity of Exp. 1, for both ions (as shown in Fig. 8.19), as the lower

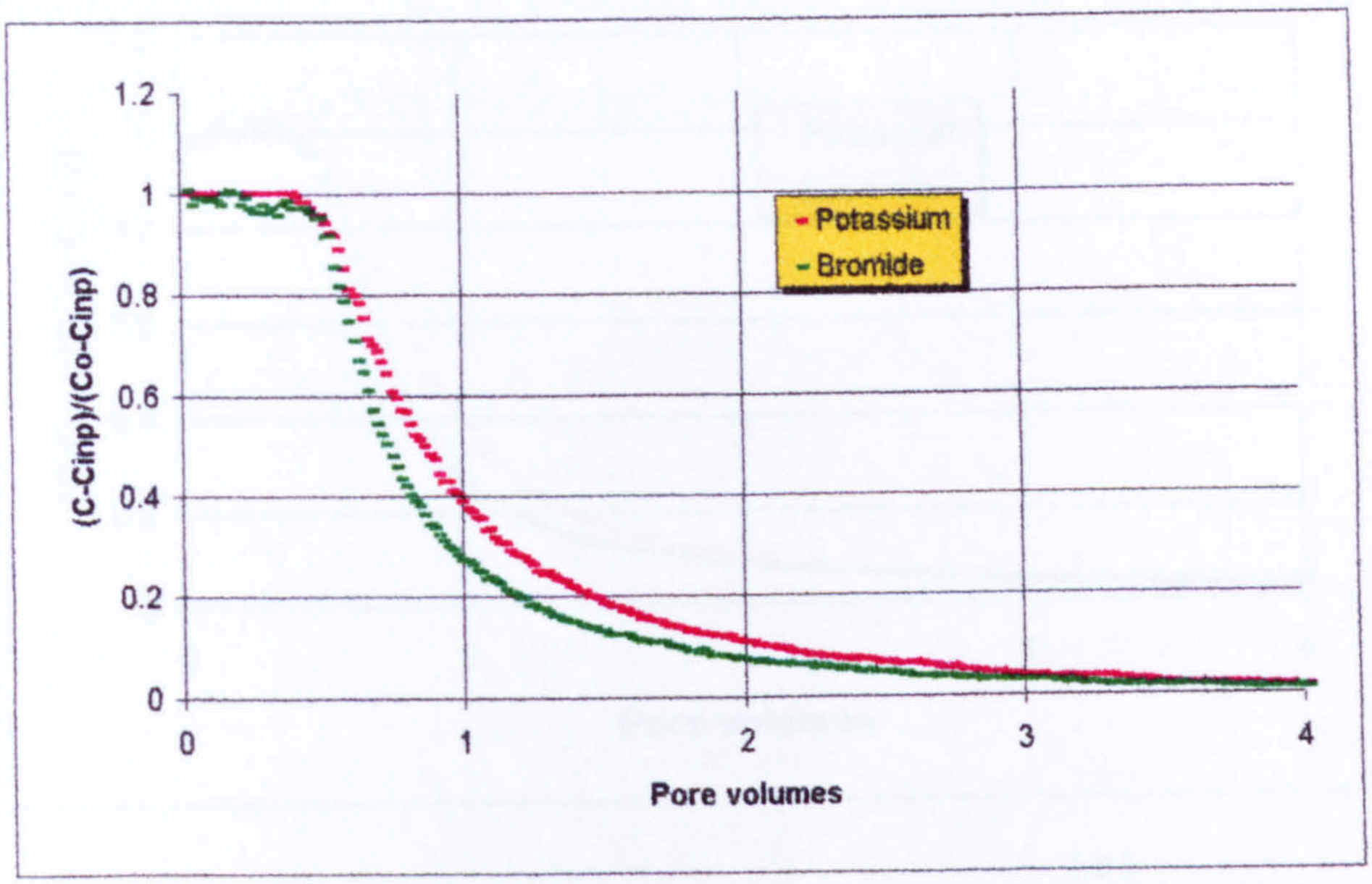

(a)

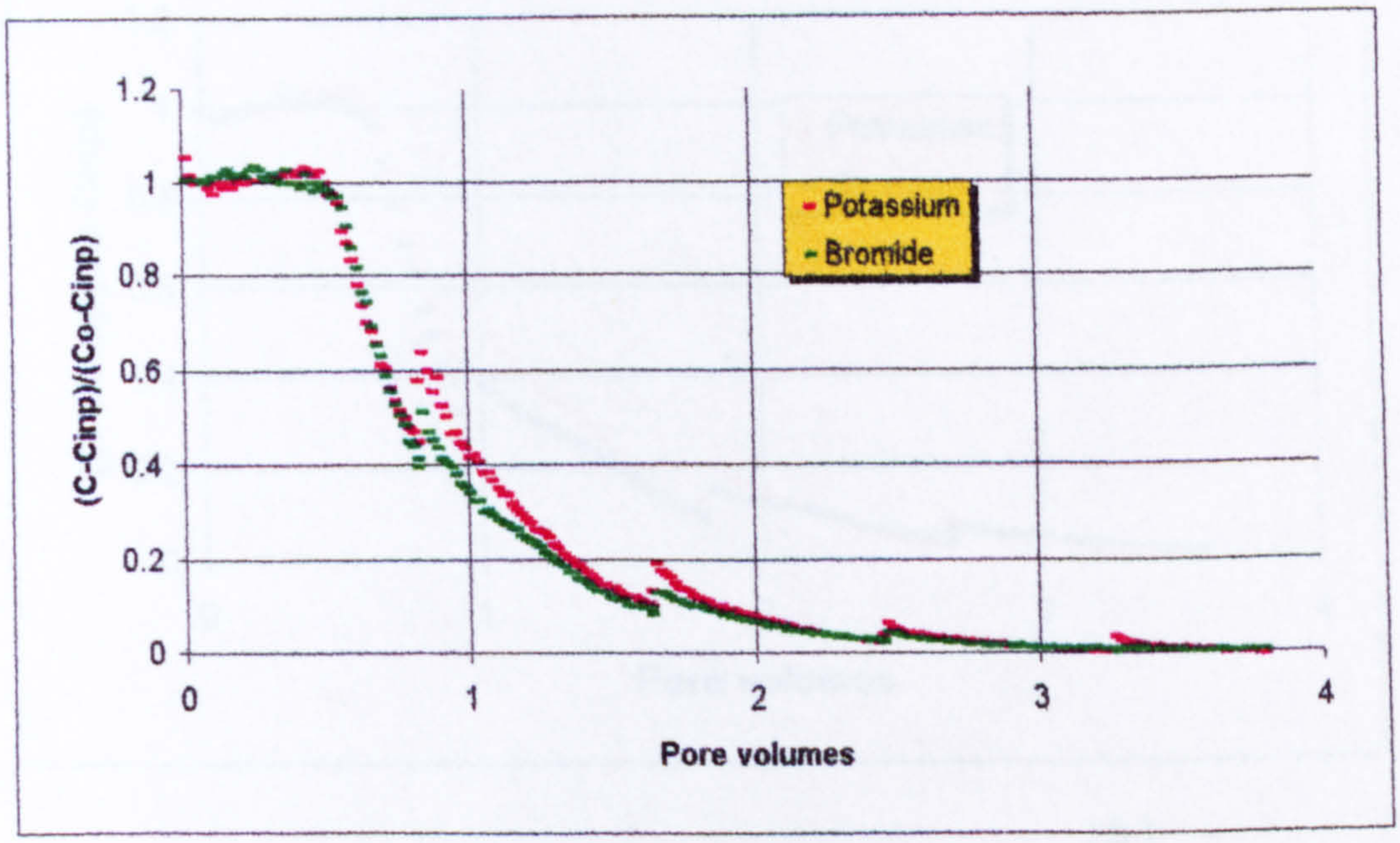

(b)

Fig. 8.16: $\frac{C - C_{inp}}{C_o - C_{inp}}$ against pore volumes for (a) Exp. 1a, and (b) Exp. 1b.

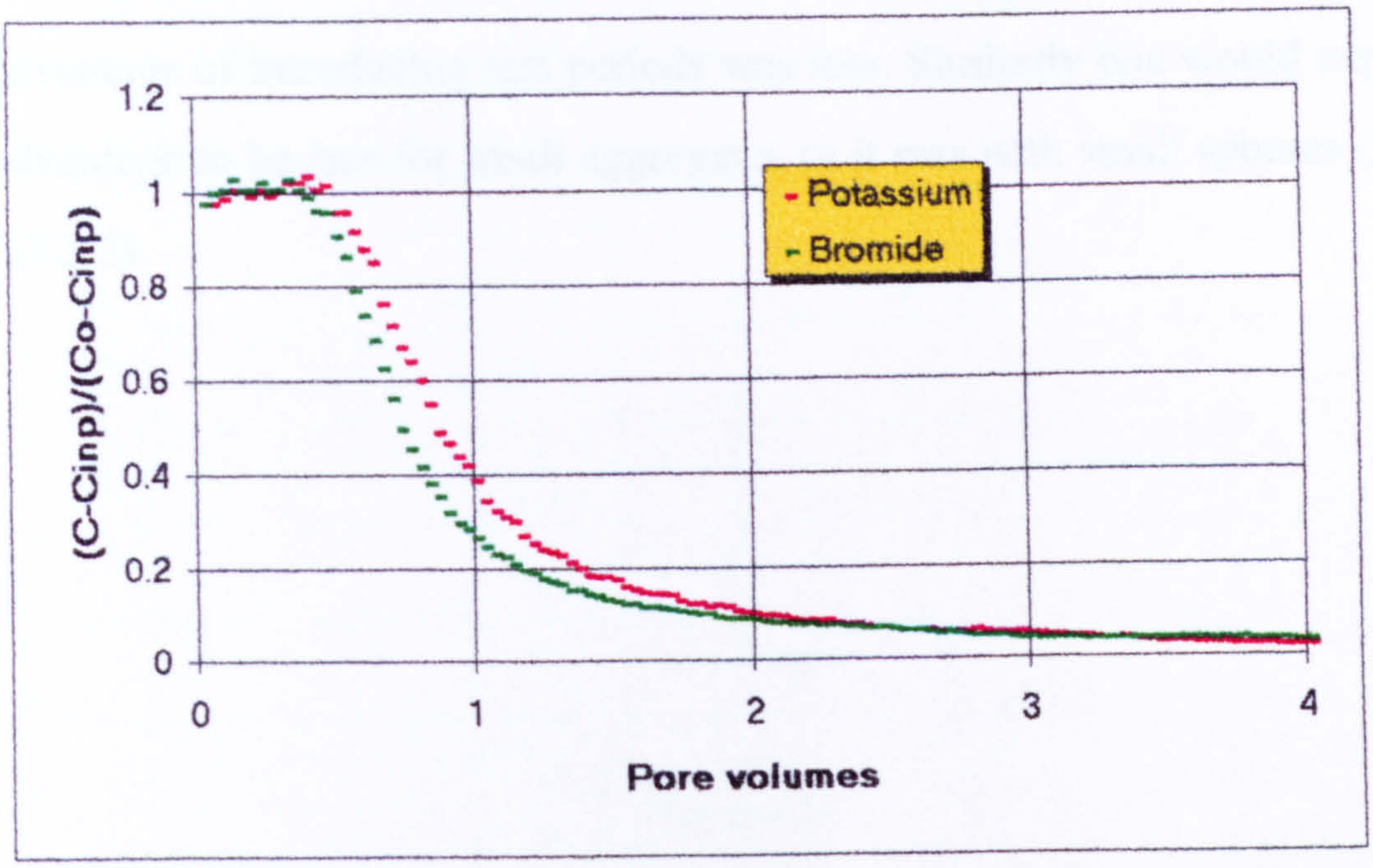

(a)

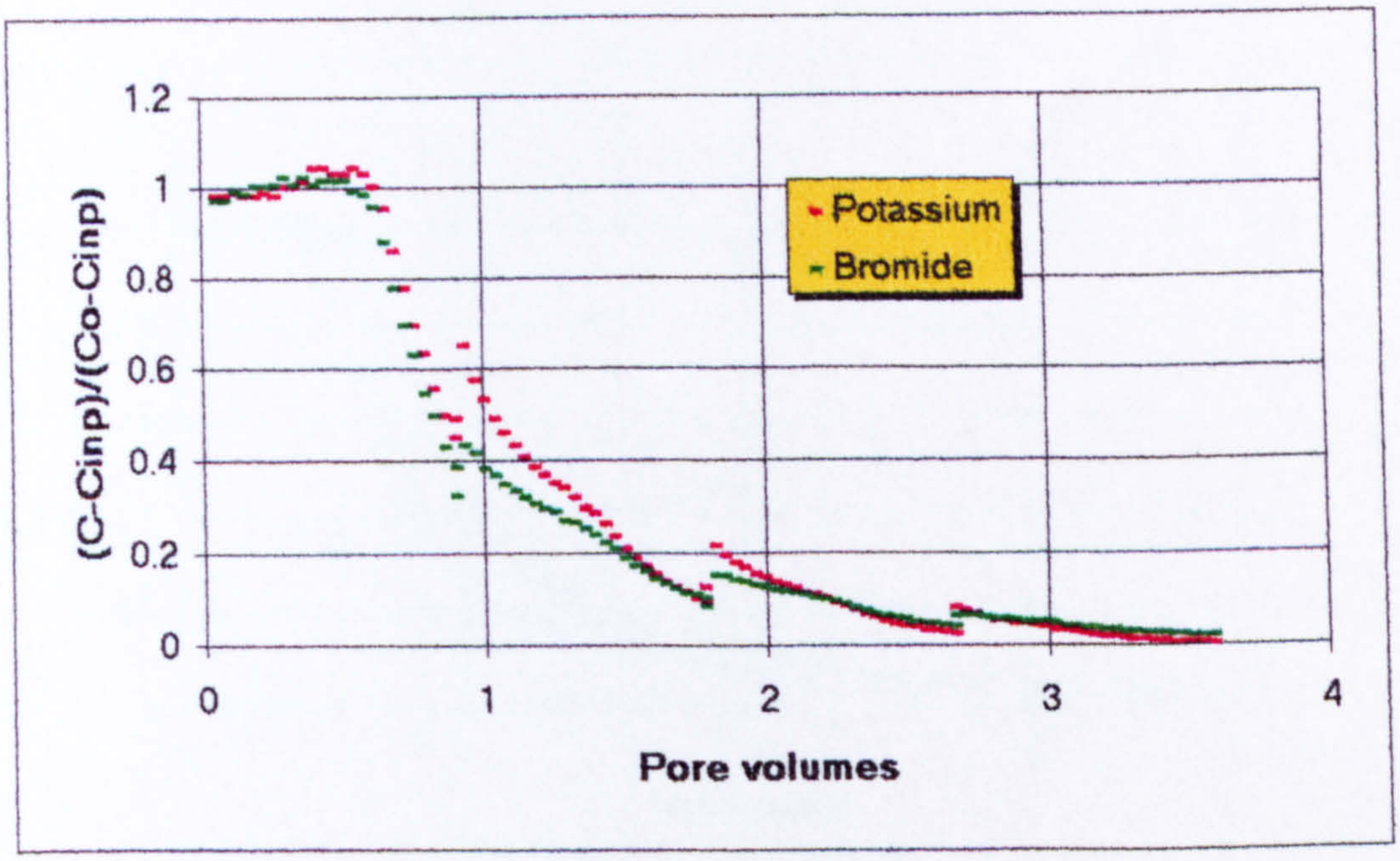

(b)

Fig. 8.17: $\frac{C - C_{inp}}{C_o - C_{inp}}$ against pore volumes for (a) Exp. 2a, and (b) Exp. 2b.

velocity allowed more time for diffusion out of aggregates and therefore the advantage of introducing rest periods was less. Similarly one would expect the advantage to be less for small aggregates as it was with small spheres (Section 5.3.2.2).

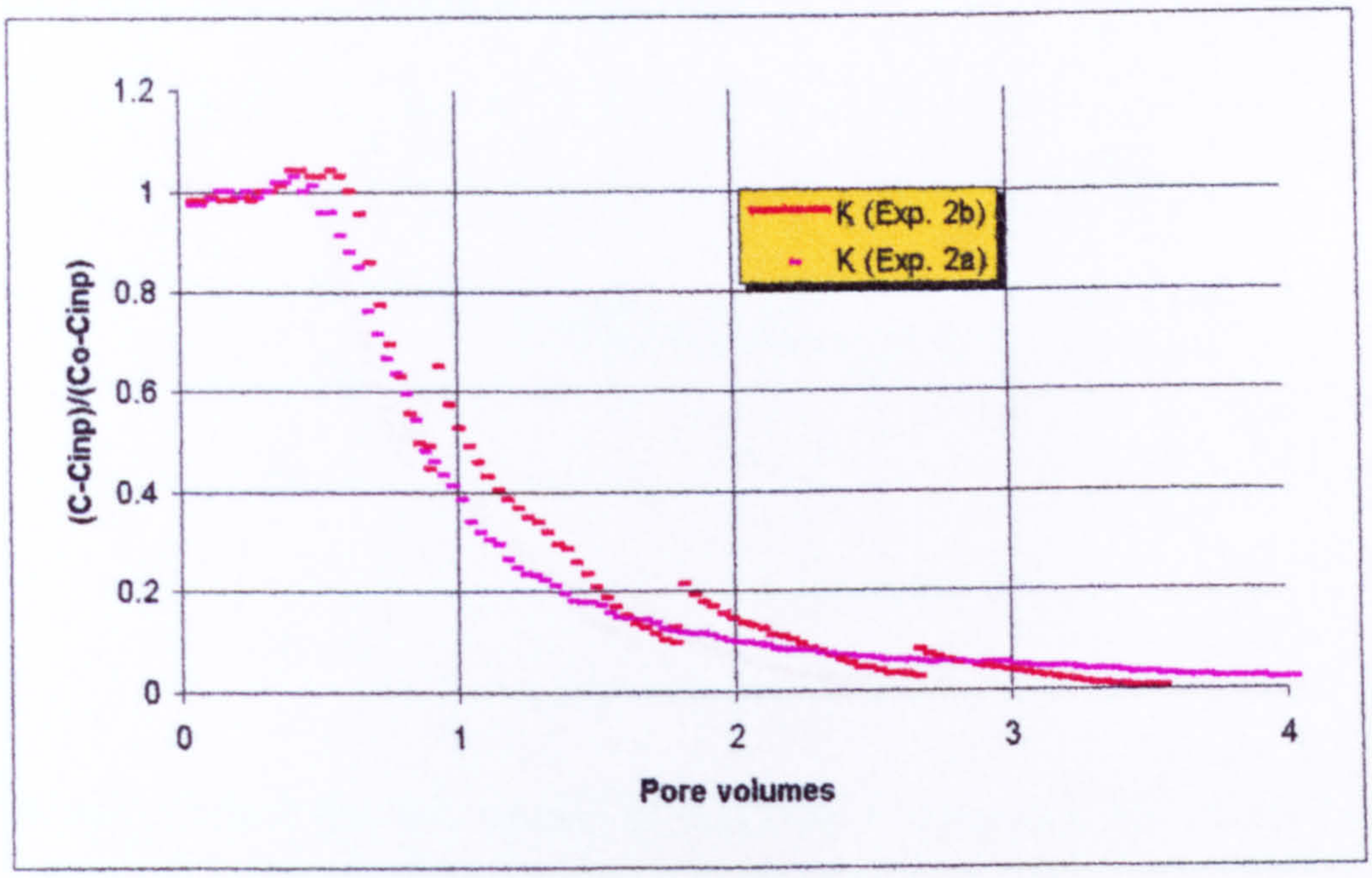

(a)

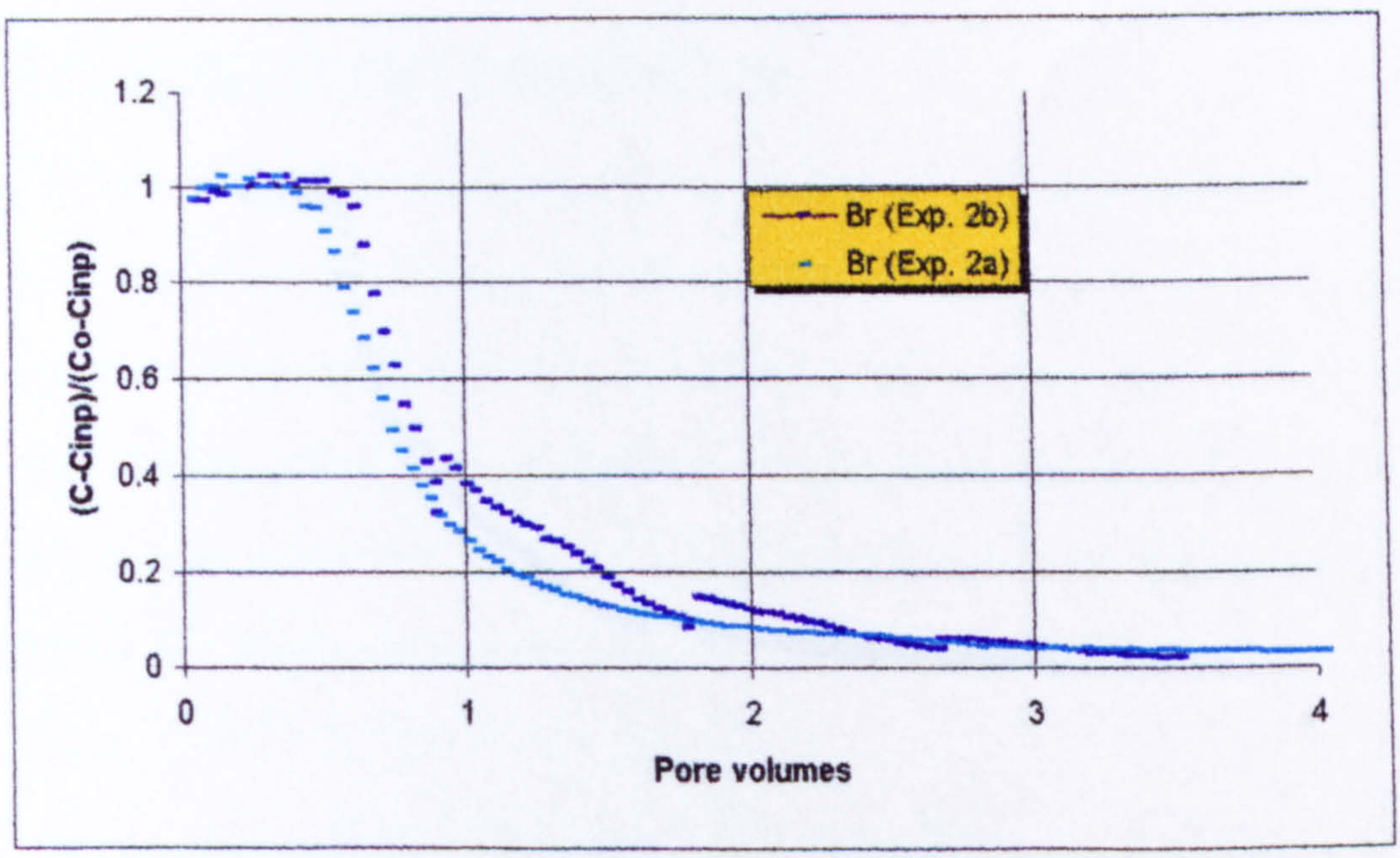

(b)

Fig. 8.18: $\frac{C - C_{inp}}{C_o - C_{inp}}$ against pore volumes for Exp. 2: (a) Potassium, and (b)Bromide.

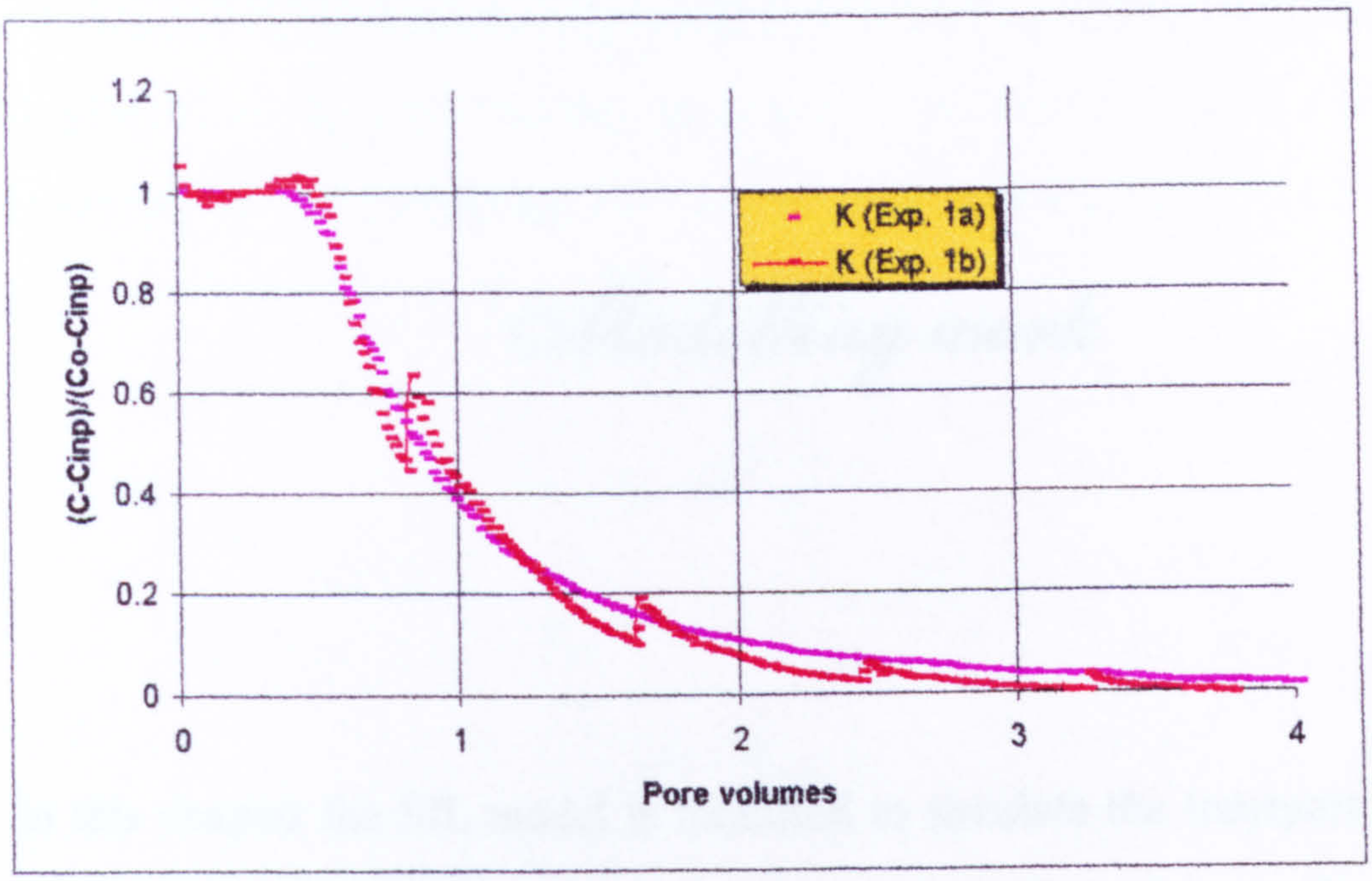

(a)

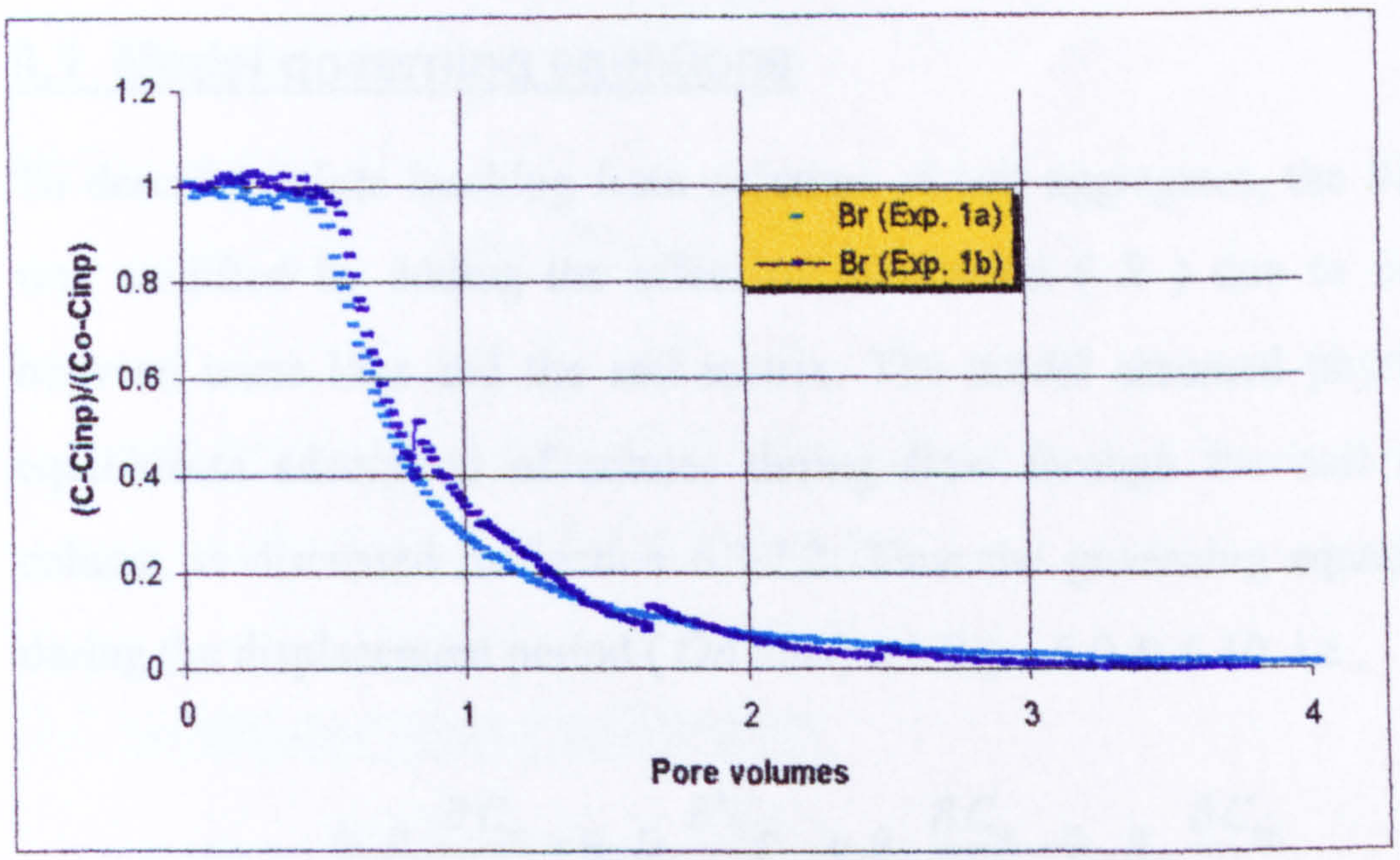

(b)

Fig. 8.19: $\frac{C - C_{inp}}{C_o - C_{inp}}$ against pore volumes for Exp. 1: (a) Potassium, and (b)Bromide.

Chapter Nine

Modelling work

In this chapter the SIL model is modified to simulate the transport of sorbing solute through a column of soil aggregates. The chapter discusses the estimation of model parameters, particularly the values of θ_m, θ_{im}, and f, and ends by testing the modified model against the analytical solution to check its stability and convergence.

9.1 Model governing equations

To describe solute leaching from columns of soil aggregates, the SIL model was modified by adding the effect of retardation (R) due to interaction between some ions and the soil matrix. The model assumed physical non-equilibrium adsorption of solutes during flow through the soil aggregate column as discussed in Section 6.3.2.2. Thus the governing equations used during the displacement period (*On* time) are Eqs. 6.9 & 6.10. i.e.,

$$\theta_m R_m \frac{\partial C_m}{\partial t} = \theta_m D_s \frac{\partial^2 C_m}{\partial z^2} - v_m \theta_m \frac{\partial C_m}{\partial z} - \theta_{im} R_{im} \frac{\partial C_{im}}{\partial t}$$

$$\theta_{im} R_{im} \frac{\partial C_{im}}{\partial t} = \alpha \left(C_m - C_{im} \right)$$

where the retardation factors R_m and R_{im} account for equilibrium type adsorption processes in the regions of mobile and immobile water respectively. Section 8.2.2 showed that the potassium desorption followed a Freundlich isotherm. For such isotherms, the retardation factors are given by:

$$R_m = 1 + \frac{f\rho K\, bC_m^{\,b-1}}{\theta_m}$$

$$R_{im} = 1 + \frac{(1-f)\rho K\, bC_{im}^{\,b-1}}{\theta_{im}}$$

$$R = R_{im} + R_m \quad .$$

During rest periods (*Off* times) the only process assumed to occur was the diffusion of solute from the aggregates. The governing equation is therefore obtained from Eqs. 6.9 & 6.10 assuming that v_m and $D_s = 0$. i.e.,

$$R_m\, \theta_m \frac{\partial C_m}{\partial t} = -\, R_{im}\, \theta_{im} \frac{\partial C_{im}}{\partial t} \qquad (9.1)$$

where

$$\theta_{im} R_{im} \frac{\partial C_{im}}{\partial t} = \alpha \left(C_m - C_{im} \right) \quad .$$

The SIL model of Section 4.2 was modified to solve the above equations. A copy of the computer code can be found in Appendix C.

9.2 Model parameter estimation

9.2.1 Mobile and immobile water content

The only known method for estimating the proportions of mobile θ_m and immobile θ_{im} water in the soil is based on the measurement of θ at an arbitrarily chosen water tension ψ (*Passioura & Rose*, 1971; *Ma & Selim*,

1995). From the shape of ψ - θ curve, *Smettem & Kirkby* (1990) chose ψ of 14 cm as the *matching point* between mobile and immobile water regions (Fig. 9.1). This point occurs when the curve slope, $d\Psi / d\theta$, increases suddenly from low values (corresponding with the mobile water region) to higher values (corresponding with the immobile water region).

Other water tensions have been used to differentiate mobile from immobile water, including 10 cm (*Wilson et al.*, 1992), 20 cm (*Selim et al.*, 1987), field capacity (50 cm) (*Seyfried & Rao*, 1987), 75 cm (*Passioura & Rose*, 1971), and 80 cm (*Nkedi-Kizza et al.*, 1982). Clearly, there is no standard definition of mobile or immobile water and it probably depends upon the structure of the soil and the size of the aggregates. However, using the shape of ψ - θ curve seems more realistic than using a constant value. Therefore this method was adopted in this study.

9.2.2 Fraction of adsorption sites (f)

The second parameter to be estimated is f which represents the fraction of adsorption sites in the mobile water region.

Different assumptions have been made since there is no direct measurement for f (*Selim et al.*, 1987). *Nkedi-Kizza et al.* (1983) assumed $f = \Phi$ (where Φ is the fraction of mobile water) while *Seyfried & Rao* (1987) proposed an intermediate approximation of $f = \Phi /2$. *Nkedi-Kizza et al.* (1982) proposed that, since the absorbing surface area associated with a unit volume of water in the small pores of the immobile water region is probably much greater than the surface area associated a similar unit volume of water in the mobile water region, f may be approximated to zero. *Selim & Ma* (1995) found that the assumptions of $f = 0$ and $f = 1$ could be used to examine the significance of physical *vs.* chemical non-equilibrium behaviour in their study of atrazine transport in Sharkey soil. A value of $f \approx 0$ might suggest that physical non-equilibrium plays an important role whereas a value of $f \approx 1$

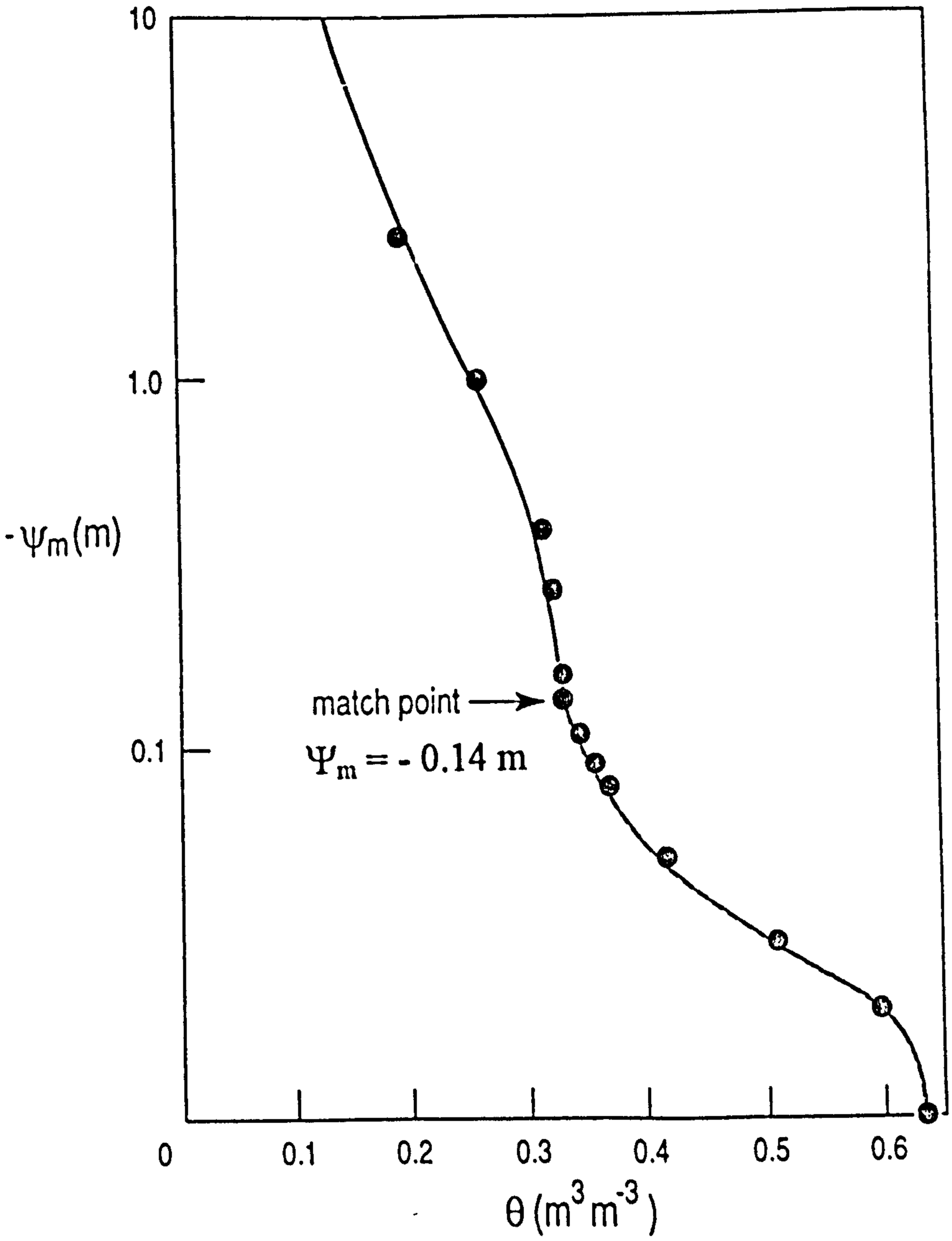

Fig. 9.1: Water release curve ($-\psi$ *vs.* θ) showing the position of the *matching point* (adopted from *Smettem & Kirkby*, 1990).

might imply that physical non-equilibrium was insignificant. However, in all approximations of f, the magnitude of any error in the eventual estimation of the solute transport is influenced by the value of R (*Anamosa et al.*, 1990). If there is almost no chemical adsorption or repulsion (R approaches 1.0), then the location of the sites becomes less important (as in the case of bromide). For an adsorbed solute, like potassium, it is usual practice for f to be estimated using one of the optimisation programs discussed next.

9.2.3 Using the best-fit optimisation program

The parameters required by the SIL model are: v_m, θ_{im} , θ_m , K, b, f, D_S, and α . Five parameters (θ_m ,θ_{im} ,v_m ,K ,b) can be estimated either directly from displacement experiments (i.e., v_m) or by independent experiments (i.e., θ_m ,θ_{im} ,K ,b). The remaining parameters (D_S ,α ,f) cannot be determined by independent experiments (*Davidson et al.*, 1980; *Selim & Ma*, 1995). Therefore, these must be estimated using the non-linear least-squares optimisation program CXTFIT1 of *Parker & van Genuchten* (1984) by fitting the programme predictions to the measured BTCs. This program uses the analytic solution of the dimensionless Eqs. 6.12 & 6.13 assuming a **linear adsorption /desorption isotherm** and is based on minimising the differences between simulated and measured BTCs by successive refinement of the initial parameters. The parameters which can be optimised are D_s , β ,ω ,v ,and R.

The relations between α ,f (used in the SIL model) and β ,ω (used in the optimisation programme), are given by:

$$\alpha = \frac{\omega\, v_d}{L_r}$$

$$f = \frac{\beta\ (\theta + \rho\ K) - \theta_m}{\rho\ K} \qquad (9.2)$$

However, one should always be careful when using curve-fitting techniques to estimate unknown parameters, especially for sorbed solutes. *Davidson et al.* (1980) concluded that, although these techniques are useful in parameter estimation, they fail to ensure identification of the process.

In the literature, if only the input concentration was changed, *Rao et al.* (1979) found that a different set of optimised parameters was required to describe the resulting BTC. *Nkedi-Kizza et al.* (1983) found that optimised α and Φ values changed with Darcy flow velocity and aggregate size. α was also found to be a function of column length, the duration of the experiment, and solute retardation (*Young & Ball,* 1995). *Kutilek & Nielsen* (1994) noticed from optimised results that the immobile water fraction, θ_{im}, was sensitive to hysteresis, the concentration of soil solution , the soil water content and soil water flux.

Despite this, curve fitting is still a useful tool for parameter estimation and may be the only way when there are no independent experiments for determining these parameters. However, during testing the model in the next chapter (Chapter 10), a minimum number of parameters were optimised, especially when testing the model against IL experimental results.

9.3 Model stability and convergence

The SIL model was tested against the analytic solution of *Parker & van Genuchten* (1984) for continuous leaching with a linear adsorption/desorption isotherm. A set of parameters as used by *Nkedi-Kizza et al.* (1983) (to describe the movement of tritiated water through a column of an aggregated Oxisol) was used with both the SIL model and the analytic solution. The results are shown in Fig. 9.2 as effluent concentration against time. The results indicate excellent agreement between the model and the analytic solution ($R^2 > 0.99$) demonstrating the stability and the convergence of the numerical procedure used in the model.

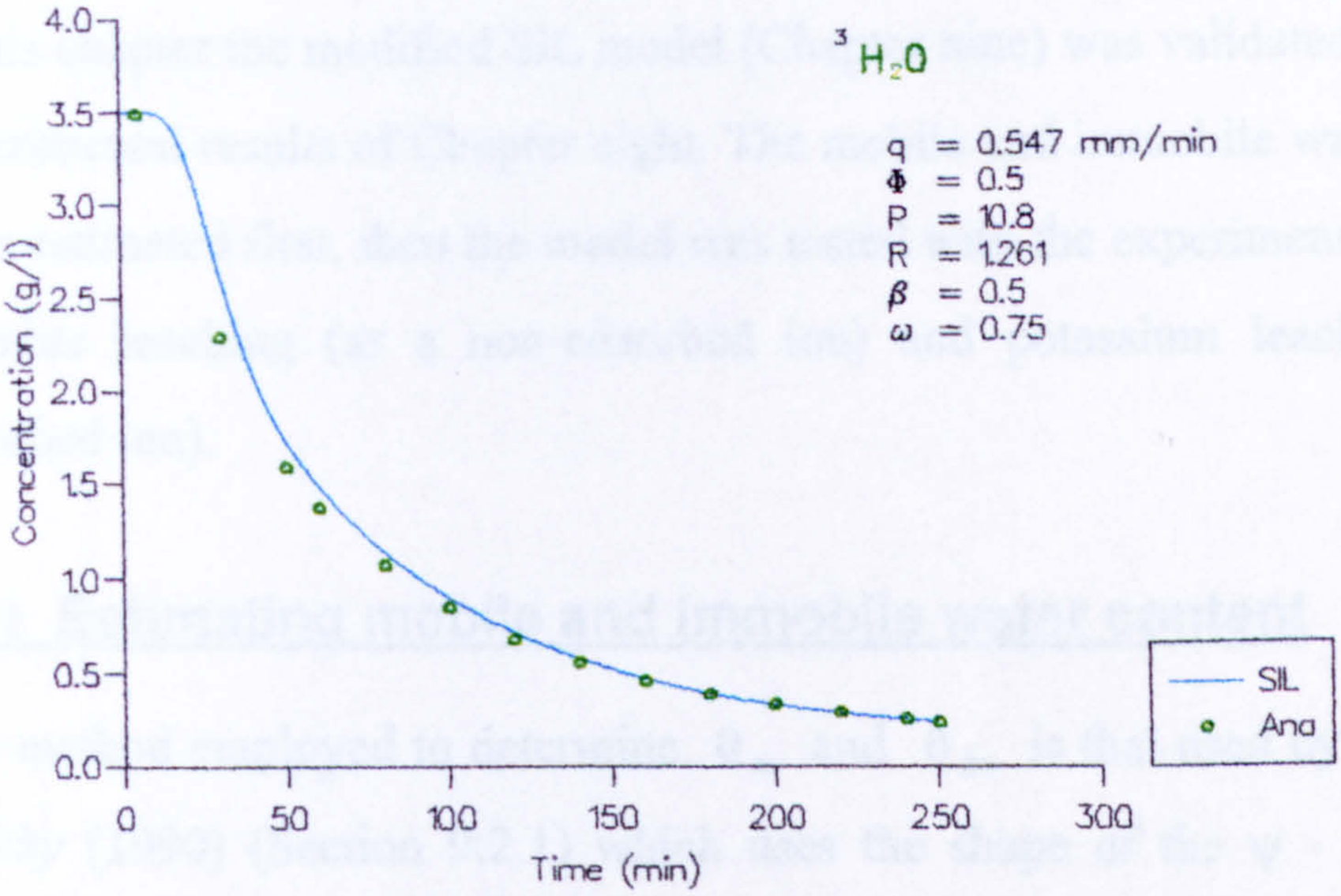

***Fig. 9.2*: Effluent concentration against time for SIL model and analytical solution results (parameter values are from *Nkedi-Kizza et al.*, 1983).**

Chapter Ten

Testing the model

In this chapter the modified SIL model (Chapter nine) was validated against the experimental results of Chapter eight. The mobile and immobile water contents were estimated first, then the model was tested with the experimental results of bromide leaching (as a non-adsorbed ion) and potassium leaching (as an adsorbed ion).

10.1 Estimating mobile and immobile water content

The method employed to determine θ_m and θ_{im} is that used by *Smettem & Kirkby* (1990) (Section 9.2.1) which uses the shape of the ψ - θ curve to define the tension (and water content) at the *matching point* which differentiates the mobile water (mainly inter-aggregate) from the immobile water (mainly intra-aggregate).

The ψ - θ curves for aggregates of 4-6.7 and 11.2-13.2 mm diameter respectively are shown in Figs. 10.1a & 10.1b. From these curves the *matching points* (MPs) were defined when the curve slope changes its value suddenly. The tension and the corresponding water content values at the MPs for each aggregate fraction are shown in Table 10.1.

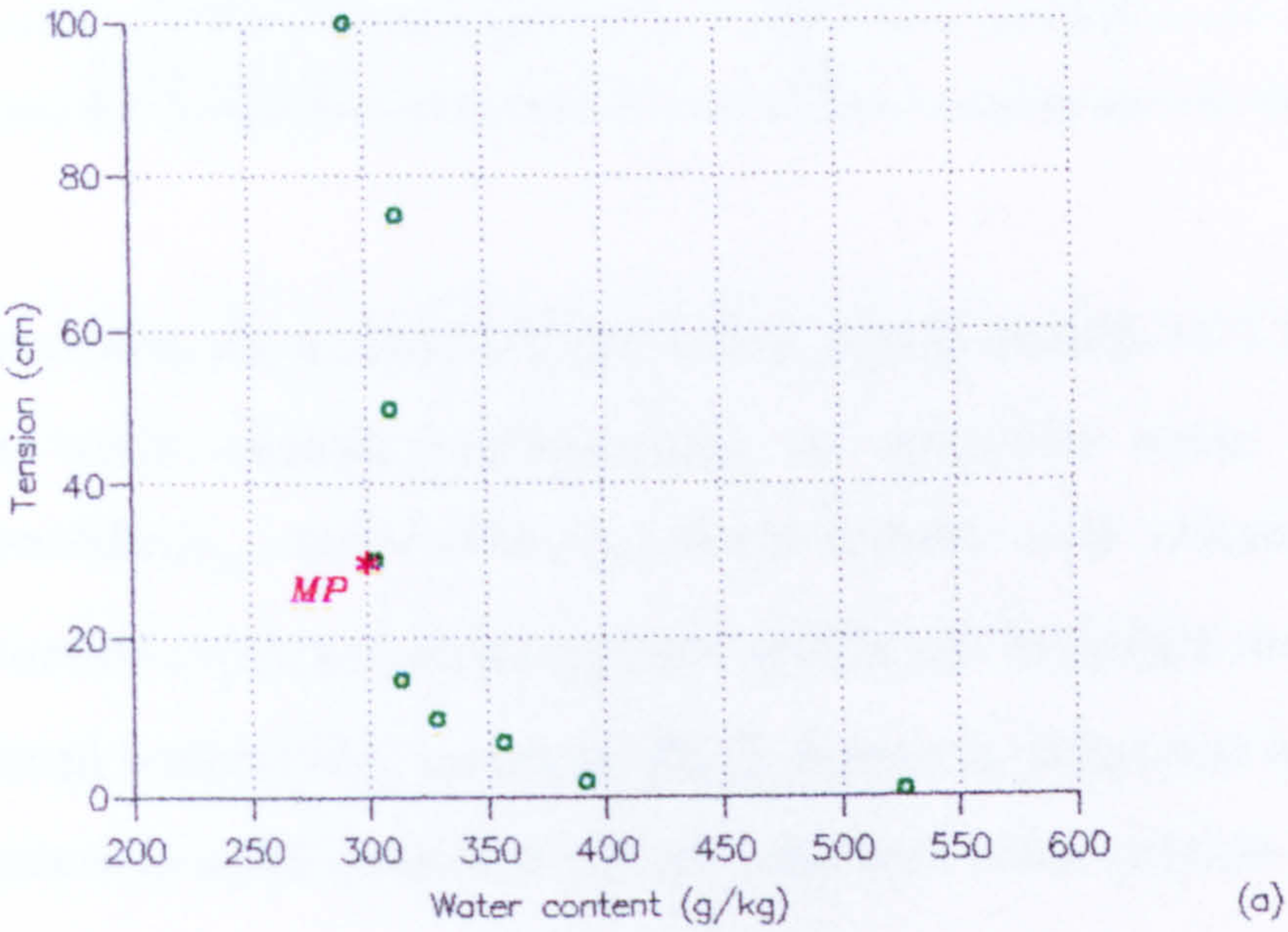

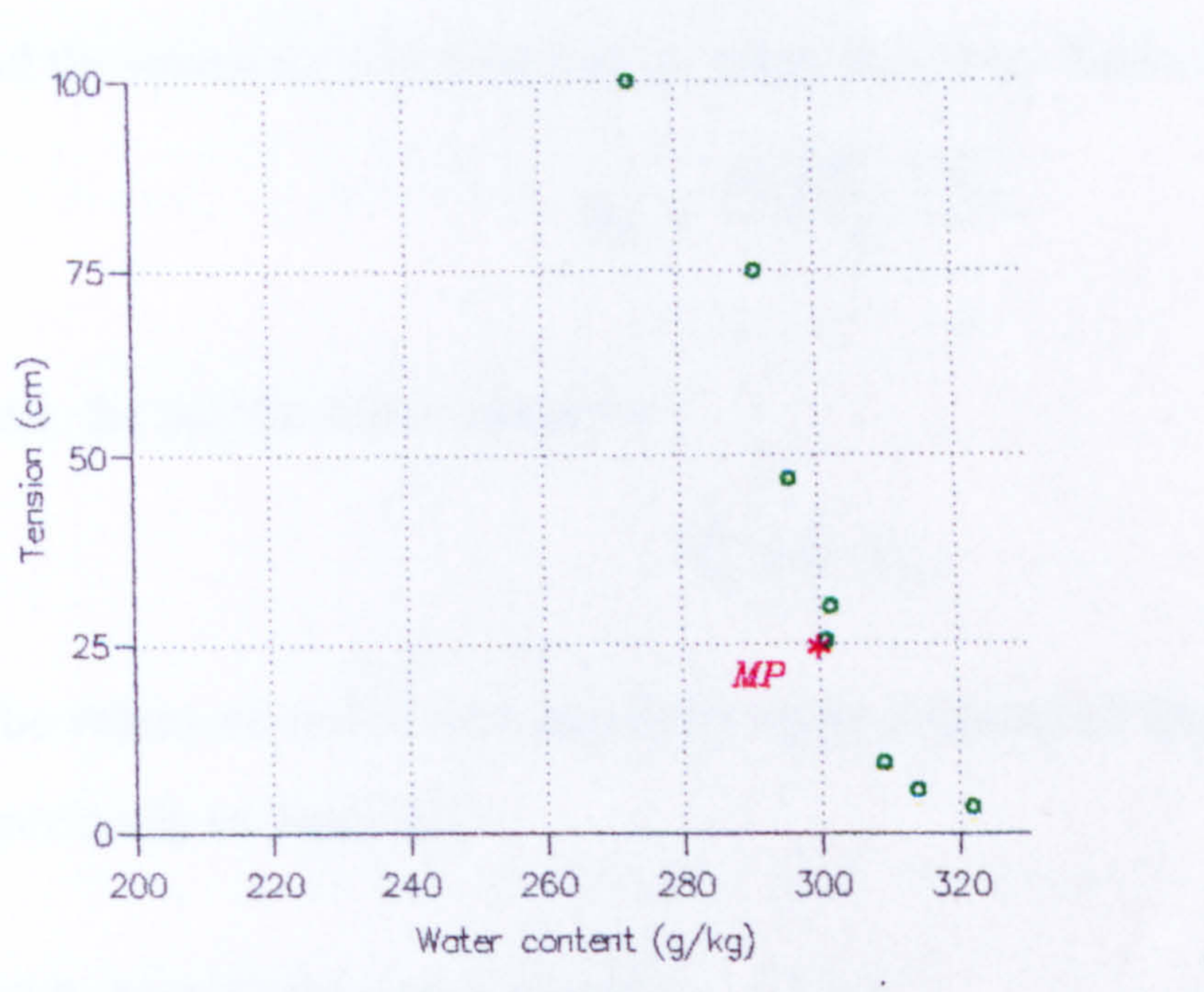

***Fig. 10.1*:** Tension against water content for soil aggregates of diameter : (a) 4-6.7 mm, (b) 11.3-13.2 mm. MP = 30 and 25 cm for case (a) and (b) respectively.

Table 10.1: Tensions and water content values at matching points.

Aggregate diameter (mm)	Tension at MP (cm)	Water content at MP (g/kg)
4 - 6.7	30	300
11.2 - 13.2	25	300

The results show that for Exps. 1 & 2, which contain 11.2-13.2 mm aggregates, the water content corresponding to immobile water is 300 g/kg. The immobile, θ_{im}, and mobile, θ_m, water content were calculated as follows: the saturated column (containing both mobile and immobile water) was poured into a tared beaker (W_b), weighed (W_{sat}), then oven dried and weighed again (W_{dry}). Assuming water density = 1 g cm^{-3}, the total water content $\theta = \theta_{im} + \theta_m$ is

$$\theta = \frac{W_{sat} - W_{dry}}{V_T},$$

and the immobile water content is, using data from Table 10.1:

$$\theta_{im} = \frac{0.3\,(W_{dry} - W_b)}{V_T},$$

thus, the mobile water content is

$$\theta_m = \theta - \theta_{im}.$$

The values of mobile and immobile water contents of Exps. 1 & 2 were shown previously in Table 8.3.

10.2 Validating the model

The SIL model was validated against experimental results of bromide and potassium leaching (Section 8.4). The results of CL experiments were used to optimise the unknown parameters. These parameters were used later in simulating the results from IL experiments.

10.2.1 With experimental results of bromide leaching

10.2.1.1 For continuous leaching

A previous experiment (Section 8.2.3) had shown that there was no bromide adsorption in the soil (i.e., $K= 0$). Therefore the β value is given by:

$$\beta = \frac{\theta_m + f\rho K}{\theta + \rho K} = \frac{\theta_m}{\theta} \qquad (10.1)$$

and the R value is equal to:

$$R = 1 + \frac{\rho K}{\theta} = 1 .$$

With R and β known, and v measured, D_s and ω were optimised. The results of bromide continuous leaching experiments (Exps. 1a & 2a, Section 8.4.5) were used in optimising these unknown parameters (D_s and ω) using the best-fit non-linear optimisation program CXTFIT1 of *Parker & van Genuchten* (1984). The resulting parameters are shown in Table 10.2.

Table 10.2 : Optimised parameters (with R, β being estimated) using the optimisation program of *Parker & van Genuchten* (1984) (CXTFIT1).

			Optimised parameters			
	R	β	D_s (mm²/min)	ω	α (min⁻¹) *	R^2
Exp. 1a	1	0.586	6.71	0.708	0.0063	0.989
Exp. 2a	1	0.614	22.70	0.498	0.0091	0.996

R^2 = coefficient of determination

$$*\alpha = \frac{\omega v_d}{L_r} .$$

However, since the soil particles were found to have a net negative charge (Section 8.1.2), one could expect a value of R less than one. Optimising R, in addition to D_s and ω, gave values very close to one (0.97 and 1.05 for Exp. 1a and 2a respectively). Thus, using a fixed value of R=1 seems reasonable and limits the number of optimised parameters.

Using the optimised parameters (D_s ,α), the SIL model was run to simulate the continuous leaching experiment results. Fig. 10.2 shows the

experimental data, and both SIL and CXTFIT1 results as relative bromide concentration of the effluent against the number of pore volumes. The SIL and CXTFIT1 results are almost identical since both the SIL model and the CXTFIT1 program used the same parameters. The agreement with the experimental data for both experiments was also very good (R^2> 0.98). The SIL model was able to simulate the early breakthrough of the solute and the tailing with a small overestimation by both models between 1 and 3 pore volumes. The difference could arise from an underestimation of the values of the immobile water fraction or there may be a proportion of "dead end" pores in the assumed mobile water region. Such water is effectively immobile and would not transport the solute by mass flow and would therefore give a lower effluent bromide concentration than predicted by the model.

10.2.1.2 For intermittent leaching

IL experiments, Exps. 1b and 2b, have almost the same conditions as the CL experiments, Exps. 1a and 2a, respectively (Table 8.3). Therefore, keeping the same previously optimised values of the parameters (D_s ,α), the SIL model should be able to predict the breakthrough curves (BTCs) obtained from IL experiments. Table 10.3 shows the parameter values used in the SIL model.

Table 10.3 **: Parameter values used in the SIL model to predict IL results.**

	R	$\beta^{\#}$	D_s * (mm^2/min)	α * (min^{-1})
Exp. 1b	1	0.608	6.71	0.0063
Exp. 2b	1	0.535	22.70	0.0091

$^{\#}$ calculated using Eq. 10.1
* values were taken from Table 10.2.

The results are shown in Fig. 10.3 as relative bromide concentration of the effluent against number of pore volumes. The SIL model was able to simulate the intermittent leaching results successfully using the same

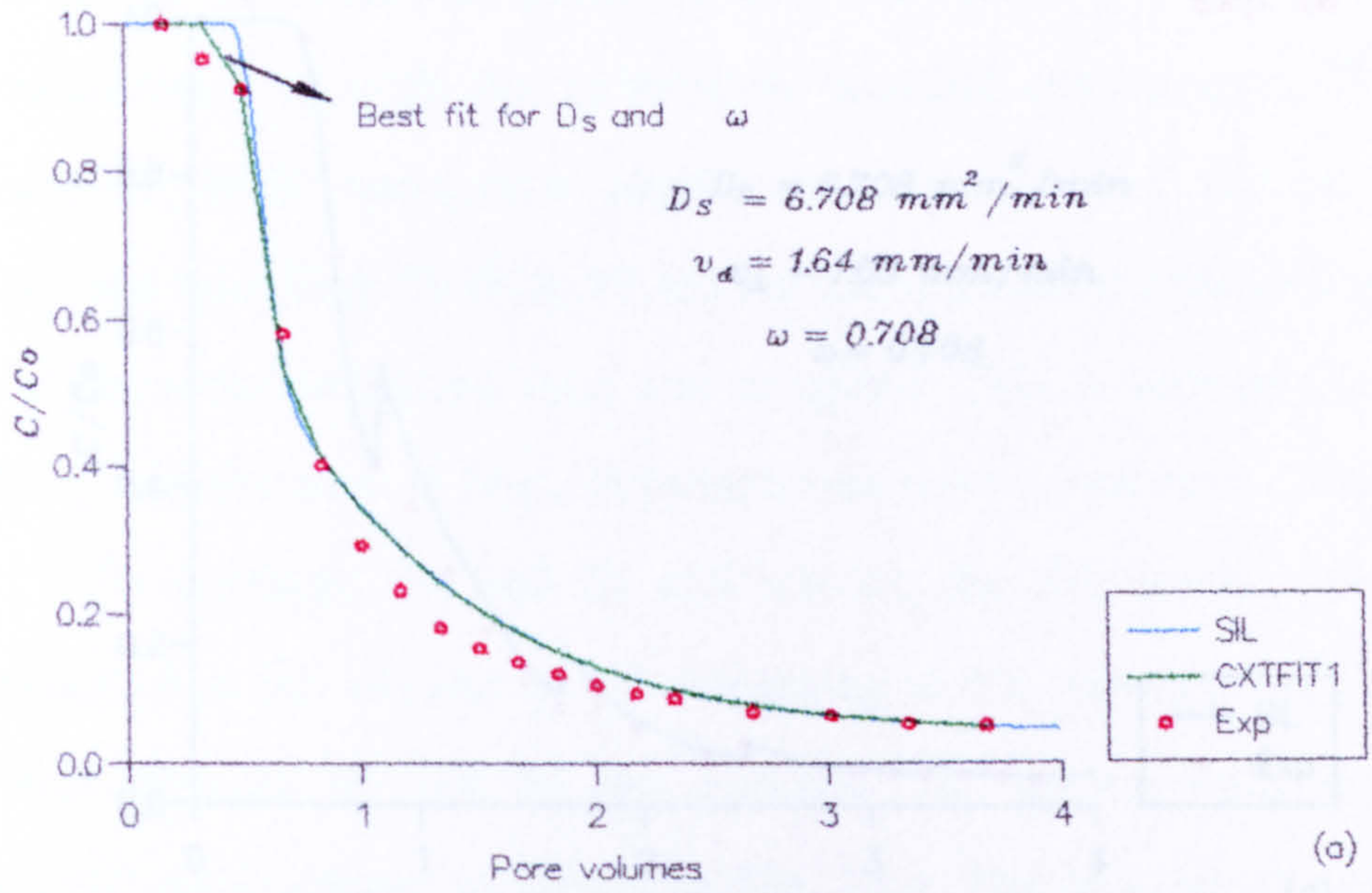

***Fig. 10.2*: Relative bromide concentration against number of pore volumes for (a) Exp. 1a, (b) Exp. 2a .**

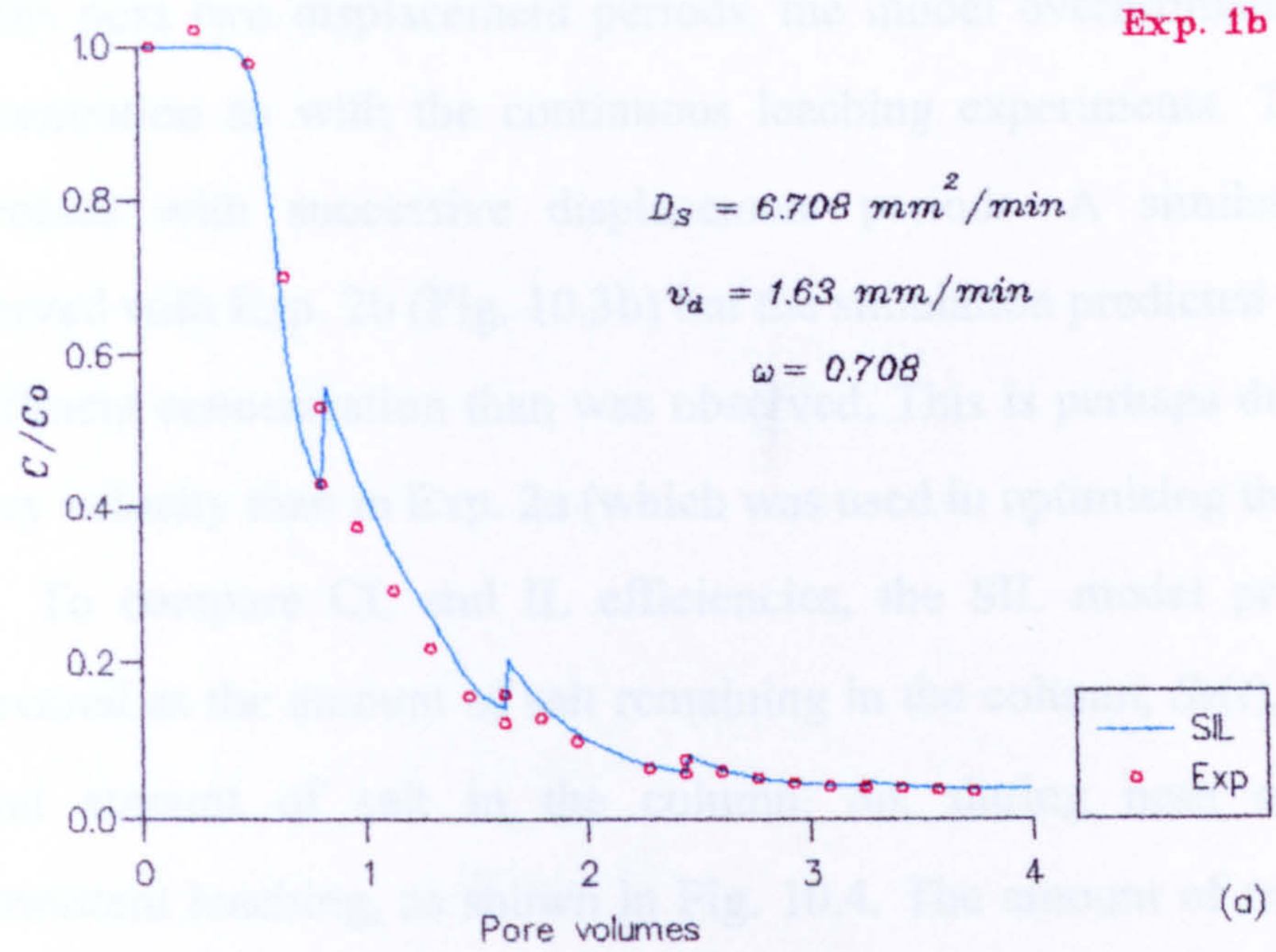

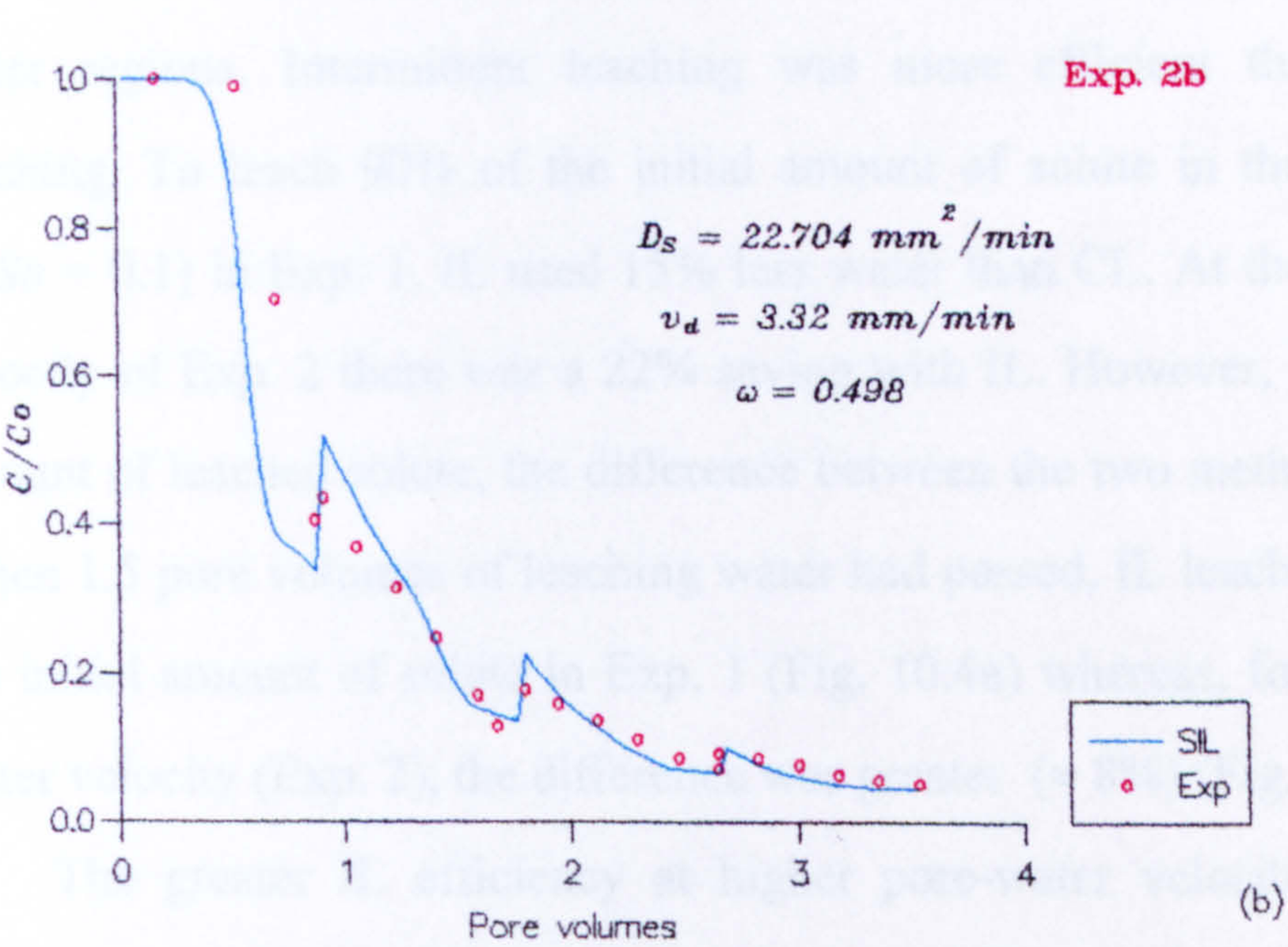

Fig. 10.3: Relative bromide concentration against number of pore volumes for: (a) Exp. 1b, (b) Exp. 2b . A duration of 50 min as *off* time is given after passing 0.814 and 0.884 pore volumes of water in Exps. 1b & 2b respectively.

optimised parameters as the CL experiments. With Exp. 1b (Fig. 10.3a) the predicted concentration started identically to the experimental data. However, for the next two displacement periods, the model overestimated the effluent concentration as with the continuous leaching experiments. This difference decreases with successive displacement periods. A similar pattern was observed with Exp. 2b (Fig. 10.3b) but the simulation predicted an earlier drop in effluent concentration than was observed. This is perhaps due to the lower Darcy velocity than in Exp. 2a (which was used in optimising the parameters).

To compare CL and IL efficiencies, the SIL model predictions were expressed as the amount of salt remaining in the column, $Ss(t)$, relative to the initial amount of salt in the column, So, during both continuous and intermittent leaching, as shown in Fig. 10.4. The amount of remaining solute started to decrease rapidly due to the leaching of solute in the mobile water and then more slowly due to the slower leaching of solute from the immobile water regions. Intermittent leaching was more efficient than continuous leaching. To leach 90% of the initial amount of solute in the column (i.e., $Ss/So = 0.1$) in Exp. 1, IL used 15% less water than CL. At the higher Darcy velocity of Exp. 2 there was a 22% saving with IL. However, in terms of the amount of leached solute, the difference between the two methods was small. When 1.5 pore volumes of leaching water had passed, IL leached 4% more of the initial amount of solute in Exp. 1 (Fig. 10.4a) whereas, for a higher pore water velocity (Exp. 2), the difference was greater ($\approx$ 8%) (Fig. 10.4b).

The greater IL efficiency at higher pore-water velocities is expected because there is then relatively less time for diffusive flow from within the aggregate to the exterior where solute may be removed by mass flow. There was therefore a greater advantage from the use of rest periods. This was previously observed with the ceramic spheres (Section 5.3.1.1).

It is also interesting to note that the differences between the intermittent and continuous leaching started directly after the first "*Off*" time (the

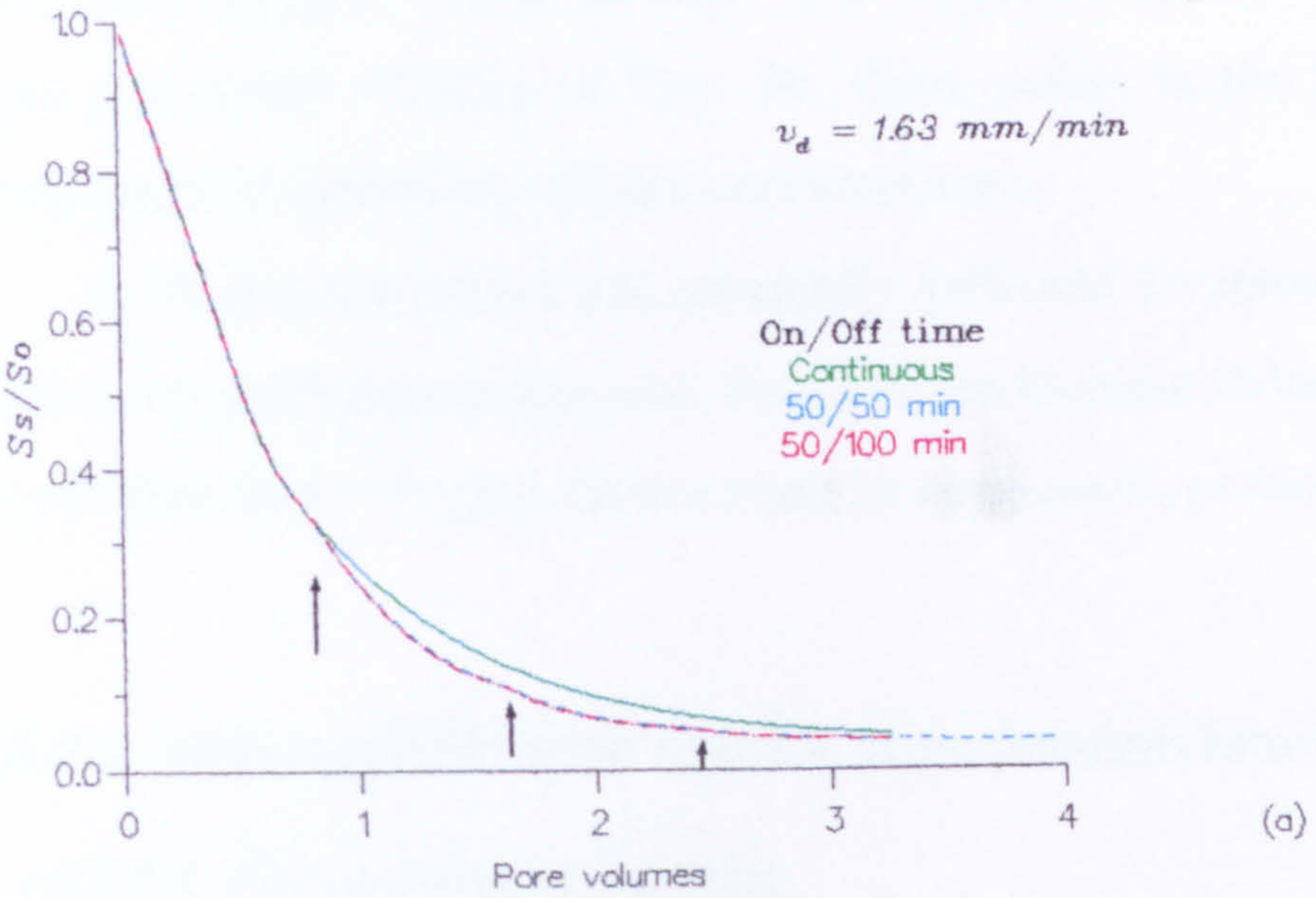

Ss is the amount of salt remaining in the column

So is the initial amount of salt in the column

Fig. 10.4: *Ss/So* against number of pore volumes for: (a) Exp. 1b and (b) Exp. 2b. Arrows indicate the beginning of each leaching cycle.

beginning of each leaching cycle is indicated by an arrow on the graphs), and that the curve slope increased (i.e., higher solute leaching rate) after each *Off* time. Such changes in curve slopes were more easily recognised with the higher pore-water velocity of Exp. 2b. These points in the leaching process corresponded to enhanced effluent concentrations.

A 50 min rest period was eventually sufficient for immobile and mobile solutions to reach equilibrium and, therefore, an increase in the duration of rest periods from 50 to 150 min did not result in any benefit, as shown in Fig. 10.4.

10.2.2 With experimental results of potassium leaching

10.2.2.1 For continuous leaching

Potassium differs from bromide because it is retarded due to adsorption/desorption processes in the soil.

In order to use the CXTFIT1 optimisation program, it was necessary to approximate the non-linear desorption isotherm of Fig. 8.5 by a straight line since the fitting program CXTFIT1 assumes linear adsorption (or desorption) isotherms. The following procedure (*van Genuchten et al.*, 1977) was used to linearize the equilibrium isotherm.

The linearized isotherm was denoted by $S = K_L C$ where K_L is the linearized distribution coefficient, such that the area under the isotherm over the range of potassium concentration of 0.156 to 3.91 g/l (0.004 M, concentration of leaching water to 0.1 M, initial concentration) for both the linearized and non-linear Freundlich equations should be the same, i.e.

$$\int_{0.156}^{3.91} K_L C \, dC = \int_{0.156}^{3.91} 0.00339 C^{0.105} \, dC$$

which gives K_L = 1.76 cm³/g. The non-linear equation used is the same as Eq. 8.2.

The value of R is calculated from

$$R = 1 + \frac{\rho K_L}{\theta} \qquad (10.2)$$

where ρ is bulk density of the soil. The calculated values of R (Table 10.4) show a retardation factor $R > 1$ as was expected. With negative charge on the surface of soil particles, the cations will be adsorbed and retarded. *Nkedi-Kizza et al.* (1982) found a retardation factor R=3.03 for calcium ions during miscible displacement through an aggregated Oxisol. However, such values will depend on K (i.e. soil particle-ion interactions), ρ , and θ (Eq. 10.2).

For the remaining parameters, since there is retardation, β will not only depend on the mobile water fraction (as for bromide) but also on the distribution coefficient K_L (Table 6.2). The value of ω could be different from that of bromide due to the smaller diffusion rate.

Using the experimental data of continuous leaching (Figs. 8.16a & 8.17a), the fitting program CXTFIT1 was used to optimise the values of β , ω, and D_s . The fitted parameters ω and β were then used to calculate the parameters f and α of the SIL model using Eq. 9.2. The optimisation results are shown in Fig. 10.5 & Table 10.4.

Table 10.4 **:** Optimised parameters for potassium (with estimated R) using the optimisation program of *Parker & van Genuchten* (1984) (CXTFIT1).

		Optimised Parameters					
	R^*	D_S (mm^2/min)	ω	β	$\alpha^{\#}$ (1/min)	$f^{\#}$	R^2
Exp. 1a	3.43	67.55	0.044	0.243	0.00039	0.102	0.994
Exp. 2a	3.28	129.63	0.032	0.251	0.00058	0.091	0.997

R^2 coefficient of determination

* values are calculated using Eq. (10.2)

\# values are calculated from optimised parameters using Eq. (9.2).

The lower values of the dimensionless parameter ω for potassium compared with bromide (Table 10.2) were expected because these values are

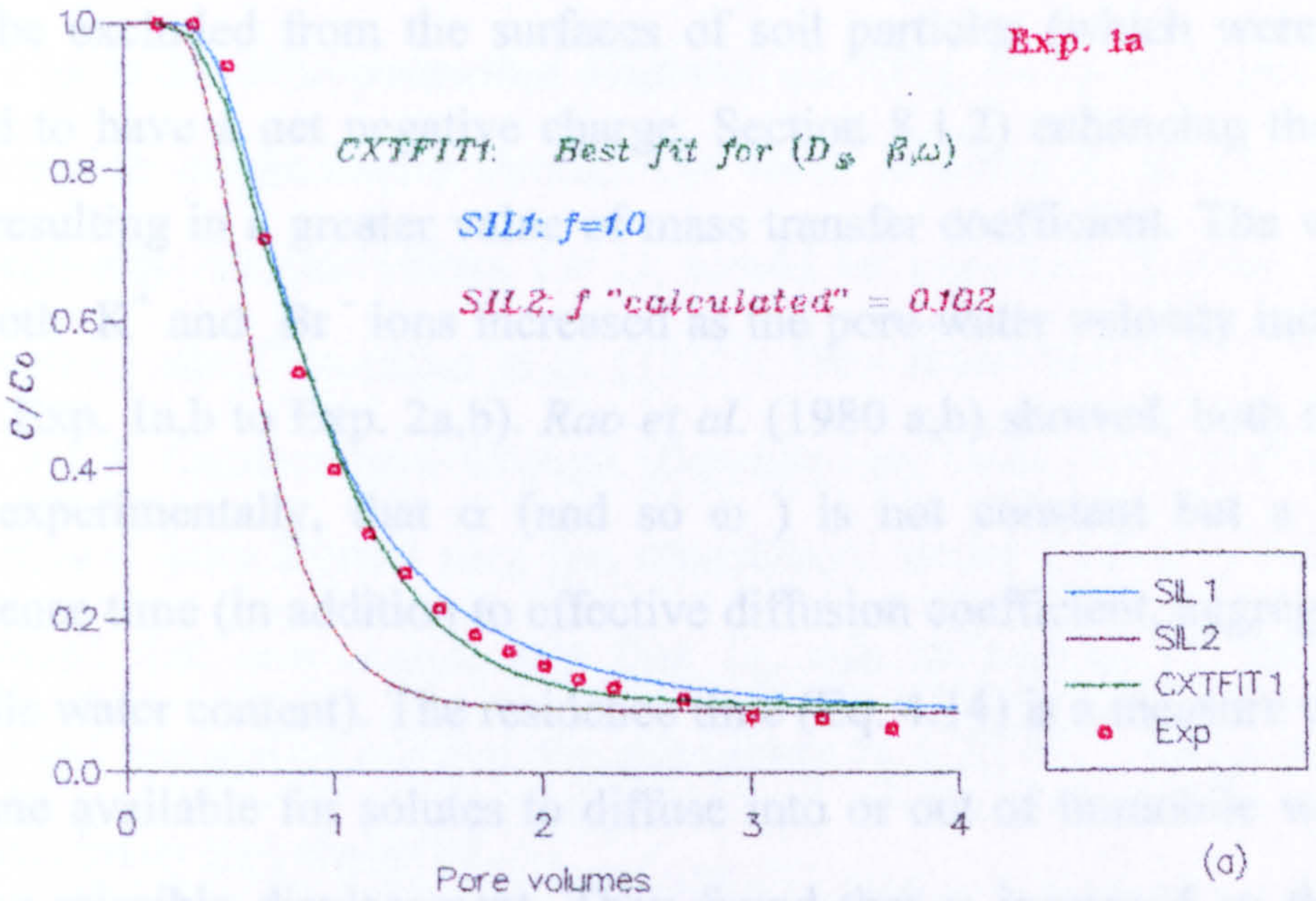

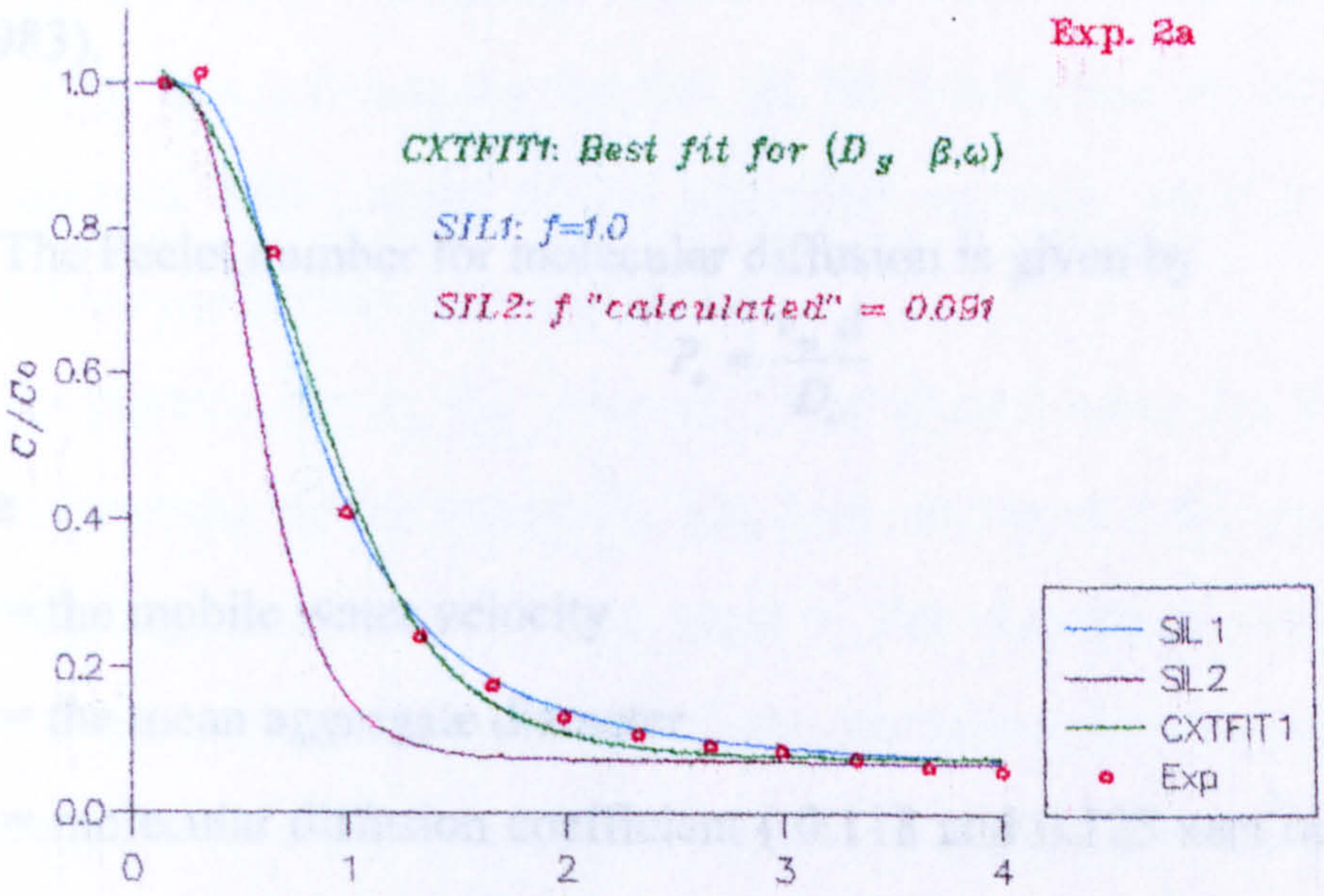

Fig. 10.5 **: Relative potassium concentration against number of pore volumes for: (a) Exp. 1a and (b) Exp. 2a .**

directly related to the values of the mass transfer coefficient, α $\left(\omega = \frac{\alpha L}{v_d}\right)$, which describes the diffusion of the ions through the aggregate. Bromide ions will be excluded from the surfaces of soil particles (which were previously found to have a net negative charge, Section 8.1.2) enhancing their mobility and resulting in a greater value of mass transfer coefficient. The values of α for both K^+ and Br^- ions increased as the pore-water velocity increased (i.e., from Exp. 1a,b to Exp. 2a,b). *Rao et al.* (1980 a,b) showed, both theoretically and experimentally, that α (and so ω) is not constant but a function of residence time (in addition to effective diffusion coefficient, aggregate size and mobile water content). The residence time (Eq. 4.14) is a measure of the length of time available for solutes to diffuse into or out of immobile water regions during miscible displacement. They found that α increased as the residence time decreased. The residence time is inversely related to pore-water velocity, thus α should increase with an increase in pore-water velocity (*Nkedi-Kizza et al.*, 1983).

The Peclet number for molecular diffusion is given by

$$P_e = \frac{v_m d}{D_o}$$

where

v_m = the mobile water velocity

d = the mean aggregate diameter

D_o = molecular diffusion coefficient (0.118 and 0.125 mm^2/min for K^{+1} and Br^{-1} respectively (*Shackelford & Daniel*, 1991)).

Using this equation Peclet numbers are approximately 527 and 1110 for Exps. 1a,b and 2a,b respectively. These values are high enough ($P_e >> 20$) to ensure that mechanical dispersion dominates the hydrodynamic dispersion coefficient D_S for both experiments (*Perkins & Johnson*, 1963; *Kutilek & Nielsen*, 1994). Mechanical dispersion depends only on pore-water velocity

(Section 2.1.1) which is the same for both ions. This means that similar values of D_s are expected for both bromide and potassium leaching.

Tables 10.2 & 10.4 show that the hydrodynamic dispersion coefficients, D_s, used to describe potassium displacement (Fig. 10.5) are higher than those for bromide displacement through the same columns at the same velocities. Theoretically, similar values for D_s would be expected. Similar results were obtained by *van Genuchten et al.* (1977). They found that the D_s values based on 2,4,5-T displacement through Glendale clay loam were smaller than those determined from tritium data (no retardation) under similar conditions. They suggested that one reason was that D_s was influenced by the fact that a linearized adsorption relation was used (here by CXTFIT1 program), instead of the non-linear one observed.

When the f and α values were calculated from the optimised parameters β and ω (Eq. 9.2) and used in the SIL model, the model predicted, for both experiments, lower effluent potassium concentration than actually observed (Fig. 10.5). This is due to the fact that the SIL model uses the actual desorption equation (Eq. 8.2) instead of the linearized equation used in CXTFIT1 by which these parameters were optimised.

To improve the fit, the value of f was altered using the SIL model (the effect of varying α was marginal). The best optimised value was found to be f =1. This high value implies that most of the desorption occurred from the mobile water soil regions with very little desorption from immobile water soil regions. The amount of desorbed solute, S, depends on the equilibrium concentration, C, of the surrounding solution ($S=K\,C^b$). The desorption curve for this soil (Fig. 8.5) showed a very small desorption at high concentrations with a sharp increase in desorption at very low concentrations (<1 g/l). The main obstacle to decreasing the concentration of potassium in the immobile water is the slow diffusion rate of potassium (the mass transfer coefficient, α , for potassium was found to be 10 to 20 times smaller than for bromide (Table

10.2 and 10.4)). This means that there is a greater difference in potassium concentration between immobile and mobile water and that the mobile water will have low concentrations much sooner than the immobile. Bearing in mind the desorption behaviour of the potassium, such concentration differences will cause much more desorption in the mobile water soil regions than in the immobile water soil regions.

10.2.2.2 For intermittent leaching

The SIL model was run using the same previously determined parameters (f, D_s and α ; Table 10.4) to simulate the results of intermittent leaching experiments (Exp. 1b, 2b) with the R value calculated using Eq. 6.11.

As with CL, the SIL model failed to simulate the IL results using the calculated f value (Table 10.4) and for the same reason. Using the SIL model, the optimal value for f was found to be ($R^2 = 0.995$ and 0.946 for Exp. 1b and 2b respectively) $f = \Phi$ (the volumetric fraction of mobile water, $\Phi = \theta_m / \theta$) (Fig. 10.6).

The difference in the optimal f value of IL from that of CL (f=1) is due to the greater diffusion time available during IL. Since intermittent leaching gives more time for solute to diffuse out of the immobile water regions (during rest periods), the concentration inside such regions will decrease and therefore more desorption will occur. Such an increase in potassium desorption in the immobile water soil regions will decrease the value of f. When complete equilibrium with the mobile water occurs, the soil in the immobile and mobile water regions will be equally active in potassium desorption, thus f will equal Φ (i.e. desorption is partitioned between immobile and mobile water regions in the same ratio as the water is partitioned between mobile and immobile water regions) .

Fig. 10.6 shows that the SIL model fits the experimental results very well in the early stages, but fails to simulate the "tailing" during the later stages

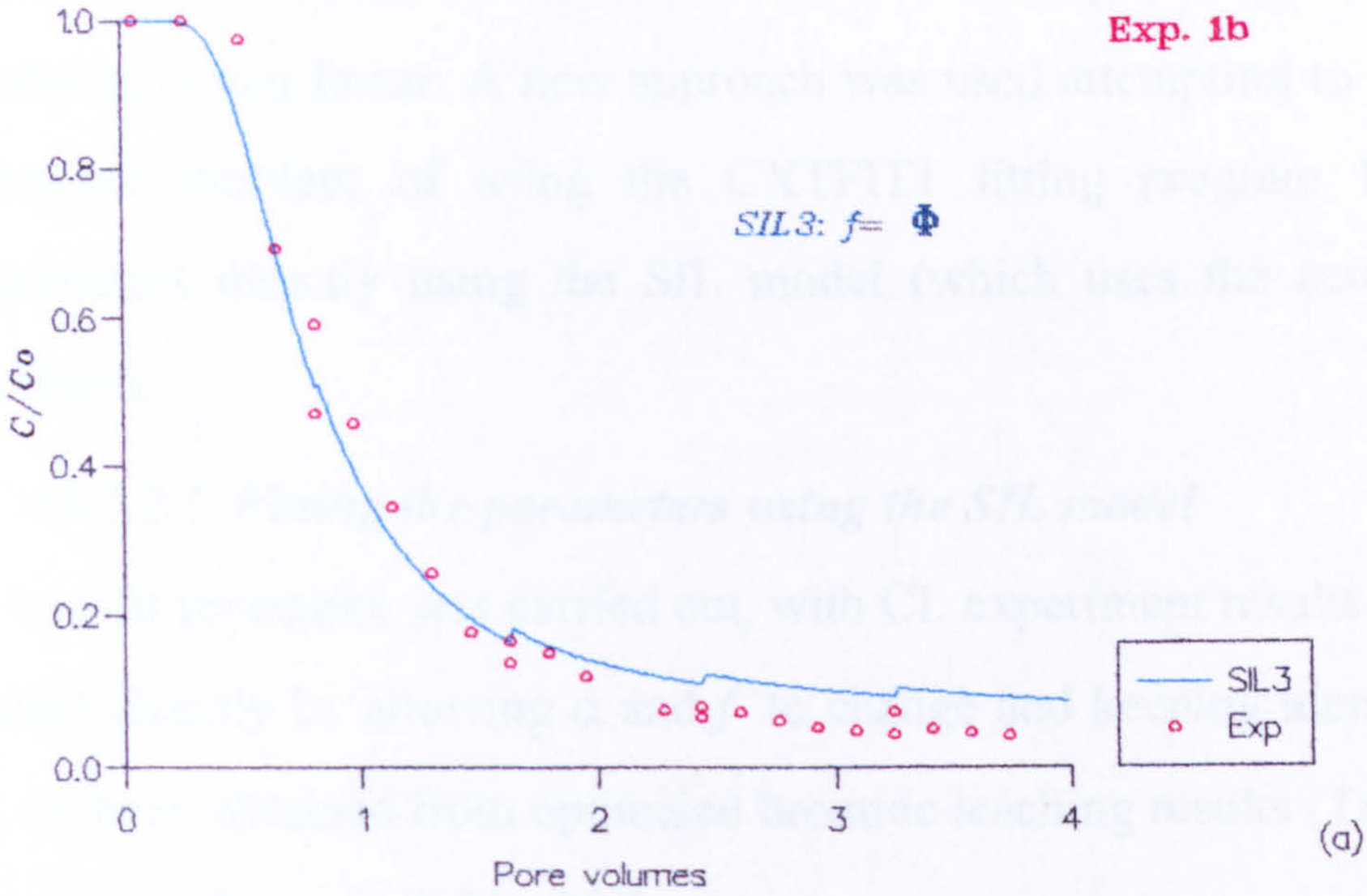

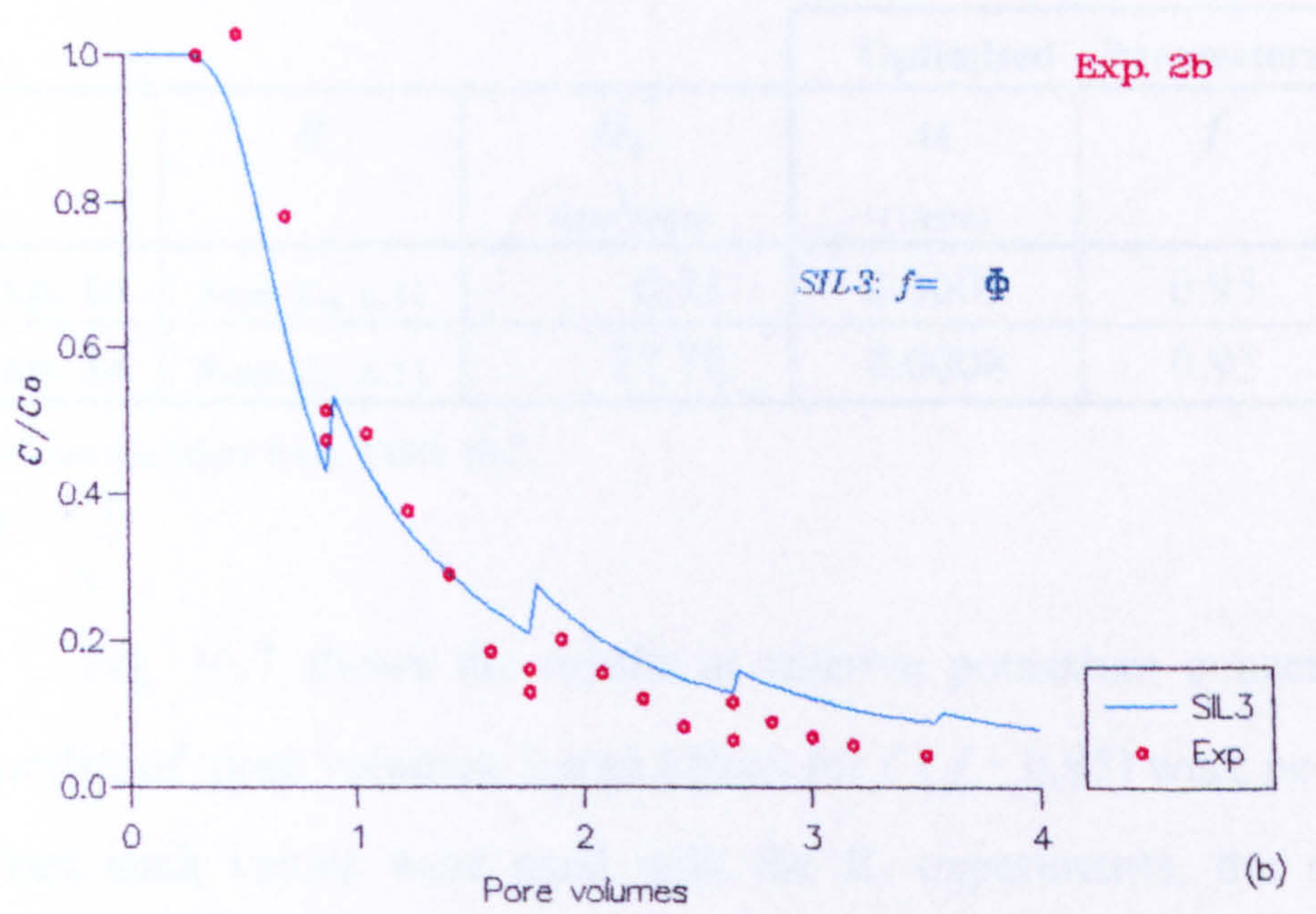

Fig. 10.6: Relative potassium concentration against number of pore volumes for: (a) Exp. 1b, (b) Exp. 2b .

where the model overestimates the effluent concentration. It seems that using CXTFIT1, which uses the linearized desorption isotherm to optimise the unknown parameters, influences the values of these parameters since the actual isotherm is non-linear. A new approach was used attempting to overcome this inherited problem of using the CXTFIT1 fitting program by fitting the parameters directly using the SIL model (which uses the actual desorption isotherm).

10.2.2.3 Fitting the parameters using the SIL model

A best-fit procedure was carried out, with CL experiment results, using the SIL model directly by allowing α and f to change and keeping identical values of D_s to those obtained from optimised bromide leaching results (Table 10.2). The results are shown in Table 10.5.

Table 10.5 : Optimised α and f (with a given D_S) using SIL model.

			Optimised Parameters			
	R	D_S^* (mm^2/min)	α (1/min)	f	$\omega^{\#}$	R^2
Exp. 1a	From Eq. 6.11	6.71	0.0005	0.95	0.056	0.996
Exp. 2a	From Eq. 6.11	22.70	0.0008	0.95	0.044	0.982

* values are taken from Table 10.2.

$^{\#}\omega = \frac{\alpha\, l}{v_d}$

Fig. 10.7 shows the results as relative potassium concentration against number of pore volumes. Large values for f (f= 0.95) were needed. However, when such values were used with the IL experiments, the model failed to successfully simulate the tailing (Fig. 10.8). The fit improved when the values of f were decreased successively for each *on* cycle (Fig. 10.9) using the following empirical equation:

$$f = f_o\,[1 - 0.45\,N_c] \quad , \qquad N_c < 3$$

$$f = 0 \quad , \qquad N_c \geq 3$$

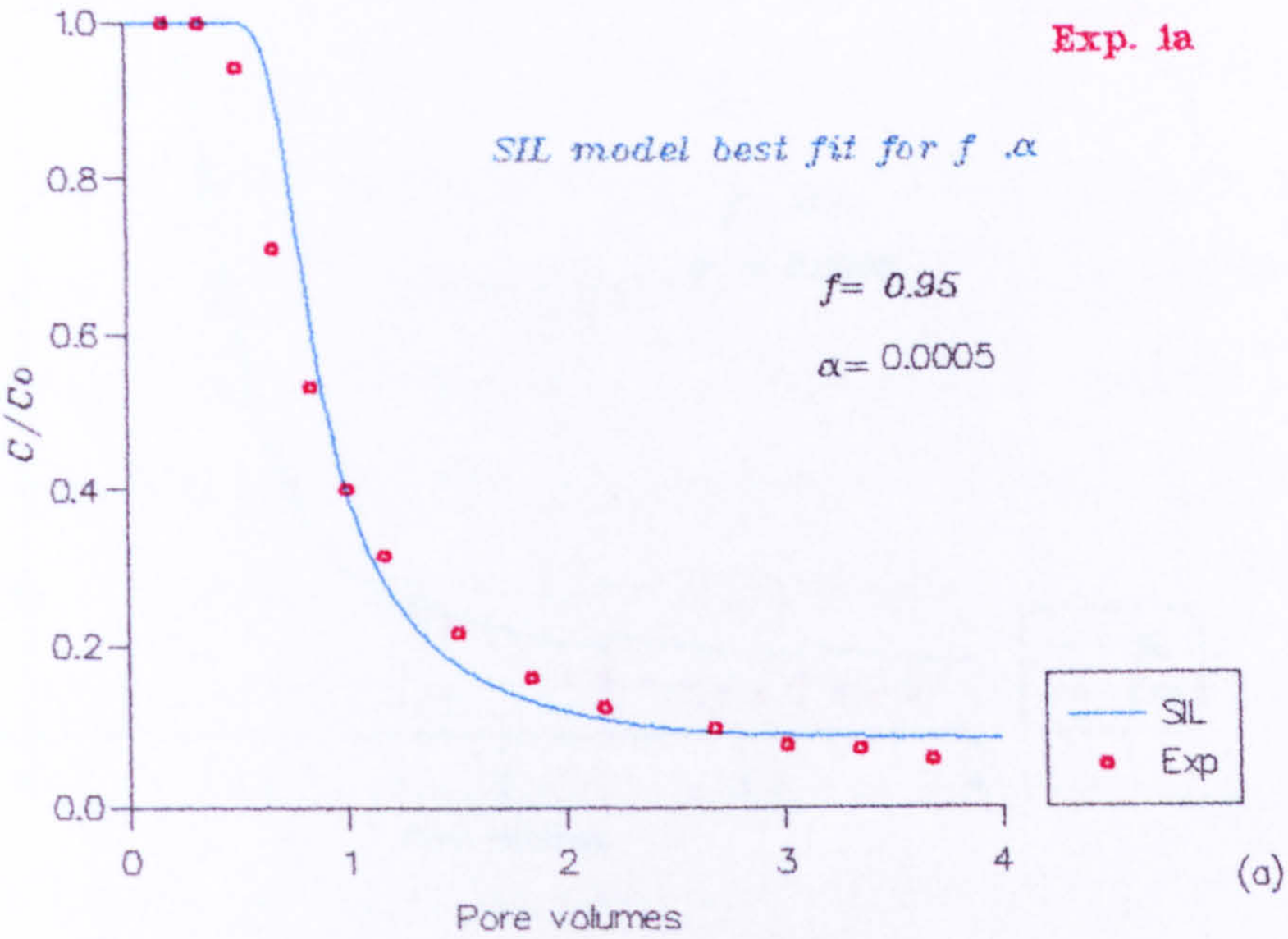

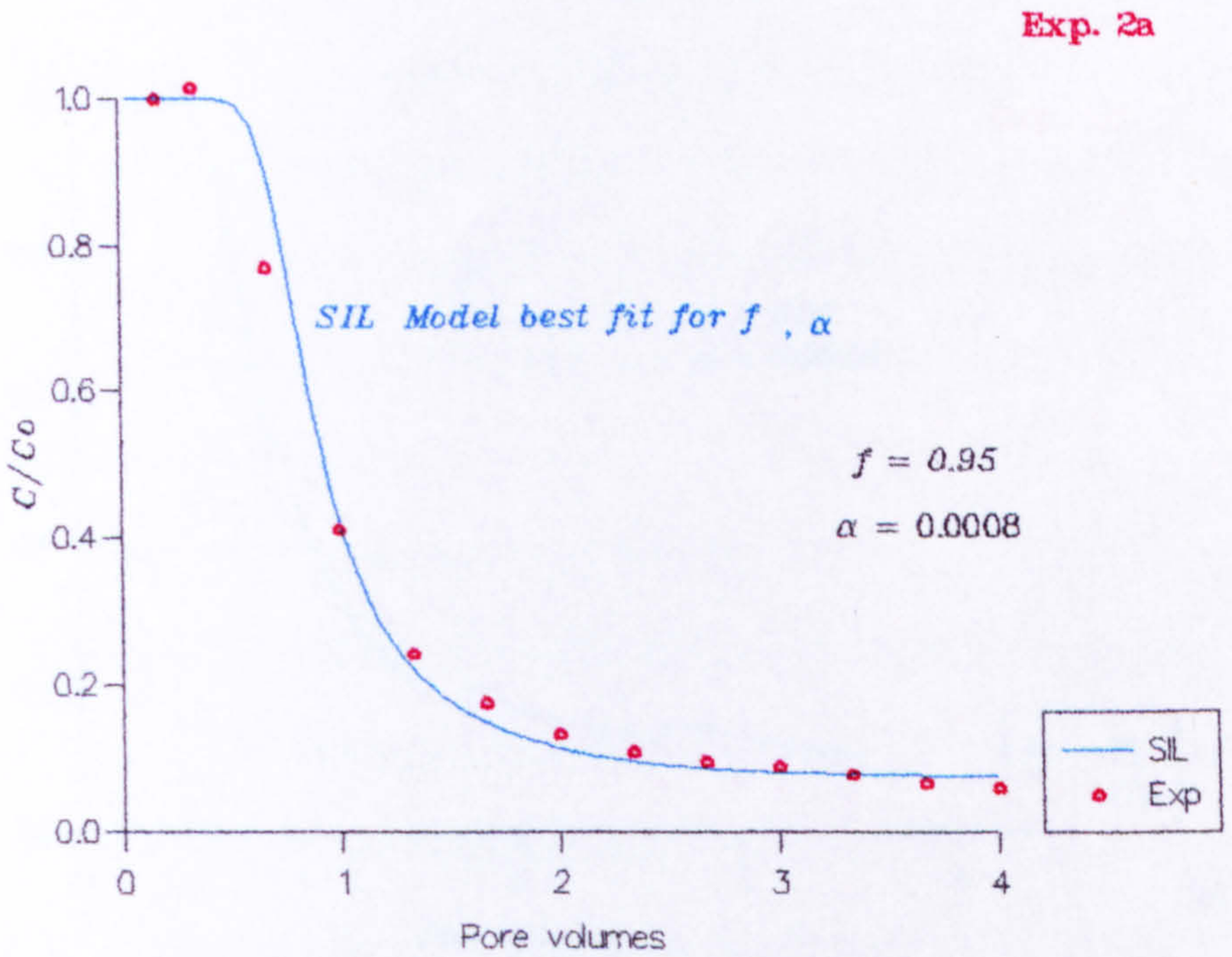

Fig. 10.7: Relative potassium concentration against number of pore volumes for : (a) Exp. 1a and (b) Exp. 2a .

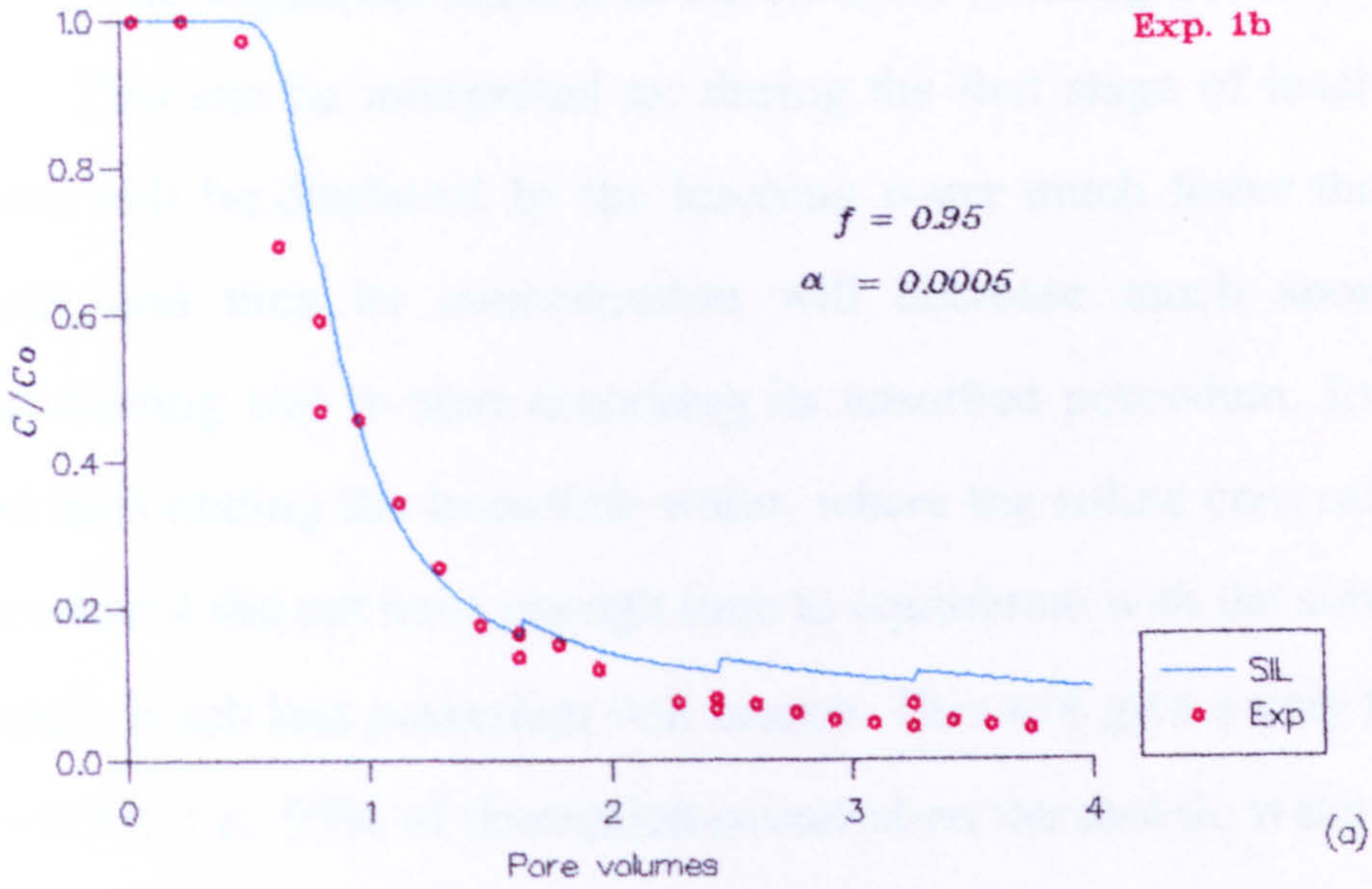

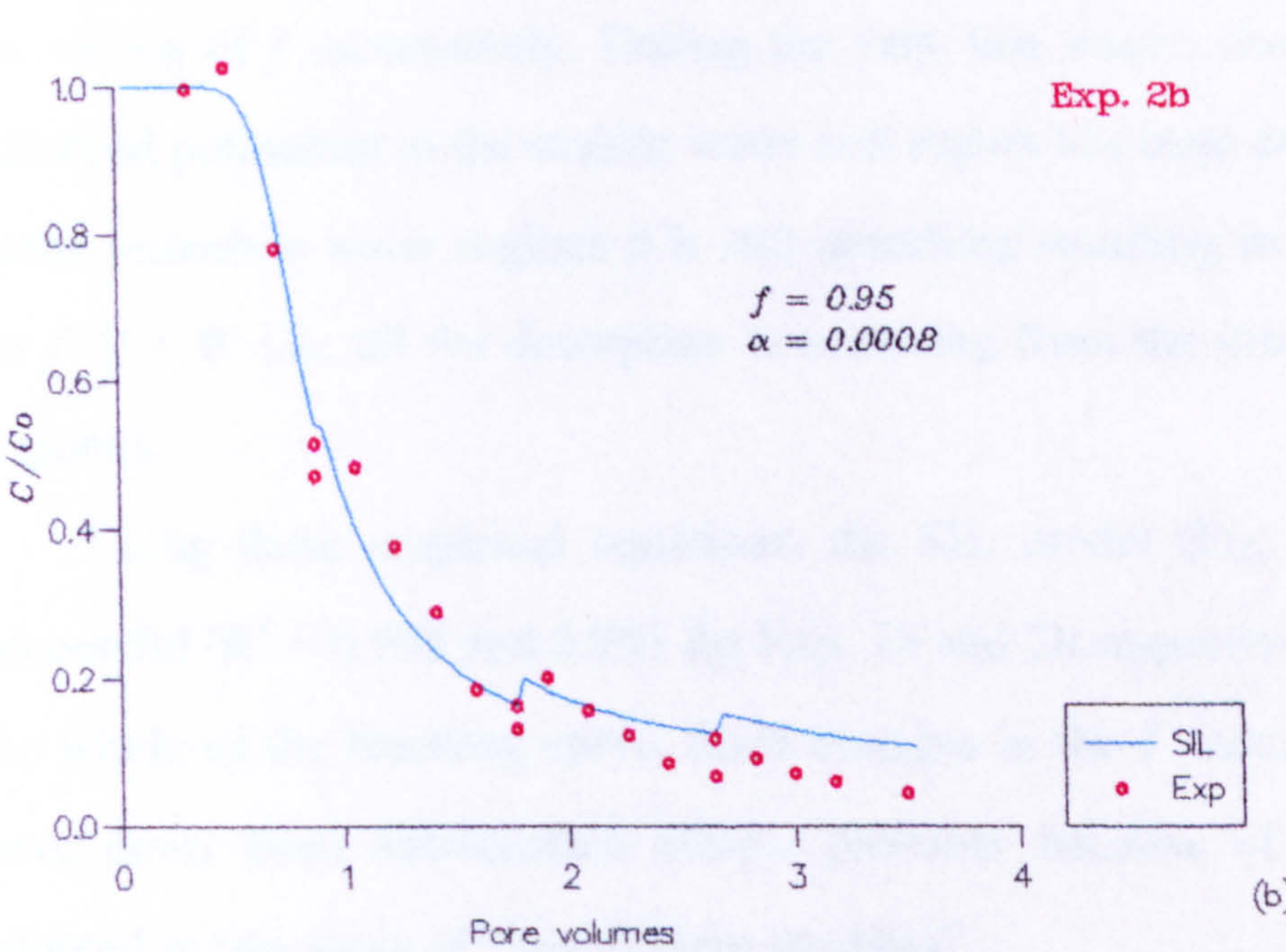

***Fig. 10.8*: Relative potassium concentration against number of pore volumes for: (a) Exp. 1b and (b) Exp. 2b .**

where

f_o = the initial value of f (0.95 in these experiments),

N_c = the sequential number of the *on* cycle (starting from zero).

This can be interpreted as: during the first stage of leaching, the mobile water will be displaced by the leaching water much faster than the immobile water and thus its concentration will decrease much sooner causing the surrounding soil to start desorbing its adsorbed potassium. In contrast, in the soil surrounding the immobile water, where the solute concentration is greater (because it did not have enough time to equilibrate with the solute in the mobile water), much less potassium will desorb. This will give a very high value for f (f = 0.95; i.e., 95% of desorption occurred on the mobile water soil regions). In the later stages the immobile water has had more chance to equilibrate with mobile water (during rest periods) so decreasing its concentration. Thus more desorption will occur in the immobile water soil regions which will decrease the values of f successively. During the very late stages, the majority of the adsorbed potassium in the mobile water soil region has been desorbed, whereas in the immobile water regions it is still desorbing resulting in the lowest value for f (f = 0 i.e., all the desorption is occurring from the immobile water soil regions).

Using these empirical equations, the SIL model (Fig. 10.9) was more successful (R^2 = 0.998 and 0.995 for Exp. 1b and 2b respectively) in describing the whole of the leaching curve. Such changes in the f value during leaching have never been documented before, probably because of the special case adopted in this study of "intermittent leaching" .

The SIL model was then used to calculate the amount of solute remaining in the column under both intermittent and continuous leaching. The results are shown in Fig. 10.10 as the ratio $Ss(t)/Sa$ against number of pore volumes, where;

$Ss(t)$ = the amount of potassium remaining in the column

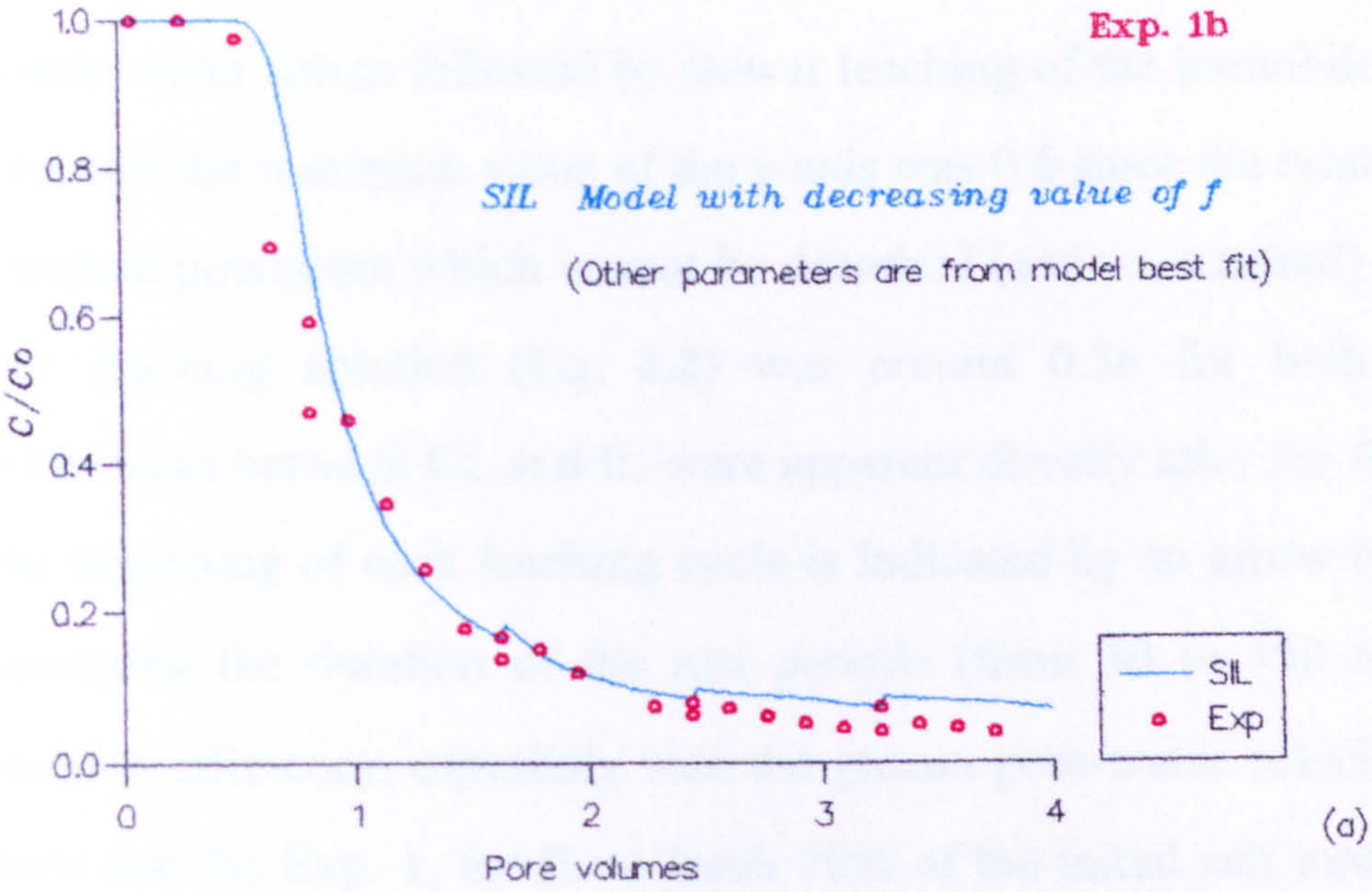

***Fig. 10.9*: Relative potassium concentration against number of pore volumes for: (a) Exp. 1b and (b) Exp. 2b .**

Sa = the initial amount of potassium in the column (including the solute adsorbed).

Fig. 10.10 shows that, as for bromide, there was rapid leaching of the mobile-water solute followed by slower leaching of the immobile-water solute. Note that the minimum value of the y-axis was 0.6 since the relative amount of adsorbed potassium which cannot be desorbed (and so, leached) with 0.004 M KCl leaching solution (Eq. 8.2) was around 0.56 for both experiments. Differences between CL and IL were apparent directly after the first rest period (the beginning of each leaching cycle is indicated by an arrow on the graphs). Increasing the duration of the rest periods (from 50 to 150 min) increased leaching efficiency, especially with the greater pore-water velocity. The results show that for Exp. 1, for IL to leach 70% of the initial salt load, 22 and 35% less leaching water is required with 50 and 150 min *off* times respectively. For Exp. 2 these savings increased to 32 and 43% respectively.

10.3 Conclusions

The results of bromide and potassium leaching can be used to examine the efficiency of intermittent leaching for adsorbed and non-adsorbed ions. A few conclusions can be deduced from comparison of the results of Figs. 10.3 and 10.10:

1) Intermittent leaching is more efficient, in terms of use of leaching water and amount of leached solute, than continuous leaching for both adsorbed and non-adsorbed ions.

2) As with ceramic spheres, the benefit of using intermittent leaching is greater the higher the pore velocity and/or the larger the aggregate size.

3) Since non-adsorbed ions are not retarded, they will be leached faster, and thus will need less leaching water than adsorbed ions (continuous or intermittent leaching). This was also found by *Verma & Gupta* (1989) during chloride leaching. They attributed the lower requirement for leaching water to

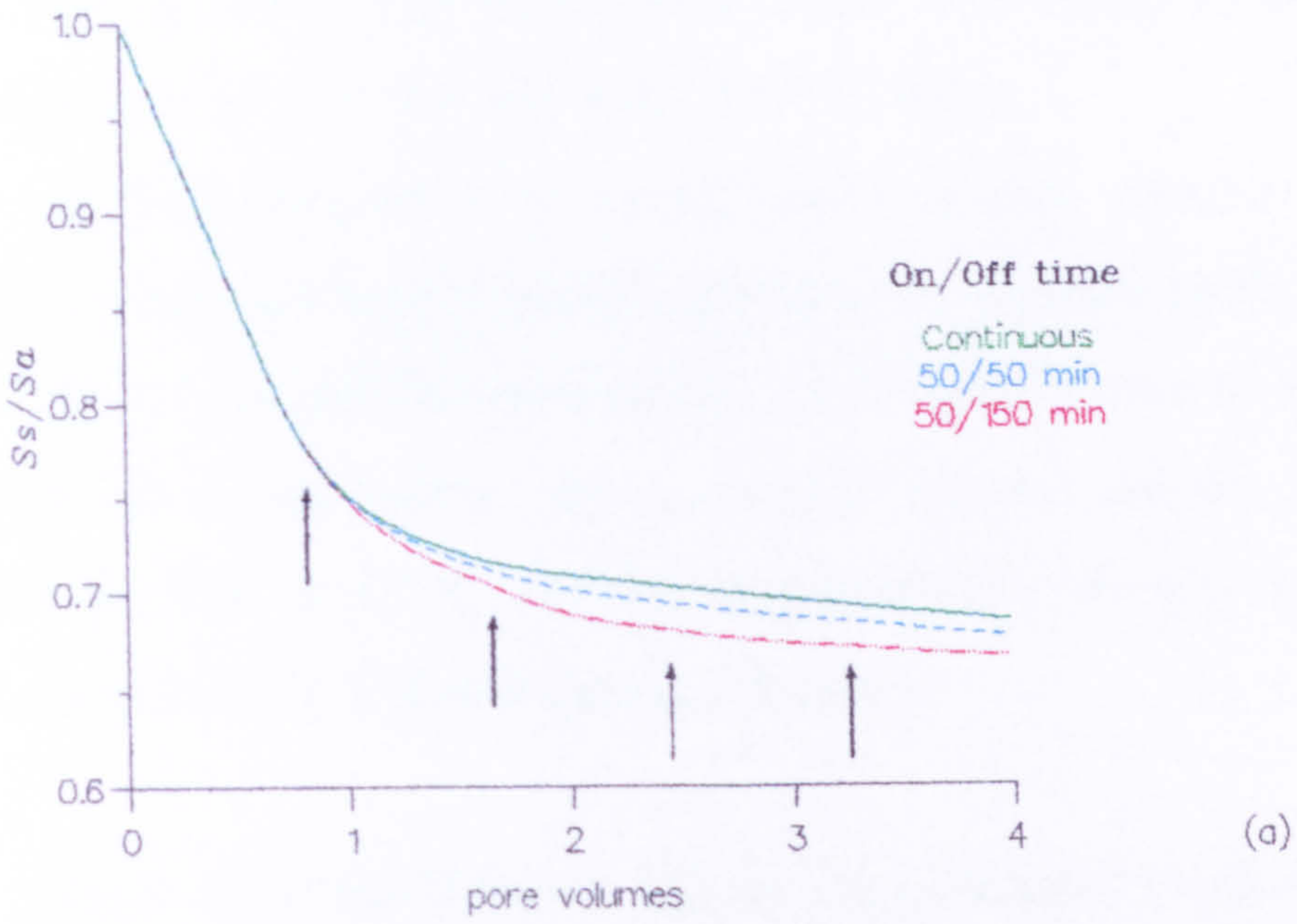

Ss is the remaining amount of potassium in the column

Sa is the initial amount of potassium in the column.

Fig. 10.10: Ratio of the remaining amount of potassium in the column to the initial amount against number of pore volumes for (a) Exp. 1b, (b) Exp. 2b. . Arrows indicate the beginning of each leaching cycle.

the relatively fast movement of anions (such as chloride or bromide) through their montmorillonitic clay soils. For adsorbed ions the ion mobility is much less and adsorbed ions will desorb slowly (according to the shape of the desorption curve), which will delay their leaching.

4) Non-adsorbed ions transfer more quickly between immobile and mobile water and hence shorter *off* times are efficient (with same *on* time). Thus the 50 min *off* time used in Exp. 1 & 2 was sufficient to allow bromide to diffuse out of aggregates, and any further increase did not result in greater efficiency (Fig. 10.4). By contrast, for potassium an increase in the *off* time (to at least 150 min) resulted in greater efficiency.

From all of the above, it can be concluded that leaching adsorbed ions requires more and longer *off* time periods than for more mobile ions. This should be borne in mind when planning the number and periods of intermittent leaching cycles.

PART THREE

Solute transport through columns of ceramic spheres under drained conditions

Chapter Eleven

Intermittent leaching under drained conditions

11.1 Introduction

So far the study has focused on intermittent leaching under saturated conditions. The porous media (ceramic spheres or soil aggregates) were saturated and subsequently leached by a less concentrated solution. During the rest periods, the column remained saturated, the outflow simply being stopped using a tap. However, in the field, this is rarely the case. The initial water content of the soil is less than saturation most of the time, and the water content profile may not be uniform. During leaching, water will infiltrate into the soil, increasing the water content, and leaching the solute. After the leaching event, water redistributes through the soil profile, large pores will empty first, and thus most of the mobile water regions will be drained. The soil will be unsaturated and will have different water content profiles depending upon the initial water content, time, amount and method of water application (e.g., Fig. 2.4), properties of the soil..., etc. All of these factors will keep the soil unsaturated during the rest periods. The question is now:

how does this affect the efficiency of intermittent leaching ?

One answer could be that, for the saturated system, at the end of a displacement period the solute concentration within soil aggregates is not

the displacement period the solute within the aggregate will diffuse out to the less concentrated solution in the mobile water region due to a concentration gradient (Section 2.2.1). Thus, the solute concentration will be greater at the centre of the aggregate and lower near the surfaces closer to the mobile water region. During the rest period, with most of the mobile water drained, Fick's equation (Eq. 2.2) suggests that solute will diffuse within the aggregates in order to establish a more uniform concentration across the aggregate. The approach to equilibrium will depend on the duration of the rest period and the aggregate size, in addition to the effective diffusion coefficient. During the next displacement period solute within the aggregates will move into the mobile water region more quickly than if still concentrated in the aggregate centre. The longer the rest period, the closer to a uniform concentration across the aggregate and more quickly will solute move out of the aggregates during the subsequent displacement period. A simple description of this hypothesis is shown in Fig. 11.1.

11.2 Experimental set-up

11.2.1 Aim of the experiment

An experiment was designed to investigate and answer the previous question. The idea was to arrange an experiment closer to field conditions, in which during the rest periods the mobile water regions were empty and only the immobile water region remained saturated.

11.2.2 Method and materials

Columns of ceramic spheres were saturated with 0.1 M KCl and prepared in a similar way to Section 3.3.2. An on-off valve was installed on the side of the column (Fig. 11.2) and connected to a distilled water container. The effluent was passed through an in-line conductivity probe (connected to a data logger *via* conductivity meter) and controlled by a peristaltic pump downstream. The

(a) At the end of drained period

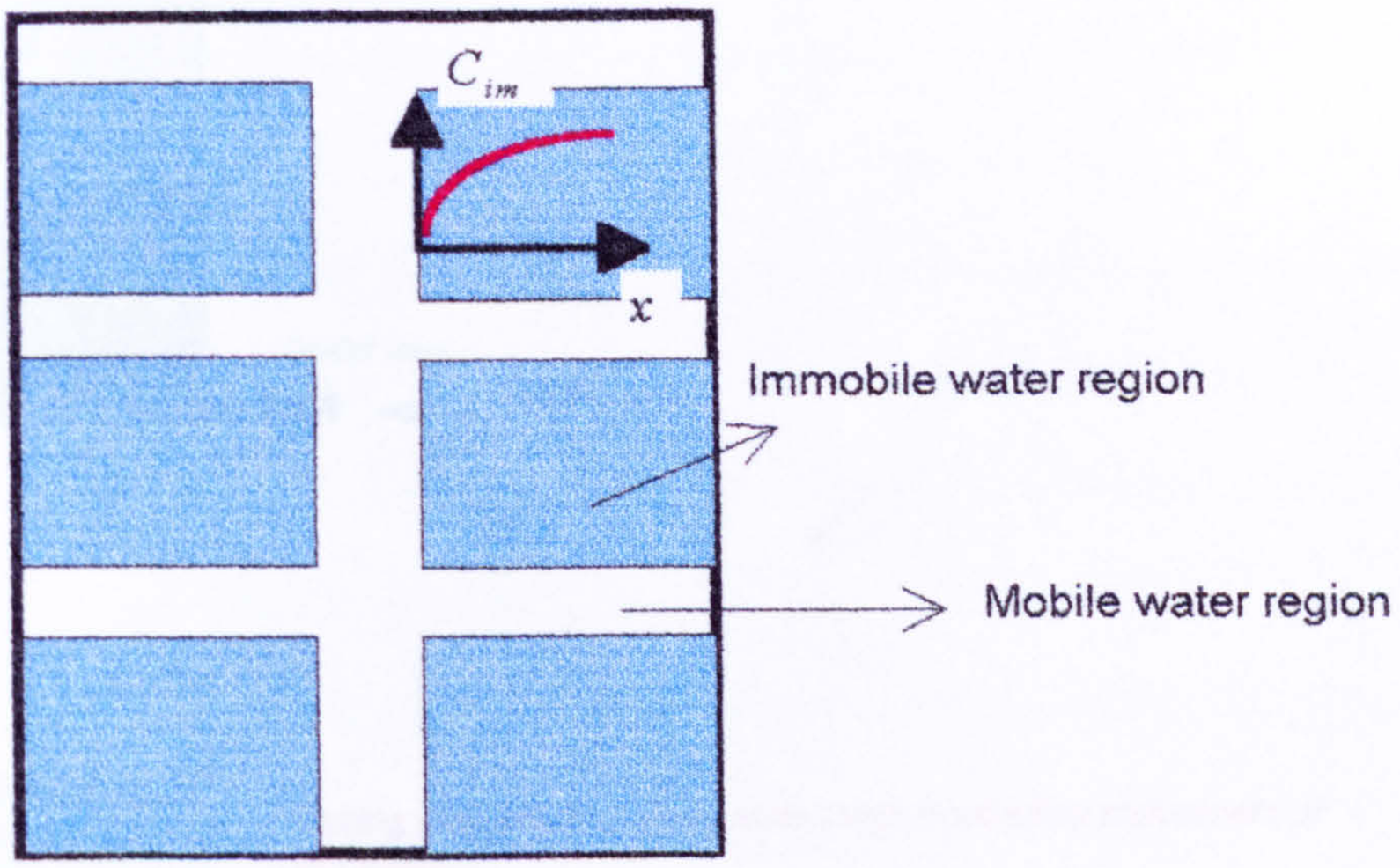

(b) At the end of rest period

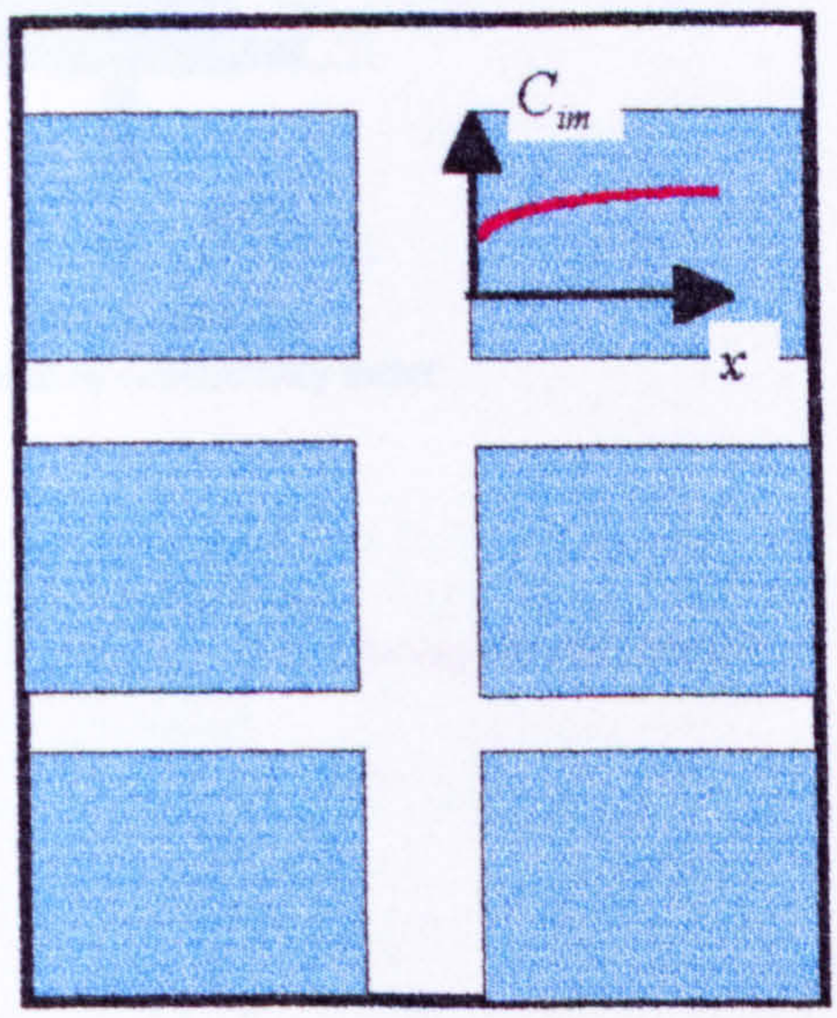

C_{im} is the concentration inside the immobile water region

x is the distance co-ordinate, starting from the interface between mobile and immobile water regions

***Fig. 11.1*: A simplified diagram of mobile and immobile water regions in the column, showing the solute concentration within the latter at the end of drained and rest periods.**

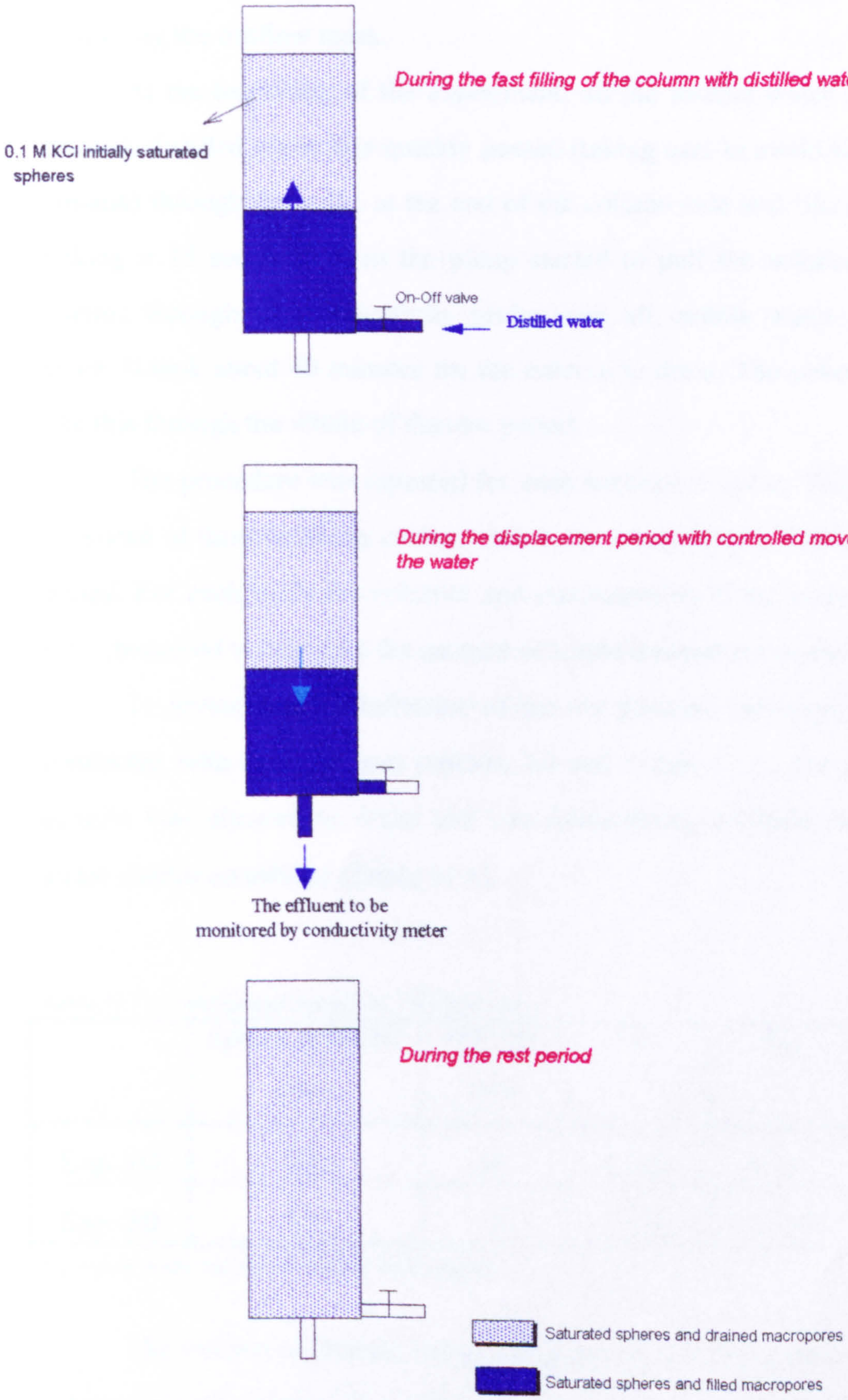

Fig. 11.2: Experimental set-up for drained experiment during saturation, the subsequent displacement period and the rest period.

effluent was collected at the end in a container placed on a balance for measuring the outflow mass.

At the beginning of the experiment, all the mobile water regions were drained, distilled water was quickly passed (taking care to avoid bubbles in the column) through the valve at the end of the column side and filled the column (taking ≈ 15 seconds), then the pump started to pull the solution out of the column through the conductivity probe until all mobile water was drained again. It took about 40 minutes for the column to drain. The column remained like this through the whole of the rest period.

The procedure was repeated for each successive cycle. The experiments consisted of three leaching cycles, each cycle comprising a drained and a rest period. For each cycle the volumes and concentration of the collected effluent were measured to calculate the amount of solute leached at the end of the cycle.

To investigate the influence of the rest periods, two experiments were conducted with different rest periods, 60 and 0 min (i.e., for the latter the column was allowed to drain and was immediately refilled), but otherwise under similar conditions (Table 11.1).

Table 11.1 : Experimental conditions (drained case).

	Sphere diameter (mm)	***Off time*** (min)	θ_m	θ_{im}	v_m (mm/min)
Exp. 1D	13	60	0.462	0.265	4.51
Exp. 2D	13	0	0.470	0.270	4.47

v_m = pore-water velocity in mobile water region.

The volume of drained water was assumed to be the mobile water (inter-spheres water) volume (V_m). The difference in mass of the spheres directly after the experiment and after oven drying was considered to be the mass of immobile water, i.e. immobile water (intra-spheres water) volume (V_{im}).

11.2.3 Results and discussion

Fig. 11.3 shows the solute concentration of the leachate as a function of mobile water volumes (MWV). Curves for each of the three leaching cycles are shown. Each curve started at a low concentration which increased sharply as solute diffused out of the spheres. As the mobile water drained down, the rate of increase of effluent concentration also decreased due to a decreasing number of spheres still in contact with the mobile water and (effectively) under leaching. In addition, as concentration in the mobile water region increased so the rate of transfer from immobile to mobile water decreased resulting in a similar reduced rate of increase in effluent concentration.

For subsequent cycles, as the total amount of solute remaining in the spheres decreased, the diffusion flux within the sphere decreased as did the concentration gradient between immobile and mobile water. Thus fluxes within spheres and into the mobile water decreased. This is why the rate of change in effluent concentration decreases from one cycle to the next.

A comparison of Exps. 1D and 2D (Fig. 11.3) shows a greater concentration of effluent during Exp. 1D (i.e., more leached solute) throughout the whole experiment, confirming that there is a benefit from the rest periods.

Fig. 11.4 shows the percentage of the solute leached against MWV. The amount of solute leached after each cycle was calculated from the concentration of the collected effluent. The initial solute load of the column (*So*) was calculated by:

$$So = C_0^m V_m + C_0^{im} V_{im}$$

where

C_0^m = the initial concentration of mobile solution (= 0)

C_0^{im} = the initial concentration of immobile solution (= 0.1 M KCl) .

V_m = the mobile water volume

V_{im} = the immobile water volume.

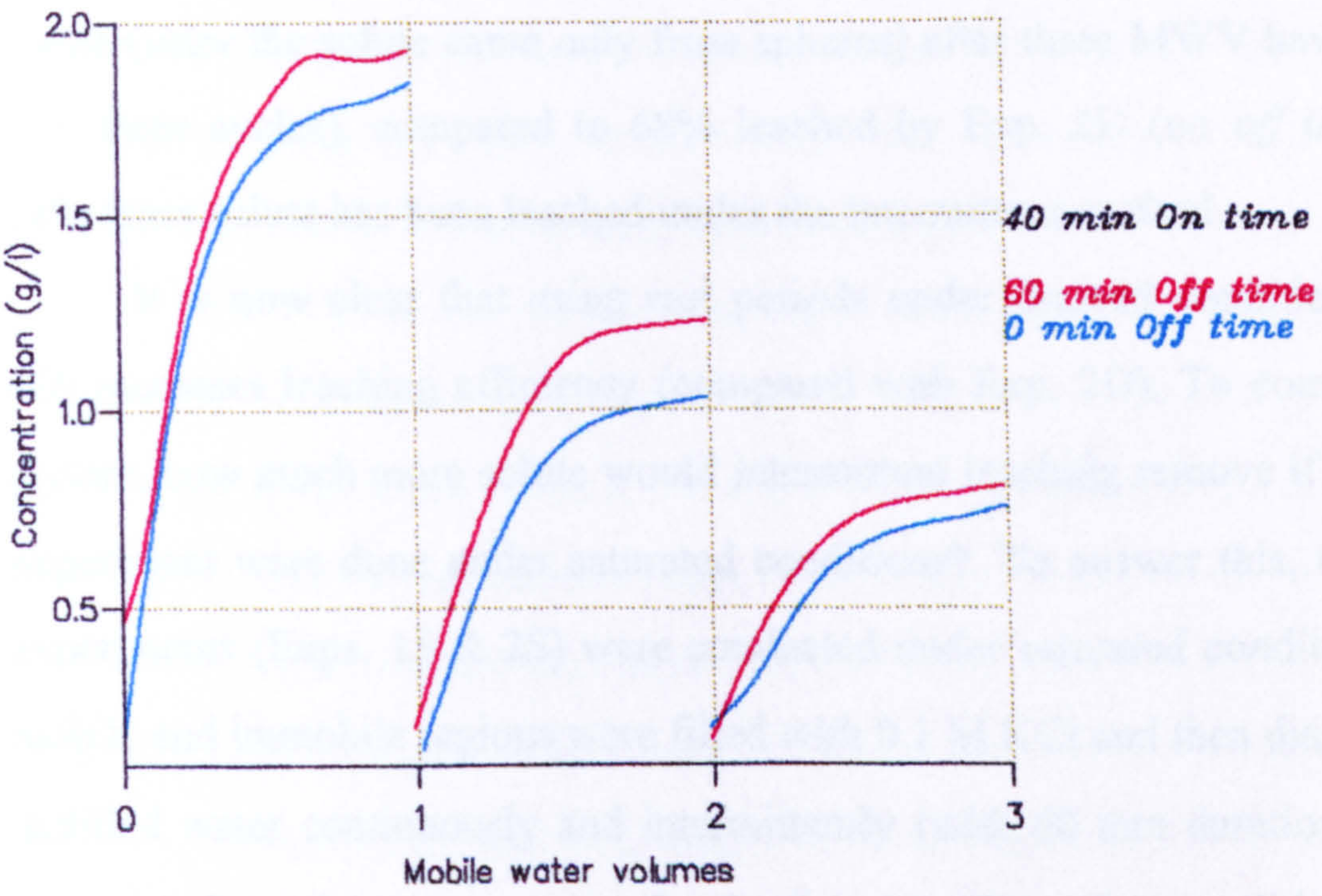

***Fig. 11.3*: A graph of effluent concentration *vs.* mobile water volumes for Exps. 1D & 2D.**

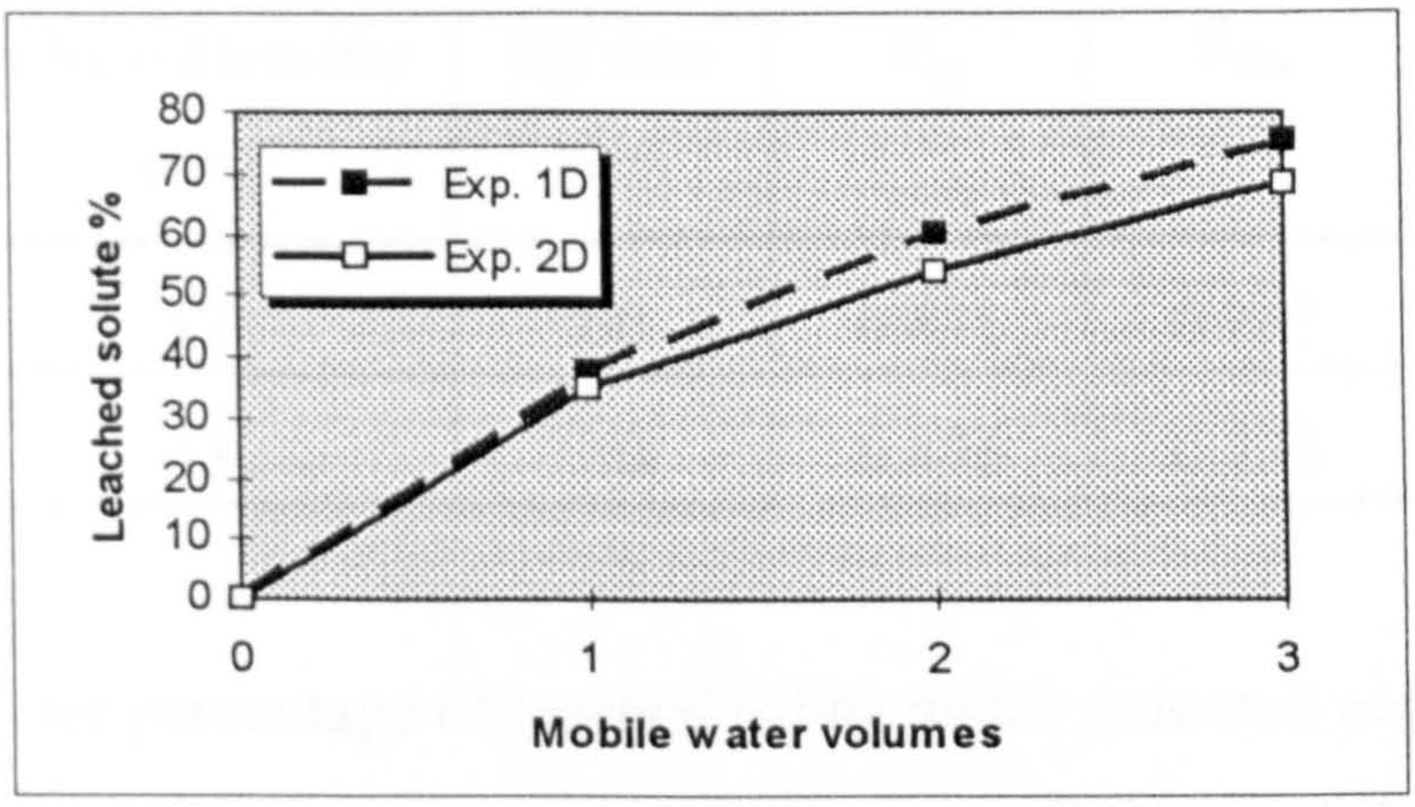

Fig. 11.4 : Percentage of leached solute *vs.* mobile water volumes for Exps. 1D&2D

The results show that Exp. 1D leached 76% of the initial immobile solute (since the solute came only from spheres) after three MWV have passed (i.e. three cycles), compared to 68% leached by Exp. 2D (no *off* time), i.e. 12% more solute has been leached under the intermittent method.

It is now clear that using rest periods under drained conditions (Exp. 1D) increases leaching efficiency (compared with Exp. 2D). To complete the picture, how much more solute would intermittent leaching remove if the same experiment were done under saturated conditions?. To answer this, two more experiments (Exps. 1S & 2S) were conducted under saturated conditions. The mobile and immobile regions were filled with 0.1 M KCl and then displaced by distilled water continuously and intermittently (with 60 min duration of each rest period) in the same way as for Section 3.3. The other conditions of the columns were similar to Exps. 1D & 2D. Table 11.2 shows the experimental conditions.

The SIL model parameters were estimated using the same procedures followed in Section 5.2. The model was run with Exp. 1S & 2S parameters to give the amount of solute leached out, only from the immobile regions, after passing a total of three MWV. Continuous leaching leached 78% of the initial immobile water solute compared to 90% leached by intermittent leaching, which means 14% more solute leached under intermittent leaching .

Table 11.2 : Experimental conditions (saturated case).

	Sphere diameter (mm)	***Off time*** (min)	θ_m	θ_{im}	v_m (mm/min)
Exp. 1S	13	60	0.471	0.267	4.45
Exp. 2S	13	0	0.476	0.276	4.31

The greater percentage of leached solute under saturated conditions than under drained conditions is attributed mainly to the fact that, when saturated, solute inside the spheres continues to move out into the mobile water throughout the whole displacement period, whereas under the drained condition solute stops diffusing out as the falling water front passes the spheres. Consequently the upper layers of the column have a shorter time in contact with leaching water and transfer into the mobile region progresses more slowly.

Fig. 11.5 shows the profile of solute concentration in immobile water (i.e. $C_{im}(z,t)$, average concentration within the spheres centred at z) for saturated and drained conditions at the end of leaching (i.e. after leaching with three MWV). The solute concentration in the upper layers of the column is much greater under drained than saturated conditions. This is because the time available for solute to diffuse out of the immobile water region is much shorter under drained conditions and will finish soon after the water front passes the spheres. However, this concentration is smaller in the lowest layers under drained conditions than under saturated conditions. This is because, near the bottom of the column, spheres are in contact with the mobile water during almost all the "drained" period as in the case of saturated conditions. Furthermore, under drained conditions, the solute concentration of the mobile water will start from zero at the beginning of each cycle (immediately after filling the column with the distilled water) which will enhance diffusion of

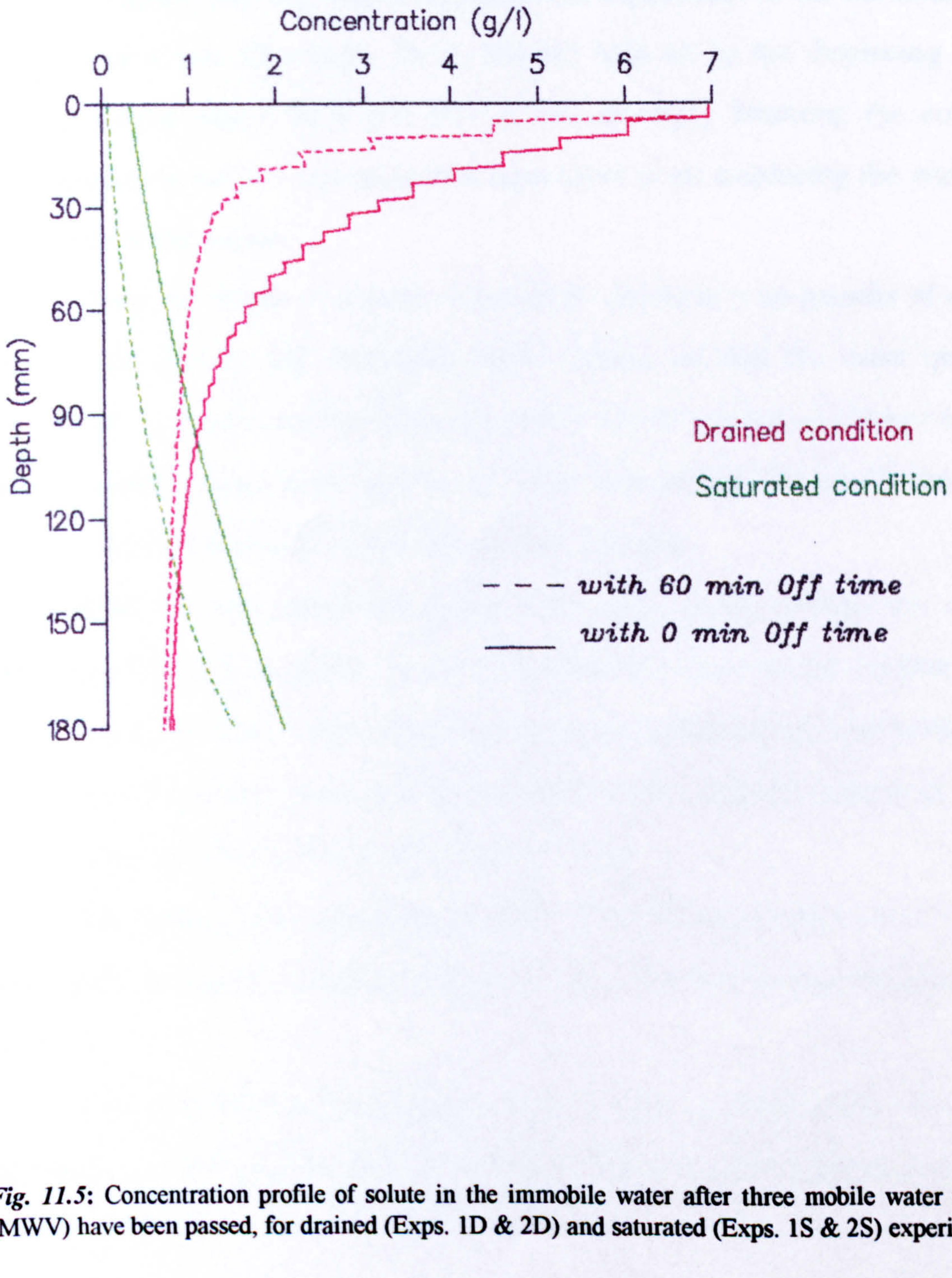

***Fig. 11.5*: Concentration profile of solute in the immobile water after three mobile water volumes (MWV) have been passed, for drained (Exps. 1D & 2D) and saturated (Exps. 1S & 2S) experiments.**

solute out of the spheres (by increasing the concentration gradient) resulting, at the end, in a lower C_{im} under drained than saturated conditions.

These experiments have proved that, even when all the mobile water is drained, there is still a benefit in using intermittent leaching.

11.3 Model modifications and simulations

To make it easier to simulate Exps. 1D & 2D, it is better to consider it as follows: suppose that this was a displacement experiment of the continuously saturated type (i.e. like Exps. 1S & 2S) but with air as the displacing fluid causing simple *piston* flow [i.e. D_s= 0, (no mixing)]. Draining the column (immediately prior to a rest period) is equivalent to air displacing the water in the mobile water region.

Along the length of column occupied by air, there is no transfer of solute between the mobile and immobile water regions, so that the mass transfer coefficient, α, is zero. On this basis, the model would suggest no change during the rest period (since there will be no mass transfer and the model does not describe the redistribution *within* the ceramic spheres).

After the rest period the solute will more readily diffuse out of the spheres as there is a greater solute concentration close to the surface (Fig. 11.1). This will increase the mass transfer rate of solute between immobile and mobile water regions during the next displacement "drained" period. In terms of the model this is translated as a higher α value.

The model was modified to allow for different values of α when solving the transport equations (Eqs. 2.17 & 2.19) during each displacement period.

The column was assumed to have length, L, greater than the actual length, L_r, of the column ($L > L_r$ and the model, in effect, describes a semi-infinite column).

At $t = 0$

$0 < z \leq L_r$

$$C_{im} = C_o \quad (0.1\ \text{M KCl})$$
$$C_m = 0$$

$L_r < z < L$

$$C_{im} = 0$$
$$C_m = 0\ .$$

The length of displacement period (*On* time) is taken as the time required to drain all the mobile water (i.e., air to displace mobile water from the length of the column). If V_m is the mobile water volume, q is the flow rate, then the *on* time is equal to

$$t_{on} = \frac{V_m}{q}$$

The rest period is assumed to begin after all mobile water has drained. Fig 11.6 shows a schematic of the model. The new model is termed the DIL (Drained Intermittent Leaching) model. The DIL model is written in FORTRAN-77. The computer program is printed in Appendix E.

11.3.1 Estimating DIL model parameters

To solve Eqs. 2.17 & 2.19, five parameters need to be estimated, namely θ_m, θ_{im}, v_m, D_S, and α. The first three parameters can be calculated from the experimental conditions. D_S is assumed to be zero during the displacement periods as discussed before. The only unknown parameter is α. This was empirically determined by optimising the fit between the experimentally observed cumulative leaching and predictions from the DIL model.

Fig. 11.7 indicates such optimised values for α for Exps. 1D & 2D. Although α was initially the same (as the starting conditions were similar), subsequently α values for Exp. 1D (with 60 min rest period) were two to four

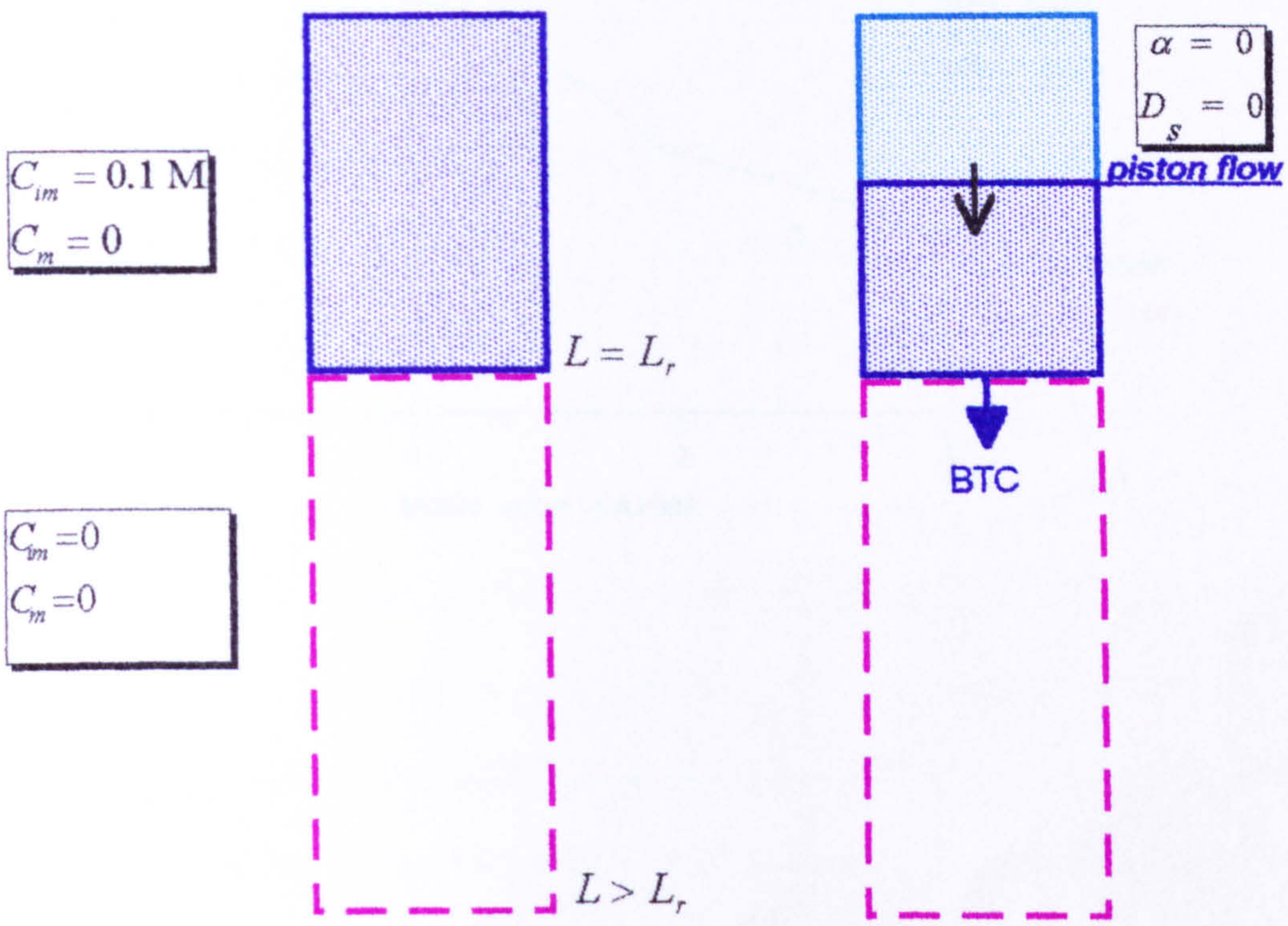

Mobile water region filled with:

Air

Solution

***Fig. 11.6*: Simple description of DIL model parameters.**

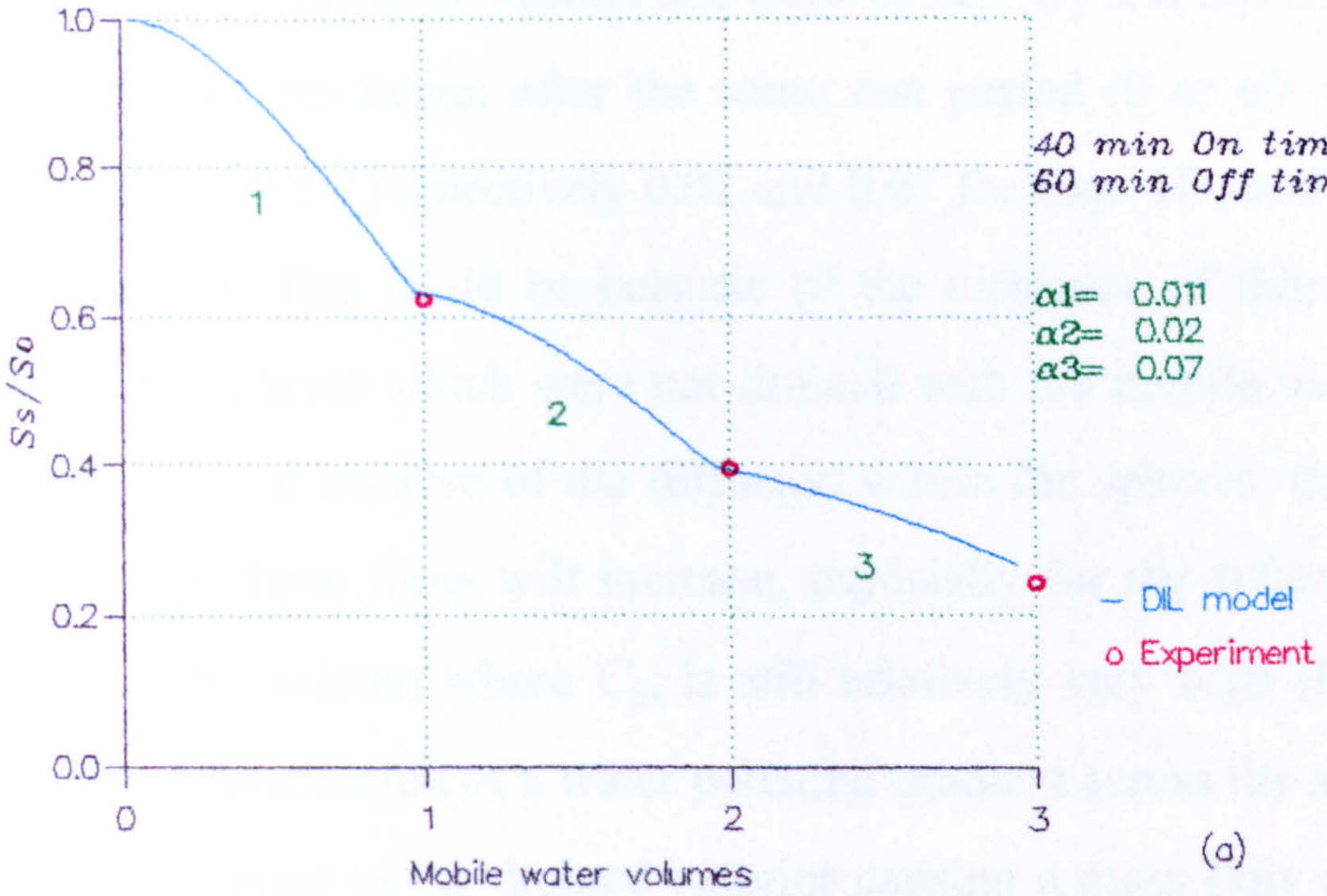

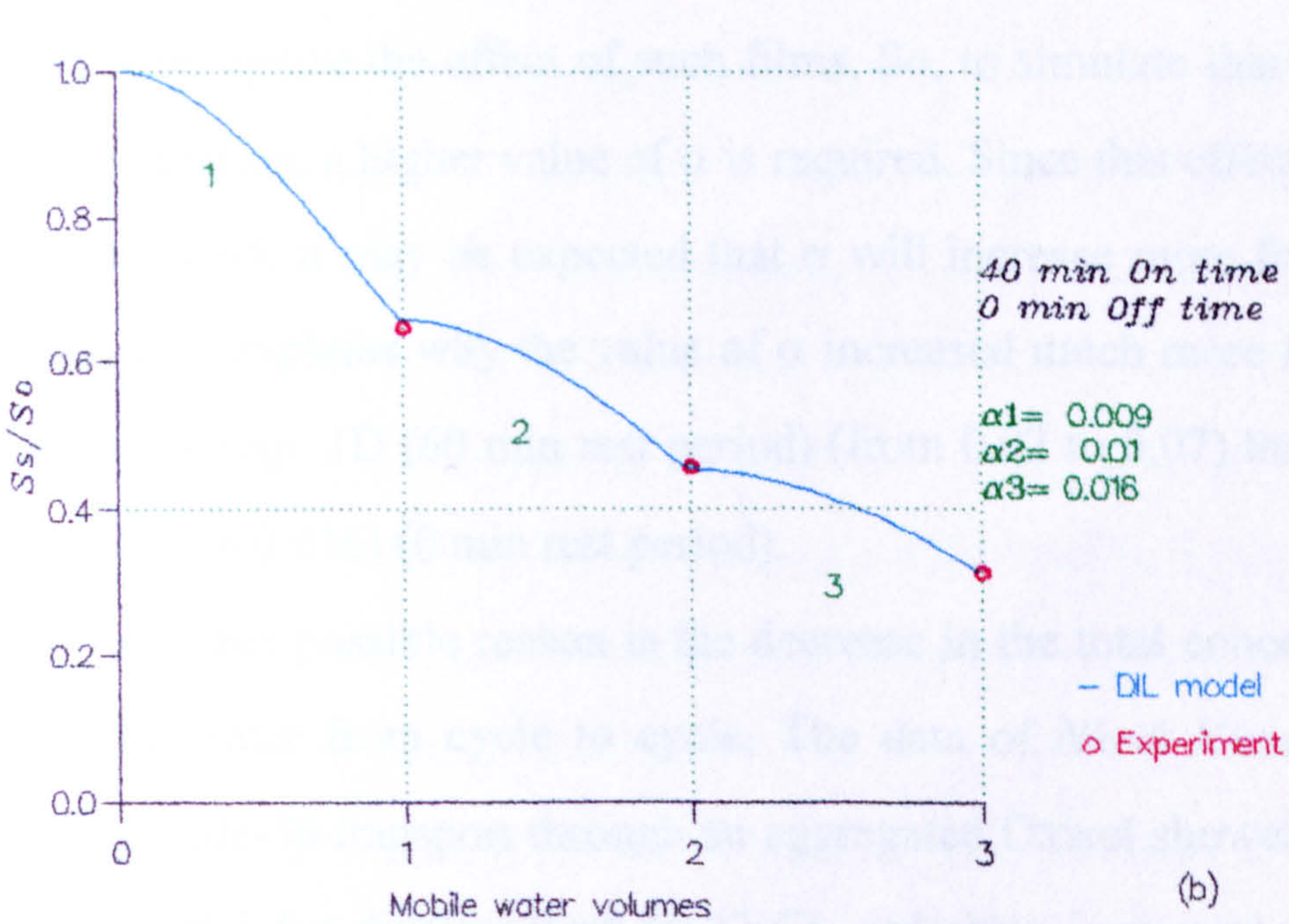

***Fig. 11.7*: A plot of relative amount of solute remaining in the column *vs.* mobile water volumes for** (a) Exp. 1D, (b) Exp. 2D.

times higher than those for Exp. 2D, in agreement with hypothesis that *the solute becomes more readily available for leaching after rest periods*.

The α values in second and third cycles (α_2 and α_3) should be similar since both cycles begun after the same rest period (0 or 60 min). However, these values were respectively 0.02 and 0.07 for Exp. 1D, and 0.01 and 0.016 for Exp. 2D. This could be because of the existence of thin films of water around the spheres which were not drained with the mobile water. During the rest period, and because of the diffusion within the spheres, the concentration of solute in these films will increase, especially for the spheres in the upper layers of the column where C_{im} is still relatively very high (Fig. 11.5). Also there is a complication of a water potential gradient across the spheres from the saturated interior to the drained exterior causing a mass flow of solute during the rest period. When the column refilled, these films will easily mix with the incoming distilled water, and quickly increase its concentration. The model does not recognise the effect of such films. So, to simulate this quick increase in concentration, a higher value of α is required. Since this effect occurs during the rest period, it may be expected that α will increase more for a longer rest period. This explains why the value of α increased much more from cycle two to three for Exp. 1D (60 min rest period) (from 0.02 to 0.07) than for.Exp. 2D (from 0.01 to 0.016) (0 min rest period).

Another possible reason is the decrease in the total concentration of the immobile water from cycle to cycle. The data of *Nkedi-Kizza et al.* (1983) from chloride-36 transport through an aggregated Oxisol showed that the value of α for ^{36}Cl for displacement by $CaCl_2$ solutions increased as the solution concentration decreased. Fig. 11.8 shows a plot created from their data for α values against the concentration of $CaCl_2$ solutions. The α value increased by a factor of three when the solution concentration decreased from 0.1 N to 0.001 N. However, this reason is not sufficient on its own as in Exps. 1D and 2D there is not much difference in concentration between cycles 2 & 3. A further

explanation of *Nkedi-Kizza et al.*'s results is that, as the experiments were on tropical soils, there may have been changes in the ion-exchange capacity of the soil with change in concentration.

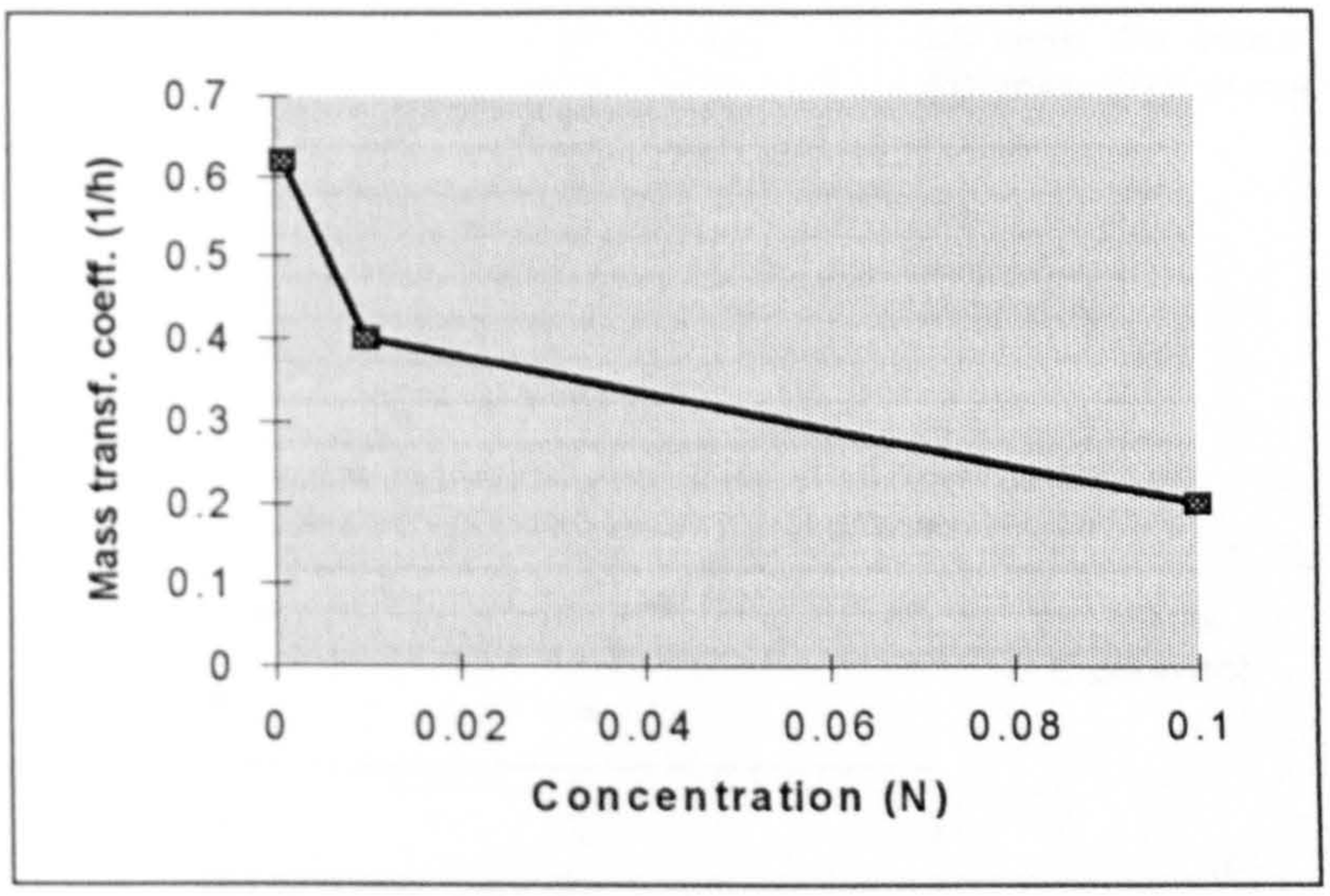

Fig. 11.8 :The mass transfer coefficient α as a function of concentration (Based on data from *Nkedi-Kizza et al.* (1983) for ^{36}Cl)

The optimised values of α were then used in the model to simulate the experimental results. Fig. 11.9 shows the effluent concentration against MWV for Exps. 1D & 2D. The results consist of three curves, each curve for each displacement period. The experimental results were steeper and with a higher concentration at the beginning of each curve and then became flatter than predicted. This could be because, during filling the column, just before the displacement period, the incoming leaching water vigorously mixed with the water films surrounding the spheres (which are relatively very concentrated) sharply raising its concentration. Then, with time, the concentration inside the spheres will decrease and the transfer of solute out of the spheres will decrease. In other words, the value of α will decrease. The model assumed a single value for α for each displacement period. By optimising the α value, the model ,in fact, averages the α value over the whole individual displacement period. The

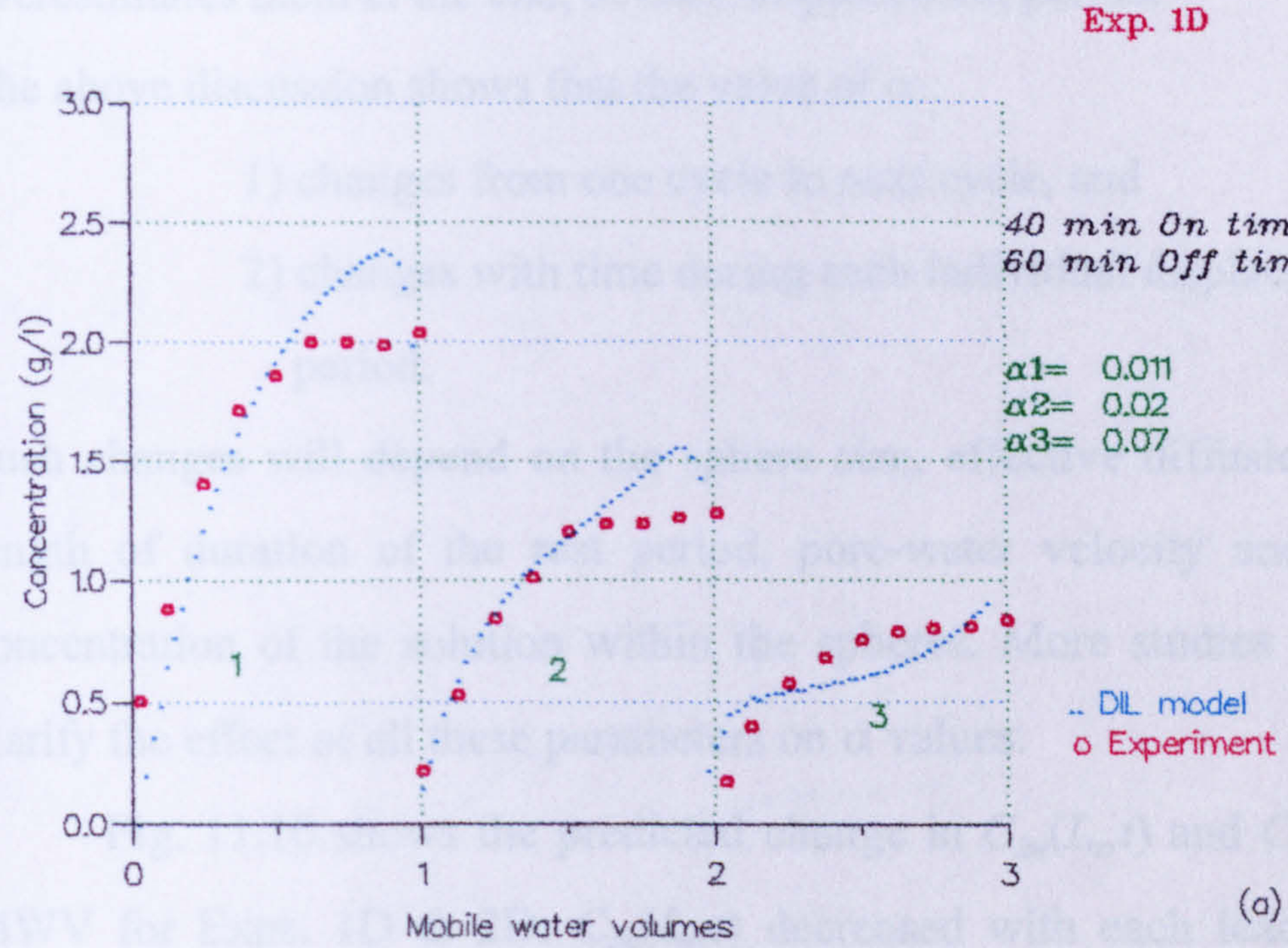

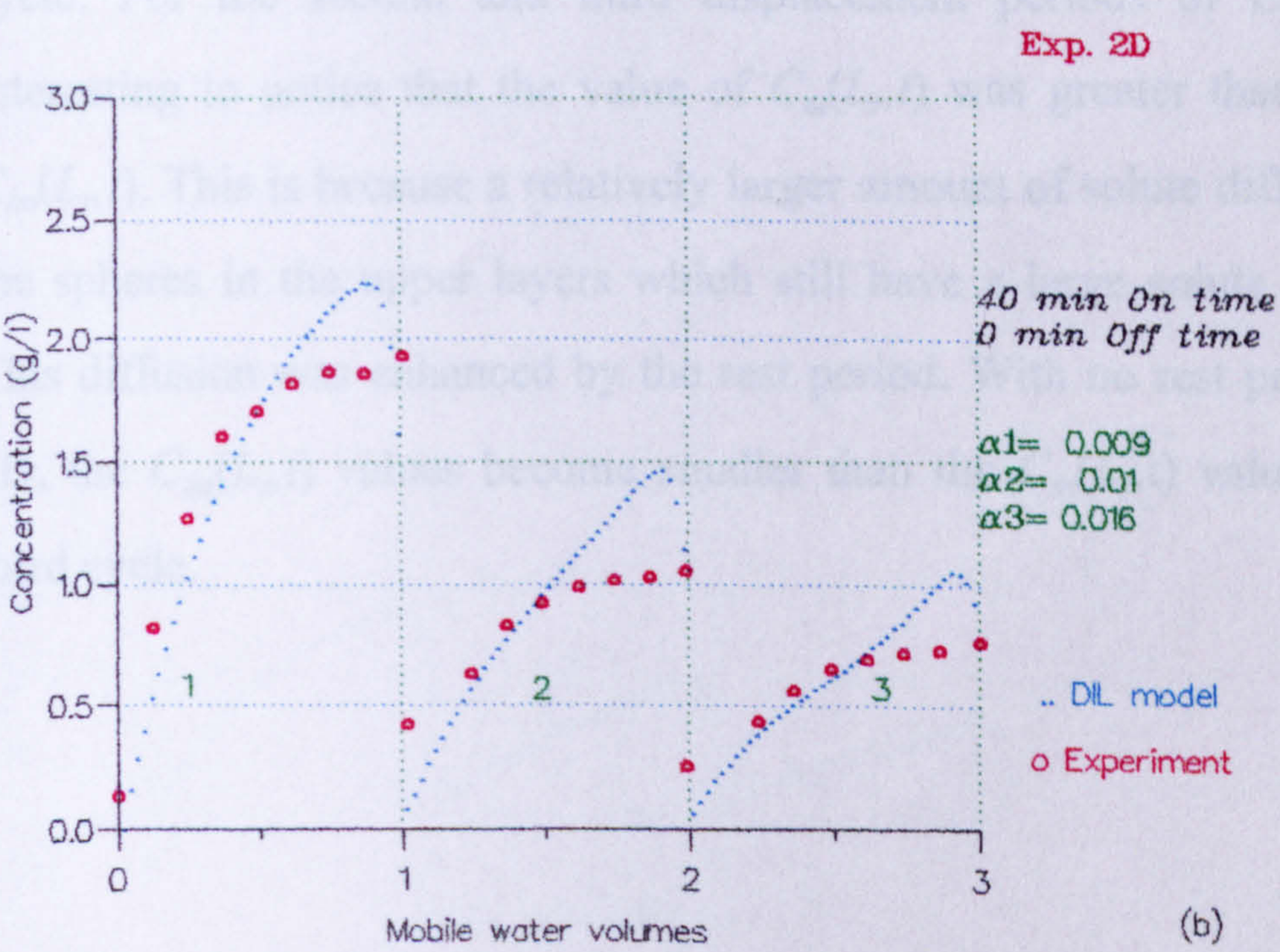

***Fig. 11.9*: Mobile water concentration *vs.* mobile water volumes for: a) Exp. 1D, b) Exp. 2D.**

model thus underestimates the experimental results at the beginning, but overestimates them at the end, of each displacement period.

The above discussion shows that the value of α :

1) changes from one cycle to next cycle, and

2) changes with time during each individual displacement period.

Such changes will depend on the sphere size, effective diffusion coefficient, length of duration of the rest period, pore-water velocity and the average concentration of the solution within the spheres. More studies are needed to clarify the effect of all these parameters on α values.

Fig. 11.10 shows the predicted change in $C_{im}(L_r,t)$ and $C_m(L_r,t)$ against MWV for Exps. 1D & 2D. $C_{im}(L_r,t)$ decreased with each leaching cycle as expected, with most of the leaching (about 42%) occurring during the first cycle. For the second and third displacement periods of Exp. 1D, it is interesting to notice that the value of $C_m(L_r,t)$ was greater than the value of $C_{im}(L_r,t)$. This is because a relatively larger amount of solute diffused out from the spheres in the upper layers which still have a large solute concentration. This diffusion was enhanced by the rest period. With no rest period, i.e. Exp. 2D, the $C_{im}(L_r,t)$ values become smaller than the $C_m(L_r,t)$ values only at the third cycle.

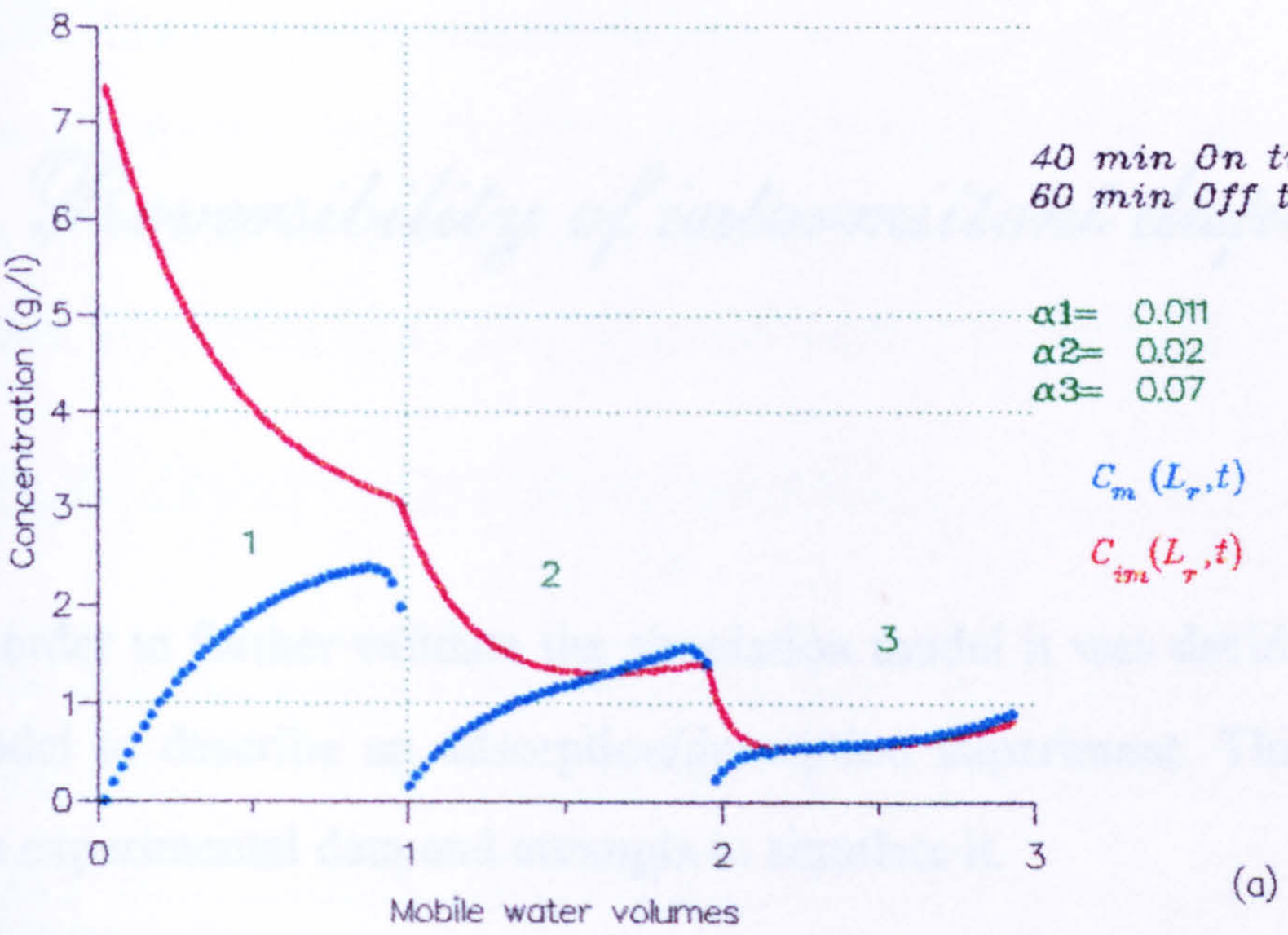

***Fig. 11.10*: Solute concentration in mobile and immobile water *vs.* mobile water volumes for: a) Exp. 1D and b) Exp. 2D.**

Chapter Twelve

Reversibility of intermittent displacement

In order to further validate the simulation model it was decided to use the SIL model to describe an adsorption/desorption experiment. This chapter reports the experimental data and attempts to simulate it.

12.1 Experimental method

The 13-mm ceramic spheres were washed, cleaned and saturated under vacuum with de-aired distilled water and left immersed overnight in excess water (to allow any possible resident solute to diffuse out), then packed in a 30-cm long glass column previously filled with distilled water. A miscible displacement procedure was conducted as in Section 3.3 & 3.4. Four separate miscible displacement experiments were conducted on the same column; two were intermittent displacement, and the other two were continuous displacement. In the first experiment (Exp. IA), the 0.1 M KCl solution was added intermittently (with 45/60 min as *on/off* time) to the column for five cycles, then continuously until the effluent concentration reached 0.1 M (i.e., the column was fully saturated with 0.1 M KCl solution).

The second experiment was then started (Exp. IL) in which distilled water displaced the 0.1 M KCl from the column intermittently (with the same *on/off* times as above) for another five cycles, then continuously until all the solute had leached out (i.e., the column was fully saturated with distilled

water). For the next two experiments, Exp. CA & CL, the same procedures were followed except that the displacement was continuous.

12.2 Results and discussion

The continuous displacement experiments were used to optimise the values of the hydrodynamic dispersion coefficient, D_S , as in Section 5.2.1. Table 12.1 shows the experimental conditions and optimisation results.

Table 12.1. : Experimental conditions and optimised D_S

	v_d (mm/min)	θ_m	θ_{im}	D_S* (mm²/min)	R^2
Exp. CA	2.15	0.489	0.230	125.75	0.968
Exp. CL	2.14	0.489	0.230	2.82	0.979

* optimised values.

The results show that two very different values of D_S were required to fit the continuous displacement results. Theoretically, similar values should have been obtained since both experiments were on the same column with the same method of water application and at almost the same mobile water velocity. The only reason one might consider is the possibility that the electrical conductivity electrode was more sensitive to an increasing concentration than to a decreasing. Such greater sensitivity meant that the electrode sensed the very early increase in concentration in Exp. IL and a higher value of D_S was required to simulate such early sensing. Since the influence of D_S on the shape of the BTC is not very large (*van Genuchten & Wierenga*, 1976), much larger values of D_S were required for simulating Exp. IL than Exp. IA.

Using these parameters the SIL model was run to simulate the intermittent displacement results. The simulation results are shown in Fig. 12.1 as effluent concentration against time. The graph consists of two branches, one for displacement with solution and the other for displacement with distilled water. In the first branch solute appeared in the effluent shortly after starting

Exp. IA

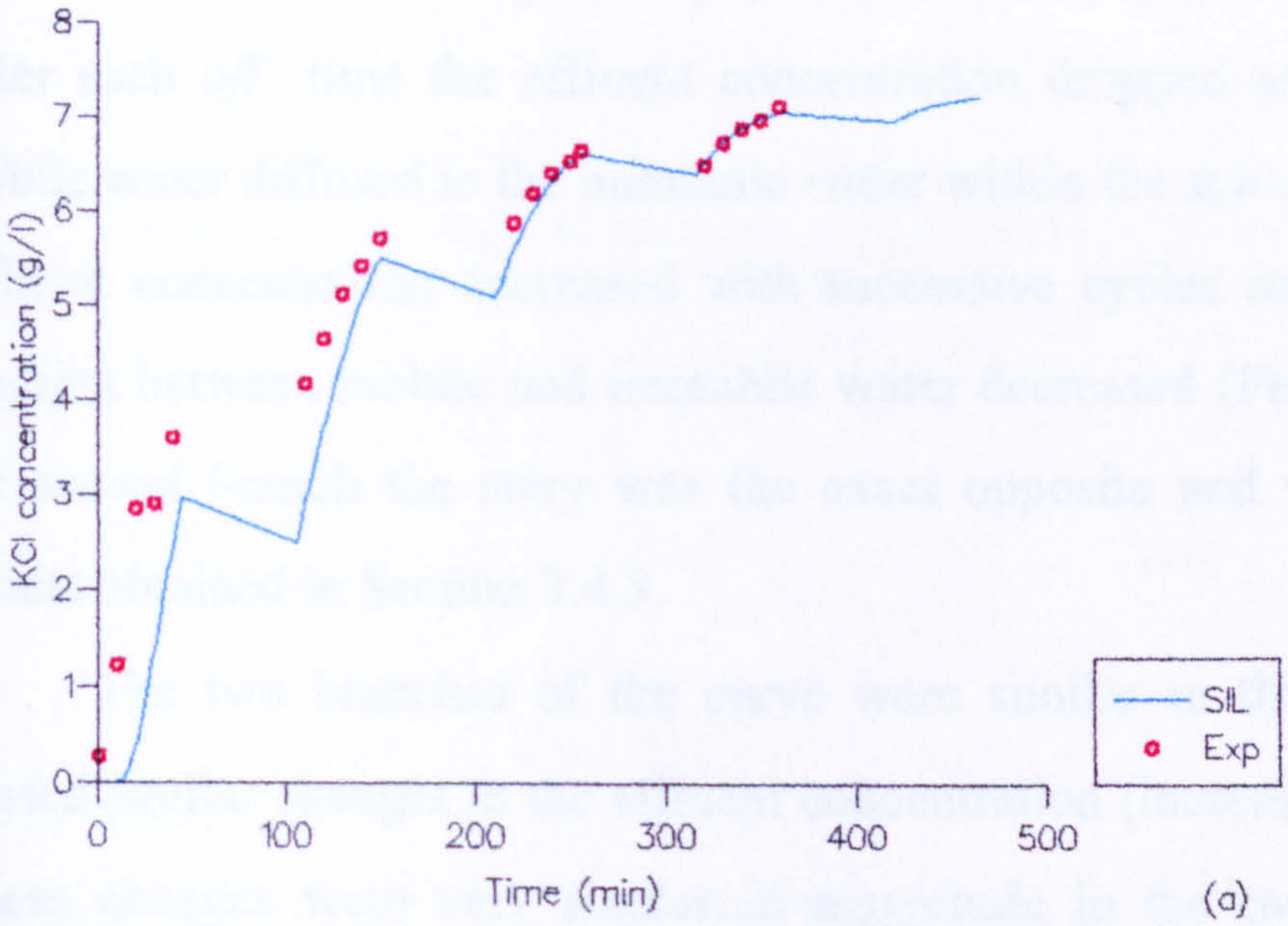

Exp. IL

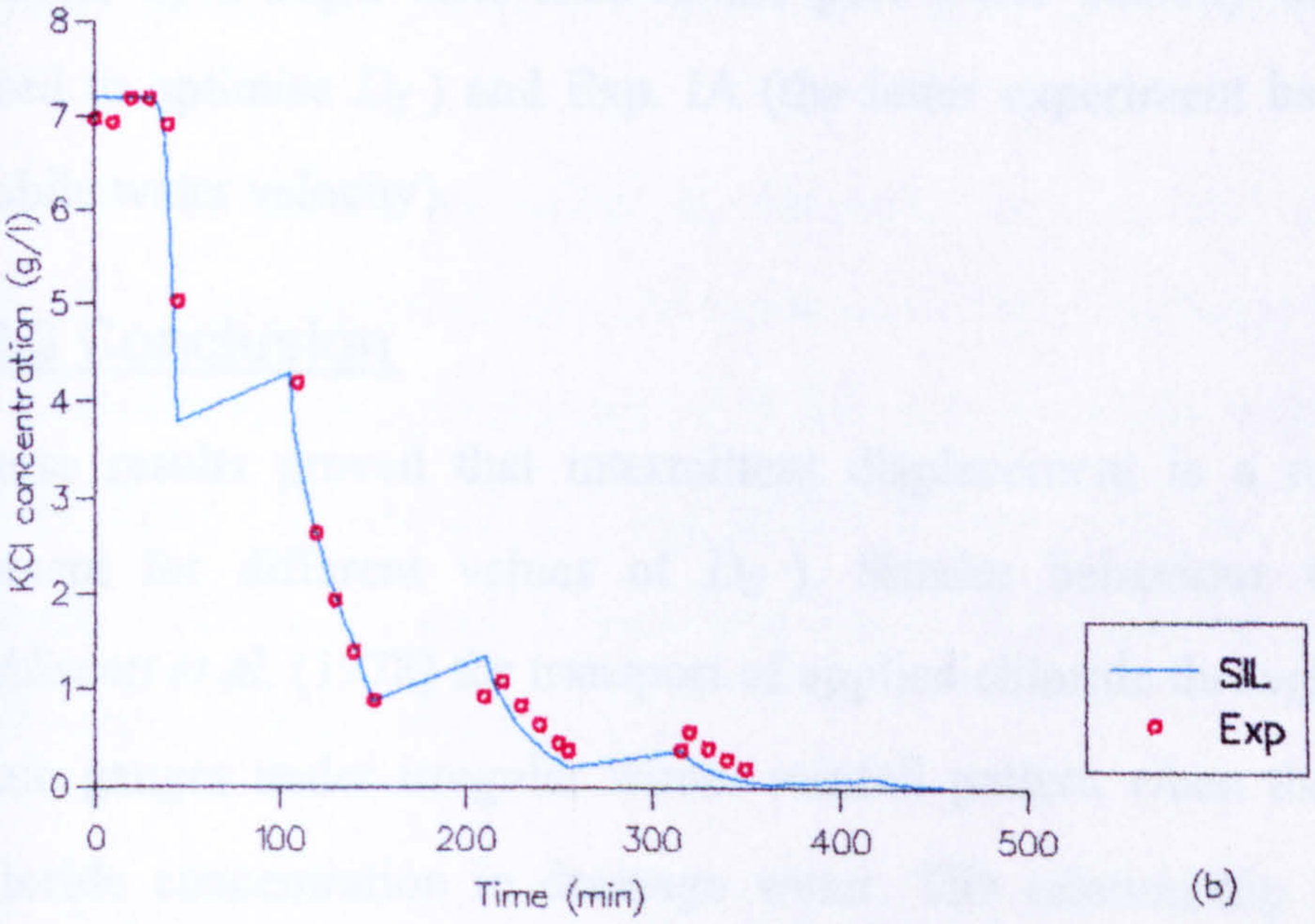

Fig. 12.1 **: Effluent concentration against time for Exps. (a) IA and (b) IL.**

the experiment and then the effluent concentration rapidly increased as the solute reached the column end *via* macropores. The effluent concentration reached the 0.1 M value gradually as solute slowly diffused into the spheres. After each *off* time the effluent concentration dropped as the solute in the mobile water diffused to the immobile water within the spheres. This change in effluent concentration decreased with successive cycles as the concentration gradient between mobile and immobile water decreased (Fick's equation). For the second branch the story was the exact opposite and was similar to the results obtained in Section 3.4.3.

The two branches of the curve were similar in that the rest periods caused similar changes in the effluent concentration (increasing or decreasing). These changes were very similar in magnitude in the two branches of the curve. The SIL model successfully simulated the two branches. There was a small difference during the early stage of adding solution which may be because of a slight difference in the pore-water velocity between Exp. CA (used to optimise D_S) and Exp. IA (the latter experiment had slightly higher mobile water velocity).

12.3 Conclusion

These results proved that intermittent displacement is a reversible process (except for different values of D_S). Similar behaviour was obtained by *Addiscott et al.* (1978) for transport of applied chloride through the Rothamsted drain gauges under irregular winter rainfall pattern when they monitored the chloride concentration in drainage water. The relationship between chloride concentration and cumulative drainage showed several subsidiary peaks on the curve when the drainage concentration was increasing and when it was declining.

The SIL model was able to satisfactorily describe both adsorption and desorption processes.

Chapter Thirteen

Conclusions and recommendations

13.1 Conclusions

This study shows that intermittent leaching (IL) has the potential to increase the efficiency (compared with continuous leaching, CL) with which water might be used to leach excess salts from a soil profile. Based on the results of the experimental and the simulation work the following conclusions can be made.

1) The advantage of using IL increases as the soil permeability increases. A low soil permeability (and consequent slow leaching) allows more time for equilibrium between regions of mobile and immobile water. Leaching of bromide from columns of soil aggregates showed that the difference in saving water between CL and IL increased almost 1.5 times when the mobile water velocity doubled (Section 10.2.1).

2) The advantage of using IL also increases as the aggregate size increases. A small aggregate size means that equilibrium between mobile and immobile water regions is reached more quickly than for a large aggregate. Leaching solute from columns of ceramic spheres indicated that the difference between the amount of water required to reach the same degree of

desalinisation with CL and with IL increased approximately 15 times when the sphere diameter increased from 2 to 13 mm (Section 5.3.2).

3) IL remains more efficient than CL even when water of lower quality is used. Section 5.2.2.2 showed that leaching of about 80% of initial amount of solute was achieved with the same quantity of water by continuously leaching with distilled water or intermittently with water containing 1 g solute /l. This is particularly important in arid and semi-arid areas where good quality water is frequently unavailable.

4) The effects of duration of *on* and *off* times on IL efficiency depend on several factors. The effect of *on* time was more distinct, especially at high velocities; at v_m= 48.11 mm/min(= 69.3 m/d) using 1 min *on* time rather than 15 min can save up to 15% of the amount of leaching water (but will require more *on* times). The effect of varying *off* time was very small for the smallest spheres. However, this effect was more pronounced for large spheres, though it was still smaller than the effect of *on* time.

5) IL is more efficient for both adsorbed and non-adsorbed ions. The dependency of IL advantage on aggregate size and mobile water velocity is the same for both adsorbed and non-adsorbed ions. However, leaching of adsorbed ions requires a greater number, and longer, *off* time periods than it requires for non-adsorbed, more mobile ions.

6) IL is an effective leaching method even when most of the macropores (the mobile water regions) are drained during the rest periods. Such rest periods result in a more uniform solute concentration across individual aggregates so that solute diffuses out of the aggregates more quickly during the next displacement period. With completely drained macropores during the rest

period, IL was able to leach 12% more of the initial amount of solute of the immobile water regions than CL (Section 12.2.3).

7) The assumptions in the SIL (Saturated Intermittent Leaching) model and the methods used for estimating its parameters are reasonably accurate as demonstrated by the validation work for the particular conditions examined. The model may be used as an investigative and/or management tool.

8) In a similar manner the DIL (Drained Intermittent Leaching) model, and the theory used to develop it, may be used in any study investigating the effect of rest periods between water applications (such as rainfall events).

9) Conversely, intermittent application of plant nutrients will reduce the losses of such nutrients by leaching. Applying plant nutrients intermittently means that they will have enough time (between the applications) to diffuse into the soil aggregates and be much less mobile, thus less subject to leaching. Such a reduction of leaching losses would be undoubtedly of great advantage for both farmer and environment.

13.2 Recommendations and further research

This study established, experimentally and mathematically, the benefit of the IL method and built a foundation for further research. However, as the study was mainly on laboratory columns, the next step must be towards conditions closer to the field situation. These include:

1) Examination of the effect of soil structure on IL under saturated conditions using undisturbed soil columns having large aggregates. Such aggregates would not be uniform in size or in shape. Optimisation technique used with the developed SIL model in Section 10.2.2.3 would be helpful in

optimising some of the parameters (e.g. f, α). Swelling could occur in a clay matrix causing some parameters to be time dependent (e.g. θ_m, θ_{im}, and v_m).

2) Study IL under unsaturated conditions. The processes are now more complicated and most of the parameters are likely to depend on the soil water content (e.g., θ_m and θ_{im}). Solute and water movement during a "single" displacement period under unsaturated conditions have been studied in detail in the literature (e.g. *van Genuchten*, 1982; *Nielsen et al.*, 1986). More studies are required in two areas:

(i) the effect of successive displacement periods (re-wetting the soil) on solute and water movement.

(ii) solute and water movement during rest periods where water is not stagnant but continues to redistribute.

3) The last step will be to investigate IL in the field. Water can be applied intermittently to the soil surface by different methods (e.g., by flooding, sprinkling, or by trickle irrigation). Choosing the most appropriate water application method depends on several factors including the existing irrigation system, land topography, and the atmospheric conditions (see also Section 2.4). With the first two methods an adequate drainage system is necessary to drain away the leached solute.

Applying leaching water by a sprinkler irrigation system is preferable when it is difficult to obtain level plots (Section 2.4.2.2) and the existence of large macropores might mean that ponded water would be quickly lost. However, because of the high evaporation rate of the sprinkled water, this method is not recommended under conditions of high evaporativity.

Applying water intermittently by a trickle irrigation system (sometimes called, pulsed trickle irrigation) has been found to reduce water loss below the root zone and to increase the horizontal diameter of the wetting area (*Zur*,

1976; *Al-Amoud & Saeed*, 1988). Therefore, in addition to driving out more solute from the soil aggregates, pulsed trickle irrigation would reduce water loss and keep the leached salts further away from the plant. This method implies a three-dimensional movement of solute and water and further research is still required.

The duration of the first application should be enough to supply a sufficient amount of water to saturate the soil profile and displace most of the mobile water. The duration of subsequent rest periods will depend on the aggregate size, the effective diffusion coefficient and the desorption characteristics of the leached ions. Conducting the first two recommended experiments on samples taken from the same field would help in developing the existing SIL & DIL models which could then be used to optimise the *on/off* times. However, long rest periods, with high evaporation rates, might result in the upward movement of water and consequent salt accumulation at the surface (Section 2.4.2.1). This should be investigated and taken into account when conducting IL under such conditions.

Restructuring the soil would enhance the leaching by providing an inter-connected macropore system to facilitate the transport of leaching water. *Tanton et al.* (1990) showed that, after restructuring a saline heavy clay soil by intensive subsoiling to 0.7 m depth, it was possible to leach 60% of the leachable salts by inducing a lateral flow of leaching water through the soil profile in two successive leachings (with an increase in drainage concentration after the rest period between the two leachings). Furthermore, without restructuring the soil, the infiltration rate decreases with each successive application of water, whereas the same previous study showed that the permeability was maintained in the subsoiled plot on re-wetting after a period of drainage and desaturation (*Armstrong et al.*, 1989; *Tanton et al.*, 1990). This enhanced permeability would increase the advantage of using IL (Section 10.2.1).

References

Abrol, I.P. & Bhumbla, D.R. 1973. Field studies on salt leaching in a highly saline sodic soil. *Soil Science* 115:429-434.

Adamson, A.W. 1976. *Physical Chemistry of Surfaces.* John Wiley & Sons Inc., USA.

Addiscott, T.M. 1977. A simple computer model for leaching in structured soil. *Journal of Soil Science* 28:554-563.

Addiscott, T.M., Rose, D.A. & Bolton, J. 1978. Chloride leaching in Rothamsted drain gauges. Influence of rainfall pattern and soil structure. *Journal of Soil Science* 29:305-314.

Addiscott, T.M. 1982. Diffusion within soil aggregates. *Journal of Soil Science* 33:37-48.

Addiscott, T.M. & Wagenet, R.J. 1985. Concepts of solute leaching in soils. A review of modelling approaches. *Journal of Soil Science* 36:411-424.

Al-Amoud, A.I. & Saeed, M. 1988. The effect of pulsed drip irrigation on water management. *Fourth International Micro-Irrigation Congress Proceedings.* Vol. I. October 1988. Australia.

Anamosa, P.R., Nkedi-Kizza, P., Blue, W.G. & Sartain, J.B. 1990. Water movement through an aggregated, gravely Oxisol from Cameroon. *Geoderma* 46:263-281

Armstrong, A.S.B., Rycroft, D.W. & Tanton, T.W. 1989. Field testing of a new reclamation technique for poorly permeable saline clay soils. Report OD 110. *Hydraulics Research*. Wallingford. UK.

ATI Orion 1995. Ion-selective electrode catalogue and guide to ion analysis. Analytical Technology Inc., Orion Research. U.K.

Atkins, P.W. 1994. *Physical Chemistry*. 5th edn. Oxford University Press. Oxford. U.K.

Avery, B.W. & Bascomb, G.L. 1982. *Soil Survey Laboratory Methods*. Technical Monograph No. 6. Bartholomew Press. Dorking. U.K.

Bachmat, Y. & Bear, J. 1964. The general equations of hydrodynamic dispersion in homogeneous isotopic porous medium. *Journal of Geophysics Research* 69:2561-2567.

Baes, C.F. & Sharp, R.D. 1983. A proposal for estimation of soil leaching and leaching constants for use in assessment models. *Journal of Environment Quality* 12:17-28.

Bailey, P.L. 1976. *Analysis with Ion-Selective Electrodes*. Heyden International Topics in Science. UK.

Bear, J. 1972. *Dynamics of Fluids in Porous Media*. Dover Publication. Inc. New York.

Bear, J. & Bachmat, Y. 1991. *Modelling of Transport Phenomena in Porous Media*. Series of theory and applications of transport in porous media. Vol. 4. Kluwer Academic Publishers. Netherlands.

Beven, K. & Germann, P. 1982. Macropores and water flow in soil. *Water Resources Research* 18:1311-1325.

Biggar, J.W. & Nielsen, D.R. 1962. Miscible displacement. II. Behaviour of tracers. *Soil Science Society of America Proceedings* 26:125-128

Biggar, J.W. & Nielsen, D.R. 1980. Mechanisms of chemical movement in soils. In *Agrochemical in Soils* (eds A. Banin & U. Kafkafi), pp. 213-227. Pergamon Press. U.K.

Bresler, E. 1973. Solute movement in soils. In *Arid Zone Irrigation* (eds. B. Yaron *et al.*), 434 p. Springer-Verlog. Berlin. Heidelberg.

Brown, K. 1991. Assessment of the agronomic benefits of FGD gypsum application on non-saline soils. Research & Development services. *Agricultural Development and Advisory Service ADAS.* UK.

Brusseau, M.L. & Rao, P.S.C. 1990. Modelling transport in structured soils. A review. *Geoderma* 46:169-192.

Burchill, S., Hayes, M.H.B. & Greenland, D.J. 1981. Adsorption of organic melecules. In *The Chemistry of Soil Processes* (eds D.J. Greenland & M.H.B. Hayes), pp. 221-400. John Wiley & Sons, Ltd. Bath. UK.

Burns, I.G. 1974. A model for predicting the redistribution of salts applied to fallow soil after excess rainfall or evaporation. *Journal of Soil Science* 25:165-178.

Cameron ,K.C. & Wild, A. 1982a. Comparative rates of leaching of chloride nitrate and tritiated water under field conditions. *Journal of Soil Science* 33:649-657.

Cameron ,K.C. & WiLd, A. 1982b. Prediction of solute leaching under field conditions. *Journal of Soil Science* 33:659-669.

Carter, D.L. & Fanning, C.D. 1964. Combining surface mulches and periodic water applications for reclaiming saline soils. *Soil Science Society of America Proceedings* 28:564-567.

Chapman, H.D. 1966. *Diagnostic Criteria for Plants and Soils.* Division of Agricultural Science. University of California. Oakland.

Coats ,K.H. & Smith, B.D. 1964. Dead end pore volume and dispersion in porous media. *Society of Petroleum Engineering Journal* 4:73-84.

Covington, A.K. 1979. Introduction. basic electrode types, classification, and selectivity considerations. In *Ion-Selective Electrode Methodology*. Vol. I. (ed. A.K. Covington), pp. 1-20. CRC Press Inc. Florida. USA.

Crank, J. 1972. *The Mathematics of Diffusion*. Oxford University Press. Oxford. U.K.

Dahiya, I.S. , Malik, R.S. & Maharaj, S. 1981. Field studies on leaching behaviour of a highly saline-sodic soil under two modes of water application in the presence of crops. *Journal of Agricultural Science, Cambridge* 97:383-389.

Dahiya, I.S., Grewal, K.S., Anlauf, R. & Richter, J. 1984. Desalinisation of a salt-affected soil in plots of various sizes under two modes of water application. *Journal of Agricultural Science, Cambridge* 104:19-26.

David, B 1979. *Soil*. Soil and Methods in Geography. Butterworths. London. U.K.

Davidson, J.M., Rao, P.S.C., Green, R.F. & Selim, H.M. 1980. Evaluation of conceptual process models for behaviour in soil-water system. In *Agrochemicals in Soil* (eds A. Banin & U. Kafkafi), pp. 241-252. Pergamon Press. U.K.

De Smedt, F. & Wierenga, P.J. 1979. Mass transfer in porous media with immobile water. *Journal of Hydrology* 41:59-67.

Elrick, D.E., Erh, K.T. & Krupp, H.K. 1966. Application of miscible displacement techniques to soil. *Water Resources Research* 2:717

Elrick, D.E. & Clothier, B.E. 1990. Solute transport and leaching. In *Irrigation of Agricultural Crops* (eds B.A. Stewart & D.R. Nielsen), pp. 94-126. Agronomy No. 30, USA.

Freeze, R.A. & Cherry, J.A. 1979. *Groundwater*. Prentic-Hall Inc. Englewood Cliffs. New Jersey .

Forth, H.D. 1990. *Fundamentals of Soil Science*. John Wiley & Sons. USA.

Freundlich, H. 1926. *Colloid and Capillary Chemistry*. Methuen. London.

Gaudet, J.P., Jegat, h., Vachaud, G. & Wierenga, P.J. 1977. Solute transfer, with exchange between mobile and stagnant water through unsaturated sand. *Soil Science Society of America Journal* 41:665-671.

Gelburd, D.E. 1985. Managing salinity, lessons from the past. *Journal of Soil and Water Conservation* 40:329-331.

Ghildyal, B.P. & Tripathi, R.P. 1987. *Soil Physics*. John Wiley & Sons. New Delhi. India.

Gilham, R.W., Sudicky, E.A., Cherry, J.A. & Frind, E.O. 1984. An advection-diffusion concept for solute transport in heterogeneous unconsolidated geological deposits. *Water Resources Research* 20:369-378.

Greenland, D.J. 1979. Structural organisation of soils and crop production. In *Soil Physical Properties and Crop Production in the Tropics*. (eds R. Lal & D.J. Greenland), pp. 47-56. Wiley. Chichester. U.K.

Grindrad, P. & Impey, M.D. 1993. Channelling and Fickain dispersion in factual simulated porous media. *Water Resources Research* 29:4077-4089.

Hall, D.G.M. 1993. An amended functional leaching model applicable to structure soils. I. Model description. *Journal of Soil Science* 44:579-588.

Han, N.W., Bhakta, J. & Carbonell, R.G. 1985. Longitudinal and lateral dispersion in packed beds: effects of column length and particle size distribution. *American Institute of Chemical Engineering Journal* 31:277-288.

Hayot, Ch. & Lafolie, F. 1993. One-dimensional solute transport modelling in aggregated porous media. Part 2. Effects of aggregate size distribution. *Journal of Hydrology* 143:85-107.

Head, K.H. 1992. *Manual of Soil Laboratory Testing*. Vol. 1. Pentech Press Ltd. U.K.

Hinz, C., Gaston, L.A. & Selim, H.M. 1994. Effect of sorption isotherm type on prediction of solute mobility in soil. *Water Resources Research* 30:3013-3021.

Hoffman, G.J. 1980. Guidelines for reclamation of salt-affected soils. 2nd Inter-American Conference. on *Salinity & Water Management Technology*. 11-12 December, pp. 49-64. Juaez. Mexico.

Hogg. R.V. & Ledolter, J. 1992. *Applied Statistics for Engineers and Physical Scientists*. 2nd edn. Maxwell Macmillan International Edition. Singapore.

Huyakorn, P. & Pinder, G.F. 1983. An efficient finite element technique for modelling transport in fractured porous media. 1: Single species transport. *Water Resources Research* 19:841-854.

International Atomic Energy Agency (IAEA) 1982. Radioactive waste management glossary. Rep. IAEA-TECDOC-264. Vienna.

International Critical Tables of Numerical Data 1927. Physical, Chemical & Technology. Vol. II. National Research Council. McGraw-Hill Book Company, Inc. New York. USA.

James, M.O. & Poole, W.G.J. 1981. *An Introduction to Numerical Methods for Differential Equations*. Pitman publishing Inc., Massachusetts. USA.

James, W. & Ross, J. 1969. Solid-state and liquid membrane ion-selective electrodes. In: *Ion-Selective Electrodes* (ed. R.S. Drust). Proceedings of a symposium held at the national breaue of standards. January 30-31 1969. Gaithersburg. Maryland. Special Publication 314. USA.

Jarvis, R.A, Bendelow, R.I., Bradley, R.I., Carroll, D.M., Furness, R.P., Kilgour, I.N.L. & King, S.J. 1984. Soils and their use in Northern England. *Soil Survey of England and Wales*. Bulletin No. 10. Harpenden. UK.

Javandel, I., Doughty, C. & Tsang, C.F. 1984. Ground water transport. Handbook of mathematical models. *Water Resources Monograph Series*.10. Washington, USA.

Jensen, J.R. 1984. Potassium dynamics in soil during steady flow. *Soil Science* 138:285-293.

Jury, W., Gardner, W.R. & Gardner, W.H. 1991. *Soil Physics*. John Wiley & Sons. New York, USA.

Kanchanasut, P. & Scotter, D.R. 1982. Leaching patterns in soil under pasture and crop. *Australian Journal of Soil Research* 20:193-202.

Kemper, W.D. & van Schaik, J.C. 1966. Diffusion of salts in clay-water systems. *Soil Science Society of America Proceedings* 30:534-540.

Kirkham, D. & Powers, W.L. 1972. *Advanced Soil Physics*. Wiley-Inter Science. USA.

Kluitenberg, G.J. & Horton, R. 1990. Effect of solute application method on preferential transport of solute in soil. *Geoderma* 46:283-297.

Krupp, H.K. & Elrick, D.E. 1968. Miscible displacement in unsaturated glass bed media. *Water Resources Research* 4:809-815.

Kutilek, M. & Nielsen, D.R. 1994. *Soil Hydrology*. GeoEcology text book. Catena vertag. Germany

Lafolie, F. & Hayot, Ch. 1993. One-dimensional solute transport modelling in aggregated porous media. Part one. Model description and numerical solution. *Journal of Hydrology* 143:63-83.

Landon, J.R. 1984. *Booker Tropical Soil Manual*. Booker Agriculture International Limited. U.K.

Langmuir, I. 1918. The adsorption of gases on plane surface of glass, mica and platinum. *Journal of American Chemical Society* 40:1361-1382.

Light, T.S. 1969. Industrial analysis and control with ion-selective electrodes. In *Ion-Selective Electrodes* (ed. R.A. Durst). Proceeding of a symposium held at the national bureau of standards. Gaithersburg. Maryland. Special Publication 314. USA.

Ma, L & Selim, H.M. 1995. Transport of a nonreactive solute in soils: A two-flow domain approach. *Soil Science* 159:224-234.

Mackay, R. & Riley, M.S. 1993. Groundwater quality modelling. In *An Introduction to Water Quality Modelling* (ed. A. James), 263-291. John Wiley & Sons.NY, USA.

Malcolm, R.L. & Kennedy, V.C. 1969. Rate of cation exchange on clay mineralises determined by specific-ion electrode techniques. *Soil Science Society of America Proceedings* 33:247-253

Mangol, D.S. & Tsang, C. 1991. A summary of subsurface hydrological and hydrochemical models. *Review of Geophysics* 29:51-79.

Mansell, R.S. & Elezeftawy, A. 1971. Measuring chloride in effluent flowing from a soil column. *Soil Science Society of America Proceedings* 36:378-380.

Marshall, T.J. & Holmes, J.W. 1988. *Soil Physics*. Cambridge University Press. Cambridge. U.K.

Martin, H.W. & Sparks, D.L. 1983. Kinetic of nonexchangeable potassium release from two coastal plain soils. *Soil Science Society of America Journal* 47:883-887

McGeary, R.K. 1961. Mechanical packing of spherical particles. *Journal of American Ceramics* 44:513-522.

Millington, R.J. & Quirk, J.P. 1961. Permeability of porous solids. *Transaction of Faraday Society* 57:1200-207.

McLay, C.D.A., Cameron, K.C. & McLaren, R.G. 1991. Effect of time of application and continuity of rainfall on leaching of surface-applied nutrients. *Australian Journal of Soil Research* 29:1-9.

Meiri, A. & Plaut, Z. 1985. Crop production and management under saline conditions. *Plant and Soil* 89:253-271.

Miller, R.J., Biggar, J.W. & Nielsen, D.R. 1965. Chloride displacement in Panoche clay loam in relation to water movement and distribution. *Water Resources Research* 1:63-73.

Minhas, P.S. & Khosla, B.K. 1986. Solute displacement in a silt loam soil as affected by the method of water application under different evaporation rates. *Agricultural Water Management* 12:63-74.

Ministry of Agriculture 1986. *The Analysis of Agricultural Materials.* Reference book 427. Ministry of Agriculture. Fisheries and Food. HMSO, UK.

Nielsen, D.R. & Biggar, J.W. 1961. Displacement in soils. I. Experimental information. *Soil Science Society of America Journal* 25:1-5.

Nielsen, D.R. & Biggar, J.W. 1962. Miscible displacement. III -theoretical consideration. *Soil Science Society of America Journal* 26:216-221.

Nielsen, D.R. & Biggar, J.W. 1963. Miscible displacement. IV. Mixing in glass beads. *Soil Science Society of America Journal* 27:10-13.

Nielsen, D.R., Biggar, J.W. & Miller, R.J. 1965. Field observation of infiltration and soil-water redistribution, *Transactions of the American Society of Agricultural Engineers* 382-387.

Nielsen, D.R., Biggar, J.W. & van Genuchten, M.Th. 1986. Water flow and solute transport processes in the unsaturated zone. *Water Resources Research* 22:89S-108S.

Nkedi-Kizza, P., Biggar, J.W., van Genuchten, M.T., Wierenga, P.J., Selim, H.M. , Davidson, J.M. , & Nielsen, D.R. 1983. Modelling tritium and chloride 36 transport through an aggregated Oxisol. *Water Resources Research* 19:691-700.

Nkedi-Kizza, P., Rao, P.S.C., Jessup, R.E. & Davidson, J.M. 1982. Ion exchange and diffusive mass transfer during miscible displacement through an aggregated Oxisol. *Soil Science Society of America Journal* 46:471-476.

Nye, P.H. 1979. Diffusion of ions and uncharged solutes in soils and soil clays. *Advances in Agronomy* 31:225-272.

Olsen, S.R. & Kemper, W.D. 1968. Movement of nutrients to plant roots. *Advances in Agronomy* 20:91-151.

Oster, J.D., Willardson, L.S. & Hoffman, G.J. 1972. Sprinkling and ponding techniques for reclaiming saline soils. *Transactions of the American Society of Agricultural Engineers* 15:1115-1117.

Panayiotopoulos, K.P. 1989. Packing of sands. A review. *Soil and Tillage Research* 13:101-121.

Parker, J.C. 1984. Analysis of solute transport in column tracer studies. *Soil Science Society of America Journal* 48:719-724.

Parker, J.C. & van Genuchten, M.Th. 1984. Determining transport parameters from laboratory and field tracer experiments. Bulletin 84-3. Virginia Agricultural Experimental Station. Virginia Polytechnic Institute and State University. Virginia. USA.

Passioura, J.B. 1971. Hydrodynamic dispersion in aggregated media. Theory. *Soil Science* 111:339-344.

Passioura, J.B. & Rose, D.A. 1971. Hydrodynamic dispersion in aggregated media. II: effect of velocity and aggregate size. *Soil Science* 111:345-351.

Peaceman, D.W. 1977. Fundamentals of numerical reservoir simulation. *Development in Petroleum Science 6.* Elsevier Scientific Publication Co. Amsterdam. Netherlands.

Peek, D.C. & Volk, V.V. 1985. Fluoride sorption and desorption in soils. *Soil Science Society of America Journal* 49:583-586.

Puri, A.N. & Keen, B.A. 1925. The dispersion of soil in water under various conditions. *Journal of Agricultural Science* 15:147-161.

Quirk, J.P. 1950. The stability of soil microaggregates in water. *Australian Journal of Agricultural Research* 1:276-284

Rao, P.S.C., Green, R.E., Balasubramanian, V. & Kanehiro, Y. 1974. Field study of solute movement in a highly aggregated Oxisol with intermittent flooding. II. Picloram. *Journal of Environmental Quality* 3:197-202.

Rao, P.S.C. & Davidson, J.M. 1979. Adsorption and movement of selected pesticides at high concentrations in soils. *Water Research* 13:375-380.

Rao, P.S.C., Davidson, J.M., Jessup, R.E. & Selim, H.M. 1979. Evaluation of conceptual models of describing nonequilibrium adsorption-desorption of pesticides during steady-flow in soils. *Soil Science Society of America Journal* 43:22-28.

Rao, P.S.C., Jessup, R.E., Rolston, D.E., Davidson, J.M. & Kilcrease, D.P. 1980a. Experimental and mathematical description of non adsorbed solute transfer by diffusion in spherical aggregates. *Soil Science Society of America Journal* 44:684-688.

Rao, P.S.C., Rolston, D.E., Jessup, R.E. & Davidson, J.M. 1980b. Solute transport in aggregated porous media. Theoretical and experimental evaluation . *Soil Science Society of America Journal* 44:1139-1146.

Rao, P.S.C., Jessup, R.E. & Addiscott, T.M. 1982. Experimental and theoretical aspect of solute diffusion in spherical and non-spherical aggregates. *Soil Science* 133:342-349.

Rich, C.I. 1968. Mineralogy of soil potassium. In *The Role of Potassium in Agriculture* (ed. V.J. Kilmer), pp. 79-108. Soil Science Society of America. Madison. Wisconsin USA.

Robinson, R.A. & Stokes, R.H. 1970. *Electrolyte Solutions*. Butterworths Scientific Publication. London. U.K.

Rose, C.W., Chichester, F.W., Williams, J.R. & Ritchie, J.T. 1982. A contribution to simplified models of field solute transport. *Journal of Environmental Quality* 17:146-150.

Rose, D.A. & Passioura, J.B. 1971. The analysis of experiments on hydrodynamic dispersion. *Soil Science* 111:252-257.

Rose, D.A. 1973. Some aspects of the hydrodynamic dispersion of solutes in porous media. *Journal of Soil Science* 24:284-293.

Rose, D.A. 1977. Hydrodynamic dispersion in porous media. *Soil Science* 123:277-283.

Rowell, D.L. 1994. *Soil Science. Methods and Applications*. Longman Scientific & Technical. UK.

Rubin, A.J. & Mercer, D.L. 1981. Adsorption of free and complexed metals from solution by activated carbon. In *Adsorption of Inorganics at Solid Liquid Interface* (eds A.W. Adamson & A.J. Rubin), pp. 295-326. Ann Arbor Science Publishers Inc., USA.

Selim, H.M. & Ma, L. 1995. Transport of reactive solutes in soils. A modified two-region approach. *Soil Science Society of America Journal* 59:75-82.

Selim, H.M. 1992. Modeling the transport and retention of inorganics in soils. *Advances in Agronomy* 47:331-384.

Selim, H.M., Schulin, R., & Fluhler, H. 1987. Transport and ion exchange of calcium and magnesium in an aggregated soil. *Soil Science Society of America Journal* 51:876-884.

Selim, H.M., Mansell, R.S. & Zelanzy, L.W. 1976a. Modelling reactions and transport of potassium in soils. *Soil Science* 122:77-84.

Selim, H.M., Davidson, J.M. & Mansell, R.S. 1976b. Evaluation of a two-site adsorption-desorption in soil. *Proceedings of Summer Computer Simulation Conference*, pp.444-448. Washington. USA.

Seyfried, M.S. & Rao, P.S.C. 1987. Solute transport in undisturbed columns of an aggregated tropical soil. Preferential flow effects. *Soil Science Society of America Journal* 51:1434-1444.

Shalhevet, J. 1973. Irrigation with saline water, In *Arid Zone Irrigation* (eds. B. Yaron *et al.*), pp.263-276. Springer-Verlog. Berlin. Heidelberg.

Simpson, R.J. 1979. Practical techniques for ion-selective electrodes, In *Ion-Selective Electrode Methodology*. Vol. I. (ed. A.K. Covington), pp. 43-66. CRC Press Inc., USA.

Singer, M.J. & Munns, D.N. 1991. *Soil, an Introduction*. Maxwell Macmillan International Editions. Singapore.

Skoog, D.A., West, D.M., & Holler, F.J. 1992. *Fundamentals of Analytical Chemistry*. Saunders College Publishing. USA.

Smettem, K.R.J. & Kirkby, C. 1990. Measuring the hydraulic properties of a stable aggregated soil. *Journal of Hydrology* 117:1-13.

Smith, G.D. 1985. *Numerical Solution of Partial Difference Equations. Finite Difference Methods*. Oxford University Press. Oxford.

Smith, K.A. & Scott, A. 1991. Continuous-flow, flow-injection, and discrete analysis. In *Soil Analysis. Modern Instrument Techniques* (ed. K.A. Smith), pp. 183-228. Books in soils, plants, and the environment. Marcel Dekker Inc., USA.

Sparks, D.L. & Huang, P.M. 1985. Physical chemistry of soil potassium. In *Potassium in Agriculture* (ed. R.D. Munson), pp. 201-276. *American Society of Agronomy*. Madison. Wisconsin. USA.

Sposito, G. 1981. *The Thermodynamics of Soil Solutions*. Oxford University Press. Oxford.

Sposito, G. 1989. *The Chemistry of Soils*. Oxford University Press. New York.

Szabolcs, I. 1989. *Salt-Affected* Soils. CRC Press Inc. Boca Raton. Florida.

Talibudeen, O. 1991. Ion-selective electrodes. In *Soil analysis. Modern Instrument Techniques* (ed. K.A. Smith), pp. 111-182. Books in soils, plants, and the environment. Marcel Dekker, Inc., USA.

Talsma, T. 1967. Leaching of tile-drained saline soils. *Australian Journal of Soil Research* 5:37-46.

Tan, K.H. 1993. *Principles of Soil Chemistry*. 2nd edn. Marcel Dekker Inc. USA.

Tanji, K.K. 1990 (ed.). Agricultural salinity assessment and management. *American Society of Civil Engineers*. Manual and Reports on Engineering Practice No. 71, USA.

Tanton, T.W., Armstrong, A.S.B. & Dervis, O. 1990. Leaching of salts from clays by subsoiling and induced lateral drainage. *Soil Use and Management* 6:36-41.

Tillman, R.W., Scotter, D.R., Clotheir, B.E. & White, R.E. 1991. Solute movement during intermittent water flow in a field soil and some implications for irrigation and fertiliser application. *Agricultural Water Management* 20:119-133.

Toth, K., Nogy, G. & Pungor, E. 1979. Analytical methods involving ion-selective elctrodes (includung flow methods). In *Ion-Selective Electrode Methodology.* Vol. II. (ed. A.K. Covington), pp. 65-122. CRC Press Inc. Florida. USA.

Travis, C.C. & Etnier, E.L. 1981. A survey of sorption relationships for reactive solutes in soil. *Journal of Environment Quality* 10:8-17.

Valocchi, A.J. 1985. Validity of the local equilibrium assumption for modelling sorbing solute transport through Homogeneous soils. *Water Resources Research* 21:808-820.

van Genuchten, M.Th. & Wierenga, P.J. 1976. Mass transfer studies in sorbing porous media. Analytical solution. *Soil Science Society of America Journal* 40:473-480.

van Genuchten, M.Th., Weirenga, P.J. & O'Connor, G.A. 1977. Mass transfer studies in sorbing porous media. III Experimental evaluation with 2,4,5-T. *Soil Science Society of America Journal* 41:278-284.

van Genuchten, M.Th. & Cleary, R.W. 1979. Movement of solutes in soil. Computer-Simulated and laboratory results. In *Soil Chemistry, Physico-Chemical Models* (ed. G.H. Bolt), pp. 349-386. Development in Soil Science 5B. Elsevier Scientific Publication Company. Netherlands.

van Genuchten, M.Th. 1980. Determing transport parameters from solute displacement experiments. Research report No. 118. US. Salinity laboratory. Riverside. California.

van Genuchten, M.Th. 1981. Non-equilibrium transport parameters from Miscible displacement experiment. Research report No. 119. US. Salinity laboratory. Riverside. California.

van Genuchten, M.Th. 1982. A comparison of numerical solution of the one-dimensional unsaturated-saturated flow and mass transport equation. *Advances in Water Resourses* 5:47-55.

van Genuchten, M.Th. & Parker, J.C 1984. Boundary conditions for displacement experiments through short laboratory soil columns. *Soil Science Society of America Journal* 48: 703-708.

van Genuchten, M.Th. & Dalton, F.N. 1986. Models for simulating salt movement in aggregated field soils. *Geoderma* 38:165-183.

Verma, S.K. & Gupta, R.K. 1989. Leaching behaviour of saline clay soil under two modes of water application. *Journal of Indian Society of Soil Science* 37:803-808.

Wagenet, R.C. 1983 . Principles of salt movement in soils. In *Chemical Mobility and Reactivity in Soil Systems* (ed. D.W. Neilsen), pp. 123-140. *Soil Science Society of America.* Publication No. 11. USA.

White, R.E. , Thomas, G.W. & Smith, M.S. 1984. Modelling water flow through undisturbed soil cores using a transfer function model derived from ^{3}HOH and Cl transport. *Journal of Soil Science* 35:159-168.

White, R.E. 1985. The influence of macropores on the transport of dissolved and suspended matter through soil. *Advances in Soil Science* 3:95-120.

White, R.E. 1987. *Introduction to the Principles and Practice of Soil Science.* Blackwell Scientific Publications. London. UK.

Wierenga, P.J. 1984. Equivalence of two conceptual models for describing ion exchange during transport through an aggregated Oxisol. *Water Resources Research* 20:1123-1130.

Wilson, G.V. , Jardine, P.M. & Gwo, J.P. 1992. Modelling the hydraulic properties of a multi-region soil. *Soil Science Society of America Journal* 56:1731-1737.

Wood, L.K. & De Turk, E.E. 1940. The absorption of potassium in soils in non-replaceable forms. *Soil Science Society of America Proceedings* 5:152-161.

Yaron, D 1981. The salinity problem in irrigation. An introductory review. In *Salinity in Irrigation and Water Resources.* (ed. D. Yaron), pp. 1-20. Marcel Dekker Inc., New York.

Yong, R.N., Mohamed, A.M.O. & Workentin, B.P. 1992. Principles of contaminant transport in soils. *Developments in Geotechnical Engineering* No. 73, Elsevier.

Young, D.F. & Ball, P.B. 1995. Effects of column conditions on the first-order rate modeling of nonequilibrium solute breakthrough. *Water Resources Research* 31:2181-2192.

Zur, B. 1976. The pulsed irrigation principle for controlled soil wetting. *Soil Science* 122:282-291.

APPENDICES

Abbreviations used in the models

Abbreviation		Equivalent	Units
ALFA	= α	mass transfer coefficients	min^{-1}
AREA	= A	column cross-section area	mm^2
AS	=	initial amount of adsorbed solute	µg
BC	= b	constant in Eq. 6.2	
C0	= C_0	initial solute concentration	µg mm^{-3}
CIM	= C_{im}	solute concentration in the immobile water	µg mm^{-3}
CIN	= C_{inp}	solute concentration in the added water	µg mm^{-3}
CM	= C_m	solute concentration in the mobile water	µg mm^{-3}
DE	= D_e	effective diffusion coefficient	mm^2 min^{-1}
DELTT	= Δt	time increment	min
DELTZ	= Δz	space increment	mm
DK	= K	distribution coefficient	
DS	= D_S	hydrodynamic dispersion coefficient	mm^2 min^{-1}
EM	=	mean value	
FF	= f	the fraction of adsorption sites in the mobile water phase	
IOFF	=	length of rest period duration	min
ION	=	length of displacement period duration	min
IR	=	number of spheres for diffusion model	
ITERA	=	number of iteration loops	
ITIME	=	total leaching time	min
LO	= L	imaginary column length	mm
LR	= L_r	real column length	mm
NP	=	number of different diameters	
P	=	mass proportion of sphere diameters	
POR	= θ_m	volume of mobile water to total column volume	mm^3 mm^{-3}
PORI	= θ_{im}	volume of immobile water to total column volume	mm^3 mm^{-3}

Q	$= q$	flux	$mm^3\ min^{-1}$
Q1	$= q_1$	constant in Eq. 4.13	
RID	$= a$	aggregate/sphere radius	mm
RU	$= \rho$	soil bulk density	$\mu g\ mm^{-3}$
SEG	$= \sigma$	variance in normal and log-normal distribution	
TOLR	=	the allowed difference in concentration required to exit the loop (error tolerance)	$\mu g\ mm^{-3}$
VEX	=	volume of external solution	cm^3

Appendix A

```
C=============================================================
c                    MODEL    SIL
c                 (Saturated Intermittent Leaching)
c
c     Program for simulating solute transport under intermittent
c       leaching for aggregated media and saturated conditions
c
c                 (case 1: for uni-diameter spheres)
C=============================================================

      PROGRAM INTERMITTENT SATURATED

      DIMENSION CIM(500,3,2)
      DIMENSION A(500,2),B(500,2),C(500,2)
      DIMENSION E(500,2),F(500,2),G(500,2)
      DIMENSION CM(500,2),RHS(500,2),EE1(500,2),FF1(500,2)
      DIMENSION XXCM(500),RESID(500)
      DOUBLE PRECISION RHS
      DOUBLE PRECISION EE1,FF1,XXCM,RESID
      DOUBLE PRECISION A,B,C,E,F,G
      DOUBLE PRECISION ZZ,PZ,ALFA

      OPEN(UNIT=8,FILE='result1i.dat')
C-------------------------------------------------------------------
C---------------- DATA -------------------------------------------
      DELTT=1.0
      DELTZ=1.0
      S=0.0
      SI=0.0

      Q=3.62*1000
      AREA=16.982*100
      V=Q/AREA
      DS=1.153

      C0=0.1
      POR=0.486
      PORI=0.231
      LO=300
      LR=180
      CIN=7.45
      ITERA=18
      ITIME=620
      ION=45
      IOFF=60

      ICYCLE=ITIME/(ION+IOFF)
```

```
      ZZ=DELTZ*DELTZ
      FI=POR/(POR+PORI)
      PZ=POR*DELTZ
C-----------------------HEADINGS-----------------------------------

C.....................................V/VO & S/SO.FOR LR.....................
c      WRITE(8,11)
c   11 FORMAT(5X,'V/VO',10X,'S/SO')
C.....................................V/VO & C/CO.FOR LR.....................
      WRITE(8,8)
    8 FORMAT(5X,'V/VO',10X,'C/CO')
C.....................................TIME & C FOR L.........................
C      WRITE(8,9)
C    9 FORMAT(5X,'TIME',10X,'CONCENT.')
C.....................................DEPTH & C @ V/VO.......................
C      WRITE(8,10)
C   10 FORMAT(5X,'DEPTH',10X,'Cm',10X,'Cim')


C-------------------------------------------------------------------------
C=====================  THE PROGRAM  ==========
      IJ=0
      IC=ICYCLE-1

      DO 5000 JJ=0,IC
      J1=JJ*(ION+IOFF)

      DO 3000 J=J1+1,ION+J1

C-------------  Calculating of ALFA  ------------------------------
      DE=0.0575
      RID=6.5
      Q1=3.57

      TETA=PORI


      TIM=LR*POR/(Q/AREA)
      B1=0.14472*LOG(167.0/(FI*Q1**2.))
      T=DE*TIM/RID**2.
      IF(T.GE.0.1)THEN
      ALFA=((FI*Q1**2.)*(1.+(0.1*B1/((1.-B1)*T))))*DE*
     &TETA/RID**2
      ELSE

      ALFA=((FI*Q1**2./(1.-B1))*(0.1/T)**B1)*DE*TETA/RID**2
      ENDIF


c     PRINT*,'ALFA=',ALFA,'FI=',FI,' T=',T,' B1=',B1,' v=',V
C-------------------------------------------------------------------------
C-------------------------Initial condition-------------------------------

      IF (J.GT.1)GO TO 2990
      DO 7 I=1,LO
      CM(I,1)=C0
      CIM(I,1,1)=C0
```

```
  7 CONTINUE
    GO TO 2970
2990 CONTINUE
    DO 2980 I=1,LO
    CM(I,2)=CM(I,1)
2980 CONTINUE
C----------Iteration loop----------

2970 DO 2000 ITER=1,ITERA
    DO 777 I=1,LO
    CIM(I,1,2)=0
 777 CONTINUE

    DO 999 I=1,LO
    IF (J.EQ.1)GO TO 550
C.....Calculating Cim.....

    CIM(I,1,2)=((ALFA*DELTT/(2*PORI))*(CM(I,1)+CM(I,2))+CIM(I,1,1)*
   &(1-(DELTT*ALFA/(2*PORI))))/(1+(ALFA*DELTT/(2*PORI)))
    GO TO 999

 550 IF(ITER.EQ.1)GO TO 553
    CIM(I,1,2)=((ALFA*DELTT/(PORI*2))*(CM(I,1)+CM(I,2))+CIM(I,1,1)*
   &(1-(DELTT*ALFA/(2*PORI))))/(1+(ALFA*DELTT/(2*PORI)))

    GO TO 999

 553 CIM(I,1,2)=((ALFA*DELTT/(PORI*2))*2*CM(I,1)+CIM(I,1,1)*
   &(1.-(DELTT*ALFA/(2*PORI))))/(1.+(ALFA*DELTT/(2*PORI)))

 999 CONTINUE
C.....

    DO 1 I=2,LO
    A(I,2)=(DS*DELTT)/(2*ZZ)+(V*DELTT)/(4*PZ)
    B(I,2)=1.+(DS*DELTT)/(ZZ)
    C(I,2)=(DS*DELTT)/(2*ZZ)-(V*DELTT)/(4*PZ)
    E(I,2)=A(I,2)
    F(I,2)=1.-(DS*DELTT)/(ZZ)
    G(I,2)=C(I,2)

  1 CONTINUE

    B(1,2)=V+(POR*DS)/DELTZ
    C(1,2)=(POR*DS)/DELTZ

C----------Calculating RHS----------
    LOLES1=LO-1
    DO 1100 I=2,LOLES1
    IF(J-1.EQ.0)GO TO 1090
    RHS(I,2)=E(I,2)*CM(I-1,1)+F(I,2)*CM(I,1)+G(I,2)*CM(I+1,1)
   &-(PORI/POR)*(CIM(I,1,2)-CIM(I,1,1))
    GO TO 1100
1090 RHS(I,J)=C0

 1100 CONTINUE
C.....Boundary conditions.....
```

```
  IF (J-1.NE.0)GO TO 45
  RHS(1,1)=V*CIN
  GO TO 47
45 CONTINUE
  RHS(1,2)=V*CIN
47 IF (J-1.NE.0)GO TO 48
  RHS(LO,1)=C0
  GO TO 49
48 COUT=C0

  RHS(LO,2)=E(LO,2)*CM(LO-1,1)+F(LO,2)*CM(LO,1)+G(LO,2)*COUT
 &-(PORI/POR)*(CIM(LO,1,2)-CIM(LO,1,1))
  49 CONTINUE

c.....Storing the old Cm(I,2) in XXCM(I) and Calculate new.....
c              Cm(I,2)

    DO 711 I=1,LO
    XXCM(I)=0.0
 711 CONTINUE

    IF(J.EQ.1)GO TO 815
 805 CONTINUE
    DO 811 I=1,LO
    XXCM(I)=CM(I,2)
    CM(I,2)=0
 811 CONTINUE
    GO TO 821
 815 CONTINUE
    IF (ITER.EQ.1)GO TO 816
    GO TO 805
 816 CONTINUE
    DO 819 I=1,LO
    XXCM(I)=CM(I,1)
 819 CONTINUE
 821 CONTINUE
C.....Calculating Cm(I,2) using Rhychmyer Algorithm.....

    IF(J.EQ.1)GO TO 840
    K=2
    GO TO 845
 840 K=1
 845 CONTINUE

    EE1(1,K)=C(1,2)/B(1,2)
    FF1(1,K)=RHS(1,K)/B(1,2)

    DO 1300 I=2,LO
     EE1(I,K)=C(I,2)/(B(I,2)-A(I,2)*EE1(I-1,K))
    IF (FF1(I-1,K).LT.1.0E-74) FF1(I-1,K)=0.0
     FF1(I,K)=(RHS(I,K)+(A(I,2)*FF1(I-1,K)))/(B(I,2)-(A(I,2)
   &  *EE1(I-1,K)))
1300 CONTINUE

    I=LO
    COUT=C0
    CM(I,2)=EE1(I,K)*COUT+FF1(I,K)
```

```
      LOLES1=LO-1
      DO 1400 II=1,LOLES1
       I=LO-II
      CM(I,2)=EE1(I,K)*CM(I+1,2)+FF1(I,K)
C      WRITE(8,*)'CM(',I,',2)',CM(I,2)
 1400 CONTINUE

C.....Storing the highest difference between old and.....
C                 new Cm into variable BIG
C....the BIG compared with the tolerant differnce TOLR (g/l).....

      BIG=0.0
      DO 720 I=1,LO
       RESID(I)=(ABS(CM(I,2)-XXCM(I)))
       RES=RESID(I)
       IF (RES.GT.BIG) BIG=RES
  720 CONTINUE

      TOLR=0.0001

      IF (BIG.LT.TOLR)GO TO 730


 2000 CONTINUE
C.....
  730 CONTINUE
      DO 2500 I=1,LO
      CIM(I,1,1)=0
      CIM(I,1,1)=CIM(I,1,2)

 2500 CONTINUE

C""""""""""""""""""""""""""""""""""""""Printing""""""""""""""""""""""""""""""""""""""""""""""""

      M=(JJ*ION)+J-J1
      VOL=M*Q
      V0=LR*(POR+PORI)*AREA
      VR=VOL/V0
      S0=V0*C0
      XR=CM(LR,2)/C0
      DELTV=DELTT*Q
      S=S+CM(LR,2)*DELTV
      SI=SI+CIN*DELTV
      SS=S0-S+SI
       SR=SS/S0
C.....V/V0 & S/S0 @ L=LR.....
c      WRITE(8,91)VR,SR
c   91 FORMAT(10X,F8.4,10X,F8.4)
C.....V/V0 & C/C0 @ L=LR.....
       WRITE(8,89)VR,XR
    89 FORMAT(10X,F8.4,10X,F8.4)
C.....TIME & C @ L=LR.....
C
c      WRITE(8,88)J,CM(LR,2)
c   88 FORMAT(5X,I5,10X,F8.4,10X,F8.4)
C.....DEPTH & C @ V/VO.....
```

```
C   IF(VR.LT.2.99.OR.VR.GT.3.0)GOTO 14
C   WRITE(8,*)VR
C   DO 13 I=1,LR
C   WRITE(8,90)I,CM(I,2),CIM(I,1,2)
C 90 FORMAT(5X,I5,10X,F8.4,10X,F8.4)
C 13 CONTINUE
C 14 CONTINUE
C""""""""""""""""""""""""""""""""""""""""""""""""""""""""""""""""""""""""""""""""""""""
   DO 2700 I=1,LO
   RHS(I,2)=0
   A(I,2)=0
   B(I,2)=0
   C(I,2)=0
   E(I,2)=0
   F(I,2)=0
   G(I,2)=0
   EE1(I,2)=0
   FF1(I,2)=0
   CM(I,1)=0
   CM(I,1)=CM(I,2)
   CM(I,2)=0
 2700 CONTINUE
 3000 CONTINUE
   IJ=J-1
C^^^^^^^^^^^^^^^^^^^^^^^^^^^^^^^^^^ Off time ^^^^^^^^^^^^^^^^^^^^^^^^^^^^^^^^^^^^^^

   IJF=IOFF+IJ
   DO 4000 J=IJ+1,IJF

C---------------   Calculating of ALFA   ---------------------------------

   TETA=PORI

   TIM=IOFF
   B1=0.14472*LOG(167.0/(FI*Q1**2.))
   T=DE*TIM/RID**2.
   IF(T.GE.0.1)THEN
   ALFA=((FI*Q1**2.)*(1.+(0.1*B1/((1.-B1)*T))))*DE*
  &TETA/RID**2
   ELSE

   ALFA=((FI*Q1**2./(1.-B1))*(0.1/T)**B1)*DE*TETA/RID**2
   ENDIF

C   PRINT*,'ALFA=',ALFA,'FI=',FI,' T=',T,' B1=',B1,' v=',V
C--------------------------------------------------------------------------



   DO 2981 I=1,LO
   CM(I,2)=CM(I,1)
 2981 CONTINUE
C-------------------------Iteration loop-------------------------------------

 2971 DO 2001 ITER=1,ITERA
   DO 771 I=1,LO
   CIM(I,1,2)=0
```

```
 771 CONTINUE
c.....Calculting Cim.....

    DO 991 I=1,LO

    CIM(I,1,2)=((ALFA*DELTT/(2*PORI))*(CM(I,1)+CM(I,2))+CIM(I,1,1)*
   &(1-(DELTT*ALFA/(2*PORI))))/(1+(ALFA*DELTT/(2*PORI)))
 991 CONTINUE


C-------------------------------------------------------------------

    DO 712 I=1,LO
    XXCM(I)=0.0
 712 CONTINUE

    IF(J.EQ.1)GO TO 1815
1805 CONTINUE
    DO 1811 I=1,LO
    XXCM(I)=CM(I,2)
    CM(I,2)=0
1811 CONTINUE
    GO TO 1821
1815 CONTINUE
    IF (ITER.EQ.1)GO TO 1816
    GO TO 1805
1816 CONTINUE
    DO 1819 I=1,LO
    XXCM(I)=CM(I,1)
 1819 CONTINUE
 1821 CONTINUE
C-------------------------------------------------------------------
    DO 345 I=1,LO
    CM(I,2)=CM(I,1)-(PORI/POR)*(CIM(I,1,2)-CIM(I,1,1))
 345 CONTINUE
C.....
    BIG=0.0
    DO 721 I=1,LO
     RESID(I)=(ABS(CM(I,2)-XXCM(I)))
     RES=RESID(I)
     IF (RES.GT.BIG) BIG=RES
 721 CONTINUE

    TOLR=0.0001

    IF (BIG.LT.TOLR)GO TO 731


 2001 CONTINUE
C.....
 731 CONTINUE
    DO 2501 I=1,LO
    CIM(I,1,1)=0

    CIM(I,1,1)=CIM(I,1,2)

 2501 CONTINUE
```

```
C     WRITE(8,88)J,CM(LR,2),CIM(LR,1,2)

      DO 2701 I=1,LO
      RHS(I,2)=0
      A(I,2)=0
      B(I,2)=0
      C(I,2)=0
      E(I,2)=0
      F(I,2)=0
      G(I,2)=0
      EE1(I,2)=0
      FF1(I,2)=0
      CM(I,1)=0
      CM(I,1)=CM(I,2)
      CM(I,2)=0
 2701 CONTINUE
 4000 CONTINUE

C^^^^^^^^^^^^^^^^^^^^^^^^^^^^^^^^^^^^^^^^^^^^^^^^^^^^^^^^^^^^^^^^^^^^^^^^^^^^^^^

 5000 CONTINUE

      STOP
      END
C============END OF THE PROGRAM==================
```

Appendix B

```
C=====================================================================
c                    MODEL    SIL
c                 (Saturated Intermittent Leaching)
c
c     Program for simulating solute transport under intermittent
c       leaching for aggregated media and saturated conditions
c
c                 (case 2: for multi-diameter spheres)
C=====================================================================

      PROGRAM INTERMITTENT SATURATED

      DIMENSION CIM(500,3,2),XCX(500,10,2)
      DIMENSION A(500,2),B(500,2),C(500,2)
      DIMENSION E(500,2),F(500,2),G(500,2)
      DIMENSION CM(500,2),RHS(500,2),EE1(500,2),FF1(500,2)
      DIMENSION XXCM(500),RESID(500)
      DIMENSION DE(10),RID(10),P(10),ALFA(10)
      DOUBLE PRECISION CIM,CM,RHS
      DOUBLE PRECISION EE1,FF1,XXCM,RESID
      DOUBLE PRECISION A,B,C,E,F,G
      DOUBLE PRECISION ZZ,PZ

      OPEN(UNIT=8,FILE='result3i.dat')
C-----------------------------------------------------------
C---------------- DATA ----------------------------------------------
      DELTT=1.0
      DELTZ=1.0
      S=0.0
      SI=0.0
      Q=7.3*1000
      AREA=56.7*100
      C0=7.634
      POR=0.337
      PORI=0.298
      LO=350
      LR=250
      XCIN=0.0
      ITERA=18

c.....Mass proportion of sphere diameters...
      NP=2
      P(1)=0.56
      P(2)=0.44
c.....
      ITIME=1300
      ION=20
```

```
      IOFF=69
      ICYCLE=ITIME/(ION+IOFF)
      ZZ=DELTZ*DELTZ
      FI=POR/(POR+PORI)
      PZ=POR*DELTZ
C-------------------------HEADINGS-----------------------------------

C.....................................V/VO & S/SO.FOR LR.....
       WRITE(8,11)
   11 FORMAT(5X,'V/VO',10X,'S/SO')
C.....................................V/VO & C/CO.FOR LR.....
C      WRITE(8,8)
C    8 FORMAT(5X,'V/VO',10X,'C/CO')
C.....................................TIME & C FOR LR.....
c      WRITE(8,9)
c    9 FORMAT(5X,'TIME',10X,'CONCENT.')
C.....................................DEPTH & C @ V/VO.....
C      WRITE(8,10)
C    10 FORMAT(5X,'DEPTH',10X,'Cm',10X,'Cim')


C-------------------------------------------------------------------
C========================= THE PROGRAM ==========
      IJ=0
      IC=ICYCLE-1

      DO 5000 JJ=0,IC
      J1=JJ*(ION+IOFF)

      DO 3000 J=J1+1,ION+J1

C-------------- Calculating of ALFA ------------------------------
      V=Q/AREA


      DS=3.71


      DE(1)=0.0575
      DE(2)=0.0528
      RID(1)=6.43
      RID(2)=1.19
      Q1=3.496

      TETA=PORI
      TIM=LR*POR/(Q/AREA)
      B1=0.14472*LOG(167.0/(FI*Q1**2.))

      DO 2991 N=1,NP
      T=DE(N)*TIM/RID(N)**2.
      IF(T.GE.0.1)THEN
      ALFA(N)=((FI*Q1**2.)*(1.+(0.1*B1/((1.-B1)*T))))*DE(N)
     &*TETA/RID(N)**2
      ELSE

      ALFA(N)=((FI*Q1**2./(1.-B1))*(0.1/T)**B1)*DE(N)
     &*TETA/RID(N)**2
```

```
      ENDIF

C     PRINT*,'ALFA=',ALFA(N),'FI=',FI,' T=',T,' B1=',B1,' v=',V
 2991 CONTINUE
C-------------------------------------------------------------------------
C-------------------------Initial condition-------------------------------
      IF (J.GT.1)GO TO 2990
      DO 7 I=1,LO
      CM(I,1)=C0
      CIM(I,1,1)=C0

      DO 2503 N=1,NP
      XCX(I,N,1)=C0
 2503 CONTINUE

    7 CONTINUE

      GO TO 2970
 2990 CONTINUE
      DO 2980 I=1,LO
      CM(I,2)=CM(I,1)
 2980 CONTINUE
C-------------------------Iteration loop----------------------------------
 2970 DO 2000 ITER=1,ITERA
      DO 777 I=1,LO
      CIM(I,1,2)=0.
      DO 776 N=1,NP
      XCX(I,N,2)=0.
  776 CONTINUE
  777 CONTINUE

C.....................Calculating Cim.....................................
      DO 999 I=1,LO
      DO 997 N=1,NP
      IF (J.EQ.1)GO TO 550

      XCX(I,N,2)=((ALFA(N)*DELTT/(2*PORI))*(CM(I,1)+CM(I,2))+XCX(I,N,1)*
     &(1-(DELTT*ALFA(N)/(2*PORI))))/(1+(ALFA(N)*DELTT/(2*PORI)))
      GO TO 998

  550 IF(ITER.EQ.1)GO TO 553
      XCX(I,N,2)=((ALFA(N)*DELTT/(PORI*2))*(CM(I,1)+CM(I,2))+XCX(I,N,1)*
     &(1-(DELTT*ALFA(N)/(2*PORI))))/(1+(ALFA(N)*DELTT/(2*PORI)))
      GO TO 998

  553 XCX(I,N,2)=((ALFA(N)*DELTT/(PORI*2))*2*CM(I,1)+XCX(I,N,1)*
     &(1.-(DELTT*ALFA(N)/(2*PORI))))/(1.+(ALFA(N)*DELTT/(2*PORI)))

  998 CONTINUE
      CIM(I,1,2)=CIM(I,1,2)+XCX(I,N,2)*P(N)
  997 CONTINUE
  999 CONTINUE
C-------------------------------------------------------------------------

      DO 1 I=2,LO
      A(I,2)=(DS*DELTT)/(2*ZZ)+(V*DELTT)/(4*PZ)
      B(I,2)=1.+(DS*DELTT)/(ZZ)
```

```
      C(I,2)=(DS*DELTT)/(2*ZZ)-(V*DELTT)/(4*PZ)
      E(I,2)=A(I,2)
      F(I,2)=1.-(DS*DELTT)/(ZZ)
      G(I,2)=C(I,2)

    1 CONTINUE

      B(1,2)=V+(POR*DS)/DELTZ
      C(1,2)=(POR*DS)/DELTZ

C----------Calculating RHS----------
      LOLES1=LO-1
      DO 1100 I=2,LOLES1
      IF(J-1.EQ.0)GO TO 1090
      RHS(I,2)=E(I,2)*CM(I-1,1)+F(I,2)*CM(I,1)+G(I,2)*CM(I+1,1)
     &-(PORI/POR)*(CIM(I,1,2)-CIM(I,1,1))
      GO TO 1100
 1090 RHS(I,J)=C0

 1100 CONTINUE
C.....Boundary conditions.....

      IF (J-1.NE.0)GO TO 45
      RHS(1,1)=V*XCIN
      GO TO 47
   45 CONTINUE
      RHS(1,2)=V*XCIN
   47 IF (J-1.NE.0)GO TO 48
      RHS(LO,1)=C0
      GO TO 49
   48 COUT=C0

      RHS(LO,2)=E(LO,2)*CM(LO-1,1)+F(LO,2)*CM(LO,1)+G(LO,2)*COUT
     &-(PORI/POR)*(CIM(LO,1,2)-CIM(LO,1,1))
   49 CONTINUE
c.....Storing the old Cm(I,2) in XXCM(I) and Calculate new.....
c                  Cm(I,2)


      DO 711 I=1,LO
      XXCM(I)=0.0
  711 CONTINUE

      IF(J.EQ.1)GO TO 815
  805 CONTINUE
      DO 811 I=1,LO
      XXCM(I)=CM(I,2)
      CM(I,2)=0
  811 CONTINUE
      GO TO 821
  815 CONTINUE
      IF (ITER.EQ.1)GO TO 816
      GO TO 805
  816 CONTINUE
      DO 819 I=1,LO
      XXCM(I)=CM(I,1)
  819 CONTINUE
  821 CONTINUE
```

```
C.....Calculating Cm(I,2) using Rhychmyer Algorithm.....

    IF(J.EQ.1)GO TO 840
    K=2
    GO TO 845
 840 K=1
 845 CONTINUE

    EE1(1,K)=C(1,2)/B(1,2)
    FF1(1,K)=RHS(1,K)/B(1,2)

    DO 1300 I=2,LO
     EE1(I,K)=C(I,2)/(B(I,2)-A(I,2)*EE1(I-1,K))
     IF (FF1(I-1,K).LT.1.0E-74) FF1(I-1,K)=0.0
     FF1(I,K)=(RHS(I,K)+(A(I,2)*FF1(I-1,K)))/(B(I,2)-(A(I,2)
    &  *EE1(I-1,K)))
 1300 CONTINUE

    I=LO
    COUT=C0
    CM(I,2)=EE1(I,K)*COUT+FF1(I,K)

    LOLES1=LO-1
    DO 1400 II=1,LOLES1
     I=LO-II
    CM(I,2)=EE1(I,K)*CM(I+1,2)+FF1(I,K)
C     WRITE(8,*)'CM(',I,',2)',CM(I,2)
 1400 CONTINUE

C.....Storing the highest difference between old and.....
C                 new Cm into variable BIG
C....the BIG compared with the tolerant differnce TOLR (g/l).....

    BIG=0.0
    DO 720 I=1,LO
     RESID(I)=(ABS(CM(I,2)-XXCM(I)))
     RES=RESID(I)
     IF (RES.GT.BIG) BIG=RES
 720 CONTINUE

    TOLR=0.0001

    IF (BIG.LT.TOLR)GO TO 730

 2000 CONTINUE
C.....
 730 CONTINUE
    DO 2500 I=1,LO
    DO 2502 N=1,NP

    XCX(I,N,1)=0.
    XCX(I,N,1)=XCX(I,N,2)
2502 CONTINUE

    CIM(I,1,1)=0.
    CIM(I,1,1)=CIM(I,1,2)
2500 CONTINUE
```

```
C""""""""""""""""""""""""""""""""Printing""""""""""""""""""""""""""""""""""""""""

      M=(JJ*ION)+J-J1
      VOL=M*Q
      V0=LR*(POR+PORI)*AREA
      VR=VOL/V0
      S0=V0*C0
      XR=CM(LR,2)/C0
      DELTV=DELTT*Q
      S=S+CM(LR,2)*DELTV
      SI=SI+XCIN*DELTV
      SS=S0-S+SI
      SR=SS/S0

C....................................V/V0 & S/S0.FOR LR......
      WRITE(8,91)VR,SR
   91 FORMAT(10X,F8.4,10X,F8.4)
C....................................V/V0 & C/C0.FOR LR......
C     WRITE(8,89)VR,XR
C  89 FORMAT(10X,F8.4,10X,F8.4)
C....................................TIME & C FOR LR..........
C     WRITE(8,88)J,CM(LR,2),CIM(LR,1,2),XCX(LR,1,2),XCX(LR,2,2)
C  88 FORMAT(5X,I5,4(10X,F8.4))
c     WRITE(8,88)J,CM(LR,2)
c  88 FORMAT(5X,I5,10X,F8.4)
C....................................DEPTH & C @ V/VO........
C     IF(VR.LT.2.99.OR.VR.GT.3.0)GOTO 14
C     WRITE(8,*)VR
C     DO 13 I=1,LR
C     WRITE(8,90)I,CM(I,2),CIM(I,1,2)
C  90 FORMAT(5X,I5,10X,F8.4,10X,F8.4)
C  13 CONTINUE
C  14 CONTINUE
C""""""""""""""""""""""""""""""""""""""""""""""""""""""""""""""""""""""""""""""""
      DO 2700 I=1,LO
      RHS(I,2)=0
      A(I,2)=0
      B(I,2)=0
      C(I,2)=0
      E(I,2)=0
      F(I,2)=0
      G(I,2)=0
      EE1(I,2)=0
      FF1(I,2)=0
      CM(I,1)=0
      CM(I,1)=CM(I,2)
      CM(I,2)=0
 2700 CONTINUE
 3000 CONTINUE
      IJ=J-1
C^^^^^^^^^^^^^^^^^^^^^^^^^^^^^^^^ Off time ^^^^^^^^^^^^^^^^^^^^^^^^^^^^^^^^^^^

      IJF=IOFF+IJ
      DO 4000 J=IJ+1,IJF
C---------------   Calculating of ALFA   --------------------------------
```

```
 TIM=IOFF
 DO 2891 N=1,NP
 T=DE(N)*TIM/RID(N)**2.
 IF(T.GE.0.1)THEN
 ALFA(N)=((FI*Q1**2.)*(1.+(0.1*B1/((1.-B1)*T))))*DE(N)
&*TETA/RID(N)**2
 ELSE

 ALFA(N)=((FI*Q1**2./(1.-B1))*(0.1/T)**B1)*DE(N)
&*TETA/RID(N)**2
 ENDIF
C     PRINT*,'ALFA=',ALFA(N),'FI=',FI,' T=',T,' B1=',B1,' v=',V
 2891 CONTINUE
C-------------------------------------------------------------------------
    DS=0.0
    V=0.0
    DO 2981 I=1,LO
    CM(I,2)=CM(I,1)
 2981 CONTINUE
C-------------------------Iteration loop-----------------------------------

    DO 2001 ITER=1,ITERA
    DO 771 I=1,LO
    CIM(I,1,2)=0.
  771 CONTINUE

    DO 991 I=1,LO
    DO 992 N=1,NP

c.....Calculting Cim.....

    XCX(I,N,2)=((ALFA(N)*DELTT/(2*PORI))*(CM(I,1)+CM(I,2))+XCX(I,N,1)*
   &(1-(DELTT*ALFA(N)/(2*PORI))))/(1+(ALFA(N)*DELTT/(2*PORI)))
    CIM(I,1,2)=CIM(I,1,2)+XCX(I,N,2)*P(N)
  992 CONTINUE
  991 CONTINUE


C-------------------------------------------------------------------


    DO 712 I=1,LO
    XXCM(I)=0.0
  712 CONTINUE

    IF(J.EQ.1)GO TO 1815
 1805 CONTINUE
    DO 1811 I=1,LO
    XXCM(I)=CM(I,2)
    CM(I,2)=0
 1811 CONTINUE
    GO TO 1821
 1815 CONTINUE
    IF (ITER.EQ.1)GO TO 1816
    GO TO 1805
 1816 CONTINUE
    DO 1819 I=1,LO
```

```
      XXCM(I)=CM(I,1)
 1819 CONTINUE
 1821 CONTINUE
C------------------------------------------------------------
      DO 345 I=1,LO
      CM(I,2)=CM(I,1)-(PORI/POR)*(CIM(I,1,2)-CIM(I,1,1))
  345 CONTINUE
C..............................................
      BIG=0.0
      DO 721 I=1,LO
       RESID(I)=(ABS(CM(I,2)-XXCM(I)))
       RES=RESID(I)
       IF (RES.GT.BIG) BIG=RES
  721 CONTINUE

      TOLR=0.0001

      IF (BIG.LT.TOLR)GO TO 731

 2001 CONTINUE
C.............................................................
  731 CONTINUE
      DO 2501 I=1,LO

      DO 2504 N=1,NP
      XCX(I,N,1)=0.
      XCX(I,N,1)=XCX(I,N,2)
      XCX(I,N,2)=0.
 2504 CONTINUE
      CIM(I,1,1)=0.
      CIM(I,1,1)=CIM(I,1,2)

 2501 CONTINUE

C     WRITE(8,88)J,CM(LR,2),CIM(LR,1,2)

      DO 2701 I=1,LO
      RHS(I,2)=0
      A(I,2)=0
      B(I,2)=0
      C(I,2)=0
      E(I,2)=0
      F(I,2)=0
      G(I,2)=0
      EE1(I,2)=0
      FF1(I,2)=0
      CM(I,1)=0
      CM(I,1)=CM(I,2)
      CM(I,2)=0
 2701 CONTINUE
 4000 CONTINUE

C^^^^^^^^^^^^^^^^^^^^^^^^^^^^^^^^^^^^^^^^^^^^^^^^^^^^^^^^^^^^^^^^^
 5000 CONTINUE
      STOP
      END
C============END OF THE PROGRAM===================
```

Appendix C

```
C=============================================================
c                    DIFFUSION MODEL
c
c
c     Program for predicting the diffusion of solute out
c       of inert spheres into a fixed volume of solution
c
c
c
C=============================================================
      PROGRAM DIFFUSION
      REAL MSR,MVR,MER,K1
      DIMENSION RID(400),ARID(6),QN(6),V(400),CM(1000),XCM(1000,6),CD(6)
      DOUBLE PRECISION TM
      OPEN(UNIT=8,FILE='resdiff2.dat')
      OPEN(UNIT=9,FILE='resdiff2A')
      WRITE(8,201)
  201 FORMAT(5X,'TIME',6X,'Reference',3X,'MSR',6X,'MVR',7X,'MER'
     &,8X,'AMR',6X,'WAR',6X,'VWR')

C.....Normal Size Distribution.....
C     EM=0.5
C     SEG=0.05
C     DO 500 I=1,3
C     KI=2*I
C     RID(KI-1)=EM+SQRT(2*SEG**2.*ALOG(1./((I/12.)*SEG*
C    &SQRT(2.*3.1416))))
C     RID(KI)=EM-SQRT(2*SEG**2.*ALOG(1./((I/12.)*SEG*
C    &SQRT(2.*3.1416))))
C  500 CONTINUE

C.....Log-Normal Size Distribution.....
C     EM=0.5
C     SEG=1.9
C     DO 505 I=1,3
C     KI=2*I
C     RID(KI-1)=EXP(-(SEG**2.-EM)+SQRT((SEG**2.-EM)**2.
C    &-EM**2.-2*SEG**2.*ALOG((I/12.)*SEG*(2.*3.1416)**.5)))
C     RID(KI)=EXP(-(SEG**2.-EM)-SQRT((SEG**2.-EM)**2.
C    &-EM**2.-2*SEG**2.*ALOG((I/12.)*SEG*(2.*3.1416)**.5)))
C  505 CONTINUE
C.....Assumed Size Distribution.....
      IR=372
      DE=0.033
      RID(1)=0.68
      RID(2)=0.68
      DO 18 I=3,372
      RID(I)=0.11
```

```
 18 CONTINUE


C---------------- DATA ----------------------------------------
C------------ (Unites:  min, mg, cm )--------
      ITIME=500
      VEX=400
      C0=7.55
      PORI=0.45

C     IR=12
C     RID(3)=0.617
C     RID(4)=0.617
C     RID(5)=0.382
C     RID(6)=0.382
C     RID(7)=RID(3)
C     RID(8)=RID(4)
C     RID(9)=RID(5)
C     RID(10)=RID(5)
C     RID(11)=RID(6)
C     RID(12)=RID(6)


C=================== THE PROGRAM ==========


      DO 13 I=1,IR
       WRITE(9,*)I,RID(I)
  9 FORMAT(2I,5X,F8.4)
 13 CONTINUE
       DO 2 K=1,ITIME
       K1=K/60.
       CM(K)=0.0
       SEGMA1=0.0
       SEGMA2=0.0
       VT=0.
       DO 1 I=1,IR

       V(I)=4.*3.14*RID(I)*RID(I)*RID(I)/3.
       VT=VT+V(I)
  1 CONTINUE
       BETA=VEX/(PORI*VT)
       VS=VEX+VT

      POR=VEX/VS
      FI=VEX/(VEX+VT*PORI)
      MT=PORI*VT*C0
      CE=MT/(VT*PORI+VEX)
      GAMA=VS*(VEX+VT*PORI)/(VEX*VT*PORI)


      QN(1)=3.3668
      QN(2)=6.4098
      QN(3)=9.5113
      QN(4)=12.6319
      QN(5)=15.7607
      QN(6)=18.89
```

```
      TM=0.0
      DO 3 I=1,IR
      SEGMA2=0.0
      DO 100 N=1,6
C      SEGMA1=SEGMA1+((6.*BETA*(BETA+1.)*QN(N)**2./(9.+9.*BETA+
C     &QN(N)**2.*BETA**2.))
C     &*EXP(-(DE*QN(N)**2.*K1/RID(I)**2.)))
      SEGMA2=SEGMA2+((6.*BETA*(BETA+1.)/(9.+9.*BETA+QN(N)**2.*BETA**2.)).
     &*EXP(-(DE*QN(N)**2.*K1/(RID(I)**2.))))
  100 CONTINUE
C      XK=(DE*FI*PORI/RID(I)**2.)*(SEGMA1/SEGMA2)
C      CATI=CE+(C0-CE)*EXP(-GAMA*XK*K1)

      CATI=CE+(C0-CE)*SEGMA2
      TMI=(C0-CATI)*V(I)*PORI
      TM=TM+TMI

    3 CONTINUE
      CM(K)=TM/(VEX+VT*PORI)


C-------------------------------------------------------
C============================== MEAN VALUES ============================================
C.....THE MEAN SQUARE RADIUS (MSR)
      RS=0.0
      RC=0.0
      AM=0.0
      XS=0.0
      XWA=0.0
      VW=0.0
      DO 4 I=1,IR
      RC=RC+RID(I)*RID(I)*RID(I)*V(I)/VT
      RS=RS+RID(I)*RID(I)*V(I)/VT
      AM=AM+RID(I)
      VW=VW+V(I)*RID(I)/VT
    4 CONTINUE
      DO 5 I=1,IR
      XS=XS+(3./RID(I))*(V(I)/VT)
      XWA=XWA+V(I)/((RID(I)*RID(I))*VT)
    5 CONTINUE
      PRINT*,XS
      MSR=(RS)**0.5
C.....THE MEAN AGGREGATE VOLUME RADIUS (MVR)
      MVR=RC/(RS)

C..... THE MEAN EXCHANGE AREA RADIUS (MER)
      MER=3/XS

C..... THE ARTHIMATIC MEAN RADIUS (AMR)
      AMR=AM/IR

C.....  WEIGHTED-AVERAGE RADIUS (WAR)
      WAR=1/XWA**(0.5)

C.....  VOLUME-WEIGHT AVERAGE RADIUS
```

```
      VWR=VW

C-----------------------------------------------------------------------------

      ARID(1)=MSR
      ARID(2)=MVR
      ARID(3)=MER
      ARID(4)=AMR
      ARID(5)=WAR
      ARID(6)=VWR

      DO 10 M=1,6
       VM=4.*3.14*ARID(M)*ARID(M)*ARID(M)/3.
       BETA=VEX/(PORI*VT)
       VS=VEX+VT
       POR=VEX/VS
       FI=VEX/(VEX+VT*PORI)
       MT=PORI*VT*C0
       CE=MT/(VT*PORI+VEX)
       GAMA=VS*(VEX+VT*PORI)/(VEX*VT*PORI)
       SEGMA1=0.0
       SEGMA2=0.0
       DO 101 N=1,6
C       SEGMA1=SEGMA1+((6.*BETA*(BETA+1.)*QN(N)**2./(9.+9.*BETA+
C      &QN(N)**2.*BETA**2.))
C      &*EXP(-(DE*QN(N)**2.*K1/ARID(M)**2.)))
       SEGMA2=SEGMA2+((6.*BETA*(BETA+1.)/(9.+9.*BETA+QN(N)**2.*BETA**2.))
      &*EXP(-(DE*QN(N)**2.*K1/ARID(M)**2.)))
     101 CONTINUE

C      XK=(DE*FI*PORI/ARID(M)**2.)*(SEGMA1/SEGMA2)

       CATII=CE+(C0-CE)*SEGMA2
       TMM=(C0-CATII)*VT*PORI



       XCM(K,M)=TMM/(VEX+VT*PORI)

      10 CONTINUE


C      WRITE(8,200)K,CM(K),XCM(K,1),XCM(K,2),XCM(K,3),XCM(K,4),
C     &XCM(K,5),XCM(K,6)
C    200 FORMAT(5X,I4,7(2X,F8.4))

       2 CONTINUE
        DO 205 K=1,ITIME,10
        WRITE(8,206)K,CM(K),XCM(K,1),XCM(K,2),XCM(K,3),XCM(K,4),
       &XCM(K,5),XCM(K,6)
     206 FORMAT(5X,I4,7(2X,F8.4))
     205 CONTINUE

       WRITE(9,312)
     312 FORMAT('AR',2X,'Vt',4X,'Ce')
       DO 203 I=1,6
       WRITE(9,*)ARID(I),VT,CE
     203 CONTINUE
```

```
      CMT=0.0
      DO 300 K=1,ITIME
      CMT=CMT+CM(K)
      CMA=CMT/ITIME
  300 CONTINUE

      DO 301 I=1,6
      SU=0.0
      SD=0.0
      DO 303 K=1,ITIME
      S1=(CM(K)-XCM(K,I))**2.
      SU=SU+S1
      S2=(CM(K)-CMA)**2.
      SD=SD+S2
      CD(I)=1.-(SU/SD)
  303 CONTINUE
  301 CONTINUE
      WRITE(9,310)
  310 FORMAT('Coffi. of Determination')
      DO 304 I=1,6
      WRITE(9,*)CD(I)
  304 CONTINUE
      STOP
      END
C==========END OF THE PROGRAM==========
```

Appendix D

```
C=============================================================
c                    MODEL    SIL
c                (Saturated Intermittent Leaching)
c
c     Program for simulating solute transport under intermittent
c       leaching for aggregated media and drained conditions
c
c
c              (case 3:  for soil aggregates)
C=============================================================

      PROGRAM INTERMITTENT SATURATED

      DIMENSION CIM(500,3,2)
      DIMENSION A(500,2),B(500,2),C(500,2)
      DIMENSION E(500,2),F(500,2),G(500,2),RM(500),RIM(500)
      DIMENSION CM(500,2),RHS(500,2),EE1(500,2),FF1(500,2)
      DIMENSION XXCM(500),RESID(500)
      DOUBLE PRECISION CIM,CM,RHS
      DOUBLE PRECISION EE1,FF1,XXCM,RESID
      DOUBLE PRECISION A,B,C,E,F,G
      DOUBLE PRECISION ZZ,PZ,ALFA

      OPEN(UNIT=8,FILE='resul1si.dat')
C-------------------------------------------------------------
C------------------ DATA -------------------------------------
      DELTT=1.0
      DELTZ=1.0
      S=0.0
      SI=0.0

c.....
c             adsorbed solute
      AS=1618*1000

c.....
c             Desorption isotherm

      RU=747
      DK=0.00339
      BC=0.105
      FF=0.95

c.....
c             Initial conditations

      C0=3.6318
      POR=0.258
```

```
PORI=0.224
LO=350
LR=195
CIN=0.156
Q=6.79*1000
AREA=20.428*100
ITERA=18
ITIME=200
ION=25
IOFF=0
    ICYCLE=ITIME/(ION+IOFF)
    ZZ=DELTZ*DELTZ
    FI=POR/(POR+PORI)
    PZ=POR*DELTZ

C----------HEADINGS----------

C.....V/VO & S/SO.FOR LR.....
    WRITE(8,11)
  11 FORMAT(5X,'V/VO',10X,'S/SO')
C.....V/VO & C/CO.FOR LR.....
c     WRITE(8,8)
c   8 FORMAT(5X,'V/VO',10X,'C/CO')
C.....TIME & C FOR L.....
C     WRITE(8,9)
C   9 FORMAT(5X,'TIME',10X,'CONCENT.')
C.....DEPTH & C @ V/VO.....
C     WRITE(8,10)
C   10 FORMAT(5X,'DEPTH',10X,'Cm',10X,'Cim')


C-------------------------------------------------------------
C========== THE PROGRAM ==========

    IJ=0
    IC=ICYCLE-1

    DO 5000 JJ=0,IC
    J1=JJ*(ION+IOFF)

    DO 3000 J=J1+1,ION+J1

C---------- Calculating of ALFA & f ----------
    ALFA=0.0008
    NCYCLE=(J/(ION+IOFF))
    IF (NCYCLE.GT.1) FF=0.95*(1.-0.45*NCYCLE)
    IF (FF.LT.0) FF=0.0000001


    V=Q/AREA

    DS=22.708
c     PRINT*,ALFA,NCYCLE
C----------Initial condition----------

    IF (J.GT.1)GO TO 2990
```

```
      DO 7 I=1,LO
      CM(I,1)=C0
      CIM(I,1,1)=C0
    7 CONTINUE
      GO TO 2970
 2990 CONTINUE
      DO 2980 I=1,LO
      CM(I,2)=CM(I,1)
 2980 CONTINUE
C----------Iteration loop----------

 2970 DO 2000 ITER=1,ITERA
 C.....Calculating Cim.....

      DO 777 I=1,LO
      IF (J.EQ.1) CM(I,2)=CM(I,1)
      RM(I)=1.+(RU*FF*DK*BC*CM(I,2)**(BC-1)/POR)
      RIM(I)=1.+(RU*(1-FF)*DK*BC*CIM(I,1,2)**(BC-1)/PORI)
      CIM(I,1,2)=0
  777 CONTINUE
      DO 999 I=1,LO
      IF (J.EQ.1.AND.ITER.EQ.1)GO TO 553

      CIM(I,1,2)=((ALFA*DELTT/(RIM(I)*2*PORI))
     &*(CM(I,1)+CM(I,2))+CIM(I,1,1)*
     &(1-(DELTT*ALFA/(RIM(I)*2*PORI))))/(1+(ALFA*DELTT/(RIM(I)*2*PORI)))
      GO TO 999

  553 CIM(I,1,2)=((ALFA*DELTT/(RIM(I)*PORI*2))*2*CM(I,1)+CIM(I,1,1)*
       &(1.-(DELTT*ALFA/(RIM(I)*2*PORI))))/(1.+(ALFA*DELTT/(RIM(I)*2*PORI)))


  999 CONTINUE
C-----------------------------------------------------------

      DO 1 I=2,LO
      A(I,2)=(DS*DELTT)/(RM(I)*2*ZZ)+(V*DELTT)/(4*PZ*RM(I))
      B(I,2)=1.+(DS*DELTT)/(RM(I)*ZZ)
      C(I,2)=(DS*DELTT)/(2*ZZ*RM(I))-(V*DELTT)/(4*PZ*RM(I))
      E(I,2)=A(I,2)
      F(I,2)=1.-(DS*DELTT)/(RM(I)*ZZ)
      G(I,2)=C(I,2)

    1 CONTINUE

      B(1,2)=V+(POR*DS)/DELTZ
      C(1,2)=(POR*DS)/DELTZ

C----------Calculating RHS----------
      LOLES1=LO-1
      DO 1100 I=2,LOLES1
      IF(J.EQ.1)GO TO 1090
      RHS(I,2)=E(I,2)*CM(I-1,1)+F(I,2)*CM(I,1)+G(I,2)*CM(I+1,1)
     &-(PORI/POR)*(RIM(I)/RM(I))*(CIM(I,1,2)-CIM(I,1,1))
      GO TO 1100
 1090 RHS(I,J)=C0
```

```
1100 CONTINUE

C.....Boundary conditions.....

    IF (J-1.NE.0)GO TO 45
    RHS(1,1)=V*CIN
    GO TO 47
 45 CONTINUE
    RHS(1,2)=V*CIN
 47 IF (J-1.NE.0)GO TO 48
    RHS(LO,1)=C0
    GO TO 49
 48 COUT=C0

    RHS(LO,2)=E(LO,2)*CM(LO-1,1)+F(LO,2)*CM(LO,1)+G(LO,2)*COUT
   &-(PORI/POR)*(RIM(I)/RM(I))*(CIM(LO,1,2)-CIM(LO,1,1))

 49 CONTINUE

c.....Storing the old Cm(I,2) in XXCM(I) and Calculate new.....
c               Cm(I,2)

    DO 711 I=1,LO
    XXCM(I)=0.0
711 CONTINUE

    IF(J.EQ.1)GO TO 815
805 CONTINUE
    DO 811 I=1,LO
    XXCM(I)=CM(I,2)
    CM(I,2)=0
811 CONTINUE
    GO TO 821
815 CONTINUE
    IF (ITER.EQ.1)GO TO 816
    GO TO 805
816 CONTINUE
    DO 819 I=1,LO
    XXCM(I)=CM(I,1)
819 CONTINUE
821 CONTINUE
C.....Calculating Cm(I,2) using Rhychmyer Algorithm.....

    IF(J.EQ.1)GO TO 840
    K=2
    GO TO 845
840 K=1
845 CONTINUE
C.....
    EE1(1,K)=C(1,2)/B(1,2)
    FF1(1,K)=RHS(1,K)/B(1,2)

    DO 1300 I=2,LO
     EE1(I,K)=C(I,2)/(B(I,2)-A(I,2)*EE1(I-1,K))
    IF (FF1(I-1,K).LT.1.0E-74) FF1(I-1,K)=0.0
     FF1(I,K)=(RHS(I,K)+(A(I,2)*FF1(I-1,K)))/(B(I,2)-(A(I,2)
   &  *EE1(I-1,K)))
```

```
 1300 CONTINUE

     I=LO
     COUT=C0
     CM(I,2)=EE1(I,K)*COUT+FF1(I,K)

     LOLES1=LO-1
     DO 1400 II=1,LOLES1
      I=LO-II
     CM(I,2)=EE1(I,K)*CM(I+1,2)+FF1(I,K)
C      WRITE(8,*)'CM(',I,',2)',CM(I,2)
 1400 CONTINUE

C.....Storing the highest difference between old and.....
C                  new Cm into variable BIG
C....the BIG compared with the tolerant differnce TOLR (g/l).....

     BIG=0.0
     DO 720 I=1,LO
      RESID(I)=(ABS(CM(I,2)-XXCM(I)))
      RES=RESID(I)
      IF (RES.GT.BIG) BIG=RES
  720 CONTINUE

     TOLR=0.0001

     IF (BIG.LT.TOLR)GO TO 730

 2000 CONTINUE
C.....
  730 CONTINUE
     DO 2500 I=1,LO
     CIM(I,1,1)=0

     CIM(I,1,1)=CIM(I,1,2)

 2500 CONTINUE

C"""""""""""""""""""""""""""""""""""Printing"""""""""""""""""""""""""""""""""""""""""""""

     M=(JJ*ION)+J-J1
     VOL=M*Q
     V0=LR*(POR+PORI)*AREA
     VR=VOL/V0
     S0=(V0*C0)+AS
     XR=CM(LR,2)/C0
     DELTV=DELTT*Q
     S=S+CM(LR,2)*DELTV
     SI=SI+CIN*DELTV
     SS=S0-S+SI
     SR=SS/S0

C.....V/V0 & S/S0.FOR LR.....
c      WRITE(8,91)VR,SR
c   91 FORMAT(10X,F8.4,10X,F8.4)
C.....V/V0 & C/C0.FOR LR.....
```

```
c     WRITE(8,89)VR,XR
c   89 FORMAT(10X,F8.4,10X,F8.4)
C.....TIME & C FOR LR.....
C
C     WRITE(8,88)J,CM(LR,2)
C   88 FORMAT(5X,I5,10X,F8.4,10X,F8.4)
C.....DEPTH & C @ V/VO.....
      IF(VR.LT.0.99.OR.VR.GT.1.0)GOTO 14
      WRITE(8,*)VR
      DO 13 I=1,LR
      WRITE(8,90)I,CM(I,2),CIM(I,1,2)
   90 FORMAT(5X,I5,10X,F8.4,10X,F8.4)
   13 CONTINUE
   14 CONTINUE
C**********************************************************************
      DO 2700 I=1,LO
      RHS(I,2)=0
      A(I,2)=0
      B(I,2)=0
      C(I,2)=0
      E(I,2)=0
      F(I,2)=0
      G(I,2)=0
      EE1(I,2)=0
      FF1(I,2)=0
      CM(I,1)=0
      CM(I,1)=CM(I,2)
      CM(I,2)=0
 2700 CONTINUE
 3000 CONTINUE
      IJ=J-1
C^^^^^^^^^^^^^^^^^^^^^^^^^^^^^^^^ Off time ^^^^^^^^^^^^^^^^^^^^^^^^^^^^^^^^^^^^

      IJF=IOFF+IJ
      DO 4000 J=IJ+1,IJF

C----------  Calculating of ALFA ----------------------------

      DS=0.0
      V=0.0
      FF=0.95

      DO 2981 I=1,LO
      CM(I,2)=CM(I,1)
 2981 CONTINUE
C-------------------------Iteration loop-----------------------------------

2971 DO 2001 ITER=1,ITERA
      DO 771 I=1,LO
      RM(I)=1.+(RU*FF*DK*BC*CM(I,2)**(BC-1)/POR)
      RIM(I)=1.+(RU*(1-FF)*DK*BC*CIM(I,1,2)**(BC-1)/PORI)
      CIM(I,1,2)=0
 771 CONTINUE
c.....Calculting Cim.....

      DO 991 I=1,LO
      CIM(I,1,2)=((ALFA*DELTT/(RIM(I)*2*PORI))
```

```
     &*(CM(I,1)+CM(I,2))+CIM(I,1,1)*
     &(1-(DELTT*ALFA/(RIM(I)*2*PORI))))/(1+(ALFA*DELTT/(RIM(I)*2*PORI)))

  991 CONTINUE

C-------------------------------------------------------

     DO 712 I=1,LO
     XXCM(I)=0.0
  712 CONTINUE

     IF(J.EQ.1)GO TO 1815
 1805 CONTINUE
     DO 1811 I=1,LO
     XXCM(I)=CM(I,2)
     CM(I,2)=0
 1811 CONTINUE
     GO TO 1821
 1815 CONTINUE
     IF (ITER.EQ.1)GO TO 1816
     GO TO 1805
 1816 CONTINUE
     DO 1819 I=1,LO
     XXCM(I)=CM(I,1)
  1819 CONTINUE
  1821 CONTINUE
C-------------------------------------------------------
     DO 345 I=1,LO
     CM(I,2)=CM(I,1)-(PORI*RIM(I)/(RM(I)*POR))*(CIM(I,1,2)-CIM(I,1,1))
  345 CONTINUE
C.....
     BIG=0.0
     DO 721 I=1,LO
      RESID(I)=(ABS(CM(I,2)-XXCM(I)))
      RES=RESID(I)
      IF (RES.GT.BIG) BIG=RES
  721 CONTINUE

     TOLR=0.0001
     IF (BIG.LT.TOLR)GO TO 731


  2001 CONTINUE
C.....
  731 CONTINUE
     DO 2501 I=1,LO
     CIM(I,1,1)=0

     CIM(I,1,1)=CIM(I,1,2)

  2501 CONTINUE

C     WRITE(8,88)J,CM(LR,2),CIM(LR,1,2)
```

```
      DO 2701 I=1,LO
      RHS(I,2)=0
      A(I,2)=0
      B(I,2)=0
      C(I,2)=0
      E(I,2)=0
      F(I,2)=0
      G(I,2)=0
      EE1(I,2)=0
      FF1(I,2)=0
      CM(I,1)=0
      CM(I,1)=CM(I,2)
      CM(I,2)=0
 2701 CONTINUE
 4000 CONTINUE
C^^^^^^^^^^^^^^^^^^^^^^^^^^^^^^^^^^^^^^^^^^^^^^^^^^^^^^^^^^^^^^^^^^^^^^^

 5000 CONTINUE

      STOP
      END
C=============END OF THE PROGRAM====================
```

Appendix E

```
C=======================================================================
c                    MODEL    DIL
c                 (Drained Intermittent Leaching)
c
c     Program for simulating solute transport under intermittent
c       leaching for aggregated media and drained conditions
c
c
c
C=======================================================================

      PROGRAM INTERMITTENT UNSATURATED

      DIMENSION CIM(500,3,2)
      DIMENSION A(500,2),B(500,2),C(500,2)
      DIMENSION E(500,2),F(500,2),G(500,2),RM(500),RIM(500)
      DIMENSION CM(500,2),RHS(500,2),EE1(500,2),FF1(500,2)
      DIMENSION XXCM(500),RESID(500),ALFA(500),ALFA0(10)
      DOUBLE PRECISION CIM,CM,RHS
      DOUBLE PRECISION EE1,FF1,XXCM,RESID
      DOUBLE PRECISION A,B,C,E,F,G
      DOUBLE PRECISION ZZ,PZ

      OPEN(UNIT=8,FILE='resun1si.dat')
C-----------------------------------------------------------
C------------------ DATA -----------------------------------
      DELTT=1.0
      DELTZ=1.0
      S=0.0
      SI=0.0


c.....
c          Desorption isotherm

      RU=708
      DK=0.
      BC=1.
      FF=0.95
c.....
c          Initial conditations
      Q=3.542*1000
      C0=0.
      CIM0=7.675
      AREA=16.982*100
      POR=0.462
      PORI=0.265
```

```
LO=500
LR=180
CIN=0.


ALFA0(0)=0.011
ALFA0(1)=0.02
ALFA0(2)=0.03

ICYCLE=3
ITERA=18
IOFF=60
V=Q/AREA
DS=0.
ION=LR/(V/POR)


ITIME=ICYCLE*(ION+IOFF)
ZZ=DELTZ*DELTZ
FI=POR/(POR+PORI)
PZ=POR*DELTZ

PRINT*,"ION=",ION," IOFF=",IOFF," ICYCLE=",ICYCLE,
&" ITIME=",ITIME,"ITERA",ITERA," V",V," Q",Q,
&"  AREA",AREA,"   POR",POR
```

C----------HEADINGS----------

```
C.....V/VO & S/SO.FOR LR.....
c     WRITE(8,11)
c   11 FORMAT(5X,'V/VO',10X,'S/SO')
C.....V/VO & C/CO.FOR LR.....
      WRITE(8,8)
    8 FORMAT(5X,'V/VO',10X,'C/CO')
C.....TIME & C FOR L.....
C     WRITE(8,9)
C   9 FORMAT(5X,'TIME',10X,'CONCENT.')
C.....DEPTH & C @ V/VO.....
c     WRITE(8,10)
c   10 FORMAT(5X,'DEPTH',10X,'Cm',10X,'Cim')


C-------------------------------------------------------------
```

C========== THE PROGRAM ==========

```
    IJ=0
    IC=ICYCLE-1

    DO 5000 JJ=0,IC
    J1=JJ*(ION+IOFF)

    DO 3000 J=J1+1,ION+J1
c     PRINT*,"IC",IC,"  J",J
```

C----------ALFA & f estimation----------

```
    NCYCLE=(J/(ION+IOFF))
    IF (NCYCLE.GT.1) FF=0.95*(1.-0.45*NCYCLE)
```

```
      IF (FF.LT.0) FF=0.0000001



      DO 110 I=1, LO
      ALFA(I)=ALFA0(NCYCLE)
  110 CONTINUE

C---------------------- -------------------------------
 C-------------------------Initial condition-------------------------------
      J2=J-J1

      IF (NCYCLE.GT.0) GOTO 444

      IF (J2.GT.1) GOTO 333
      DO 111 I=1, LR
      CM(I,1)=C0
      CIM(I,1,1)=CIM0
  111 CONTINUE

      DO 222 I=LR+1, LO
      CM(I,1)=C0
      CIM(I,1,1)=C0
  222 CONTINUE
  333 CONTINUE


      DO 2980 I=1,LO
      CM(I,2)=CM(I,1)
 2980 CONTINUE
      GOTO 1010
C.....
  444 IF (J2.GT.1) GOTO 666
      DO 555 I=1, LR
      CM(I,1)=C0
  555 CONTINUE

      DO 888 I=LR+1, LO
      CM(I,1)=C0
      CIM(I,1,1)=C0
  888 CONTINUE
  666 CONTINUE


      DO 2982 I=1,LO
      CM(I,2)=CM(I,1)
 2982 CONTINUE

 1010 CONTINUE
C.....

      IA=J2*V/POR
      DO 776 I=1,IA
      ALFA(I)=0.
  776 CONTINUE
C-------------------------Iteration loop-----------------------------------

 2970 DO 2000 ITER=1,ITERA
      DO 777 I=1,LO
```

```
      IF (J2.EQ.1) CM(I,2)=CM(I,1)
      RM(I)=1.+(RU*FF*DK*BC*CM(I,2)**(BC-1)/POR)
      RIM(I)=1.+(RU*(1-FF)*DK*BC*CIM(I,1,2)**(BC-1)/PORI)
      CIM(I,1,2)=0
  777 CONTINUE
      DO 999 I=1,LO
      IF (J.EQ.1.AND.ITER.EQ.1)GO TO 553

C.....Calculating Cim.....

      CIM(I,1,2)=((ALFA(I)*DELTT/(RIM(I)*2*PORI))
     &*(CM(I,1)+CM(I,2))+CIM(I,1,1)*
     &(1-(DELTT*ALFA(I)/(RIM(I)*2*PORI))))
     &/(1+(ALFA(I)*DELTT/(RIM(I)*2*PORI)))
      GO TO 998



  553 CIM(I,1,2)=((ALFA(I)*DELTT/(RIM(I)*PORI*2))*2*CM(I,1)+CIM(I,1,1)*
     &(1.-(DELTT*ALFA(I)/(RIM(I)*2*PORI))))/(1.+(ALFA(I)
     &*DELTT/(RIM(I)*2*PORI)))

  998 CONTINUE
  999 CONTINUE
C-------------------------------------------------------------

      DO 1 I=2,LO
      A(I,2)=(DS*DELTT)/(RM(I)*2*ZZ)+(V*DELTT)/(4*PZ*RM(I))
      B(I,2)=1.+(DS*DELTT)/(RM(I)*ZZ)
      C(I,2)=(DS*DELTT)/(2*ZZ*RM(I))-(V*DELTT)/(4*PZ*RM(I))
      E(I,2)=A(I,2)
      F(I,2)=1.-(DS*DELTT)/(RM(I)*ZZ)
      G(I,2)=C(I,2)

    1 CONTINUE

C-------CONTSTANT FLUX CONDITION FOR UPPER BOUNDARY
      B(1,2)=V+(POR*DS)/DELTZ
      C(1,2)=(POR*DS)/DELTZ

C--------------------Calculating RHS-----------------------------

      LOLES1=LO-1
      DO 1100 I=2,LOLES1
      IF(J.EQ.1)GO TO 1090
      RHS(I,2)=E(I,2)*CM(I-1,1)+F(I,2)*CM(I,1)+G(I,2)*CM(I+1,1)
     &-(PORI/POR)*(RIM(I)/RM(I))*(CIM(I,1,2)-CIM(I,1,1))
      GO TO 1100
 1090 RHS(I,J)=C0

 1100 CONTINUE
C.....Boundary conditions.....

      IF (J-1.NE.0)GO TO 45
      RHS(1,1)=V*CIN
      GO TO 47
   45 CONTINUE
      RHS(1,2)=V*CIN
```

```
   47 IF (J-1.NE.0)GO TO 48
      RHS(LO,1)=C0
      GO TO 49
   48 COUT=C0

      RHS(LO,2)=E(LO,2)*CM(LO-1,1)+F(LO,2)*CM(LO,1)+G(LO,2)*COUT
     &-(PORI/POR)*(RIM(I)/RM(I))*(CIM(LO,1,2)-CIM(LO,1,1))

   49 CONTINUE
c.....Storing the old Cm(I,2) in XXCM(I) and Calculate new.....
c                 Cm(I,2)

      DO 711 I=1,LO
      XXCM(I)=0.0
  711 CONTINUE

      IF(J.EQ.1)GO TO 815
  805 CONTINUE
      DO 811 I=1,LO
      XXCM(I)=CM(I,2)
      CM(I,2)=0

  811 CONTINUE
      GO TO 821
  815 CONTINUE
      IF (ITER.EQ.1)GO TO 816
      GO TO 805
   816 CONTINUE
       DO 819 I=1,LO
       XXCM(I)=CM(I,1)
   819 CONTINUE
   821 CONTINUE
C.....Calculating Cm(I,2) using Rhychmyer Algorithm.....

       IF(J.EQ.1)GO TO 840
       K=2
       GO TO 845
   840 K=1
   845 CONTINUE
C.....
       EE1(1,K)=C(1,2)/B(1,2)
       FF1(1,K)=RHS(1,K)/B(1,2)

      DO 1300 I=2,LO
       EE1(I,K)=C(I,2)/(B(I,2)-A(I,2)*EE1(I-1,K))
      IF (FF1(I-1,K).LT.1.0E-74) FF1(I-1,K)=0.0
       FF1(I,K)=(RHS(I,K)+(A(I,2)*FF1(I-1,K)))/(B(I,2)-(A(I,2)
     &  *EE1(I-1,K)))
 1300 CONTINUE

      I=LO
      COUT=C0
      CM(I,2)=EE1(I,K)*COUT+FF1(I,K)

      LOLES1=LO-1
      DO 1400 II=1,LOLES1
       I=LO-II
      CM(I,2)=EE1(I,K)*CM(I+1,2)+FF1(I,K)
```

```
C     WRITE(8,*)'CM(',I,',2)',CM(I,2)
 1400 CONTINUE

C.....Storing the highest difference between old and.....
C                new Cm into variable BIG
C....the BIG compared with the tolerant differnce TOLR (g/l).....

      BIG=0.0
      DO 720 I=1,LO
       RESID(I)=(ABS(CM(I,2)-XXCM(I)))
       RES=RESID(I)
       IF (RES.GT.BIG) BIG=RES
  720 CONTINUE

      TOLR=0.0001

      IF (BIG.LT.TOLR)GO TO 730


 2000 CONTINUE

C.....
  730 CONTINUE
      DO 2500 I=1,LO
      CIM(I,1,1)=0

      CIM(I,1,1)=CIM(I,1,2)

 2500 CONTINUE

C""""""""""""""""""""""""""""""""""""""Printing""""""""""""""""""""""""""""""""""""""""""""""

      M=(JJ*ION)+J-J1
      VOL=M*Q
      V0=LR*(POR)*AREA
      VR=VOL/V0
      S0=LR*PORI*AREA*CIM0
      XR=CM(LR,2)/C0
      DELTV=DELTT*Q
      S=S+CM(LR,2)*DELTV
      SI=SI+CIN*DELTV
      SS=S0-S+SI
      SR=SS/S0
c     PRINT*,"S0=",S0
C.....V/V0 & S/S0.FOR LR.....
c     WRITE(8,91)VR,CM(LR,2),CIM(LR,1,2)
      WRITE(8,91)VR,SR
   91 FORMAT(10X,F8.4,2(10X,F8.4))
C.....V/V0 & C/C0.FOR LR.....
c     WRITE(8,89)VR,XR
c   89 FORMAT(10X,F8.4,10X,F8.4)
C.....TIME & C FOR LR.....
C

c     WRITE(8,88)J,CM(LR,2),CIM(LR,1,2)
c   88 FORMAT(5X,I5,10X,F8.4,10X,F8.4)
c     WRITE(8,88)J,CM(LR,2)
```

```
c  88 FORMAT(5X,I5,10X,F8.4)
C.......................................DEPTH & C @ V/VO........
c     IF(VR.LT.2.9.OR.VR.GT.3.0)GOTO 14
c     WRITE(8,*)VR
c     DO 13 I=1,LO
c     WRITE(8,90)I,CM(I,2),CIM(I,1,2)
c  90 FORMAT(5X,I5,10X,F8.4,10X,F8.4)
c  13 CONTINUE
  14 CONTINUE
C"""""""""""""""""""""""""""""""""""""""""""""""""""""""""""""""""""""""""""""""
    DO 2700 I=1,LO
    RHS(I,2)=0
    A(I,2)=0
    B(I,2)=0
    C(I,2)=0
    E(I,2)=0
    F(I,2)=0
    G(I,2)=0
    EE1(I,2)=0
    FF1(I,2)=0
    CM(I,1)=0
    CM(I,1)=CM(I,2)
    CM(I,2)=0
2700 CONTINUE
3000 CONTINUE
c^^^^^^^^^^^^^^^^^^^^^^^^^^^^^^^^^^^^^^^^^^^^^^^^^^^^^^^^^^^^^^^^^^^^^^^^^^^^^^


5000 CONTINUE
    STOP
    END
C============END OF THE PROGRAM====================
```

Appendix F

How to Specify Denstone Inert Support Products

A complete set of certified specs is available on request for any product.

Typical Chemical Composition	D57 Balls	D57 Pellets	D80 Balls	D2000 Balls	D95 Balls	D99 Balls
SiO_2	67.40%	67.40%	66.10%	70.00%	0.20% max	0.20% max
Al_2O_3	24.10%	24.10%	26.20%	22.00%	94.5% min	99.00% min
TiO_3	1.18%	1.18%	1.25%	0.90%	—	0.30% max
CaO	0.39%	0.39%	0.61%	0.20%	4.5% max	—
MgO	0 51%	0.51%	0.25%	0.44%	—	—
K_2O	3.28%	3.28%	2.43%	2.97%	—	0.35% max
Na_2O	1.18%	1.18%	2.51%	1.51%	0.30% max	—
Leachable Iron	< .1%	< .1%	< 0.005%	< 0.01%	—	—
Typical Physical Properties	**D57 Balls**	**D57 Pellets**	**D80 Balls**	**D2000 Balls**	**D95 Balls**	**D99 Balls**
Free space (%)	40%	—	40%	40%	40%	40%
Particle density (gm/cc)	2.4	2.4	2.4	2.4	2.8	2.8
Mohs' hardness	6.5	6.5	6.5	6.5	8 min	8 min
Specific heat @ 100°C (cal/gm)	0.25	0.25	0.25	0.25	0.34	—
Water absorption	< 0.4%	< 0.4%	< 0.3%	< 3%	< 7%	< 7%
Apparent porosity	< 1.0%	< 1.0%	< 0.75%	< 8%	< 20%	< 20%
Crush strength - ¼"	120lb (55kg)	—	200lb (91kg)	250lb (115kg)	130lb (60kg)	165lb (75kg) min
Crush strength - ½"	370lb (170kg)	—	400lb (182kg)	500lb (225kg)	550lb (250kg)	440lb (200kg) min
Crush strength - ¾"	950lb (430kg)	—	—	1150lb (520kg)	660lb (300kg)	550lb (250kg) min
Crush strength - 1"	1400lb (635kg)	—	—	1800lb (815kg)	990lb (450kg)	1100lb(500kg)min
Max. Operating Temp.	1800°F (968°C)	1800°F (968°C)	1800°F (968°C)	1800°F (968°C)	2730°F (1500°C)	3000°F (1650°C)
Approximate Packing Density	1450kg/m³ 87-93 lb/cf	1450kg/m³ 87-93 lb/cf	1450kg/m³ 87-93 lb/cf	1400kg/m³ 85-91 lb/cf	1700kg/m³ 97-116 lb/cf	1700kg/m³ 97-116 lb/cf

SIZES AVAILABLE

D57 Balls (in.)	(mm)	D57 Pellets (in.)	(mm)	D80 Balls (in.)	(mm)	D2000 Balls (in.)	(mm)	D95 Balls (in.)	(mm)	D99 Balls (in.)	(mm)
1/8	03	1/8 x 1/8	03 x 03	1/8	03	1/8	03	1/8	03	1/8	03
1/4	06	3/16 x 1/4	04 x 06	1/4	06	1/4	06	1/4	06	1/4	06
3/8	10	1/4 x 3/8	06 x 10	3/8	10	3/8	10	3/8	10	3/8	10
1/2	13	3/8 x 1/2	10 x 13	1/2	13	1/2	13	1/2	13	1/2	13
5/8	16	1/2 x 5/8	13 x 16	3/4	19	5/8	16	3/4	19	3/4	19
3/4	19	5/8 x 3/4	16 x 19	1	25	3/4	19	1	25	1	25
1	25	3/4 x 7/8	19 x 22	—		1	25	1-1/2	38	1-1/2	38
1-1/4	32	7/8 x 1-1/4	22 x 32	—		1-1/4	32	2	50	2	50
1-1/2	38	—		—		1-1/2	38	—		—	
2	50	—		—		2	50	—		—	